RESONANCES – Experimental 1 $(B = 0)$

Chairman	R.L. COOL
Rapporteur	B. FRENCH
Discussion Leader	I.S. HUGHES
Secretaries	H. ATHERTON
	A. GRANT
	J.D. HANSEN

MESON RESONANCES

B. French

CERN, Geneva

INTRODUCTION

In the first section*) of this survey after a brief mention of statistical problems (Section 1.1), I would like to note down some of the quasi-theoretical notions which as an experimentalist I have picked up along the way and have found useful to have at the back of my mind (Sections 1.2 and 1.3). Theorists should jump these. The second section will be an attempt to show up what things have changed in the more well-established mesons, referring mainly for orientation to the

$$J^P = 0^-,\ ^1S_0(q\bar{q}) \text{ nonets}$$

$$J^P = 1^-,\ ^3S_1(q\bar{q}) \text{ nonets}$$

$$J^P = 0^+,\ ^3P_0(q\bar{q}) \text{ nonets}$$

$$J^P = 1^+,\ ^3P_1(q\bar{q}) \text{ nonets}$$

$$J^P = 1^+,\ ^1P_1(q\bar{q}) \text{ nonets}$$

$$J^P = 2^+,\ ^3P_2(q\bar{q}) \text{ nonets}$$

This essentially means masses less than 1600 MeV.

In the third section, I will discuss the data in what has become known as the R region [1600 MeV - 1880 MeV ($\simeq 2M_{\text{nucleon}}$)], and the fourth part will concern those data relevant to the mass region $> 2M_{\text{nucleon}}$. The last section will be a mixed bag of things.

I shall often refer to the Particle Data Group tables[1] as most people by now keep these in their pockets.

*) Those who wish to follow the line of the talk at Vienna should read the last section first. Those who are interested only in a survey of the experimental situation should read Sections 2 and 3.

1. GENERALITIES

1.1 Statistics

One month before the Conference, Professor Rosenfeld sent me his paper on "Far-out mesons and baryons"[2] in which he states that at the present rate of measurement of two million events/year we can expect to see "several 4σ and hundreds of 3σ fluctuation/year". After having passed away several sunny evenings reading the papers submitted to this Conference and trying to sort out the fluctuations from the real effects, I was in the right state to feel that my saviour had come, in that only papers with $\geq 5\sigma$ effects need be taken seriously (how many of those are there?!). However, two lines further on he tells us that for the theoreticians the moral is simple -- wait for 5σ effects. The poor old experimentalists on the other hand, even with a 4σ peak, have nowadays to await confirmation from another experiment before they can say the effect is real. I think all of us should be aware of this problem as it should influence, in a sense, the way we undertake our experiments. For example should a small laboratory concentrate on one large statistics experiment or dabble in several?

In more detail we have:

i) world measurement of bubble chamber events $\sim 2 \times 10^6$ events/year (estimated 1967 figure; may be low);

ii) each event contributes $\sim$15 mass combinations/event;

iii) each histogram contains $\sim$3000 combinations/histogram.

$$\therefore \text{No. of histograms} \sim \frac{2 \times 10^6 \times 15}{3 \times 10^3} = 10{,}000/\text{year}.$$

iv) No. of bins/histogram ∿40

∴ No. of bins/year ∿ 4 × 10^5/year.

However the probability of various fluctuations is

$$3\sigma : 4\sigma : 5\sigma = \frac{1}{370} : \frac{1}{1.6 \times 10^4} : \frac{1}{1.7 \times 10^6}.$$

∴ the No. of fluctuations we can expect/year is

for 3σ = 1000
4σ = 25
5σ = 0.25 .

The significance is clear -- that we can be in trouble if we are not careful. Furthermore, for the future it would seem that it would be a wise move to ensure that the expected growth in measurements of a factor of 2 in two years should be channelled into the same total number of experiments if possible and not into increasing this number.

A further small point which I feel could be helpful is a recommendation that mass [not (mass)^2 histograms] be plotted in 20 MeV bins starting from a multiple of 20 MeV. This would make the task of compiling world data much easier. When one considers the time, money, and effort being put into this field it seems to me that we should make some effort so that world compilation of data is made easier. Of course this does not exclude the plotting of histograms in 10 or 5 MeV bins if the data and resolution warrant it.

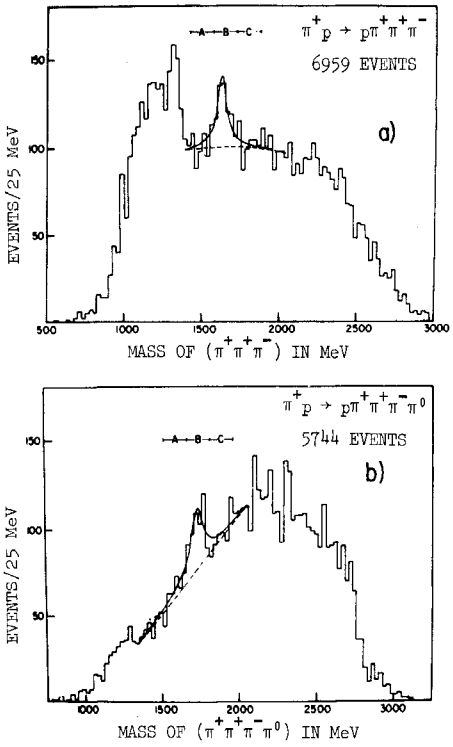

Fig. 1 a) $\pi^+\pi^+\pi^-$ effective mass spectrum, and b) $\pi^+\pi^+\pi^-\pi^0$ effective mass spectrum from the reactions $\pi^+p \to p(3\pi)^+$ and $\pi^+p \to p(4\pi)^+$, respectively, at 7 and 8.5 GeV/c.

In order not to discourage the experimentalists too much, Fig. 1 shows one of the more beautiful results presented to the Conference[3]. Clearly ≥ 5σ peaks are possible! (Note the > 5000 events/histogram.) I do not think many people will question the fact that peaks in the $\pi^+\pi^+\pi^-$ and $\pi^+\pi^+\pi^-\pi^0$ systems are present around 1700 MeV, and one does not need selections to see them! To prove convincingly that these peaks have decay modes $f^0\pi^+$ and $\omega^0\pi^+$, respectively, is another matter and probably requires a factor ≥ 3 more in statistics.

Of course, it is to be hoped that this discussion will not incite people to find ways of increasing the apparent significance of their results by calculating

TABLE 1

Mesons discussed	No. papers concerned
A_1 A_2 region	17
K*'s (Q, L region)	17
R region	17
ππ phase shift, ε^0	8
> R region	7
B	5
S*,KK(I=1)	5
X^0, E^0	5
δ	4
Exotics	3
ω	3
New mesons?	3
η	2
f*	2
H	2
D	2
Odds	5
	107 coming from 98 actual papers

the probability that a fluctuation in a "smooth hand-drawn background curve" could produce the observed peak. To my mind this is incorrect and can, in the case of low background, give very optimistic results. More realistic is an estimate based on the probability for the number of events in the peak to fluctuate down to the phase-space background as this estimate compensates for the fact that the phase-space curve itself has an uncertainty on its position.

As a last comment on statistics, Table 1 lists the number of papers contributed on various subjects and serves to give a rough idea in which sections of meson physics effort is being directed.

1.2 The quark model

Since I am an experimentalist I shall make no excuse for frequently referring to the quark model[4-7]. For me this model is a convenient mnemonic and is an aid for remembering the possible quantum numbers of the various bumps we see and call resonances. By using the quark model as a means of classifying meson states, we can hope to bring out more clearly which states appear to be unfilled, which established meson states seem not to find a place in the scheme, and thus also get some idea of how successful the model is. For the student (not to say the experimentalist) the quark model is a good demonstration of how important it is to establish in a systematic and unbiased fashion the mesonic states of matter and their properties if progress in this field is to be facilitated.

A meson is supposedly composed of a quark and an antiquark: $q\bar{q}$. Since the quarks are fermions, we have for a $q\bar{q}$ system of angular momentum L and total spin S (= 0 or 1)

$$P = (-1)^{L+1} \tag{1}$$

$$C = (-1)^{L+S} \tag{2}$$

$$G = C(-1)^{I} = (-1)^{L+S+I} \ . \tag{3}$$

The quarks having spin 1/2 allow a value of S = 0 and 1, the singlet and triplet states, for each value of orbital angular momentum L between the quarks. Since the product $q \otimes \bar{q} \rightarrow \textcircled{8} + \textcircled{1}$, we will expect to find an SU(3) octet and an unitary singlet (9 meson states) associated with each value of L and S. Each octet is composed of an I = 0, S = 0 isosinglet (η), an I = 1, S = 0 isovector triplet (π), and an I = 1/2, S = ±1 doublet (K), which can be represented as shown in Fig. 2.

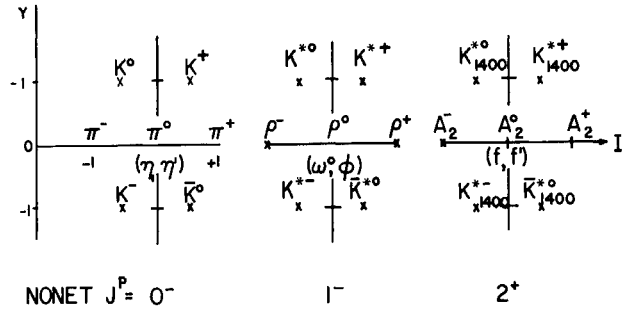

Fig. 2 The three well-known nonets.

Using the Eqs. (1)-(3) it is not too difficult to arrive at Table 2, which lists the quantum numbers one can expect for the various states in each nonet. Possible assignments of the meson states already found experimentally are also shown[8].

1.3 Mass formulae - SU(3) branching ratios - Regge trajectories

What helps us to feel that the assignment of a meson state (of known I^G, J^P, and mass) to a given nonet is reasonable?

1.3.1 Mass formulae

First there are the mass formulae. For members of a given octet there is the Gell-Mann-Okubo (GMO) mass formula

$$4M_K^2 = 3M_\eta^2 + m_\pi^2 \ . \tag{4}$$

Although this works not too badly for the $0^-(^1S_0)$ octet, it is not satisfied for the $1^-(^3S_1)$ octet. So we introduce the idea that the singlet (ϕ) and the octet (ω) I = 0 members can mix

$$\begin{aligned} \omega &= \omega_1 \cos\theta_1 + \phi_8 \sin\theta_1 \\ \phi &= -\omega_1 \sin\theta_1 + \phi_8 \cos\theta_1 \ , \end{aligned} \tag{5}$$

where now ω_1 and ϕ_8 are the (masses)^2 required to satisfy the octet GMO formula (4), and ω and ϕ are the (masses)^2 of the physical particles. From formulae (4) and (5) we solve for a mixing angle θ, which can be used in branching ratio calculations.

The vector mesons are expected to obey the Schwinger mass formula

$$(\phi^2 - \rho^2)(\omega^2 - \rho^2) - \frac{4}{3}(K^2 - \rho^2)(\phi^2 + \omega^2 - 2K^2) = \frac{8}{9}(K^2 - \rho^2)(1 - J^2), \quad J \simeq 1 . \qquad (6)$$

The $1^-(^3S_1)$ nonet, with $\theta_1 \sim 40°$, satisfies formula (6) fairly well.

TABLE 2

$P = (-1)^{L+1}$: $C = (-1)^{L+S}$: $G = C(-1)^I = (-1)^{L+S+I}$

L	S	$^{2S+1}L_J$	C	J^P	I^G	Octet	Singlet
0	0	$^1S_0$	+	0^-	0^+	$\underline{\eta}$	$\underline{\eta' \equiv X^0}$
					1/2	K	
					1^-	π	
	1	$^3S_1$	-	1^-	0^-	ω	ϕ
					1/2	K*(890)	
					1^+	ρ	
1	0	$^1P_1$	-	1^+	0^-	~~H~~	?
					1/2	K*(1320)	
					1^+	B	
	1	$^3P_0$	+	0^+	0^+	$\underline{\varepsilon^0_{700}}$	S*(1080)
					1/2	$\underline{K\pi(1100)}$	
					1^-	δ	
	1	$^3P_1$	+	1^+	0^+	D	?
					1/2	$\underline{K^*_C(1240)}$	
					1^-	$\underline{A_1}$	
	1	$^3P_2$	+	2^+	0^+	f^0	f*
					1/2	K*(1420)	
					1^-	$\underline{A_2}$	

Outstanding states E^0, $\underline{F_1}$, $\underline{A_{1.5}}$, $\underline{K^*(1280)?}$, of mass < 1600 MeV not obviously finding a place in Table 2.

The H meson is discussed in the text and seems to have died. Not listed in the Particle Data Group tables as well established mesons are ε^0_{700}, δ_{962}, $K\pi(1100)$.

Throughout our discussion we shall often refer, for orientation, to this table.

1.3.2 SU(3) branching ratios

Up to now we have made some progress in our attempts to give ourselves confidence that the assignments we have made are correct. However, if we now study the branching ratios of the decay modes of the mesons within a given nonet we find that these are functions of θ_1 and that, given sufficiently accurate data on these branching ratios, they overdetermine the situation to such an extent that we begin to feel if the mesons are correctly assigned or not[9]. Hence the interest in the accurate determination of branching ratios.

In order to make this comparison between the predicted width ($\Gamma_{SU(3)}$) and the measured width (Γ_{exp}) one may use the formula[9]

$$\Gamma_{SU(3)} = N \cdot C^2 \cdot \frac{p}{M^2} \cdot \left(\frac{p^2 X^2}{p^2 + X^2} \right)^L , \qquad (7)$$

where

N = reduced matrix element squared
C = SU(3) Clebsch-Gordan coefficient
p = momentum of decay product
M = mass of decaying particle
X = inverse interaction radius, usually put equal to ∞.

Table 3 shows the predicted rates for the $1^-(^3S_1)$ and $2^+(^3P_2)$ nonets and Tables 4 and 5 the results of a χ^2 fit to the data at that time (July 1967)[9]. Clearly the fits are not too bad but the errors on the Γ_{exp} should be reduced before one can be satisfied. However, at the present time one can say that for the 1^- and 2^+ nonets the mesons assigned to these nonets appear to have branching ratios compatible with SU(3).

1.3.3 Regge trajectories or L-excited mesonic states

We have two different points of view from which we can see how the masses of mesons of given I-spin depend on J, P, and G. There is the Regge trajectory picture in which meson states of a given I, G, P, and differing in J by multiples of two, are expected to lie on a trajectory when their spin J is plotted against their $(\text{mass})^2$. However, it seems that the I = 1 mesons ρ, A_2, R, S, T, U, where admittedly only the J^P of $\rho(=1^-)$ and $A_2(=2^+)$ are well estab-

TABLE 3

$1^- \to 0^- + 0^-$		$2^+ \to 1^- + 0^-$	
$K^* \to K\pi$	1/4	$A_2 \to \rho\pi$	4
$\phi \to K\bar{K}$	$1/2\ (\cos^2\theta_1)$	$K^{**} \to K^*\pi$	3/2
$\rho \to \pi\pi$	1/3	$K^{**} \to K\rho$	3/2
		$K^{**} \to K\omega$	$3/2\ (\sin^2\theta_1)$
		$f^* \to K^*K$	$6\cos^2\theta_2$
$\theta_1 = 40°$ $\theta_2 = 30°$			
$2^+ \to 0^- + 0^-$			
$A_2 \to K\bar{K}$	12	$f^* \to \pi\pi$	$3(2\cos\theta_2 - \alpha\sin\theta_2)^2$
$A_2 \to \eta^0\pi$	8	$f^* \to \eta^0\eta^0$	$(2\cos\theta_2 + \alpha\sin\theta_2)^2$
$f \to \pi\pi$	$3(2\sin\theta_2 + \alpha\cos\theta_2)^2$	$f^* \to K\bar{K}$	$4(\cos\theta_2 + \alpha\sin\theta_2)^2$
$f \to \eta^0\eta^0$	$(2\sin\theta_2 - \alpha\cos\theta_2)^2$	$K^{**} \to K\pi$	18
$f \to K\bar{K}$	$4(\sin\theta_2 - \alpha\cos\theta_2)^2$	$K^{**} \to K\eta^0$	2

lished, lie very well on a straight line trajectory as shown in Fig. 3. The fact that the 2^+ meson lies on the 1^- trajectory has been termed exchange degeneracy and apparently can be understood in terms of the quark model[10]. If we feel that the slope of most Regge trajectories are similar and of the same order as that of the ρ, A_2 trajectory, i.e. $dJ/dM^2 = 1\ GeV^{-2}$, then the mass of a meson together with its production mechanism (diffraction or meson exchange) may help us to guess its J^P assignment by looking on which Regge trajectory it could lie. For example, the L meson ($K\pi\pi$ at 1790 MeV), which can be produced in the reaction $K^+d \to dL^+$ in what appears a diffraction dissociation (or Pomeron exchange)*) reaction, is expected to have J^P in the series 1^+, 2^-, 3^+, etc., and lies nicely on the Regge trajectory of K(494, 0^-), K*(1320, 1^+) if its J^P is taken to be 2^-.

Another way to look at mesonic states is the spectroscopic one in which we invert the Regge plot, and plot (mass)^2 -- vertical scale -- against the spin J. This is more in line with the L-excitation model of Dalitz[6], Zweig[5] and Goldhaber[7]. Figures 4 and 5 show how the mesonic states may be displayed[11].

In this model the mesonic states are seen as the rotational and vibrational excitations of a three-dimensional harmonic oscillator, the linear dependence of the (mass)^2 on L (or J) being a "natural" consequence of the quantization of the harmonic oscillator states. Most of the mesons seen to date are expected to be the lowest-lying states with radial quantum number n = 0. The higher-lying states, which

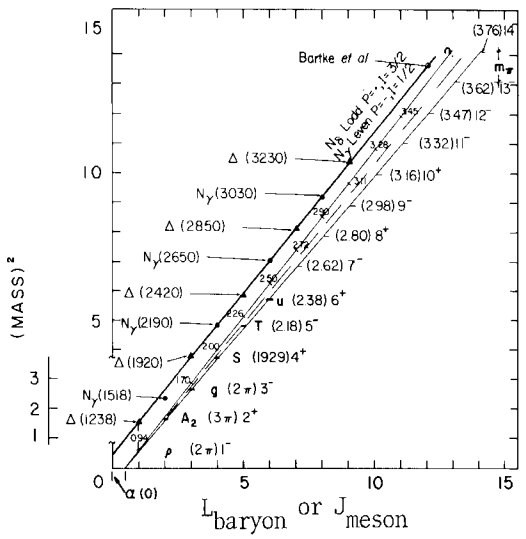

Fig. 3 Excitation diagram of the lowest lying N*'s and bosons. The lower thin full line curve is the ρ trajectory passing through $A_2^L(1270)$, g(1640), S, T, and U. The upper full line curve passes through $A_2^H(1320)$ and g(1700)? The mean of these two lines gives the dotted line which is parallel to the $N^*_{\delta,\gamma}$ trajectory.

*) See Section 1.3.4

TABLE 4

Experimental versus predicted rates

$2^+ \to 1^- + 0^-$			
			←2ΔΓ→
Decay	Γ(expt.)	Γ(pred.)	
$A_2 \to \rho\pi$	56 ± 19	59	
$K^{**} \to K^*\pi$	40 ± 16	20	
$K^{**} \to K\rho$	8 ± 8	5	
$K^{**} \to K\omega$	0 ± 3	2	
$f^* \to K^*K$	0 ± 9	9	
$\chi^2 = (3.2)_3$		Prob. = 40%	
$1^- \to 0^- + 0^-$			
$K^* \to K\pi$	50 ± 3	48	
$\phi \to K\bar{K}$	3 ± 1	3.5	
$\rho \to \pi\pi$	130 ± 30	153	
$\chi^2 = (1.1)_1$		Prob. = 31%	

TABLE 5

Experimental versus predicted rates

$2^+ \to 0^- + 0^-$			
			←2ΔΓ→
Decay	Γ(expt.)	Γ(pred.)	
$A_2 \to K\bar{K}$	2.5 ± 2	3.5	
$A_2 \to \eta^0\pi$	6.5 ± 6	7	
$f \to \pi\pi$	117 ± 21	115	
$f \to \eta^0\eta^0$	0 ± 12	0.4	
$f \to K\bar{K}$	0 ± 12	7	
$K^{**} \to K\pi$	32 ± 13	27	
$K^{**} \to K\eta^0$	0 ± 4	1	
$f^* \to \pi\pi$	0 ± 9	1	
$f^* \to \eta^0\eta^0$	0 ± 18	8	
$f^* \to K\bar{K}$	66 ± 31	31	
$\chi^2 = (2.2)_7$		Prob. = 94%	

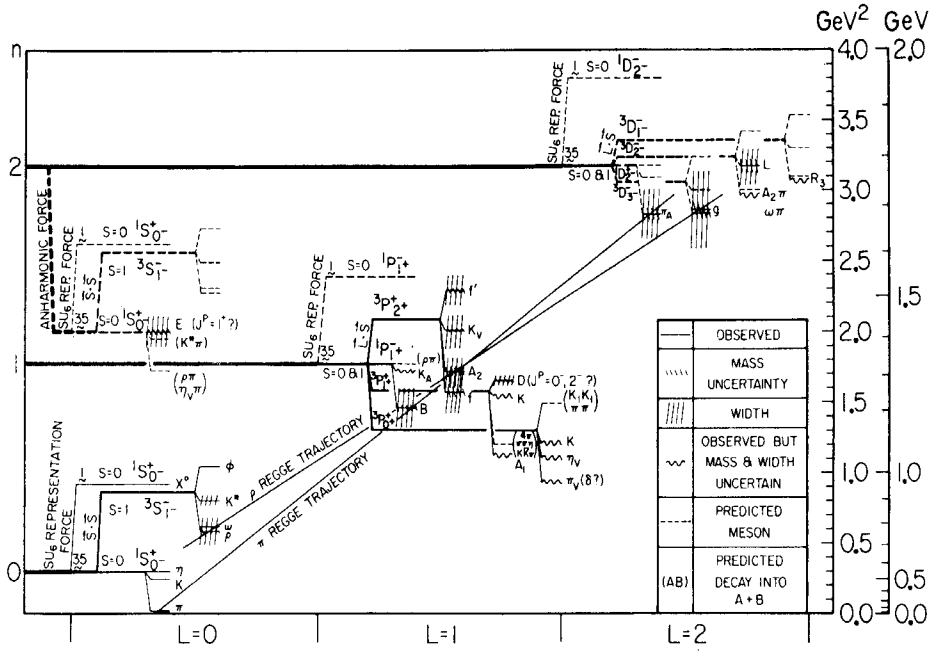

Fig. 4 Excitation diagram for boson states after Zweig[11].

probably have larger widths and are probably more difficult to excite (at least in πp or Kp collisions), may be more difficult to discover. Phase-shift analyses which have been successful in finding broad baryon resonances are difficult to apply to meson physics. Possibly the $\bar{p}p$ boson formation channel will prove of interest here for bosons of mass > $2M_{\text{nucleon}}$.

1.3.4 Dependence of cross-sections on energy

When a meson is produced in a given reaction the variation of its production cross-section with the momentum of the incident particle can be of use to give us some idea as to whether the meson produced has a J^P value in the natural series 0^+, 1^-, 2^+, ... or in the unnatural series 0^-, 1^+, 2^-, ... etc. The reasoning behind this is as follows: mesons produced

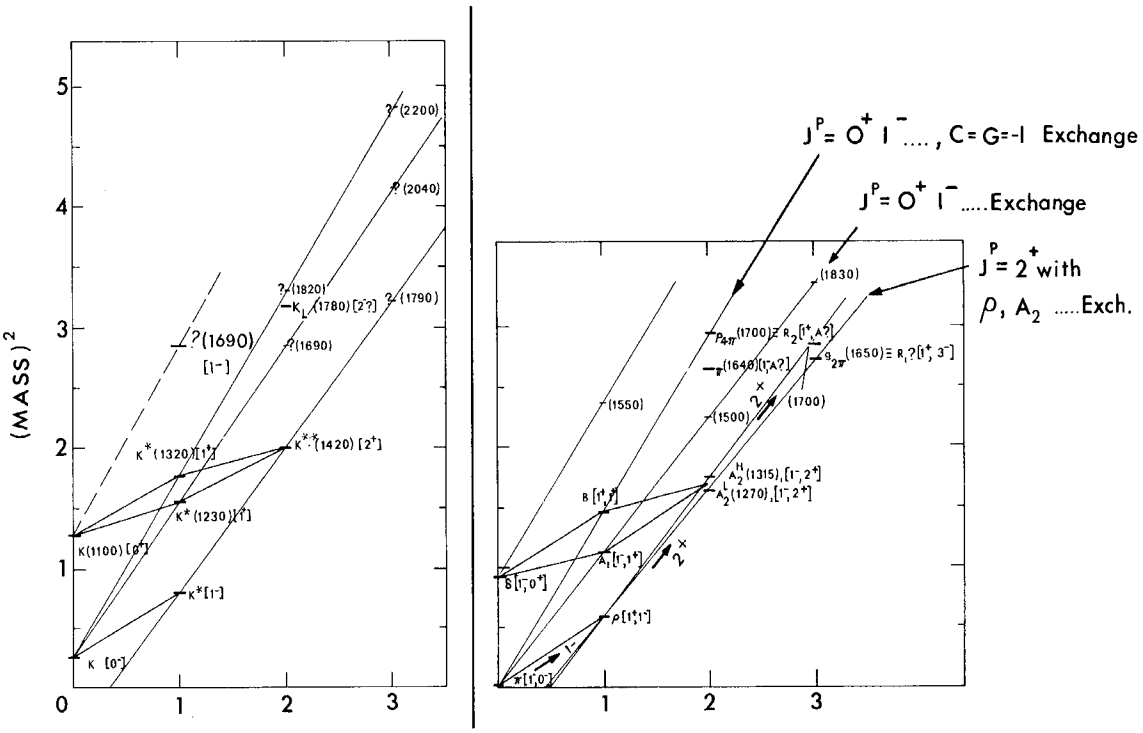

Fig. 5 Excitation diagram for I = 1/2 and I = 1 boson states. Thick lines connect states in same $q\bar{q}$ orbital angular momentum state.

peripherally are thought to involve either the exchange of the Pomeron ($J^P = 0^+$) or of a meson (e.g. π, ρ, A_2) and Regge pole theory predicts[12]

$$\sigma \simeq \left(\frac{d\sigma}{dt}\right)_{t=0} \propto S^{2\alpha(0)-2} \simeq p_i^{2\alpha(0)-2} . \qquad (8)$$

Here the assumption is that most of the cross-section comes from the region where $t \simeq 0$. p_i = incident particle momentum; $\alpha(0)$ is the intercept of the exchanged particles' trajectory at $t = 0$ on the angular momentum axis of the Chew-Frautschi diagram, Fig. 3.

For Pomeron exchange $\alpha(0) \simeq 1$ so $\sigma \simeq$ constant

For π exchange $\alpha(0) \simeq 0$ so $\sigma \simeq p_i^{-2}$

For ρ, A_2 exchange $\alpha(0) \simeq 0.5$ so $\sigma \simeq p_i^{-1}$.

Thus since the Pomeron has $J^{PC} = 0^{++}$ and $I^G = 0^+$ its exchange can only involve a change in the angular momentum of the incident particle by 0^+, 1^-, 2^+, etc., and mesons produced from incident pions or kaons which have production cross-sections that are nearly constant with energy will be expected to have values of J^P in the series 0^-, 1^+, 2^-, etc.[12].

2. MESONS (MASS < 1600 MeV)

In this section we will discuss the recent data on meson states referring, for orientation, to Table 2. We first go systematically through the I = 0 states, then the I = 1, and finally the I = 1/2 states of mass < 1600 MeV.

2.1 I = 0 mesons

2.1.1 $\eta^0(549)$

$\eta(549)$

$\eta \to \pi^+\pi^-\gamma$	5.4 ± 0.6%	28.7 ± 1.3
$\pi^+\pi^-\pi^0$	23.3 ± 1.2%	
$3\pi^0$	29.0 ± 2.5%	71.3 ± 1.3
$\gamma\gamma$	40.3 ± 1.6%	
$\pi^0\gamma\gamma$	2.0 ± 1.2%	

$3\pi^0/\pi^+\pi^-\pi^0$: 1.25 ± 0.13 (Exp.); 1.58 (Theory)

α = -0.54 ± 0.017 (REAL)

It has become customary to discuss the branching ratios of the η in the meson session although this really involves the electromagnetic interactions. Thus the η is to the study of electromagnetic interactions as the K^0 is to the study of weak interactions. At the Philadelphia Meson Conference, Baltay reviewed in detail the η branching ratios and gave the values[13] shown in the insert.

There is little change between these values and those reported at the Heidelberg Conference. The ratio $(\eta \to 3\pi^0)/(\eta \to \pi^+\pi^-\pi^0) = 1.25 \pm 0.13$ is still some way off the theoretically-predicted value of 1.58 [13]. At this Conference, a paper was presented by groups working with a heavy-liquid bubble chamber[14] in which they observe the 6γ's from the $3\pi^0$ materialize in the liquid. They were thus able in one experiment to measure directly the ratio

$$\frac{\eta \to 3\pi^0}{\eta \to \pi^+\pi^-\pi^0} = 1.37 \pm 0.20$$

in good agreement with the above value of 1.25.

As a result of two papers which have appeared during the last year[15,16] and a bubble chamber collaboration result, Baltay[13] has arrived at a best value for the parameter "α" describing the Dalitz plot distribution of the $\eta^0 \to \pi^+\pi^-\pi^0$ decay of

$$\alpha(\text{real}) = -0.54 \pm 0.017 ,$$

the decay distribution being described by a linear matrix element of the form $|f|^2 = |1 + \alpha y|^2$ and $y = 3\,T_0/Q - 1$ (T_0 = kinetic energy of the π^0, $Q = M_{\eta^0} - 3m_{\pi^0}$). This factor α is important in that it enters into the theoretical expression for the ratio[17]

$$\frac{\eta \to 3\pi^0}{\eta \to \pi^+\pi^-\pi^0} = \frac{1.15 \times 1.5}{(1 + 0.25\alpha^2)} .$$

2.1.2 $\eta'(958)$ or X^0

There was always the problem of the $\eta'(958)$ and $\delta(962)$ of similar masses and narrow widths ($\Gamma \lesssim 4$ MeV). Are they the same resonance? δ clearly does not have I = 0 (seen in charged mode). However, is $I(\eta'^0) = 0$? During the year, experiments on deuterium at LRL[18] and the SABRE[19] collaboration, studying reaction

$$K^- n \to \Lambda^0 X^- , \qquad (9)$$

show no evidence for a signal in X^- at a mass of 960 MeV.

η'(958)

- I = 0 or I = 1?

$K^-n \to \Lambda X^-$ LRL and
$K^-p \to \Lambda X^0$ SABRE $\to$ I = 0

- $J^P = 0^-$ or 1^+?

$\pi^-p \to nX^0$, $X^0 \to \gamma\gamma$ CERN $\to J^P = 0^-$

Since the η' is seen abundantly in the reaction

$$K^-p \to \Lambda\eta'^0 \qquad (10)$$

and I-spin conservation would predict twice the cross-section of reaction (10) for reaction (9) if the I(η') = 1, the evidence for I(η') = 0 seems strong. (More quantitatively the LRL group, for example, give $\sigma(\eta'^-) < 25$ μb with 99% confidence, whereas 220 ± 18 μb is expected if I = 1.)

η'(958) → γγ: Although the Dalitz plot distribution for the $\eta^0\pi^+\pi^-$ decay of η'(958) favours $J^P = 0^-$ for I = 0, the possibility of $J^P = 1^+$ has always existed if I = 1. The foregoing result, therefore, in a sense establishes $J^P = 0^-$. However, observation of the γγ decay of the η'(958) would unambiguously establish $J^P = 0^-$. At this Conference a result was presented[20] by a CERN-Bologna group studying the reaction

$$\pi^-p \to nX^0, \quad X^0 \to \gamma\gamma$$

at 1.93 GeV/c with a spark chamber technique. Figure 6 shows the γγ mass spectrum with and without charged particles accompanying the two γ's. An excess of five events occurs in the bin 945-980 MeV. Bubble chamber people should not laugh at the small statistics, as it is clearly not the easiest of experiments. If we associate this excess as being due to the γγ decay of the η', then $J^P(\eta') = 0^-$ within the limitations imposed by the small statistics.

2.1.3 H meson ($I^GJ^P = 0^-1^+$)

During the year, work has been published by groups at LRL[21] and the UCLA[22] which, I think most experimentalists agree, kills or at least severely maims

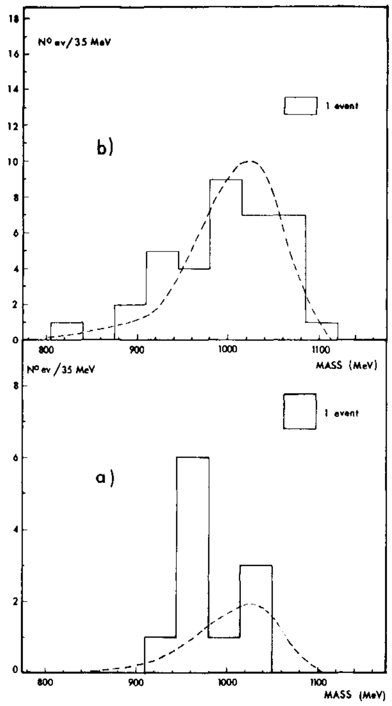

Fig. 6 γγ effective mass distribution from reaction $\pi^-p \to n + MM$ [20], a) without accompanying charged particles, b) with accompanying charged particles.

the H meson as a meson candidate. The reasons for this are primarily:

a) the effect, i.e. the bump in the $\rho^0\pi^0$ mass spectrum at ∿ 990 MeV in the reactions $\pi^+p \to N^{**}_{33}\pi^+\pi^-\pi^0$ and $\pi^+n \to p\pi^+\pi^-\pi^0$ was statistically small and was seen by only a few groups ; thus one could be subject to fluctuation problems in choosing a few experiments that see an effect out of many that do not;

b) enhancements in this region of phase space can be produced by making a ρ selection on a statistically produced 3π phase space[22];

H is dead?

- Statistics, small $\rho^0\pi^0$ effect.
- Partially reproduced by ρ cut on 3π phase space.
- Partially explained by γ faking π^0 in $\pi^+p \to p\pi^+X^0$, $\pi^+n \to pX^0$, $X^0 \to \pi^+\pi^-\gamma$

c) a spurious peak can be produced by misidentifying a γ from the $\pi^+\pi^-\gamma$ decay of the $\eta'(958)$ as a π^0 in the reactions

$$\left.\begin{array}{l} \pi^+ p \to p\pi^+ X^0 \\ \qquad\qquad \hookrightarrow \pi^+\pi^-\gamma \\ \pi^+ n \to p\, X^0 \\ \qquad\qquad \hookrightarrow \pi^+\pi^-\gamma \end{array}\right\} \gamma \text{ taken as } \pi^0.$$

From considerations of all these effects the LRL group concludes that no significant evidence for the existence of the H meson remains.

This leaves us with two unfilled states in the I = Y = 0, $^1P_1$ states of Table 2.

2.1.4 $\varepsilon^0(700) \to \pi\pi$?

The possibility of a resonance in the I = 0 $\pi\pi$ system has been around for some time. Such a state is clearly of interest to the quark model enthusiasts. To my mind the situation has hardened a little in favour of a broad state ($\Gamma \gtrsim 200$) at about 700 MeV. The variation of the I = 0, J = 0 phase shift δ_0^0 as deduced from the reaction $\pi N \to N\pi\pi$ is shown in Fig. 7 [23]. The main problem is to decide between solutions I and III, solutions I and II being essentially the same but 180° out of phase. Set I goes through 90° in the region of 700 MeV, whereas set III goes through 90° around 900 MeV but very slowly [cf. $K\pi(1100)$ in Section 2.3.1]. Clearly this is

$\varepsilon^0(700)$

- Single π production in $\pi N \to N\pi\pi$.
- Does δ_0^0 go through 90° around 700 MeV?
- Decision to be made between set I and III phase-shift solutions. Mass spectra favour set I, i.e. 90° at 700 MeV.

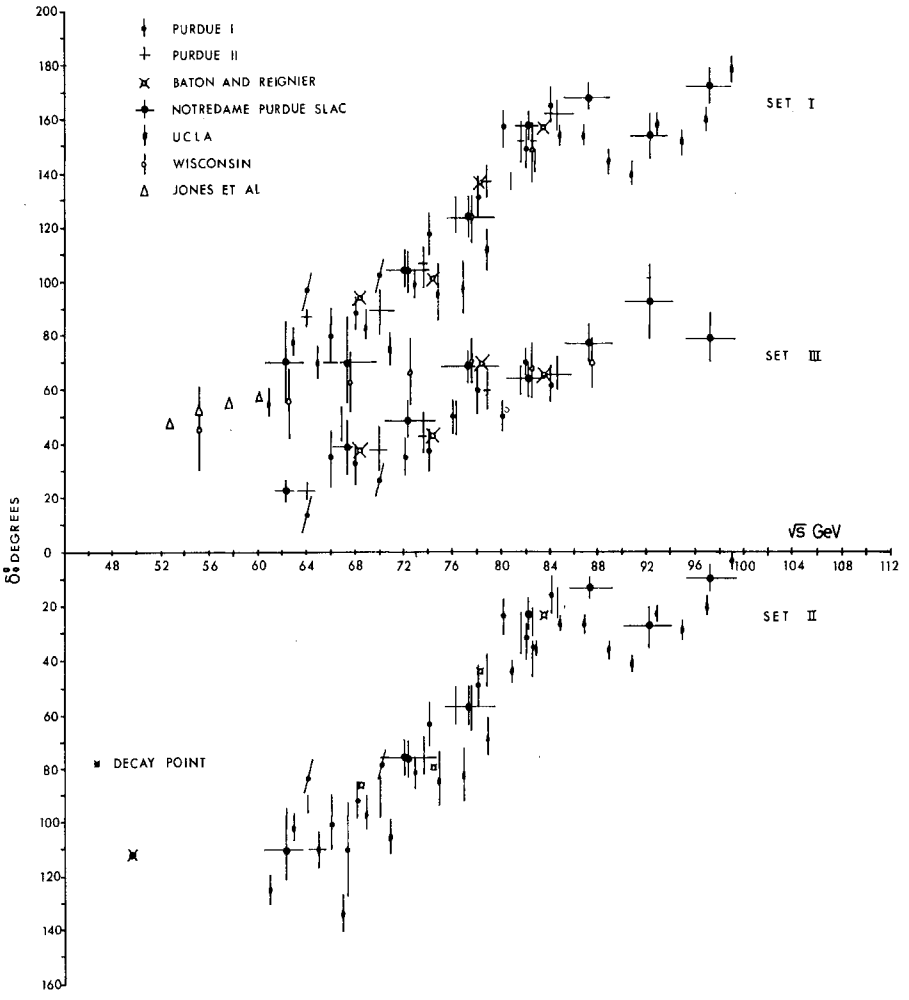

Fig. 7 Results of seven experiments on δ_0^0 [23].

where the phase-shift analysis technique, which has been so successful in the search for baryon resonances, should be more successful than the search for bumps in the $\pi\pi$ effective mass. However, at this Conference and during the year there have been papers on the $\pi^0\pi^0$ effective mass spectrum[24-26]. These three groups interpret their data as giving support to a broad $\pi^0\pi^0$ resonance around 700 MeV. Moreover, their cross-sections appear to agree in magnitude with that predicted by the phase shifters[27], which was not the case in earlier work[28]. Figures 8 and 9 show the $\pi^0\pi^0$ effective mass spectra from two experiments along with the prediction from Malamud and Schlein[27]. The agreement is good and solution I seems favoured.

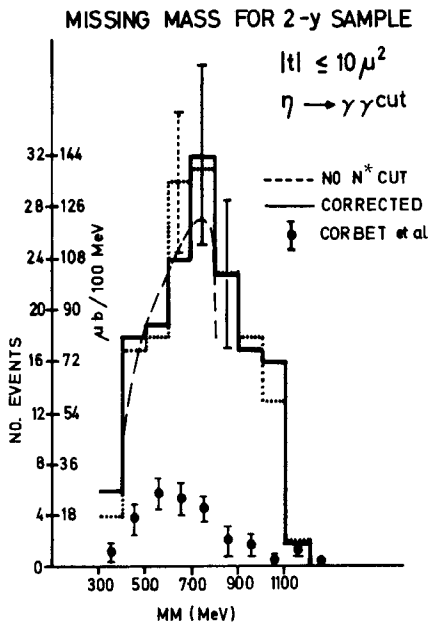

Fig. 8 $\pi^0\pi^0$ effective mass distribution calculated as the missing mass (MM) from the reaction $\pi^+d \to pp_s$ MM (MM $\to \pi^0\pi^0$) at 2.15 GeV/c [24]. Dashed curve prediction of Malamud and Schlein[27].

2.1.5 $\eta_\nu(1070)$ or $S^*(I^GJ^P = 0^+0^+)$

S*(1070)
• S-wave scattering length, resonance, or mixture of both? No clear-cut decision.
• $\pi^+\pi^-$ decay? ρ^0, f^0 complications.
• NEW: $M(\pi^+\pi^-)$ bump at 1050 MeV - requires D-wave?

$K_1^0K_1^0$ decay: As regards the $K_1^0K_1^0$ decay of the S* nothing has drastically changed. New data presented to the Conference[29] using the optical spark chamber technique served to demonstrate how difficult it is to determine in π^-p interactions whether this enhancement is due to

a) an S-wave complex scattering length,

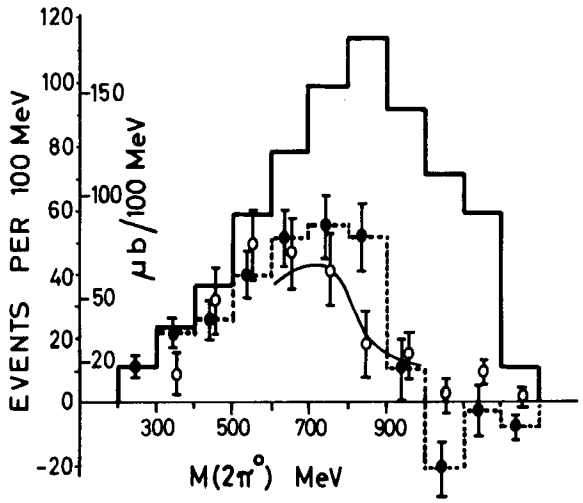

Fig. 9 (Solid histogram) Neutrals mass spectrum from the reaction $\pi^+n \to p$ + neutrals [25]; cos $\theta_{c.m.}$ (neutrals) ≥ 0.8. (Solid points) $\pi^0\pi^0$ effective mass spectrum, after subtraction of $3\pi^0$ and N* background from the solid histogram. (Open points) Data of Corbett et al.[28] multiplied by factor 2.96. The curve represents the prediction of Malamud and Schlein[27].

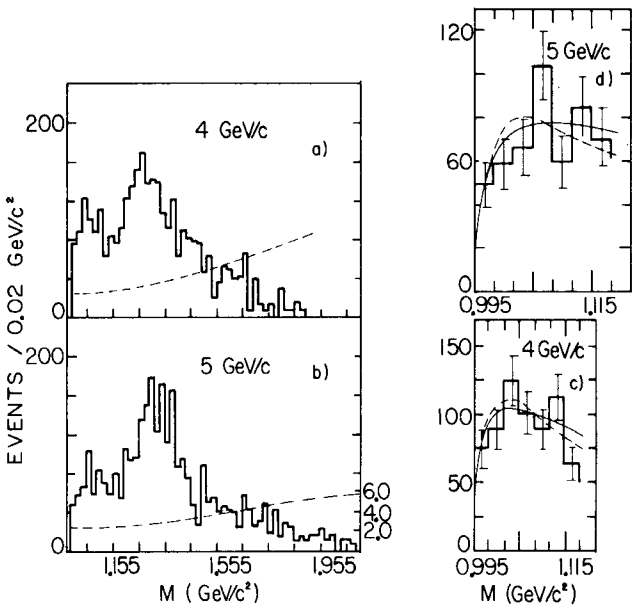

Fig. 10 Weighted $K_1^0K_1^0$ invariant mass distribution: a) at 4 GeV/c; b) at 5 GeV/c from the reaction $\pi^-p \to K_1^0K_1^0n$ [29]; c) and d) scattering length fit (solid curve) and resonance fit (dashed curved) to the data at 4 GeV/c and 5 GeV/c.

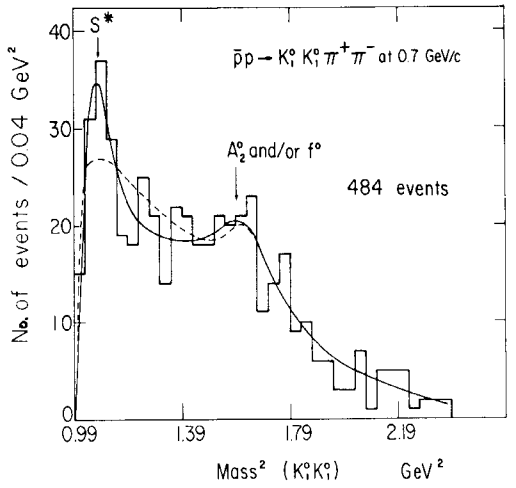

Fig. 11 Distribution of the effective mass squared of the $K_1^0K_1^0$ system for the reaction $\bar{p}p \to K_1^0K_1^0\pi^+\pi^-$ at 0.7 GeV/c [30]. The solid curve represents the fit with a Breit-Wigner for the S* with M = (1030 ± 7) MeV, Γ = (50 ± 15) MeV. Dashed curve: scattering length fit of (1.50 ± 0.5) fermi.

b) an S-wave resonance near threshold, or

c) a mixture of the two, as can be seen in Fig. 10.

In contrast, Fig. 11 shows the $K_1^0K_1^0$ mass spectrum produced in $\bar{p}p$ annihilations at 0.7 GeV/c [30]. Here the resonance interpretation seems to explain the data better. They report a value of M(S*) = (1030 ± 7) MeV and Γ(S*) = (50 ± 15) MeV.

$\pi^+\pi^-$ decay: If indeed $I^GJ^P = 0^+0^+$ for the S* we might expect to see a $\pi^+\pi^-$ decay manifest itself in the reaction

$$\pi^- p \to n\, S^{*0} \begin{cases} \to K_1^0K_1^0 \\ \to \pi^+\pi^- \end{cases}$$

This $\pi^+\pi^-$ signal will depend on the effective coupling (α) of the S* to the $\pi^+\pi^-$ system. Since the $S^* \to K_1^0K_1^0$ is produced peripherally in the π^-p reaction it would seem reasonable that the entrance channel to the S* is $\pi^+\pi^-$ (see Fig. 12a). If α were near 1 we could expect to see a $\pi^+\pi^-$ signal (proportional to α^2, Table 6) since we see a signal in $K_1^0K_1^0$ [proportional to $\alpha(1-\alpha)$]. That a $\pi^+\pi^-$ signal exists in this region was indicated already at the Heidelberg Conference [31] and has been consolidated a little more at this Conference [32,33], see Figs. 13 and 14. Figure 13 shows the $\pi^+\pi^-$ mass spectrum from the reaction $\pi^-p \to n\pi^+\pi^-$ at 6 GeV/c for those $\pi^+\pi^-$ systems with a π^- emitted into the backward hemisphere in the $\pi^+\pi^-$ c.m.s. A signal seems to exist in the S* region, and along with the $K_1^0K_1^0$ signal observed in the same experiment (shown in Fig. 15) yields a ratio of $(S^* \to \pi^+\pi^-/S^* \to K_1^0K_1^0) = 1.0^{+0.6}_{-0.3}$ (2.5 would be expected from phase-space considerations alone). Figure 14 shows the $\pi^+\pi^-$ mass spectrum from a Purdue-Notre Dame-SLAC Collaboration with 8000 $\pi^-p \to \pi^+\pi^-n$ events [33]. A clear bump is seen at $M(\pi^+\pi^-) = 1.05 \pm 0.01$ GeV; $\Gamma \leq 40$ MeV especially when the π^- is selected to have $\cos\theta^* < -0.75$ (Fig. 14d). The problem here, however, is that the angular distribution of the π^- in the c.m.s. of the dipion system is more compatible with D-wave decay than S-wave, as can be seen in Fig. 14b. This is in agreement with an observation made by a counter experiment at the Rutherford laboratory [34] which also favoured spin ≥ 0. The variation of the coefficients of a Legendre polynomial fit to the $\pi^+\pi^-$ decay angular distribution as a function of $\pi^+\pi^-$

TABLE 6

	$\pi^+\pi^-$	$K_1^0K_1^0$
$\pi^+\pi^-$	α^2	$\alpha(1-\alpha)$
$K_1^0K_1^0$	$(1-\alpha)\alpha$	$(1-\alpha)^2$

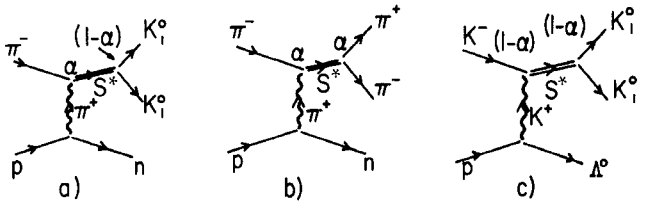

Fig. 12 Peripheral diagrams relevant to S* production.

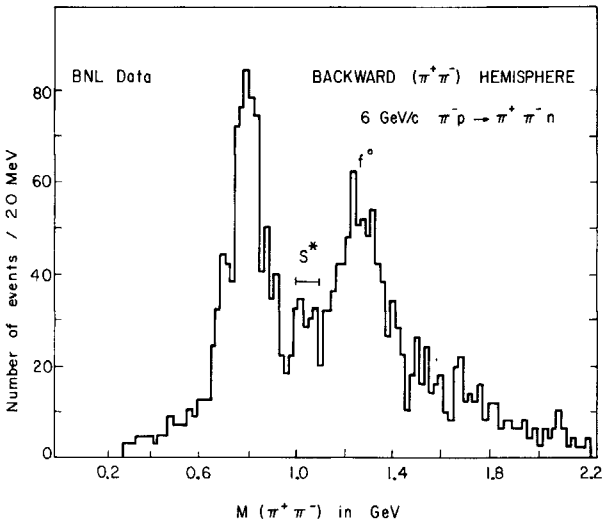

Fig. 13 $\pi^+\pi^-$ effective mass spectrum where π^- is emitted into backward hemisphere in $\pi^+\pi^-$ c.m.s. [32].

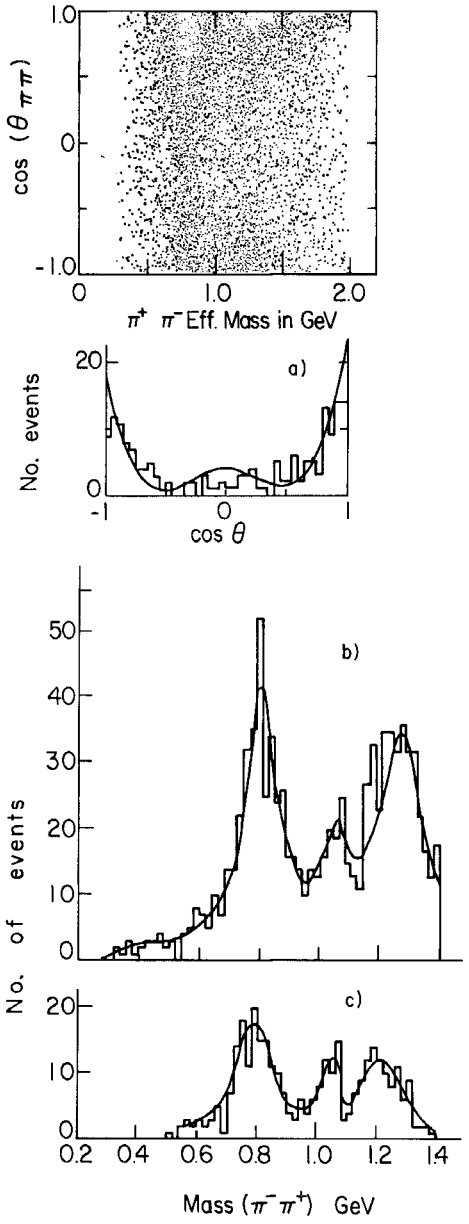

Fig. 14 a) $\pi^+\pi^-$ effective mass spectrum from reaction $\pi^-p \to n\pi^+\pi^-$ at 4 GeV/c [33] plotted against the cosine of the scattering angle in the dipion rest frame, and the decay angular distribution for $1.00 < M_{\pi\pi} < 1.10$ and Δ^2 to the $\pi\pi$ system < 0.1 GeV^2; b) $M(\pi^+\pi^-)$ for $\cos\theta < -0.75$; c) $M(\pi^+\pi^-)$ for $\cos\theta < -0.75$ and Δ^2 to $\pi\pi$ system < 0.1 GeV^2.

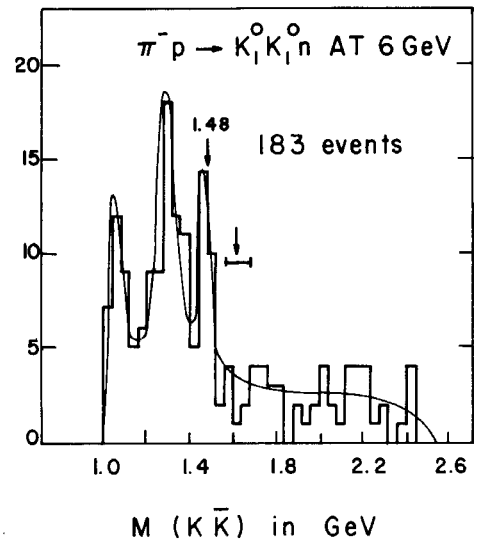

Fig. 15 $M(K_1^0K_1^0)$ from the reaction $\pi^-p \to K_1^0K_1^0n$ at 6 GeV/c [32].

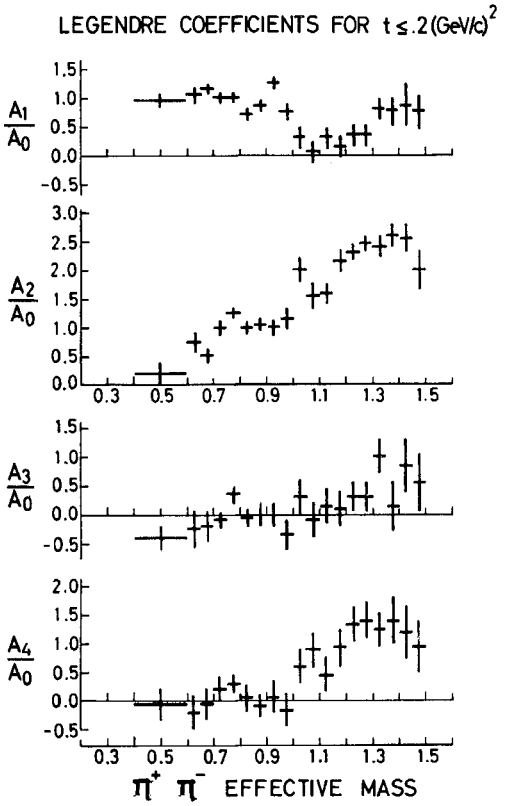

Fig. 16 Legendre coefficients from fits to the $\pi^+\pi^-$ decay angular distribution from the reaction $\pi^-p \to n\pi^+\pi^-$ at 4 GeV/c with $|t_p| < 0.2$ GeV^2 [35].

mass is shown in Fig. 16 [35]. We see a peaking of A_2/A_0 near 1.03 GeV which, as the authors state, is consistent with constructive interference between a rapidly increasing δ_0^0 (S*?) and an increasing D-wave phase shift, δ_2^0.

2.2 I = 1 mesons < 1600 MeV

2.2.1 B(1220) ($I^GJ^P = 1^+?$)

I will not discuss this state in detail except to note that during the year, and at this Conference,

B(1220) → ωπ

- New, $J^P = 1^+$ or 2^+, 3^- ... favoured in the $\pi^-p \to p\omega^0\pi^-$ 5 GeV/c.

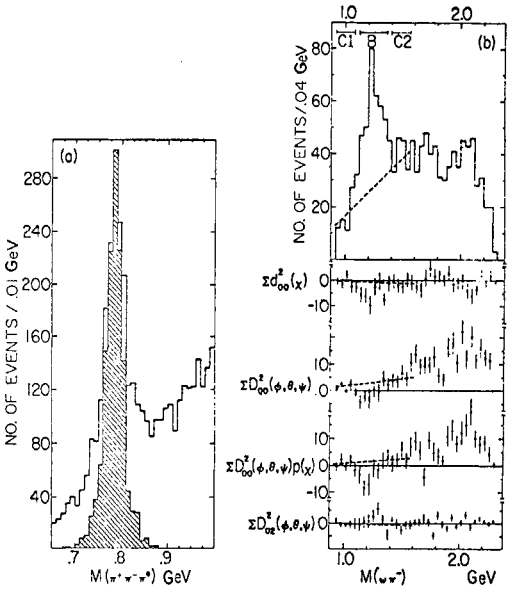

Fig. 17 a) $M(\pi^+\pi^-\pi^0)$ spectrum from $\pi^- p \to p\pi^-\pi^+\pi^0$ [36]; b) $M(\omega^0\pi^-)$ spectrum and unnormalized moment distributions.

the Illinois group[36] working with π^- at 5 GeV/c see a nice $\omega^0\pi^-$ signal at $\sim$ 1240 MeV, $\Gamma \sim$ 200 MeV (see Fig. 17) in the reaction

$$\pi^- p \to p\pi^-\omega^0 \quad \omega^0 \to \pi^+\pi^-\pi^0 .$$

This experiment gives much needed confirmation for a $\omega\pi$ state at this mass. From a moment analysis of the angular distributions they conclude that $J^P = 1^+$ or 2^+, 3^- ... is favoured. $J^P = 3^-$, 5^- ... is unlikely because of the non-observation of a $\pi\pi$ decay, although we should remember that, for instance, $f^*(1515) \not\to \pi\pi$ has nice explanations coming from SU(3). They also state that the fact that their data require $|J_z| \simeq \pm J$ for $J^P = 2^+$, 3^- ..., together with the rather peripheral production of the B, makes it difficult to believe in the possible $J^P = 2^+$, 3^- ... assignments given by the moment analysis.

2.2.2 δ(962)

Now we come to the δ problem. Seemingly only the CERN-MMS data remains. In all the other experiments, repeat experiments have not substantiated the original claims. Why do we not have more CERN-MMS-type experiments? If δ has $I^G J^P = 1^-0^+$ an expected decay mode is $\delta^- \to \eta^0\pi^-$; possible evidence for this decay mode has been reported in three experiments.

δ(962)

- Seen in CERN-MMS nothing new.
- Other former evidence vanished
- NEW

i)	$K^- p \to \Lambda^0\pi^+\pi^- M$	4.6 GeV/c	BNL
		5.5 GeV/c	ANL-NW
ii)	$\bar{p}p \to 3\pi^+3\pi^-\pi^0$	1.2 GeV/c	CERN CdF IPN

$K^- p \to \Lambda\pi^+\pi^- M$

- agree: when M = "η^0", peak at δ^- mass in $\pi^- M$.
- disagree: on % of η^0 in δ^- and on Y_1^{*+} association to δ^-

M ∿ 975 MeV Γ ∿ 80 MeV

$K^- p \to \Lambda^0\pi^+\pi^- M$: Two experiments study the reaction

$$K^- p \to \Lambda^0\pi^+\pi^- M$$

4.6 GeV/c BNL 3.5 evts/μb [37]

5.5 GeV/c ANL-NW 7 evts/μb [38]

where M is the unfitted missing mass. Both groups agree that when a region of M around the η^0 mass ("η^0") is taken a peak is obtained in the $\pi^- M$ effective mass spectrum in the region of 975 MeV with a $\Gamma \lesssim 80$ MeV which is claimed to be similar to their mass resolution in this region, see Figs. 18 and 19. The main problem comes when one asks how much of this $\pi^- M$ signal is really due to $\eta^0\pi^-$. BNL feel not more than 30% and ANL-NW a large fraction. Justification of the ANL-NW claim is given in Fig. 20, which shows that selecting events in which the $\Lambda^0\pi^+$ mass lies in the $Y^*(1385)^+$ region a signal is seen in $\pi^- M$ at ∿ 975 MeV only when 500 < M < 600 MeV. BNL on the other hand, arrive at their estimate by using the reaction

$$K^- p \to \Lambda^0\pi^+\pi^-\eta^0 \quad \eta^0 \to \pi^+\pi^-\pi^0 .$$

They have few events with an η^0 and can estimate how much $\eta^0 \to$ neutrals are left in the M spectrum after those contributing to X^0 ($\to \eta^0\pi^+\pi^-$) production have been removed. After that the further details do not seem to agree too well. Thus BNL find little associ-

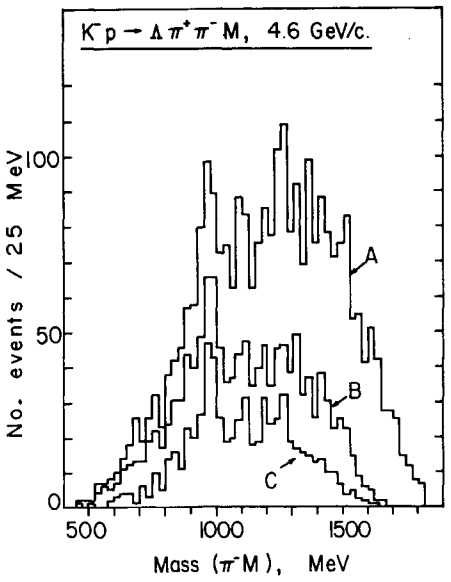

Fig. 18 π^-M mass distribution from reaction $K^-p \to \Lambda^0\pi^+\pi^-M$ at 4.6 GeV/c [37] with $M^2 > 0.05$ GeV^2.

Histogram A - 2736 events, no $\eta'(960)$
Histogram B - 1295 events, no $\eta'(960)$, $\Lambda\pi^+$ and $\Lambda\pi^-$ > 1430 MeV
Histogram C - 648 events, no $\eta'(960)$, $\Lambda\pi^+$ and $\Lambda\pi^-$ > 1430 MeV
$M^2 < 0.95$ GeV^2, $E_{lab}(\pi^+) < 1$ GeV.

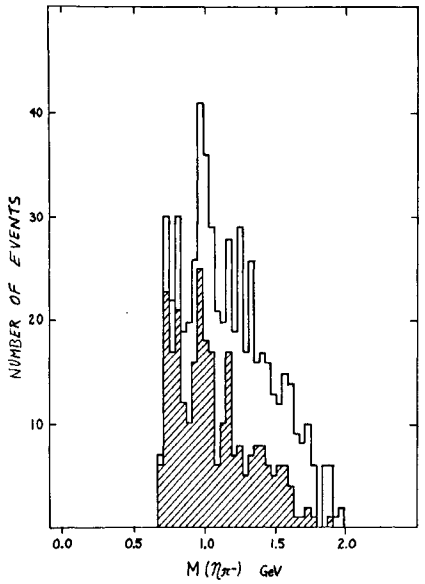

Fig. 19 π^-M mass distribution from the reaction $K^-p \to \Lambda^0\pi^+\pi^-M$ [38] where M = [M(η) ± 50] MeV.
Hatched histogram: $\Delta^2(\pi^-M) \leq 1.5$ GeV^2.

ation of the peak to Y_1^{*+}, ANL-NW do, see Fig. 20. BNL find no evidence for peripheral production whereas ANL-NW do.

$\bar{p}p \to 3\pi^+3\pi^-\pi^0$: The third experiment[39] concerns the reaction

$\bar{p}p \to 3\pi^+3\pi^-\pi^0$ at 1.2 GeV/c 3500 events.

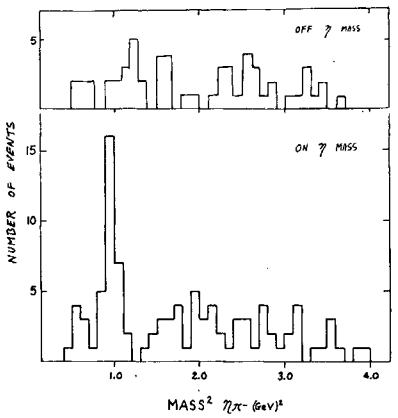

Fig. 20 π^-M mass distribution opposite $Y_1^*(1385)$ from the reaction $K^-p \to \Lambda^0\pi^+\pi^-M$ [38] for M on and off the η^0 mass.

$\bar{p}p \to 3\pi^+3\pi^-\pi^0$ (3500 evts)

- No η^0 evident in $(3\pi)^0$ but "η^0"$\pi^+\pi^-$ shows X^0, and "η^0" cut of (548 ± 20) MeV consistent with $100\eta^0$.
- "η^0"$\pi^\mp \to 3\sigma$ peak at 970 MeV.
- "$\delta^\pm$"$\pi^\mp \to$ peak at 1300 MeV (D^0?).

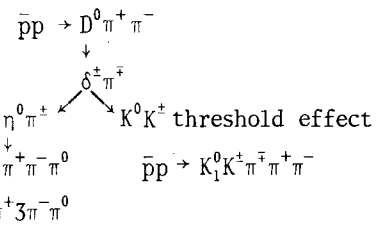

The $\pi^+\pi^-\pi^0$ mass distribution shown in Fig. 21a shows no clear η^0 signal although with the large number of combinations 100 η^0 can easily be accommodated. That η^0's are present is indicated by the "η^0"$\pi^+\pi^-$ mass distribution (Fig. 21c) which shows an X^0 signal and also a signal at ∿ 1300 MeV. [Here "η^0" means $\pi^+\pi^-\pi^0$ masses in region (548 ± 20) MeV.] When they look at the "η^0"$\pi^\pm$ mass distribution they find evidence (∿3σ) for a peak at about 970 MeV ($\Gamma \sim 25$ MeV consistent with their resolution). Taking then the "η^0"$\pi^\pm$ masses with (970 ± 20) MeV ("δ", say) and forming the "$\delta^\pm$"$\pi^\mp$ mass distribution they get back the 1300 MeV peak (Fig. 21d) suggestive of the D^0 meson. Their tentative interpretation, which to my mind has a certain beauty about it, is that they are observing the cascade decay chain shown in the insert. The reaction

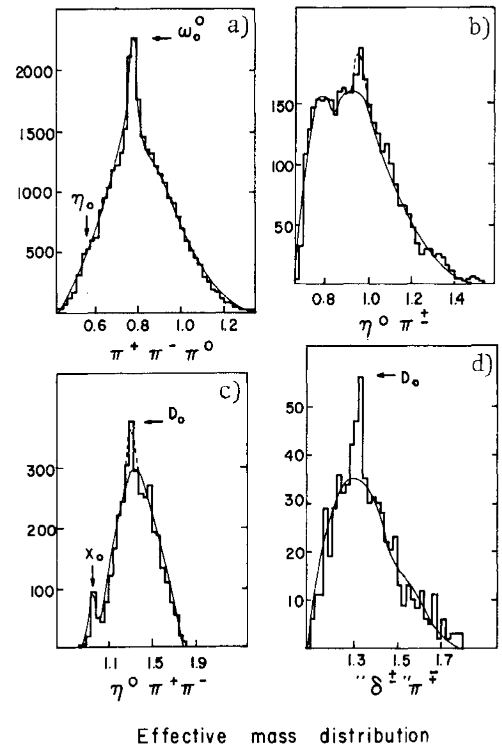

Fig. 21 $\pi^+\pi^-\pi^0$, $\eta^0\pi^\pm$, $\eta^0\pi^+\pi^-$ and "$\delta^\pm$"$\pi^\mp$ mass distributions from the reaction $\bar{p}p \to 3\pi^+3\pi^-\pi^0$ at 1.2 GeV/c [39].

branch to the right, viz. $\bar{p}p \to K_1^0K^\pm\pi^\mp\pi^+\pi^-$, has already been published[40]. Evidence was presented for the possible reaction

$$\bar{p}p \to \pi^+\pi^-D^0 \;\; \hookrightarrow \delta^\pm\pi^\mp \;\; \hookrightarrow (K^0K^\pm)$$

where threshold $K\bar{K}$ behaviour is interpreted as the effect of a virtual bound state below threshold at the δ mass. Here, if the interpretation is true, we have a nice example of the decay of the original $\bar{p}p$ excited state down to the ground state via emission of π quanta (Rutherford would be proud!). Oh, for a bubble chamber type technique with 100 times the statistics for the same amount of work!

Conclusion: The evidence is consistent with a state of mass ∿ 970 MeV, $\Gamma \lesssim 80$ MeV ($\lesssim 25$ MeV in $\bar{p}p$ experiment) which decays partially into $\eta^0\pi^\pm$ and partially into $K\bar{K}$. However, to prove this is another matter. It is tempting to associate this state to the $\delta(962)$.

2.2.3 $A_1(1070)$ $I^GJ^P = 1^-1^+$?

$\pi p \to p(3\pi)^-$: My feeling concerning the A_1 is that we still have problems here: What are they?

$A_1(1070)$
• Is A_1 seen in $\pi p \to p(3\pi)$?
- take away A_2
- understand background?
- select "ρ"π
- N* cuts?

Most claims for the A_1 come through study of the reactions

$$\pi^\pm p \to p\underbrace{(\pi^\pm\pi^+\pi^-)^\pm}_{A_1\,?} \quad .$$

Looking through the data, and how the A_1 developed, I was not convinced that it really existed from an experimental point of view. (The trouble is one always has the quark model asking for it in the background.) Figure 22 shows some of the problems[41]. Deduction that something exists in the A_1 region depends on

a) taking away the A_2 -- that is all right, most people agree that the A_2 exists;

b) a true appreciation of the background under the A_1. Here one usually uses Deck type calculations -- none of which (to date) can explain the accumulation of 3π masses in the 1.1 GeV region.

The question is: is this really enough evidence to say the A_1 exists? At 16 GeV/c [41] they need not only an $A_1(1070)$ but also $A_{1.5}(1190)$ to obtain a reasonable fit to the data.

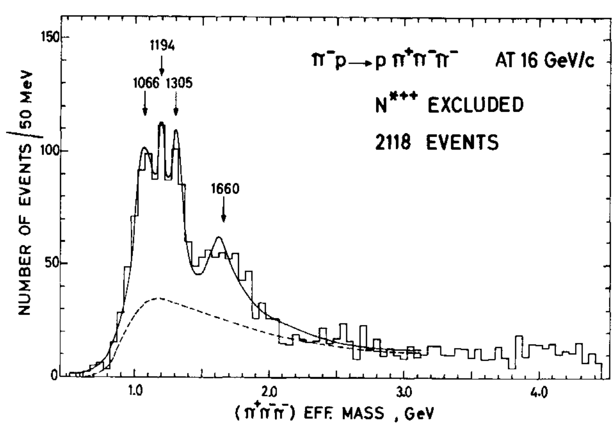

Fig. 22 $\pi^+\pi^-\pi^-$ mass distribution from the reaction $\pi^-p \to p(3\pi)^-$ at 16 GeV/c [41] when events for which the $(p\pi^+)$ system has effective mass in the N^{*++} band have been excluded.

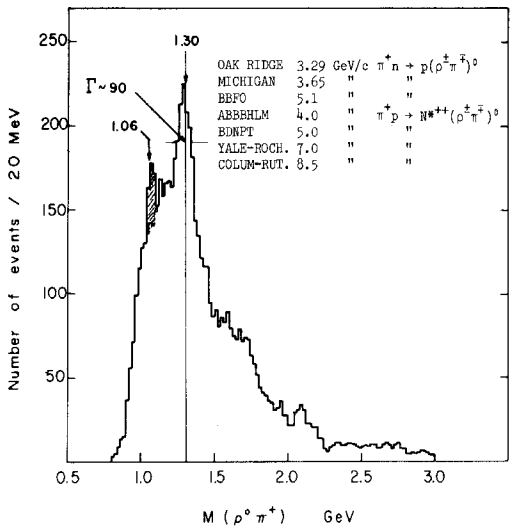

Fig. 23 Compilation of $\rho^0\pi^+$ effective mass spectra.

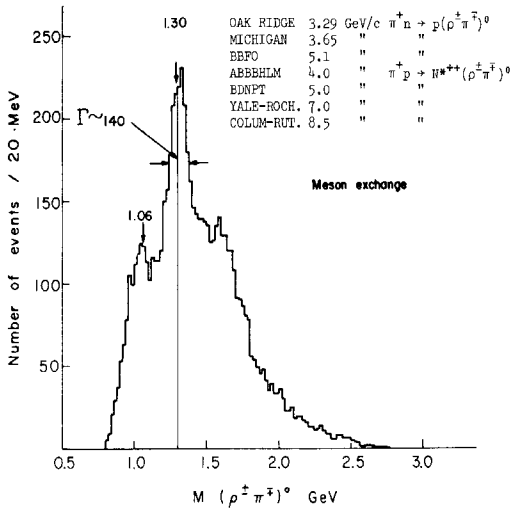

Fig. 25 Compilation of $\rho^\pm\pi$ effective mass spectra.

$\underline{M(\rho^0\pi^\pm)}$: In order to convince ourselves more that the A_1 exists we can add up all the available data -- at least we are not then so subject to fluctuations. (I am aware that this procedure also has its dangers in that interference of an A_1 with background can move the central value around.) Figures 23 and 24 show the $\rho^0\pi^+$ and $\rho^0\pi^-$ "world" mass spectra. The A_2 peak around 1.3 GeV stands out clearly. In the $\rho^0\pi^-$ one does not see much evidence for an $A_1(1070)$ and if we want to be difficult we could say we do not understand the background problem and just make a conventional hand-drawn background curve. [Of course the "in" word at this Conference seems to be "Duality"[42], the fact that we observe a large cross-section for M(3π) in the A_1 mass region being taken as an indication that resonances probably exist in this region.] In the $\rho^0\pi^+$ mass spectrum (Fig. 23) we see more evidence for a peak in the A_1 region, but then why is the $\rho^0\pi^+$ different from $\rho^0\pi^-$? Is there a problem associated with the $N^*(1238)^{++}$?

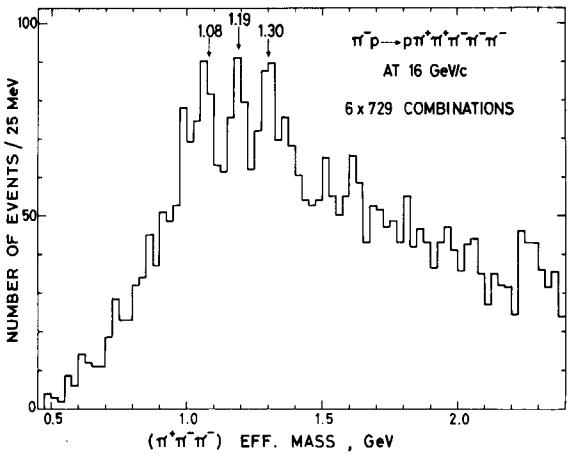

Fig. 26 $\pi^+\pi^-\pi^-$ mass distribution from the reaction $\pi^-p \to p\pi^+\pi^+\pi^-\pi^-\pi^-$ at 16 GeV/c [43].

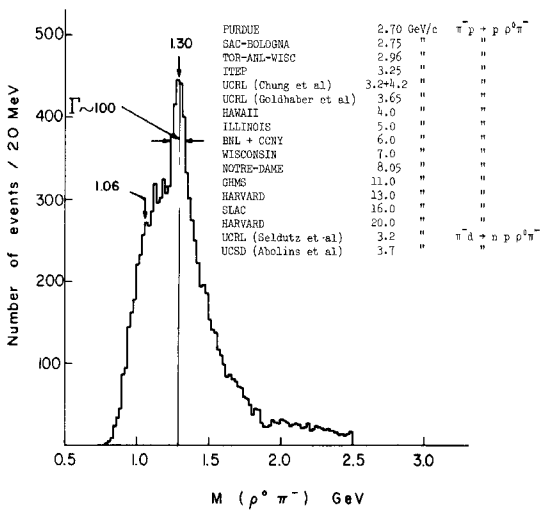

Fig. 24 Compilation of $\rho^0\pi^-$ effective mass spectra.

$\underline{M(\rho^\pm\pi^\mp)^0}$: Having, I feel, not had too much success with the $\rho^0\pi^\pm$ spectra, we can turn to the $(\rho^\pm\pi^\mp)^0$ as shown in Fig. 25. Here meson exchange processes are necessary to produce the A_1 and the problem of diffraction Deck type background should be absent.

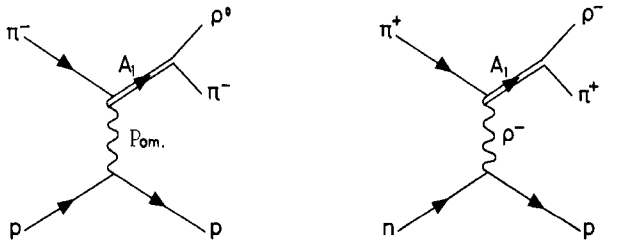

There may be some indication for a small signal at 1.06 GeV in Fig. 25 but it is marginal.

Other reactions: At this Conference, however, we have had two contributions which seem to provide some evidence for A_1 as well as an $A_{1.5}$, this time in reaction channels other than the well-known $\pi p \to p3\pi$. Figure 26 shows the $\pi^+\pi^-\pi^-$ mass spectrum from the reaction $\pi^- p \to p\pi^+\pi^+\pi^-\pi^-\pi^-$ at 16 GeV/c [43]. Three peaks are seen above the background at 1.06,

$A_1(1070)$

So, evidence not compelling in $\pi p \to p(3\pi)$

- What about other channels?
- 16 GeV/c ABBCW

$\pi^- p \to p\, 2\pi^+ 3\pi^-$

→ peaks at (1058 ± 7) MeV 4.5 σ
(1190 ± 8) MeV 2 σ
(1306 ± 7) MeV 3.5 σ

- 5 GeV/c Illinois

$\pi^- p \to p\, 3\pi^-$, $\Delta^2 > 0.1$ 6300 evts.
$p\,\pi^0\,(3\pi)^-$ 6882 evts.
$n\,\pi^+\,(3\pi)^-$ 6212 evts.

→ peaks at 1.06 2.7 σ
1.17 3 σ
1.30 6 σ

1.19, and 1.30 GeV of ∿4.5, 2, and 3.5 standard deviation significance, respectively. At a lower momentum 5.0 GeV/c the Illinois group [44], combining the $\rho^0\pi^-$ mass spectra from the reactions

$$\pi^- p \to p(3\pi)^- \qquad \Delta^2 > 0.1$$
$$\to p\pi^0(3\pi)^-$$
$$\to n\pi^+(3\pi)^-$$

as shown in Fig. 27, find evidence for three peaks at 1.06, 1.17, and 1.30 GeV of ∿2.7, 3, and 6 standard deviations significance, respectively. My feeling about these peaks (see Section 5) is that they may arise from the decay of either

a) higher mass N*'s, for example:

$$\pi^- p \to N^{*0}$$
$$\quad\quad \hookrightarrow N^{*+} A_1^-$$

or

b) higher mass bosons, for example:

$$\pi^- p \to p X^-$$
$$\quad\quad \hookrightarrow A_1^- \pi^+ \pi^-$$
$$\to p X^-$$
$$\quad\quad \hookrightarrow X^0 \pi^- \to (A_1^- \pi^+)\pi^- .$$

If this is the case we may be in a better situation as regards the background to observe peaks in the A_1 region.

Tentative conclusion: It seems to me we have not only the

A_1 M = 1.06 MeV, $\Gamma \simeq 40$ MeV

but also

$A_{1.5}$ M = 1.18 MeV, $\Gamma \simeq 40$ MeV.

Suggestion: more experiments on the higher multiplicity events may be more rewarding than the hard worked $\pi p \to p3\pi$ channel.

2.2.4 $A_2(1300)$ $I^G J^P = 1^- 2^+$

Counters: Passing onto the A_2, the main new result comes from the recent run of the CERN Boson

$A_2(1300)$

- $\pi^- p \to p X^-$

OLD MMS	NEW CBS
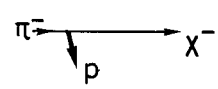	
JACOBIAN PEAK	MIN Δ^2
$0.21 < t < 0.39$	$t = 0.22$ GeV^2
$p_{\pi^-} = 6$ & 7 GeV/c	$p_{\pi^-} = 2.65$ GeV/c
$\Gamma \simeq 16$ MeV	$\Gamma \simeq 10$ MeV

- Splitting confirmed by CBS

Spectrometer (CBS) studying the reaction $\pi^- p \to p X^-$ at 2.65 GeV/c at minimum Δ^2 [45]. The dynamical situation is somewhat different in the CBS set-up from the original MMS:

a) the proton recoils with minimum Δ^2;

b) the error on the missing mass is essentially dependent on the accuracy with which the recoil proton momentum is measured, $\partial M_X/\partial\theta_p \simeq 0$;

c) the incident momentum is near threshold for A_2 production.

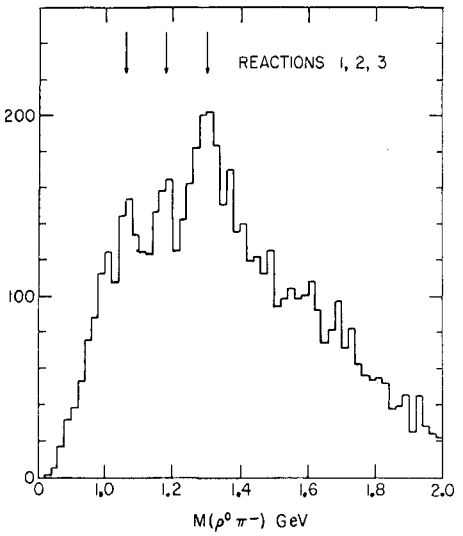

Fig. 27 $\rho^0\pi^-$ mass distribution from the reactions[44]
$\pi^-p \to p(\pi^+\pi^-\pi^-)$ $\Delta^2 > 0.1$ at 5 GeV/c
$\pi^-p \to p\pi^0(\pi^+\pi^-\pi^-)$
$\pi^-p \to n\pi^+(\pi^+\pi^-\pi^-)$

Figure 28 compares the results from the CBS experiment with that of the MMS and the splitting of the A_2 is confirmed. However, they are now able to say that a fit of the data with two incoherent Breit-Wigners can essentially be ruled out [$P(\chi^2) = 0.2\%$]. Either a dipole of the form

$$N \propto \left[\frac{(M - M_0)}{(M-M_0)^2 + \left(\frac{\Gamma}{2}\right)^2}\right]^2$$

or two coherent Breit-Wigner functions give quite acceptable fits as shown in Fig. 29 and the insert.

$A_2(1300)$

		M_1 (MeV) Γ_1	M_2 Γ_2	$P(\chi^2)$ %
2 incoh. B.W.		1278	1318	0.2
		22	21	
2 coh. B.W.	symm.	1289	1309	40
		22	22	
	asymm.	1298	1297	40
		90	12	
Dipole		1298		40
		28		

It is probably worth while to note that the height of the two peaks is similar both in the 6 to 7 GeV/c MMS and the 2.65 GeV/c CBS experiments.

Bubble chambers: Now let us see if the bubble chamber technique can shed any light on the subject.

$A_2(1300)$

- BNL 6 GeV/c $\pi^-p \to p\pi^-M$
  reproduce exp. cond. of CERN-MMS
  $\Gamma \sim 10$ MeV resolution
  2 peaks better fit than 1
  (40% versus 10%)
- $\pi^-p \to K_1^0K_1^0n$, $K_1^0K_1^0M$ - $K_1^0K_1^0$ mass
  similar to upper peak in π^-M
  $M(K_1^0K_1^0) \approx 1311$ MeV $\Gamma \sim 21$ MeV
  not in agreement with the world
  average $\Gamma \sim 120$ MeV. No $K_1^0K^-$ peak?

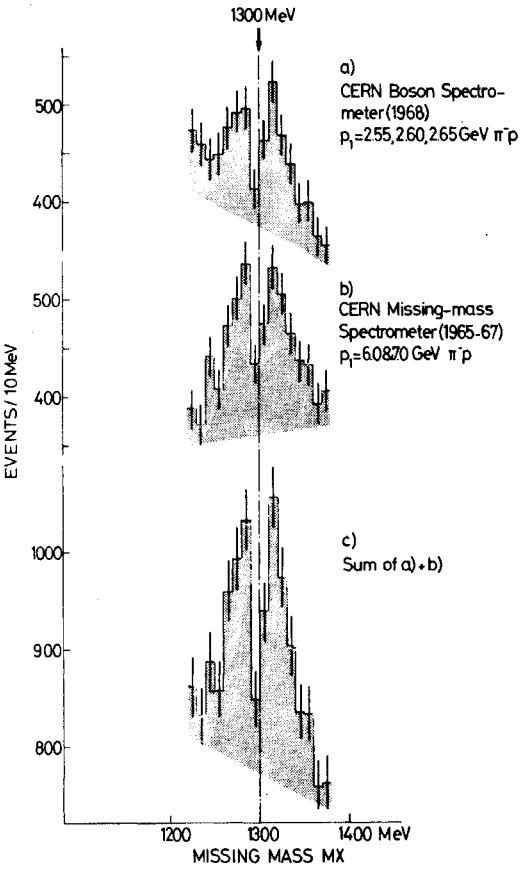

Fig. 28 Compilation of the total A_2 data from the CERN Boson Spectrometer (0° method) 1968, and CERN Missing-Mass Spectrometer (Jacobian peak method) 1965-1967.

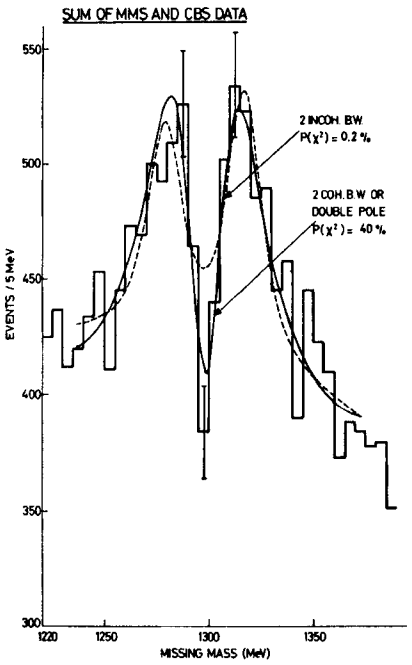

Fig. 29 Fits to the combined MMS and CBS data[45].

A BNL group submitted a paper on the reaction $\pi^- p \to p\pi^- M$ at 6 GeV/c (10,000 events)[46]. Selecting proton momenta in a region corresponding to that of the MMS experiment the $\pi^- M$ mass distribution shown in Fig. 30a is obtained. Their stated resolution is $\Gamma_{exp} \simeq 10$ MeV, full width at half height, so they are in a position to see a dip if it exists (this applies to most bubble chamber work if the same selection on the proton is made). A dip in the A_2 signal exists, but, as they state, the fit with two Breit-Wigner curves is not significantly better than with one Breit-Wigner (40% versus 10%). Their $K_1^0K_1^0$ mass spectrum from the reactions $\pi^- p \to nK_1^0K_1^0$ and $K_1^0K_1^0M$ (Fig. 30b) shows a peak centred at 1311 MeV and coincident with the upper peak in the $\pi^- M$ mass distribution and has a width of $\Gamma \sim 21$ MeV. No peak is seen in the $K^\pm K_1^0$ mass spectrum (Fig. 30c). Before one draws the obvious conclusion that two resonant states exist, one of which decays to $K\bar{K}$, perhaps we should be aware of what the "world" $K_1^0K_1^0$ and $K_1^0K^\pm$ mass spectra look like. These are shown in Figs. 31 and 32 where it is clear that not only a signal in the A_2 region exists in the $K_1^0K_1^0$ spectrum but also in the $K^\pm K_1^0$ spectrum*). Both

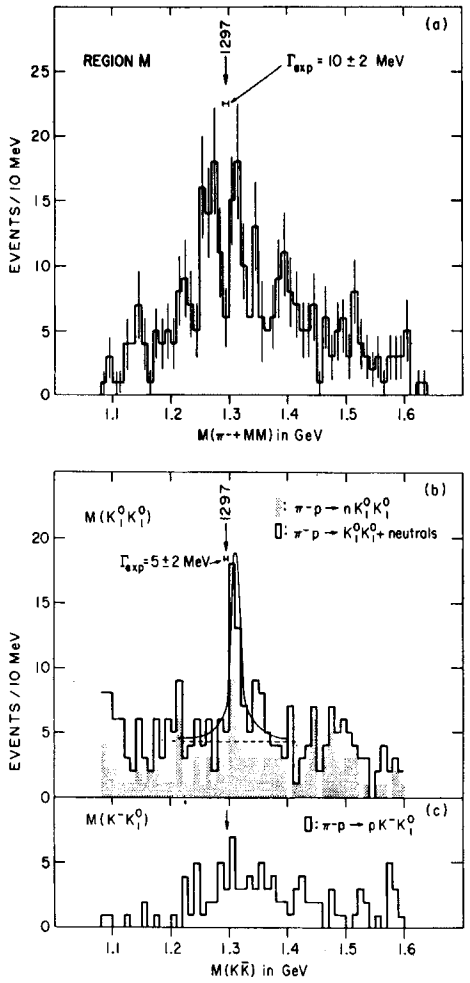

Fig. 30 a) Effective mass distributions of X^- from the reaction $\pi^- p \to pX^-$ at 6 GeV/c [46], the recoil proton being selected in a similar way to the MMS experiment. b) Effective mass distribution of $K_1^0K_1^0$ from the reaction $\pi^- p \to nK_1^0K_1^0$ and $K_1^0K_1^0$ + neutrals. c) Effective mass distribution of $K_1^0K^-$ from the reaction $\pi^- p \to pK_1^0K^-$.

peaks seem to be situated 20 MeV higher in mass (viz. 1320 MeV) than the $\rho^0\pi^\pm$ peaks as has been known for some time. The widths of the $K\bar{K}$ peaks are $\sim$ 100 MeV

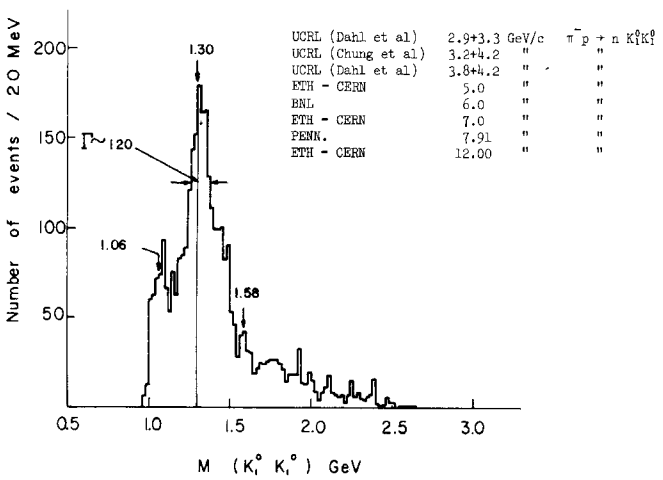

Fig. 31 Compilation of $K_1^0K_1^0$ effective mass spectra.

*) The small signal at 1.58 GeV, $\Gamma \sim 40$ MeV, in the world $K_1^0K^\pm$ mass spectrum of Fig. 32 ($\sim 3\sigma$) and repeated in the $K_1^0K_1^0$ spectrum demonstrates, if substantiated in future data, the usefulness of presenting bubble chamber data in a compilable form.

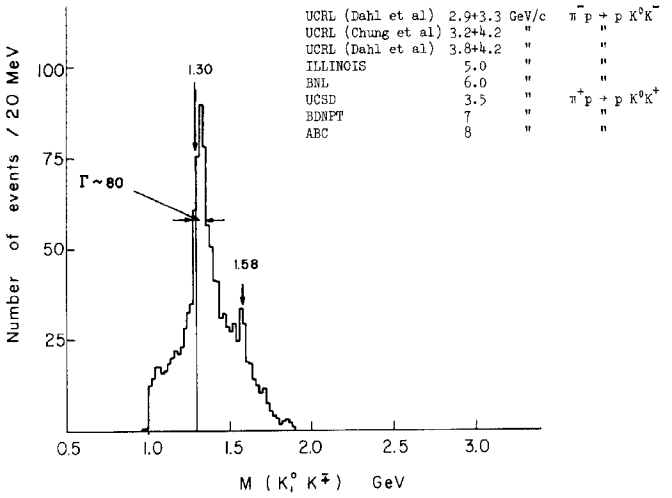

Fig. 32 Compilation of $K^0_1K^\pm$ effective mass spectra.

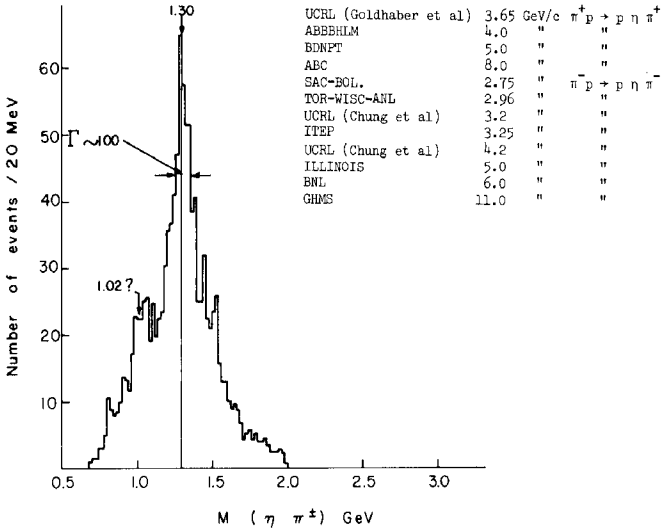

Fig. 33 Compilation of $\eta^0\pi^\pm$ effective spectra.

and so considerably wider than the $K^0_1K^0_1$ peak of the BNL group. Although some of this 100 MeV width could be due to adding different experiments, a factor of 4 would seem rather too large to accommodate.

To complete the picture, Fig. 33 shows the "world" $\eta^0\pi^\pm$ mass spectrum from $\pi^\pm p \to p\eta^0\pi^\pm$. The mass and width of the $A_2 \to \eta^0\pi^\pm$ seem to agree with the $\rho^0\pi^\pm$ spectra (is there also an enhancement around 1.02 GeV?).

$A_2(1300)$

Conclusions:

- Split of $A_2 \to (\text{neutrals})^-$ O.K.
- Coherent B.W. or dipole necessary for fit.
- Apparent shift in $K\bar{K}$ mass relative to $\rho\pi$, but $\rho\pi$ must be better understood.
- $\rho\pi$ Dalitz plot favours $J^P = 2^+$.
- $\eta\pi$ seems broad and centred at 1.30 GeV.

Wanted - 1 MMS with decay products measurable.

Finally, two other observations bearing on the split A_2 problem:

a) Two papers studying $\pi^+p \to p(3\pi)^\pm$ at 8 GeV/c and 4 GeV/c [47] have looked at the $(3\pi)^\pm$ mass when the recoil proton has momentum in the region 0.5 to 0.8 GeV/c, i.e. similar to the MMS experiment. The sum of the data, shown in Fig. 34, shows a narrow peak $\Gamma \sim 20$ MeV ($\Gamma_{\text{resolution}} \sim 10$ MeV) centred at 1298 MeV (the dip in the split A_2!) of about 4σ significance. Can this be a clue to the splitting of the A_2? We should remember that the MMS, CBS, and BNL work looks at final states involving unseen neutrals and therefore could have different properties to the $\pi p \to p3\pi$ channel.

b) In the reaction $\bar{p}p \to K^0_1K^\pm\pi^\mp$ (1563 events) at 0.70 GeV/c [48] the $K^0_1K^\pm$ mass spectrum, after $K\pi$ mass combinations < 0.95 GeV have been removed, i.e. the K*'s, is shown in Fig. 35. A splitting of the A_2 region compatible with the BNL $\rho\pi$ splitting (not

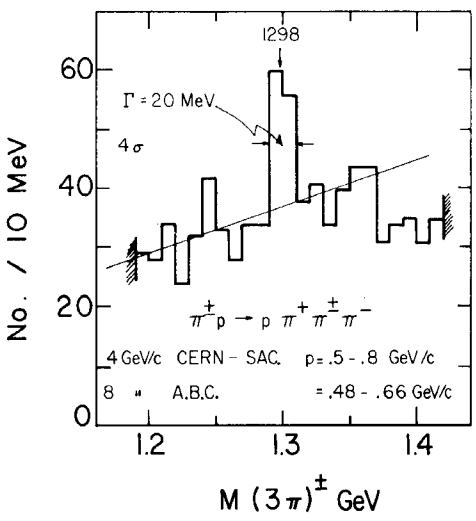

Fig. 34 $\pi^+\pi^\pm\pi^-$ mass distribution from the reaction $\pi^-p \to p\pi^+\pi^-\pi^-$ at 4 and $\pi^+p \to p\pi^+\pi^+\pi^-$ at 8 GeV/c where the recoil proton is selected to have a momentum in the region 0.5-0.8 GeV/c and 0.48-0.66 GeV/c, respectively.

$K_1^0K_1^0$) and the CBS + MMS data is evident. They quote

$$M_L = (1274 \pm 16)\ \text{MeV}, \quad \Gamma_L = (29 \pm 10)\ \text{MeV}$$

$$M_H = (1320 \pm 16)\ \text{MeV}, \quad \Gamma_H = (35 \pm 10)\ \text{MeV}\ .$$

The interplay of the missing-mass counter technique and the bubble chamber technique is nicely demonstrated by the A_2 problem. Much more data is needed, and maybe here we are entering the fine structure side of meson spectroscopy.

Conclusions:

a) The $A_2 \to (\text{neutrals})^-$ is split and requires two coherent Breit-Wigners or a dipole for a good fit.

b) "World" $K^0K^\pm$ peaks $\sim$ 20 MeV higher in mass than $\rho\pi^\pm$ and $\eta^0\pi^\pm$.

c) BNL $K_1^0K_1^0$ peak narrower than world $K_1^0K_1^0$ -- central values agree and are similar to "world" $K^0K^\pm$.

d) Narrow peak in $\rho^0\pi^\pm$, under missing-mass proton selection, falls where dip of MMS-CBS occurs -- must be verified as only two experiments.

e) compilation of cross-sections [41], shown in Fig. 36, suggests that $\sigma(A_2 \to K^0K^\pm)$ fall off faster with momentum than $\sigma(A_2 \to \rho^0\pi^\pm$ or $\eta^0\pi^\pm)$. However, the $K^0K^\pm$ data rely heavily on the 16 GeV/c point, and some slight modification to $\sigma(A_2 \to \rho\pi)$ may be necessary if we make a hand-drawn background curve instead of Deck type. More data is needed.

2.2.5 $F_1(1560)$

To finish the non-strange bosons below 1600 MeV we have a new object submitted for scrutiny. The effect concerns a bump of > 4σ observed in the $K\bar{K}\pi$ spectra from the reactions[49] at 0.7 GeV/c

$\bar{p}p \to K_1^0\pi^+\pi^-(K^0)$	1305 events
$\to K_1^0K_1^0\pi^+\pi^-$	484 events
$\to K_1^0K^\pm\pi\ \pi^0$	2114 events .

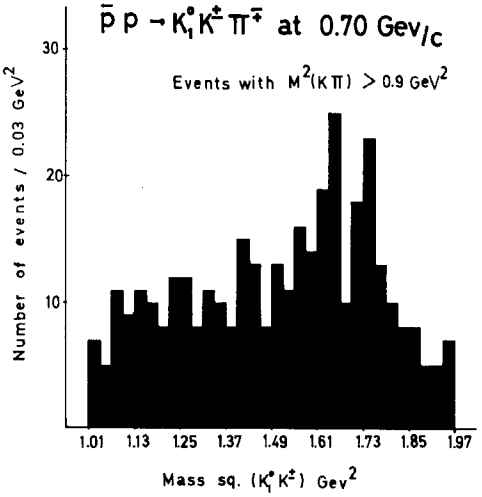

Fig. 35 $K_1^0K^\pm$ mass spectrum from the reaction $\bar{p}p \to K_1^0K^\pm\pi$ at 0.7 GeV/c [48] after removal of events with $M^2(K\pi) < 0.9$ GeV^2.

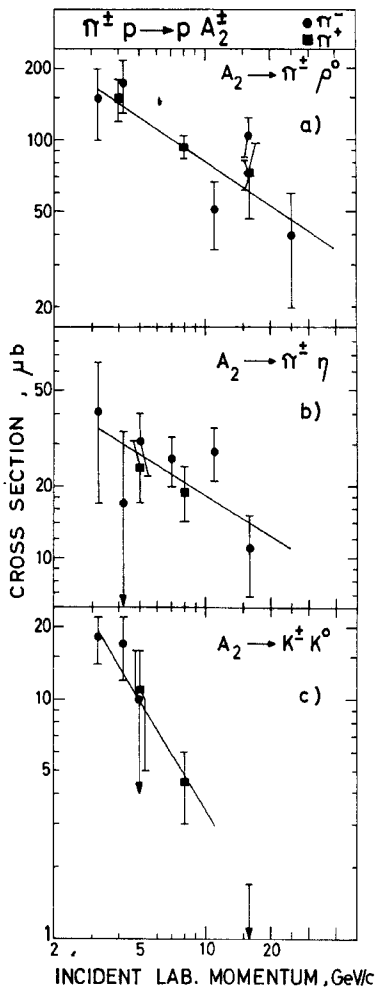

Fig. 36 Variation of the $A_2 \to \rho^0\pi^\pm$, $\eta^0\pi^\pm$, $K_1^0K^\pm$ cross-sections with primary momentum[41].

$F_1(1560)$

- NEW $K\bar{K}\pi$ peak observed in $\bar{p}p \to K\bar{K}\pi\pi$ at 0.7 GeV/c.
  Signal > 4σ in $K_1^0K_2^0\pi^\pm$.
  Decay rates $F_1 \to K_1^0K_2^0\pi^\pm$ / $K_1^0K^\pm\pi^0$ / $K_1^0K_1^0\pi^\pm$ compatible with > 80% of $F_1 \to K^*K$.
- Properties
  M $\sim$ 1560 MeV, Γ $\sim$ 70 MeV.
  I = 1, Decay $F_1 \to K\bar{K}\pi$ (mostly K^*K).

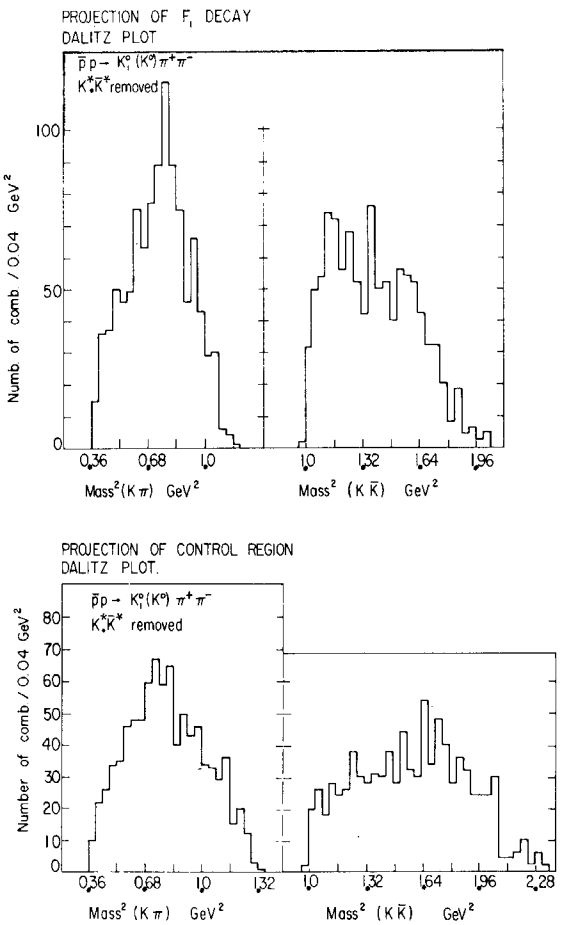

Fig. 37 a) Projections of the $F_1 \to KK\pi$ decay Dalitz plot where F_1 region is defined by $2.32 < M^2(F_1 \to K\bar{K}\pi) < 2.56$ GeV^2. b) Projection of central region Dalitz plot where $2.64 < M^2(KK\pi) < 2.88$ GeV^2 [49].

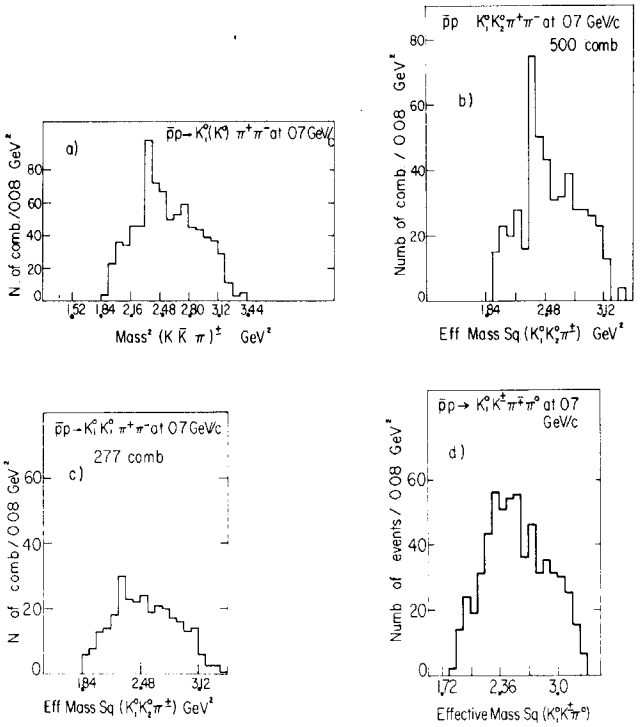

Fig. 38 $K\bar{K}\pi$ effective mass squared distributions from the reactions $\bar{p}p \to K\bar{K}\pi\pi$ at 0.7 GeV/c after selecting that the $K\pi$ or $\bar{K}\pi$ mass lies in the K* region viz. $0.735 < M^2(K\pi) < 0.845$ GeV^2.

Evidence for K* production can be seen in Fig. 37. Figure 38c shows a respectable signal in the $K^0_1K^0_2\pi^\pm$ mass spectrum. Evidence for a K*K decay are shown in Fig. 38, which shows the $K\bar{K}\pi$ mass spectra when K* is selected. The main observations are set out in the insert. No obvious place in the quark excitation model exists for this state unless it is a radially excited state.

2.2.6 Exotic states

No evidence for resonant states in either S = 2, I = 2, or I = 3/2 systems has been reported either during the past year or at this Conference.

2.3 I = 1/2 (K*'s) < 1600 MeV

2.3.1 Kπ(1100)?

A UCLA group presented a paper[50] suggesting the existence of a broad Kπ resonance (I = 1/2, $J^P = 0^+$) of mass ∿ 1100 MeV. This would then correspond nicely to the broad ππ resonance ϵ^0 from the $^3P_0$ octet of the quark model. The first piece of evidence comes from studying the variation of the m=0 spherical harmonic moments of the outgoing K as a function of Kπ mass at the Kπ vertex. These are shown in Fig. 39; the essential feature is that Y^0_1 goes to zero in the region of 0.95 GeV where one expects the P-wave phase shift due to the K*(890) to be $\delta_p \sim 150°$. The authors argue, therefore, that the S-wave phase shift must be $\delta_S^{1/2} \sim 60°$. Then, since Y^0_1 increases after 1.0 GeV, whereas δ_p is decreasing, the δ_s must be increasing and reaches 90° in the region 1.1 - 1.2 GeV of the Kπ mass. The second piece of

K*(1100)

- Reaction: $K^+p \to p\pi^+(K\pi)^0$

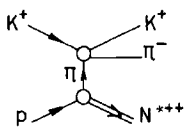

- Variation of Kπ scattering angle as f[M(Kπ)] suggest $\delta_s \sim 90°$ at 1.1 GeV.
- Variation of σ_s versus M(Kπ) suggests broad Kπ resonance at 1.1 GeV $J^P = 0^+$, I = 1/2.

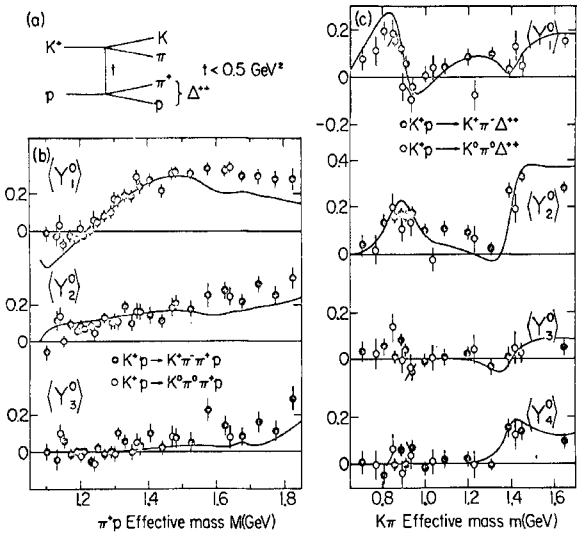

Fig. 39 a) One-pion exchange diagram for the reaction $K^+p \to (p\pi^+)(K\pi)^0$. b) Spherical harmonic moments of the π^+p angular distribution. c) Spherical harmonic moments of the $K\pi$ angular distribution[50].

evidence is obtained when they fit to their K^-p experimental data at 7.3 GeV/c the O.P.E. model with Dürr-Pilkuhn off the mass shell factors to extract the S-wave $K\pi$ cross-section (σ_S). The variation of σ_S, shown in Fig. 40b, reaches the S-wave unitary limit around 1.1 GeV. The success with which this model fits the data can be seen from the full line curves of Figs. 40a and c-g.

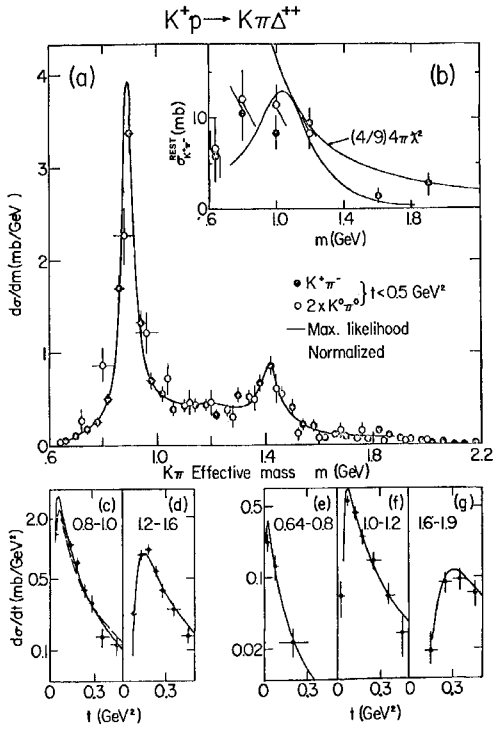

Fig. 40 a) OPE fit to experimental data. b) Variation of the S-wave $K\pi$ cross-section with mass of the $K\pi$ system. c-g) Fits to the $d\sigma/dt$ distributions for various intervals of $K\pi$ mass[50].

Thus the evidence for a broad S-wave $K\pi$ resonance in the 1.1 GeV region seems strongly suggested by the data; hopefully more statistics at different K^-p momenta will support this conclusion.

2.3.2 K's in the Q region*

$K^\pm p \to p(K\pi\pi)^\pm$: The problem of the K*'s in what has become known as the Q-region, $1.1 < M(K\pi\pi) < 1.4$ GeV, is demonstrated in Figs. 41, 42, and 43, which are "world" compilations of $K^*\pi$ from the reaction $K^\pm p \to p(K^*\pi)^\pm$. The situation is reminiscent of the A_1, as one might expect, since the production

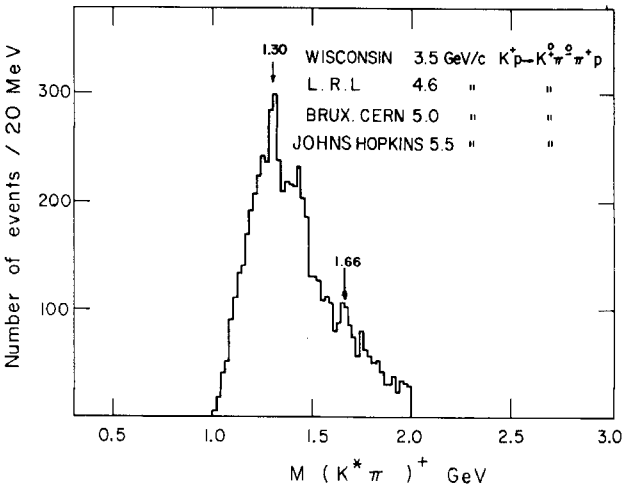

Fig. 41 Compilation of $(K^*\pi)^+$ effective mass spectra from K^+p reactions < 6 GeV/c.

K*(1230, 1320)

- Difficulties of the Q-region:

  $K^\pm p \to p(K\pi\pi)^\pm$
  - Deck type background? (cf. A_1)
  - Possibility two 1^+ interfering resonances
  - Presence of K*(1400)

- $\bar{p}p \to K\bar{K}\pi\pi \to C\pi$, necessary for fit
  $K^*\pi$ $K\rho$
  - problem of possible 1320 MeV state C'

    $M(C) = (1242 \pm 10)$ MeV,

    $\Gamma = (127 \,^{+\,7}_{-\,25})$ MeV

    $J^P = 1^+$ favoured

- $K^+p \to p(K\pi\pi)^+$ at 9 and 10 GeV/c

  4σ peak in $K^*\pi$ at 1250 MeV

  $\Gamma \simeq 40$ MeV

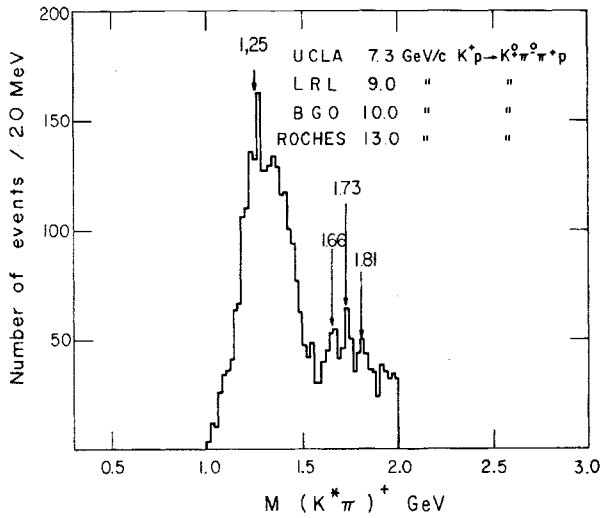

Fig. 42 Compilation of $(K^*\pi)^+$ effective mass spectra from K^+p reactions > 6 GeV/c.

mechanism appears again to be of the diffraction type with the associated background problems. However, in the $K\pi\pi$ case we have the additional complication that the two K^*'s of $J^P = 1^+$ expected in this mass region from the quark model may interfere not only with the background but also between themselves. No obvious peak exists in these compilations [the best at 1.30 GeV disagrees with present values[1]] although with all the possible interference phenomena, addition of different momenta may wash out any possible existing effect, should it exist. On the other hand, it is not obvious that we have at our disposal sufficient statistics at any one momentum to establish a peak unambiguously; this is demonstrated in Fig. 44 where the data at 5.0 GeV/c [51] are compared to those at 5.5 GeV/c [52]. The correspondence of the various peaks is remarkably poor and to say that interference effects can change the character of a distribution so drastically over such a narrow momentum interval is pushing things rather hard. All these problems are probably the reason

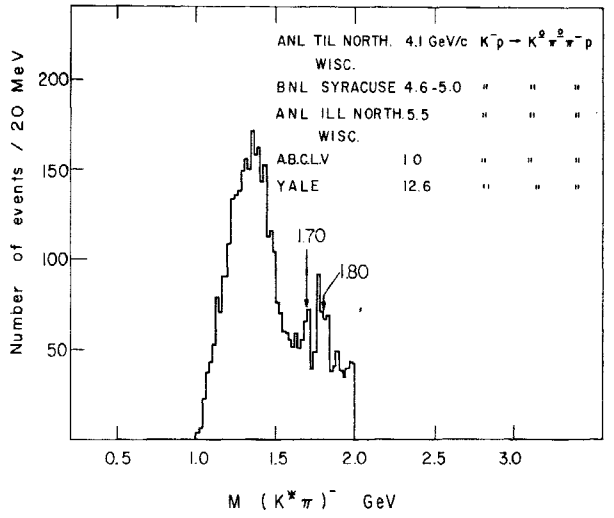

Fig. 43 Compilation of $(K^*\pi)^-$ effective mass spectra from K^-p reactions of all momenta.

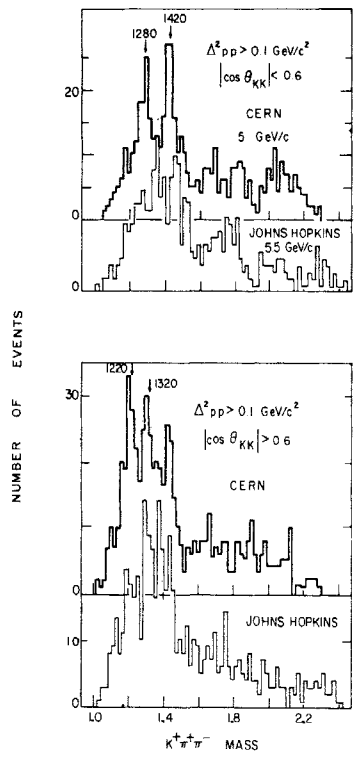

Fig. 44 Comparison of the $K^+\pi^+\pi^-$ mass spectra from the reaction $K^+p \to p(K^+\pi^+\pi^-)$ at 5 and 5.5 GeV/c.

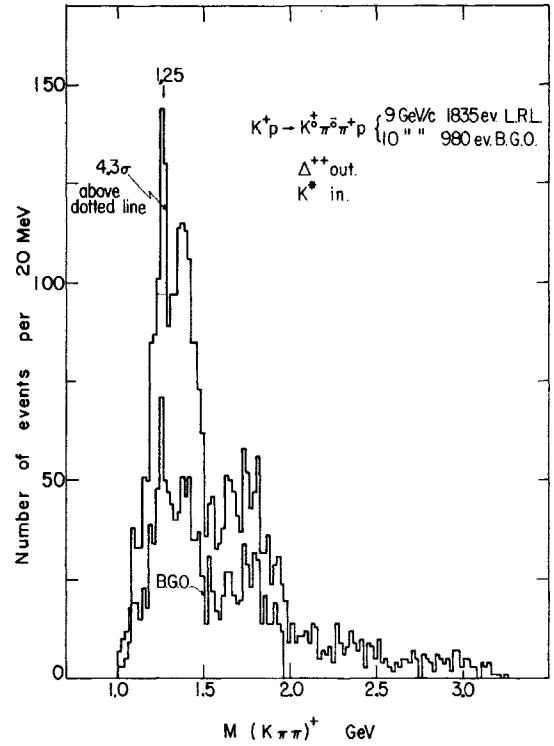

Fig. 45 Sum of the $(K\pi\pi)^+$ mass spectra from the reactions $K^+p \to pK^-\pi^+\pi^+$ at 9 and 10 GeV/c [53,54].

why most groups have a tendency to call this region the "Q-region" nowadays and, although one cannot help feeling that there is structure in this region, I think it is difficult to state of what this structure consists. Maybe, as with the A_1, we should try the higher multiplicity events. However, after this rather pessimistic note let us look at the data at 9 GeV/c [53] and 10 GeV/c [54] presented to the Conference which show Kππ mass spectra with similar structure; when they are added, see Fig. 45, a > 4σ peak appears around 1250 MeV with a rather narrow width ($\Gamma \sim 40$ MeV). If we accept this peak then we have to accept another at a higher mass ∿ 1370 MeV which is in disagreement with a state at a mass ∿ 1320 MeV proposed in the literature in the past[1].

$\bar{p}p \to K\bar{K}\pi\pi$: Evidence for a structure in the Kππ system at ∿ 1240 MeV and known as the C meson has been known for some time. At this Conference more up to date results have been presented[55] on the reactions

$$\left.\begin{array}{ll} \bar{p}p \to K_1^0 K_1^0 \pi^+\pi^- & 1143 \text{ events} \\ K_1^0 K^{\pm}\pi^{\mp}\pi^0 & 3308 \text{ events} \\ K_1^0 K_2^0 \pi^+\pi^- & 1608 \text{ events} \end{array}\right\} \bar{p}\text{'s at rest}$$

In order to fit their experimental Kππ mass distributions they find they need a state of mass ∿ 1242 MeV and width 127 MeV. The fits to the data with this hypothesis are shown in Fig. 46. A J^P assignment of 1^+ is favoured over other possible assignments and the introduction of another Kππ resonance at 1320 MeV does not improve the fits. As one can see, the width of the Kππ state proposed here does not agree with that just mentioned above found in K^+p interactions.

2.3.3 Kπ(1260)?

Kπ(1260)?

- NEW - compilation of Kπ in:
  $K^+p \to K^0\pi^+p$ at 3 and 3.5 GeV/c.
- Peak at M = (1260 ± 30) MeV, $\Gamma \sim 75$ MeV
  $J^P = 0^+, 1^- \ldots$
  $\sigma \sim (70 \pm 25)\mu b$.
- The Kπ ≠ C if $J^P(C) = 1^+$.

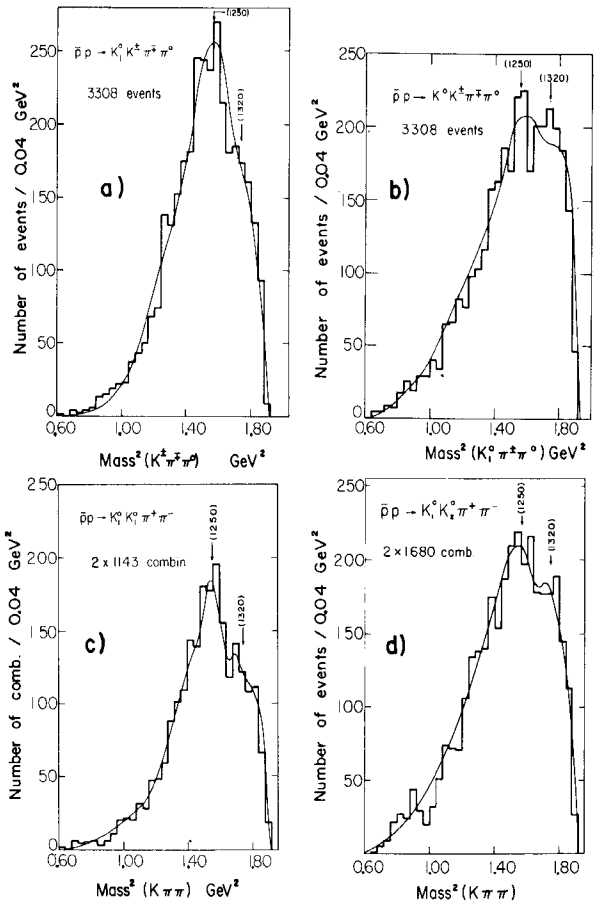

Fig. 46 Recent data relevant to the C meson[55]. Kππ mass squared spectra from the reactions $\bar{p}p \to K\bar{K}\pi\pi$ at rest.

A compilation[56] of data from the reaction $K^+p \to K^0\pi^+p$ at 3 and 3.5 GeV/c has provided evidence for a new Kπ resonance with a mass M = 1260 MeV. The bump in the region of 1260 MeV in the Kπ mass spectrum, as can be seen from Fig. 47, is a five standard deviation effect and therefore cannot be dismissed lightly. Its observation in the Kπ mode limits its J^P to the series $0^+, 1^-, \ldots$

One also notices, in passing, an enhancement around 1.1 GeV which may be associated to the Kπ(1100) proposed in Section 2.3.1.

2.3.4 Some comments and impressions on the bosons < 1600 MeV

a) The finding of states to satisfy the L = 0 and L = 1 octets has not met with amazing success since the Berkeley Conference two years ago.

b) Two I = 0 states are missing in the $^1P_1$ nonet, one I = 0 state in the $^3P_1$ nonet.

c) The situation concerning the existence of the A_1 has not really improved either, since if we take

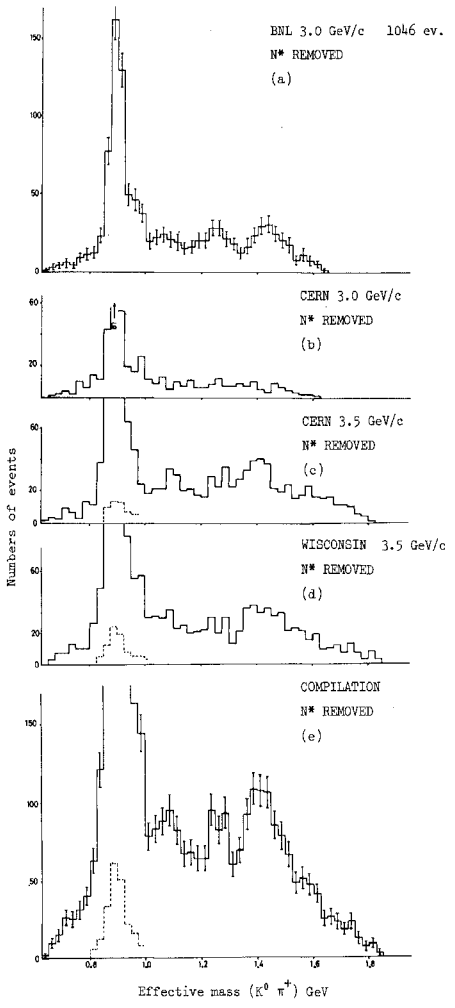

Fig. 47 Compilation of $K^0\pi^+$ effective mass spectra[56] from the reaction $K^+p \to pK^0\pi^+$ at 3 and 3.5 GeV/c.

the A_1 we have to take the $A_{1,5}$ for which no niche exists in the simple quark model (except perhaps in the new ideas of Gell-Mann and Zweig presented at this Conference).

d) The $J^P = 1^+$ K*'s, expected on the quark model, are also difficult states to establish from an experimenter's point of view.

e) No place exists either for the E^0, $F_1(1560)$, or the K*(1260), although maybe these could be radially excited states.

f) The A_2 splitting seems with us. No convincing evidence for the splitting of the other members of this nonet has yet appeared. Is a time-of-flight neutron counter experiment possible on the f^0, $\pi^- p \to nf^0; (f^0 \to \pi^+\pi^-)$ to detect any f^0 splitting? The neutron picked up in the forward direction has $\partial M_{f^0}/\partial\theta_{neutron} = 0$. The splitting of the K*(1400) would probably be more difficult without an intense K beam and a long-burst radio-frequency separator.

3. MESONS (1.6 GeV < MASS < 1.88 GeV) - "R" REGION

We now turn our attention to what has become known as the R-region, that is the mass region between 1.6 and 1.88 GeV ($\simeq 2\, M_{nucleon}$). We first discuss the S = 0 bosons then the S = -1.

3.1 S = 0, I = 0,1

R-region (MMS)

	M(MeV)	Γ(MeV)
R_1	1630 ± 15	≤ 21
R_2	1700 ± 15	≤ 30
R_3	1748 ± 15	< 38
R_4?	∿1830	-

The insert shows the charged states found by the CERN-MMS group[57]. Much steady work with the bubble chamber technique since the Berkeley Conference has gradually shown how complex this region really is. This could be predicted from the quark model where, as can be seen in Table 7 and Fig. 5, the L = 2 $q\bar{q}$

TABLE 7

L	S	$^{2S+1}L_J$	C	J^P	I^G	Octet	Singlet
2	0	$^1D_2$	+	2^-	0^+ 1/2 1^-		π(1640)?
	1	$^3D_1$	-	1^-	0^- 1/2 1^+		g(1650)? ≡ R_1?
	1	$^3D_2$	-	2^-	0^- 1/2 1^+	K_L(1790)?	ρ(1700)? ≡ R_2?
	1	$^3D_3$	-	3^-	0^- 1/2 1^+		R_3(1750)?

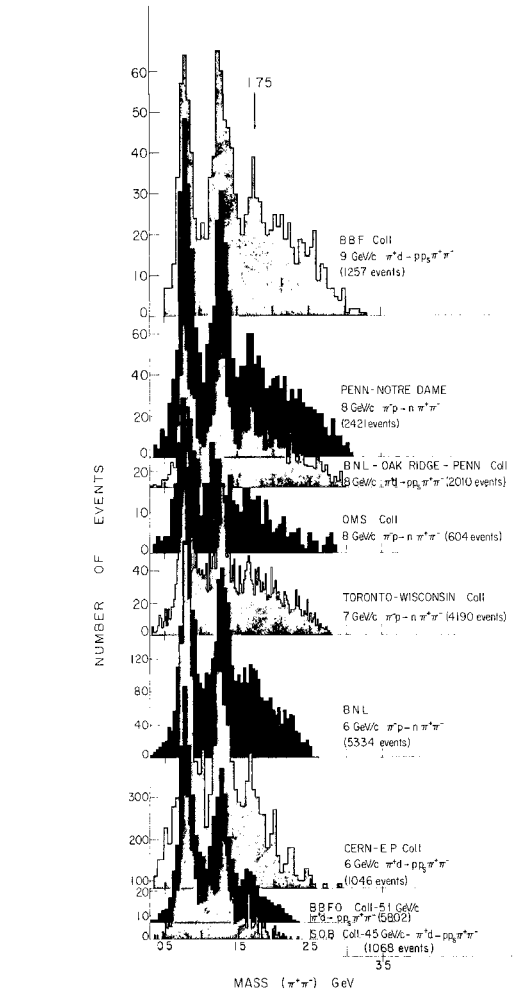

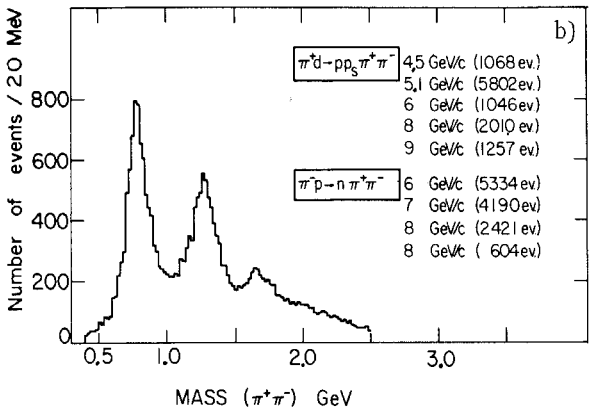

Fig. 48 a) and b) Compilation of $\pi^+\pi^-$ mass spectra.

system predicts eight I = 0 states and four I = 1 states in this mass region if the Regge trajectories all have similar slopes of $dJ/dM^2 \sim 1$ GeV^{-2}.

Taking the point of view that bumps in different mass combinations have to be considered as separate states until they are shown to be the same, one can construct a list of states which are indicated by the present experimental data. Other more dubious peaks will be mentioned at the end, more because of their interest than their statistical significance.

R-region (Bubble chamber)

	M(MeV)	Γ(MeV)	I^G	J^P
$g^{\pm} \to \pi^0\pi^{\pm}$	1640 ± 20	120 ± 30	1^+	3^-?
$g^0 \to \pi^+\pi^-$	1680 ± 15	200 ± 50	$?^+$	-
$A_3^{\pm} \to (3\pi)^{\pm}$	1648 ± 10	100 ± 20	1^-	$A(2^-?)$
$A_3^0 \to (3\pi)^0$	1651 ± 10	130 ± 20	0^-?	A?
$\rho^{\pm} \to (4\pi)^{\pm}$	1700 ± 15	120 ± 30	1^+	N?
$R_\omega \to \omega^0\pi^+\pi^-$	1670 ± 15	50 ± 15	$?^-$	-
• other emerging states?				
$\pi(1840)^-$	∿1840	∿	$?^-$	-
$\rho(1840)^0$	∿1840	∿	$?^+$	-
$\rho(1630)^- \to \omega^0\pi^-$	∿1630	∿60	$?^-$	-

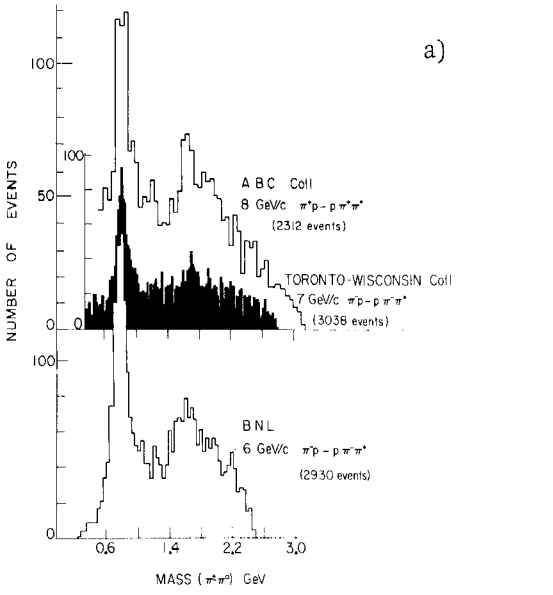

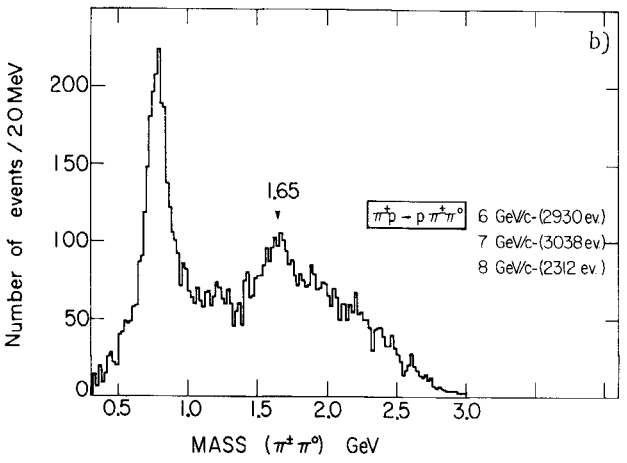

Fig. 49 a) and b) Compilation of $\pi^{\pm}\pi^0$ mass spectra.

3.1.1 $\rho_N \to 2\pi$, *alias g meson*

Compilations of the $\pi^+\pi^-$ and $\pi^\pm\pi^0$ mass spectra[58-66] observed in the reactions $\pi^- p \to n\pi^+\pi^-$ and $\pi^\pm p \to p\pi^\pm\pi^0$, respectively, are shown in Figs. 48 and 49. Fits to the summed data of Figs. 48b and 49b give widths which are very much dependent on how one estimates the background, especially true for the $\pi^+\pi^-$ due to the nearby f^0. The values of the masses and widths given in the insert are best values estimated from the fits we have made*) and those of Ferbel[67]. The higher mass of the g^0, although not significant, together with its larger width compared to the $g^\pm$ has led to the speculation that there may be an I = 0 state in the $\pi^+\pi^-$ system around 1750 MeV.

The BNL group[61] in an attempt to determine the spin of the g have calculated the Legendre polynomial coefficients, A_n, from a fit to the $\pi^+\pi^-$ and $\pi^-\pi^0$ decay angular distributions. The peaks in A_2, A_4, and A_6 in the g^- mass region, shown in Fig. 50, are interpreted in favour of a $J^P = 3^-$ assignment for the g. The same group also presented evidence, shown in Fig. 51, for a $K_1^0K^\pm$ enhancement at a mass of $\sim$ 1640 MeV (which could be a new decay mode of the g^-). No corresponding peak is seen in the $K_1^0K_1^0$ mass spectrum, which suggests G = +1, P = -1 for the $K_1^0K^\pm$ state. Thus possible quantum numbers for this state are $I^GJ^P = 1^+3^-$. If the g^- does have $J^P = 3^-$ and also corresponds to the R_1 peak seen in the MMS experiment, an elegant interpretation of the mass of the R peaks in terms of spin-orbit splitting[57] is lost since, as shown in the insert, the $J^P = 3^-$ state is expected to have the highest mass.

SPIN-ORBIT SPLITTING FOR L = 2				
$^{2S+1}L_J$	$^3D_1$	$^3D_2$	$^1D_2$	$^3D_3$
ΔM^2	$\propto -3$	-1	0	$+2$

3.1.2 $\rho(1700)^{0}_{\pm} \to (4\pi)^{0}_{\pm}$

The compiled evidence[3,62,68-70] for the charged state is shown in Figs. 52a and b, the reaction concerned being $\pi^\pm p \to p\pi^\pm\pi^+\pi^-\pi^0$. The shape of the peak in Fig. 52b does not look too good (maybe there are two nearby states here, R_2 and R_3 for example?) but the enhancement is clear. An important question is whether this peak is another decay mode of the g^-

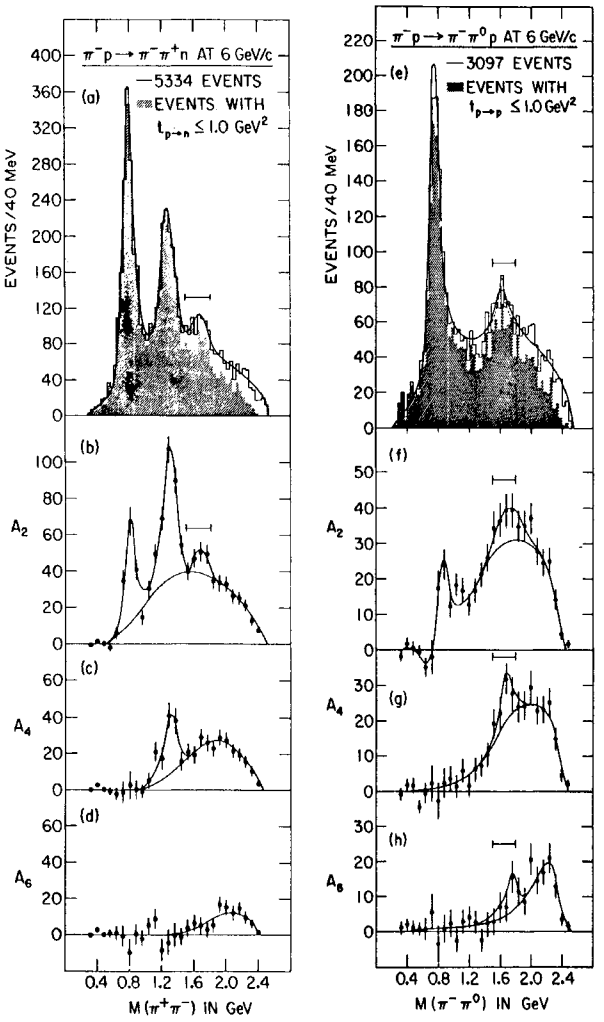

Fig. 50 a), e) $\pi^+\pi^-$ and $\pi^-\pi^0$ mass spectra from the reaction $\pi^- p \to n\pi^+\pi^-$ and $p\pi^-\pi^0$ at 6 GeV/c [61]. b-d), f-h) Legendre coefficients from a fit to the $\pi\pi$ scattering angular distribution.

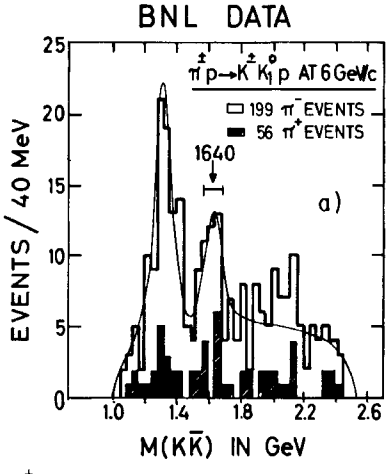

Fig. 51 $K^0K^\pm$ effective mass distribution from the reaction $\pi^\pm p \to K^\pm K_1^0 p$ at 6 GeV/c [61].

*) I thank Dr. E. Quercigh for his collaboration in fitting the summed distributions with various background curves.

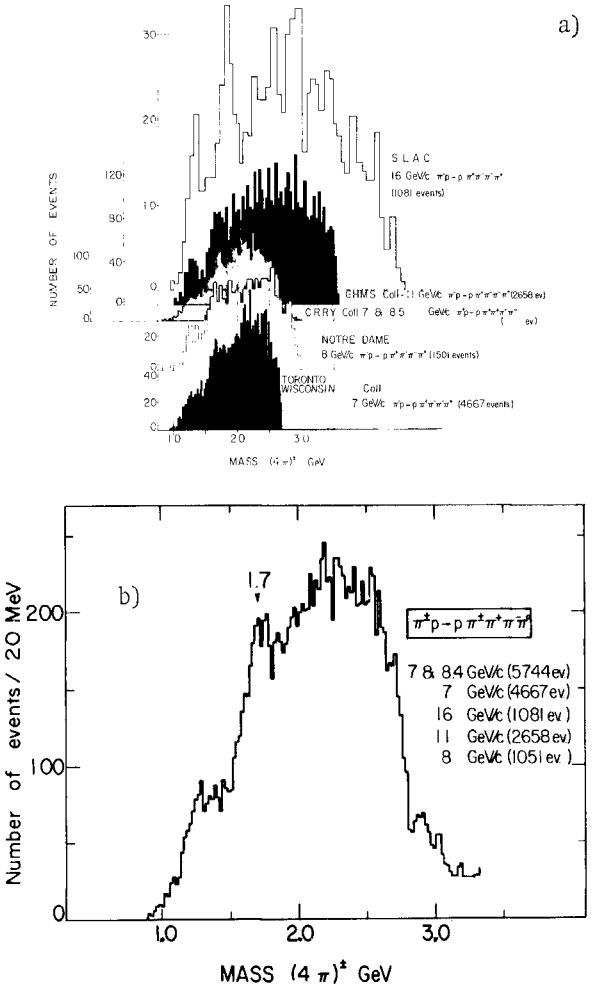

Fig. 52 a) and b) Compilation of $(4\pi)^{\pm}$ mass spectra.

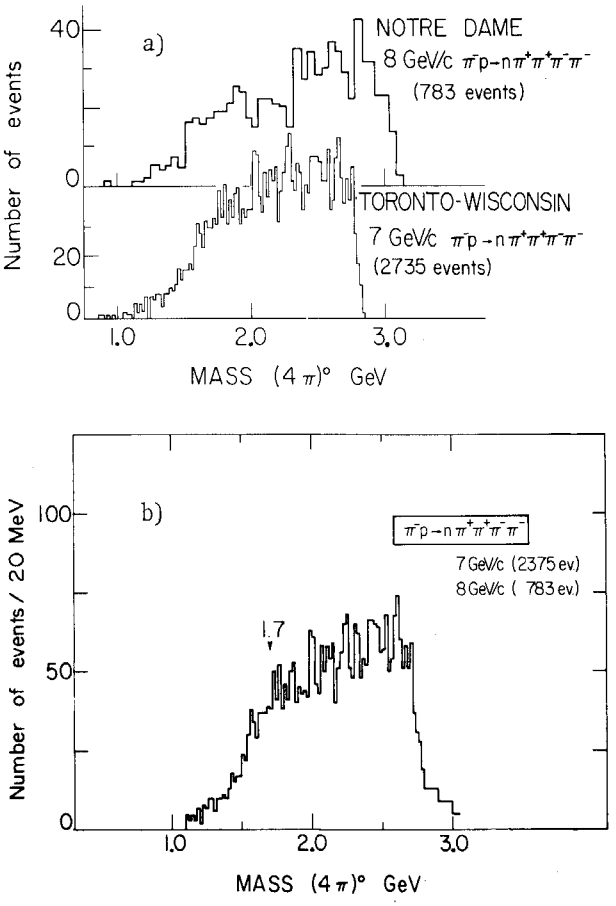

Fig. 53 a) and b) Compilation of $(4\pi)^0$ mass spectra.

state discussed above. The fitted mass values of (1700 ± 15) MeV for the $\rho(4\pi)$ and (1640 ± 20) MeV for the g^- are not sufficiently different yet to exclude this possibility. At the present level of statistics determination of the decay modes is difficult. The CRRY collaboration[3] give evidence for an $\omega^0\pi^+$ and $A_2^0\pi^+$ decay, but the $A_2^0\pi^+$ mode is not seen by the Illinois[44] group or the Toronto-Wisconsin collaboration[62]. In the $(4\pi)^0$ combination from the reaction $\pi^-p \to n\pi^+\pi^+\pi^-\pi^-$ [62,68] no signal in the mass region 1700 MeV is evident as can be seen in Fig. 53. It has been suggested[62] that a predominant $\rho^0\rho^{\pm}$ decay mode of the $\rho(4\pi)^-$ could explain this observation since $\rho^0\rho^0$ decay of the $\rho(4\pi)^0$ would then be forbidden if $I[\rho(4\pi)] = 1$.

3.1.3 $\pi_A(1640)^{\pm} \to (3\pi)^{\pm}$ *alias* A_3

There seems to be little doubt about the production of a resonant state in the reaction $\pi^{\pm}p \to p(3\pi)^{\pm}$, in the $(3\pi)^{\pm}$ mass system at a mass of (1648 ± 10) MeV [3,66,69,71-73]. The evidence for this state is shown in Fig. 54. Most groups agree that it decays partially to $f^0\pi^{\pm}$, therefore I = 1, and that the signal almost disappears when a ρ^0 is selected. A spin parity analysis by one group[74] gave preference for J^P values in the abnormal series, 0^- 1^+ 2^-, etc.

3.1.4 $\pi(1650)^0 \to (3\pi)^0$

A paper presented to the Conference[63] concerning the reaction $\pi^+d \to pp_s\pi^+\pi^-\pi^0$ at 8 GeV/c gave added support to the existence of a new 3π state at a mass (1651 ± 10) MeV (see Fig. 55) already proposed during the year by another experiment at 5.1 GeV/c [75]. That this enhancement is different from the $A_3^{\pm}$ is indicated by the fact that it does not disappear when a ρ^0 selection is made. The $\rho^0\pi^0$ decay is not as firmly established as one would like, but suggests I = 0 for this G = -1 state. Further evidence for a state at 1.65 GeV with a ρπ decay came from a group studying the reaction $\bar{p}p \to 2\pi^+2\pi^-\pi^0$ at 2.5 GeV/c [76]. Figure

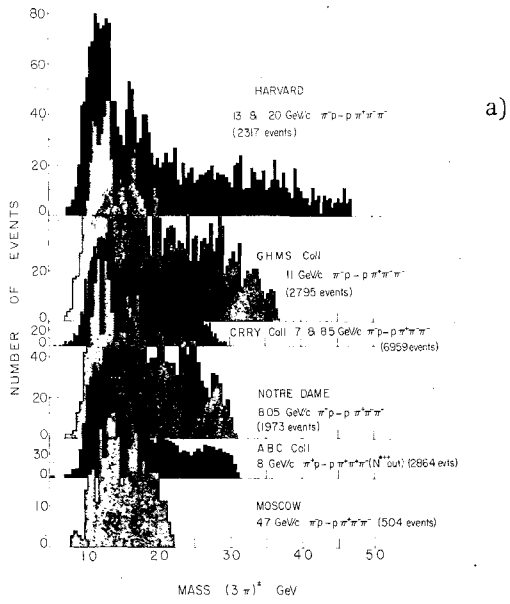

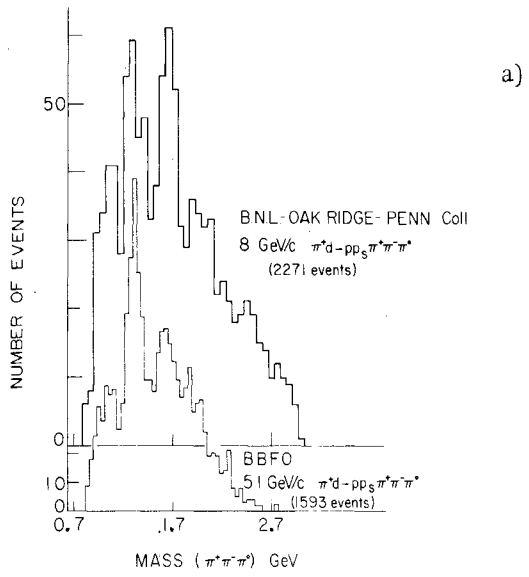

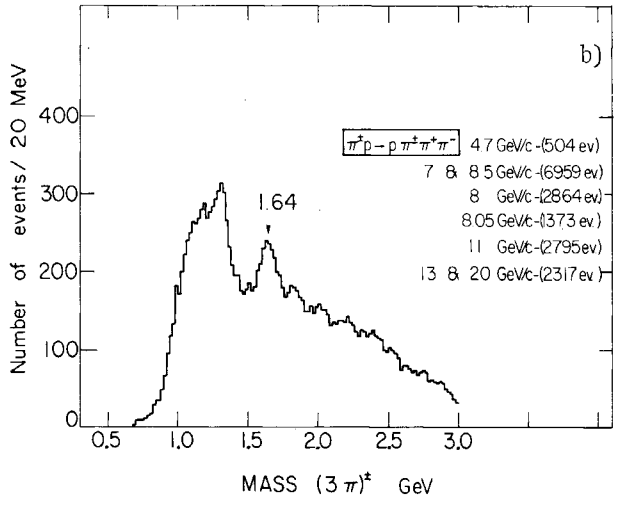

Fig. 54 a) and b) Compilation of $(3\pi)^{\pm}$ mass spectra.

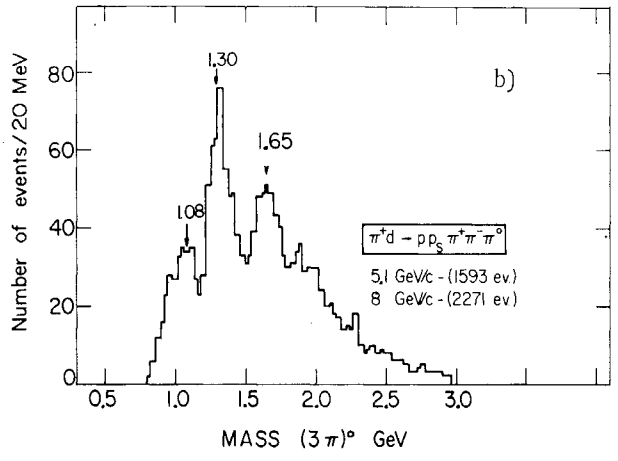

Fig. 55 a) and b) Compilation of $(3\pi)^{0}$ mass spectra.

56 shows their $\rho^{\mp}\pi^{\pm}$ mass distribution; a 4σ peak at 1.65 GeV is visible.

3.1.5 $R_{\omega}(1670) \to \omega^0\pi^+\pi^-$

Another candidate for a negative parity resonance at a mass of (1670 ± 18) MeV was submitted to the Conference[77]. A 3σ peak is observed in the mass spectrum of $\omega^0\pi^+\pi^-$ produced in the reaction $K^-p \to \Lambda^0\omega^0\pi^+\pi^-$ at 4.25 GeV/c, as shown in Fig. 57. Both the mass and the width of (50 ± 15) MeV agree with a previous observation[78] by a group studying annihilations of antiprotons. Whether this state represents another decay mode of the $A_3^{\pm}$ or A_3^0 is difficult to say at the present time.

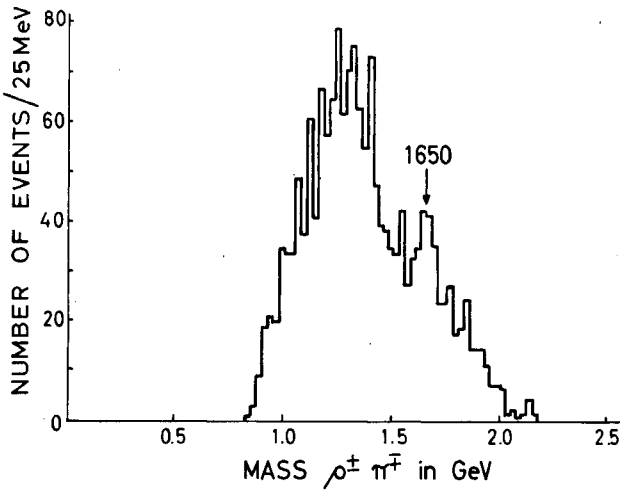

Fig. 56 $\rho^{\pm}\pi^{\mp}$ effective mass distribution from the reaction $\bar{p}p \to 2\pi^+2\pi^-\pi^0$ at 2.5 GeV/c [76].

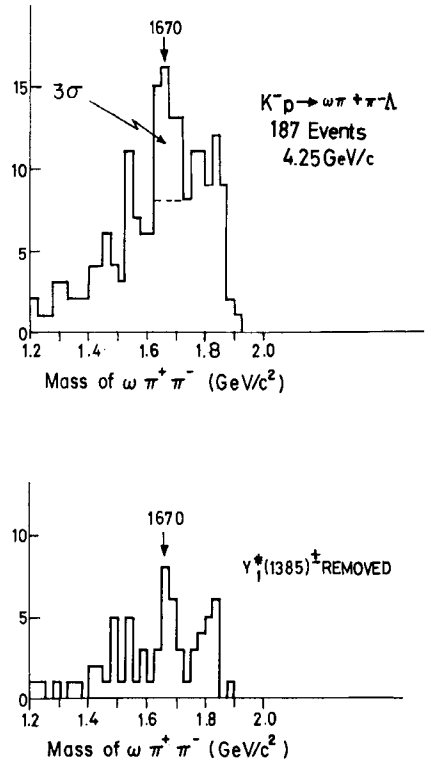

Fig. 57 $\omega^0\pi^+\pi^-$ effective mass distribution from the reaction $K^-p \to \Lambda^0\omega^0\pi^+\pi^-$ at 4.25 GeV/c [77].

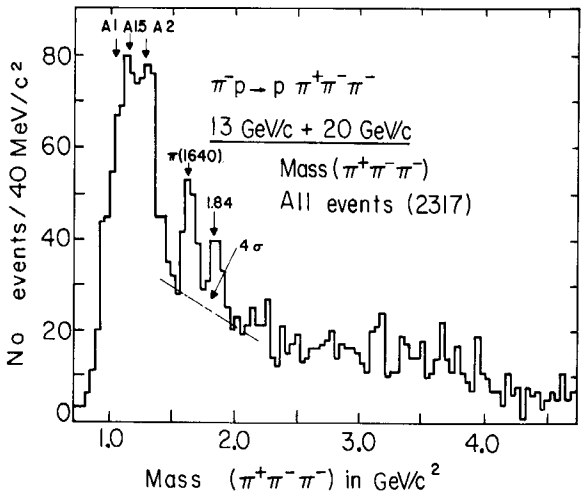

Fig. 58 $\pi^+\pi^-\pi^-$ mass distribution from the reaction $\pi^-p \to p\pi^+\pi^-\pi^-$ at 13 and 20 GeV/c [73].

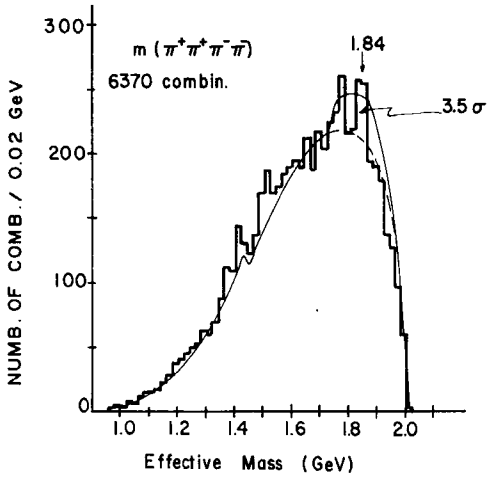

Fig. 59 $\pi^+\pi^+\pi^-\pi^-$ mass distribution from the reaction $\bar{p}p \to 2\pi^+2\pi^-\pi^0$ at 1.2 GeV/c [79].

3.1.6 *Other emerging states?*

$\pi(1840)$: Figure 58 shows the $\pi^+\pi^-\pi^-$ mass spectrum from the reaction $\pi^-p \to p(3\pi)^-$ at 13 and 20 GeV/c [73]. A peak of about 4σ at a mass 1840 MeV and with a width ∿ 80 MeV can be seen and may correspond to the peak seen in $\omega^0\pi^+\pi^-$ at a similar mass[78] in $\bar{p}p$ annihilations at 3 GeV/c.

$\rho(1840)^0 \to 4\pi$: Figure 59 shows the $\pi^+\pi^+\pi^-\pi^-$ mass spectra coming from an investigation of the reaction $\bar{p}p \to 2\pi^+2\pi^-\pi^0$ at 1.2 GeV/c [79]. The full-line curve indicates a fit to the data which is bad in the region above 1.7 GeV. A chimney of 3.5σ exists above the dotted line at a mass of 1840 MeV and is interesting to notice in view of a similar peak seen in $\bar{p}p \to 3\pi^+3\pi^-$ [80] at 3 GeV/c incident momentum.

$\rho(1630)^- \to \omega^0\pi^-$: The possibility of a resonance in the $\omega^0\pi^-$ system at 1630 MeV with $\Gamma \sim 60$ MeV has been suggested by a collaboration studying $\pi^-p \to p\pi^+\pi^-\pi^-\pi^0$ at 11 GeV/c [81]. The evidence is presented in Fig. 60 where a > 3σ peak is seen above the dotted line. The central mass seems to be lower than the usual broad peak centred at 1.7 GeV seen in the $(4\pi)^-$ mass distribution and may be an indication that the broad $(4\pi)^-$ peak consists of two or more resonances, one of which decays preferentially to $\omega^0\pi^-$. Clearly more data is needed.

3.1.7 *Widths and cross-sections, MMS versus HBC*

R-region (1630 MeV)

MMS	HBC ($A_3 \to 3\pi$)
• Γ_R < 30 MeV	Γ_R ∿ 100 MeV - WHY?
	$\sigma \simeq 70$ μb
	$\frac{d\sigma}{dt} \simeq 0.35e^{-5t}$ mb/GeV²
• $\Delta\sigma$ = 35 μb in $0.23 < t < 0.28$	$\Delta\sigma = \frac{\sigma}{12}$ = 6 μb in $0.23 < t < 0.28$

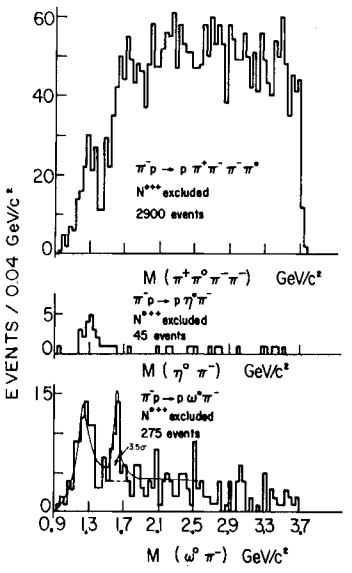

Fig. 60 $\pi^+\pi^-\pi^-\pi^0$, $\eta^0\pi^-$, and $\omega^0\pi^-$ mass distributions from the reaction $\pi^-p \to p\pi^+\pi^-\pi^-\pi^0$ at 11 GeV/c [81].

A clear discrepancy exists in the widths of the bosons seen in the R region by the MMS and hydrogen bubble chamber (HBC) techniques -- typically < 30 MeV versus ∿ 100 MeV, respectively. It is difficult to imagine where we have gone wrong in the HBC technique, typical errors being Γ < 20 MeV for four constraint (4C) fits of the type $\pi^\pm p \to p\pi^\pm\pi^+\pi^-$ and Γ < 40 MeV for 1C fits of the type $\pi^\pm p \to p\pi^\pm\pi^+\pi^-\pi^0$. Consider, for example, the 4C fit reaction $\pi^+ p \to p\, A_3(1630)^+ \to p\pi^+\pi^+\pi^-$, for which most people find cross-sections of the order 50 μb. If we add in the $A_3^+ \to \pi^+\pi^0\pi^0$ decay mode a cross-section of 70 μb is obtained[74]. The differential cross-section can be expressed in the form $d\sigma/dt = A\, e^{-Bt}$ with $B = (5.5 \pm 0.6)$ GeV^{-2}, and predicts a $\Delta\sigma$ = 6 μb in the t range, 0.23 < t < 0.28 GeV^2. This should be compared to the value of $\Delta\sigma$ = = (35 ± 12) μb given for the $R_1(1630)$ [82]. As the MMS does not distinguish between final states at the same mass [for example $\rho(1630)^- \to \omega^0\pi^-$ and $g^- \to \pi^-\pi^0$] it is satisfactory that the $\Delta\sigma$ of the MMS is larger, by a factor six, than that of the HBC. If the MMS detects all resonances one would think that it would be easier for the superposition of two or three resonances to give a broad enhancement with this technique than the HBC which detects one resonance. Maybe one should study the resonance production with the MMS technique as a function of t to make sure that Γ is independent of t. This is difficult to do for the HBC in view of the statistics required.

3.2 S = -1 bosons (L region)

L-region (1.6 - 1.88) GeV

- $K^-d \to d(K\pi\pi)$ at 12.6 GeV/c
  M = 1780 MeV, I = 1/2, $J^P = 1^+, 2^- \ldots$
- K^-p at 10 GeV/c
  M = (1785 ± 12) MeV, Γ = (127 ± 13) MeV
  $J^P = 1^+, 2^-, 3^+$
- NEW: $K^*(1660)$, $K^+p \to pK^+3\pi$ at 5 GeV/c
  M = 1660 MeV, Γ ∿ 80
- More than one resonance in Kππ spectrum?

The presence of a Kππ resonance at 1.79 GeV has been known for some time. More recent data[83] shown in Fig. 61 show a large peak centred at (1785 ± 12) MeV with a Γ of (127 ± 13) MeV. A peak seen in the $(K\omega)^-$ system at the same mass suggests I = 1/2 for this state. A detailed spin parity analysis favours a solution for J^P in the series $1^+, 2^-, 3^+, \ldots$ Is this mass region more complicated, however? On the quark model we can expect four K* resonances in this region. A sum of all the Kππ data from $K^\pm p$ experi-

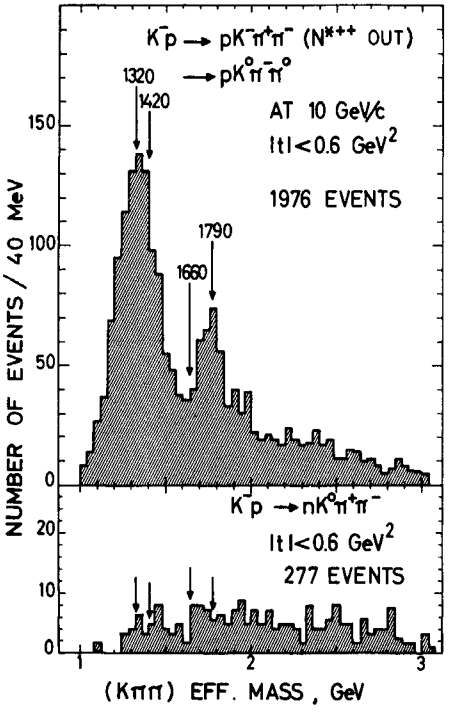

Fig. 61 Kππ effective mass distribution from the reaction $K^-p \to pK^-\pi^+\pi^-$ at 10 GeV/c [83].

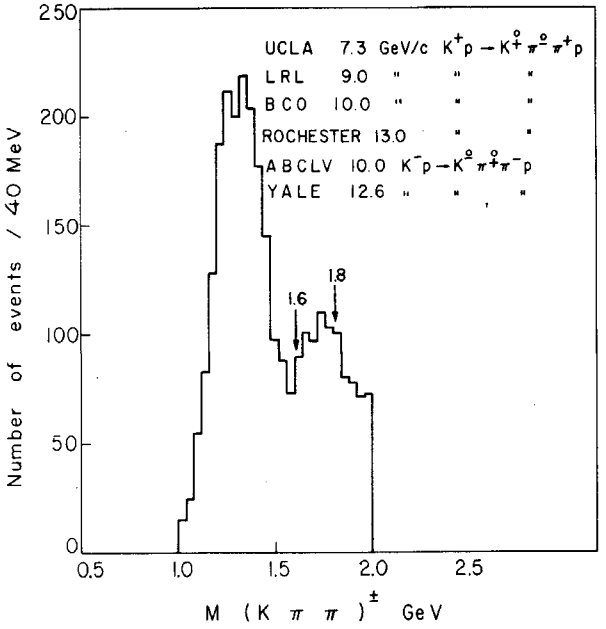

Fig. 62 Compilation of $(K\pi\pi)^{\pm}$ mass spectra from the reaction $K^{\pm}p \to (K\pi\pi)^{\pm}p$ greater than 7 GeV/c.

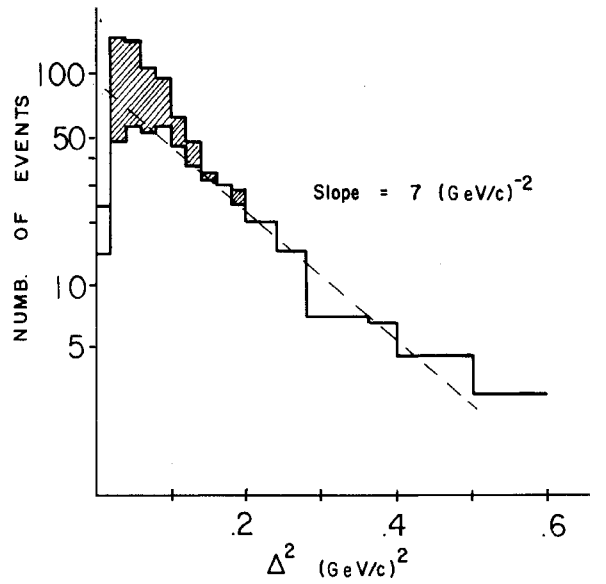

Fig. 63 Momentum transfer distribution to the target for all events fitting the reaction $K^-d \to K^-\pi^+\pi^-pn$ at 12.6 GeV/c. Shaded area corresponds to events fitting $K^-d \to K^-\pi^+\pi^-d$ [84].

ments with incident momenta > 7 GeV/c is shown in Fig. 62. The enhancement in the L-region is rather broad and spans 240 MeV. Reference to Figs. 41, 42, and 43 indeed suggest structure in this region: the optimistic observer could put his finger on three peaks in the region of 1660, 1720, and 1810 MeV. Clearly more data, as always, is required.

3.2.1 $K^-d \to d(K\pi\pi)^-$

A paper was presented to the Conference[84] on the coherent production of $(K\pi\pi)$ systems off deuterium at 12.6 GeV/c. Absence of a peak in the $(K\pi)^-$ system at 890 MeV in the reaction $K^-d \to d(K\pi)^-$ is taken as evidence that only states with unnatural parity (0^-, 1^+, 2^-, etc.) are produced in these reactions. The momentum transfer to the deuteron, shown in Fig. 63, is confined to a region < 0.1 GeV^2, as is expected of coherent production. The $K^-\pi^+\pi^-$ mass spectrum is shown in Fig. 64d, and peaks in the Q- and L-regions are evident. In Fig. 64a the $K^-\pi^+$ mass spectrum shows that K*(890) and K*(1400) are produced as daughters of the decay of the Q- and L-states. The peak at 1.28 GeV could either be a fluctuation or correspond to the $K\pi(1260)$ already mentioned in Section 2. The lack of background under the resonant states produced seems to be a nice feature of these coherent reactions and is particularly evident when the decay properties

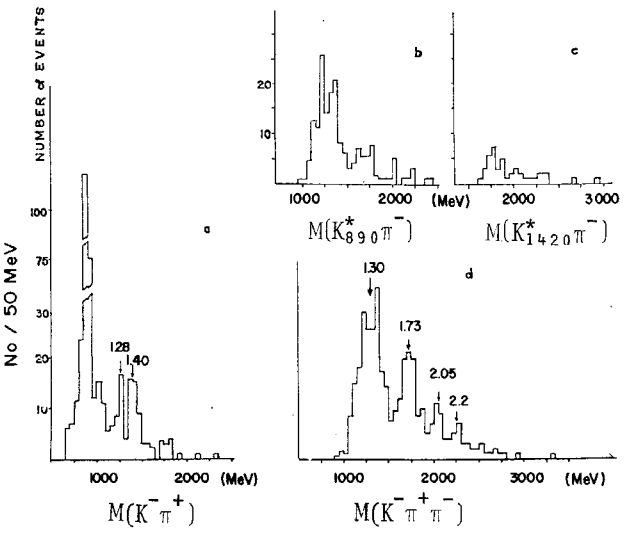

Fig. 64 Invariant mass distributions from the reaction $K^-d \to K^-\pi^+\pi^-d$ at 12.6 GeV/c.
a) $K^-\pi^+$ mass
b) $K^-\pi^+\pi^-$ mass where $0.85 < M(K^-\pi^+) < 0.94$ GeV
c) $K^-\pi^+\pi^-$ mass where $1.33 < M(K^-\pi^+) < 1.55$ GeV
d) $K^-\pi^+\pi^-$ mass.

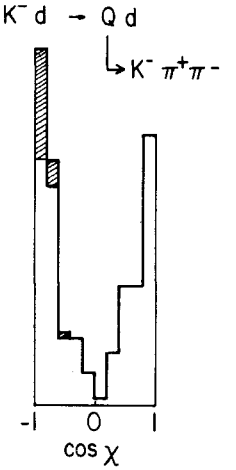

Fig. 65 Distribution of cos χ (see text for definition of χ) in the $K^-d \to Qd$ ($Q \to K\pi\pi$) events at 12.6 GeV/c.

of the Q-region are studied, as can be seen in Fig. 65. The angular distribution of the outgoing π^+ relative to the incoming K^- in the K*(890) c.m.s. (cos χ) in the Q-region goes to zero at cos χ = 0 and makes it possible to rule out $J^P = 2^-$ for the Q region. $J^P = 1^+$ is left as the only possibility. More statistics are necessary before J^P of the L-region can be determined but the outlook is promising.

3.2.2 K(1660)*

At this Conference additional evidence for the 1660 MeV state, already suggested earlier[85], was presented by the same group studying the reaction

$$K^+p \to K^0p\pi^+\pi^+\pi^- \quad (987 \text{ events})$$

at 5 GeV/c. In Fig. 66, showing the $K^0\pi^+\pi^-\pi^-$ mass distribution, a 4σ peak at 1660 MeV with a width ∿ 60 MeV can be seen. Study of the $K^0\pi^+\pi^-$ mass spectrum for $K^0(3\pi)^-$ mass in and near the 1660 MeV peak suggests a possible decay mode of this state is

$$K^*(1660) \to K^*(Q)\,\pi^+$$
$$\qquad\qquad \hookrightarrow K^0\pi^+\pi^-.$$

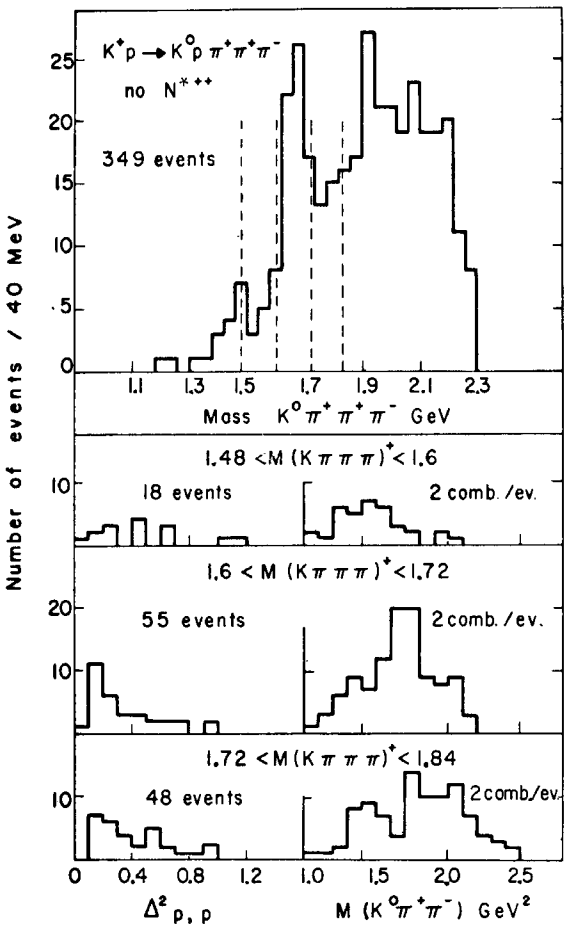

Fig. 66 Effective mass distribution of $K^0\pi^+\pi^+\pi^-$ from the reaction $K^+p \to pK^0\pi^+\pi^+\pi^-$ at 5 GeV/c.

4. MESONS (MASS > 1.88 GeV)

> R-region (M > 1.88 GeV)

- $\bar{p}p$ backward scattering

  $\bar{p}$ 0.3 - 0.7 GeV/c (3934 events)

M(MeV)	Γ(MeV)	L(?)
∿ 1925	∿ 10	odd
∿ 1945	∿ 20	even
≳ 1975	> 20	even

- Nice counter experiment required?

The baryon-antibaryon system is clearly an interesting system from the point of view of bosons. At this Conference and during the past year, results suggest that the study of this system has and will yield interesting results in the future.

4.1 S = 0 bosons

An interesting paper presented to the Conference by a Wisconsin group[86] serves to demonstrate how the study of backward elastic $\bar{p}p$ scattering can be a powerful tool in the study of bosons which are coupled to the $\bar{p}p$ system. The technique is both simple and elegant. They scan for heavily ionizing negative tracks in the hydrogen bubble chamber and thus eliminate most of the forward elastic scattering. Any boson formed will decay symmetrically forward and backward in the c.m.s. (ignoring interference effects). Their results are shown in Figs. 67 and 68. The change in the structure of the backward peak as a function of the $\bar{p}$ momentum is evident in Fig. 67. The variation of the differential cross-section dσ/d(cos θ) with $\bar{p}$ momentum provides (Fig. 68) evidence for three boson resonances at ∿ 1925, 1945, and 1975 MeV with widths of ∿ 10, 20 and > 20 MeV, respectively. Observation of the 1945 and 1975 MeV bumps in the region of cos θ near zero indicates that these states have even spin and that the 1925 MeV bump has odd spin. The faster fall-off in cos θ of the 1925 and 1945 MeV bumps than the 1975 MeV bump suggests that the latter have lower spin than the former. Although the I-spin cannot be determined, the narrow peak at

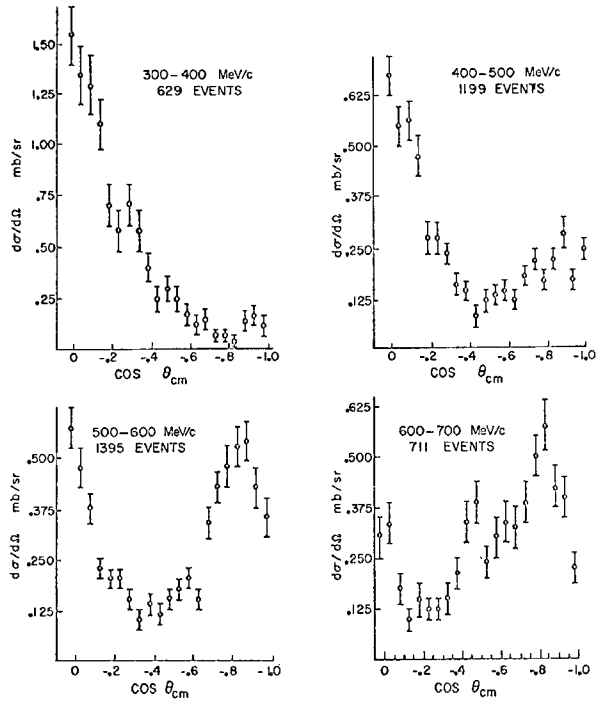

Fig. 67 Differential cross-sections for backward hemisphere $\bar{p}p$ elastic scattering below 700 MeV/c [86].

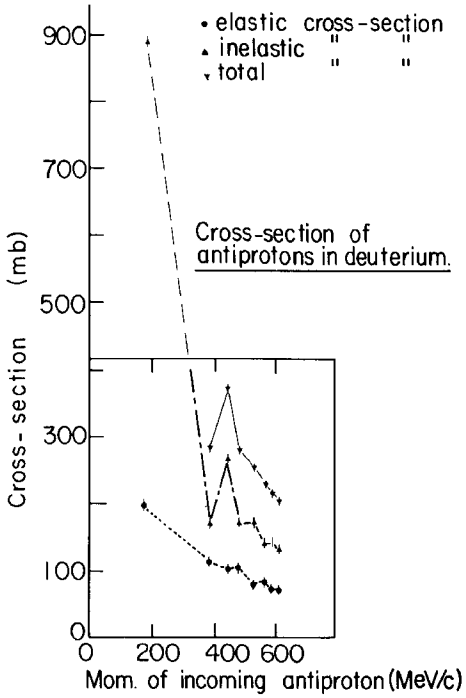

Fig. 69 Variation of the total, elastic, and inelastic $\bar{p}d$ cross-sections with antiproton momentum[87].

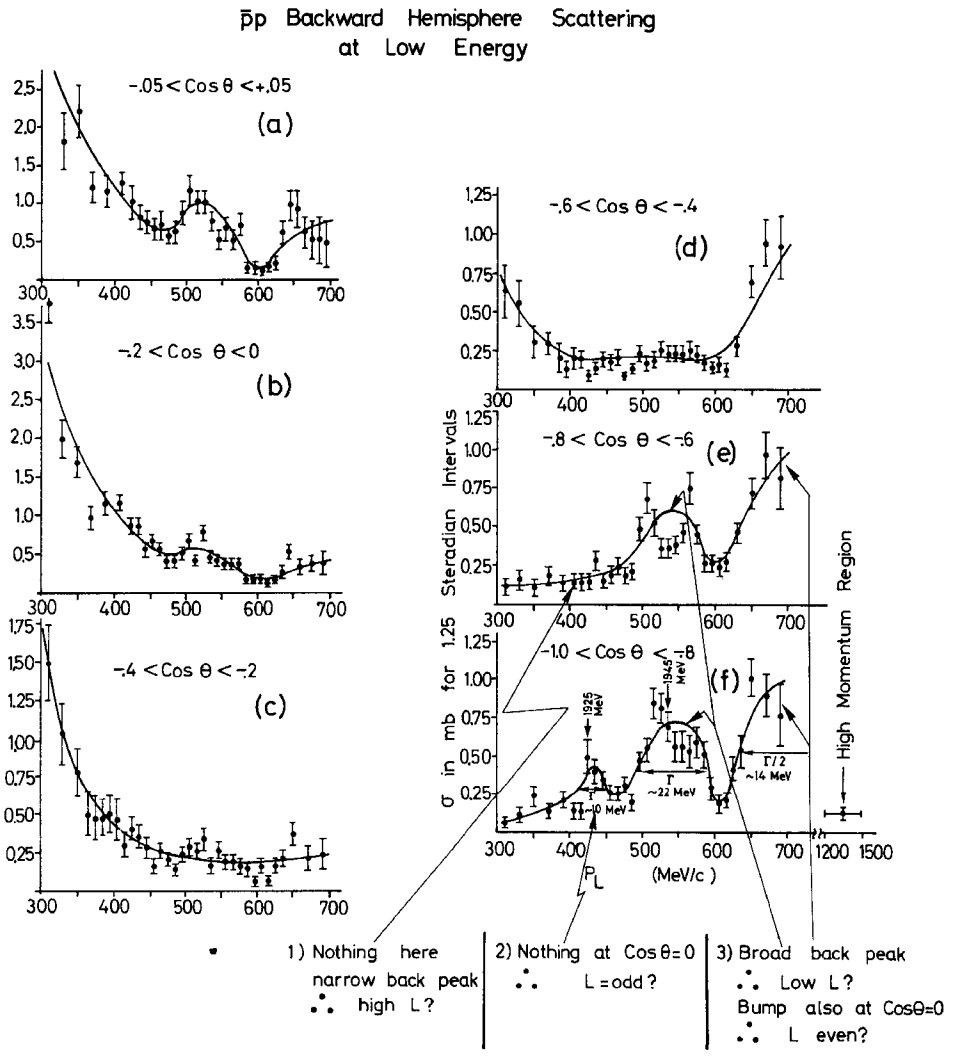

Fig. 68 Energy dependence of the differential cross-section for various cos θ cuts [86].

1925 MeV may correspond to the peak at the same mass seen in the CERN-MMS experiment.

Evidence for a narrow (Γ < 30 MeV) $\bar{p}n$ state was presented by a group [87] studying the elastic, inelastic and total cross-sections of $\bar{p}d$ interactions in the momentum range 0 to 630 MeV/c. The cross-sections are shown in Fig. 69 where a peak can be seen at an incident momentum of 450 MeV/c corresponding to a mass 1927 MeV in the (I = 1) $\bar{p}n$ system.

4.1.1 M = 2220 MeV state?

Figure 70 shows the variation of the backward elastic scattering cross-section for $\bar{p}$'s in the momentum region 1.5 to 2.0 GeV/c [88]. A peak seems to exist at a mass of 2220 MeV. No corresponding peak is seen in the one-pion production channel.

4.1.2 $\pi^- p \to \Lambda\bar{\Lambda}n$

Data were presented at the Conference[89] by a group using a magnetic spark chamber system to study the rare reaction ($\sigma \simeq 0.3$ μb)

$\pi^- p \to \Lambda^0\bar{\Lambda}^0 n$ at 7 and 12 GeV/c (100 events) .

The $\Lambda^0\bar{\Lambda}^0$ system has the nice feature that I = 0 and J^P analysis of any boson would be helped by observing the Λ and $\bar{\Lambda}$ polarizations through their weak decay. However, as Fig. 71 shows, no evidence for a peak in the $\Lambda^0\bar{\Lambda}^0$ mass spectrum exists.

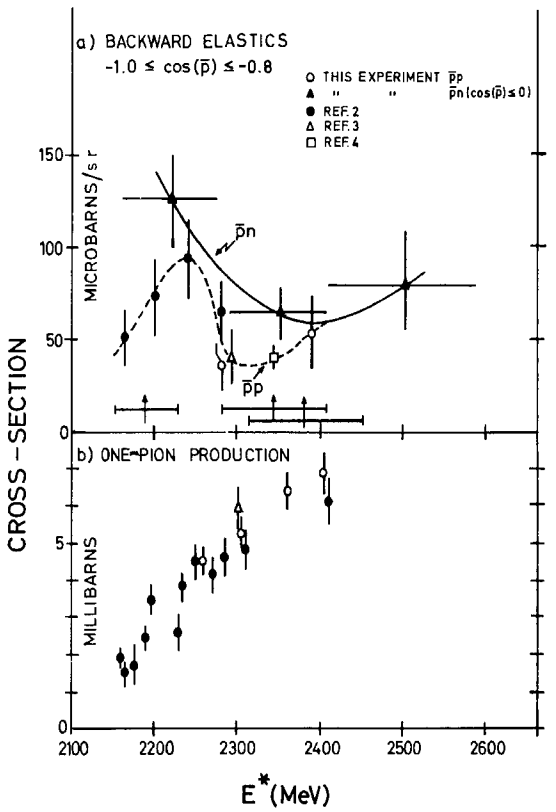

Fig. 70 a) Backward $\bar{p}p$ and $\bar{p}n$ elastic cross-sections versus the over-all c.m. energy. b) Variation in the one-pion production cross-section of $\bar{p}p$ collisions with c.m. energy[88].

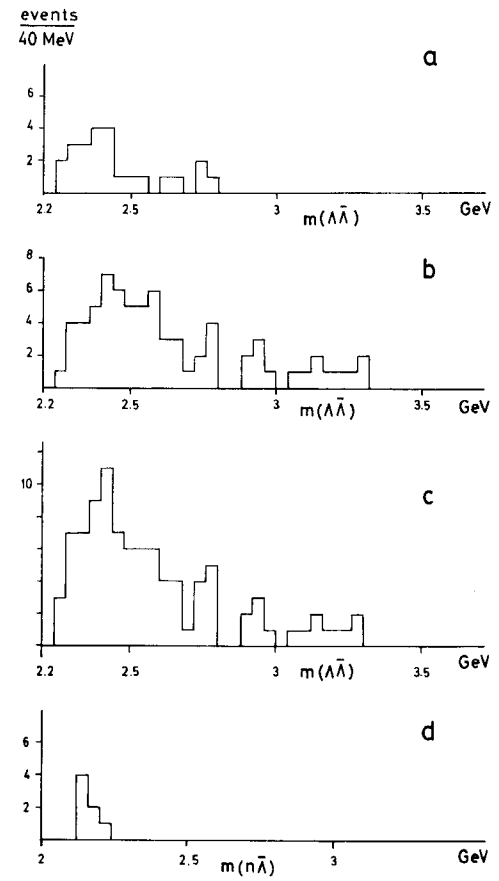

Fig. 71 $\Lambda^0\bar{\Lambda}^0$ invariant mass distributions from the reaction $\pi^- p \to n\Lambda\bar{\Lambda}$ [89]. a) 7 GeV/c; b) 12 GeV/c, $t(p \to n) > -2.5$ GeV^2; c) a and b combined; d) $n\bar{\Lambda}$ mass for $t(p \to \Lambda) > -1$ GeV^2.

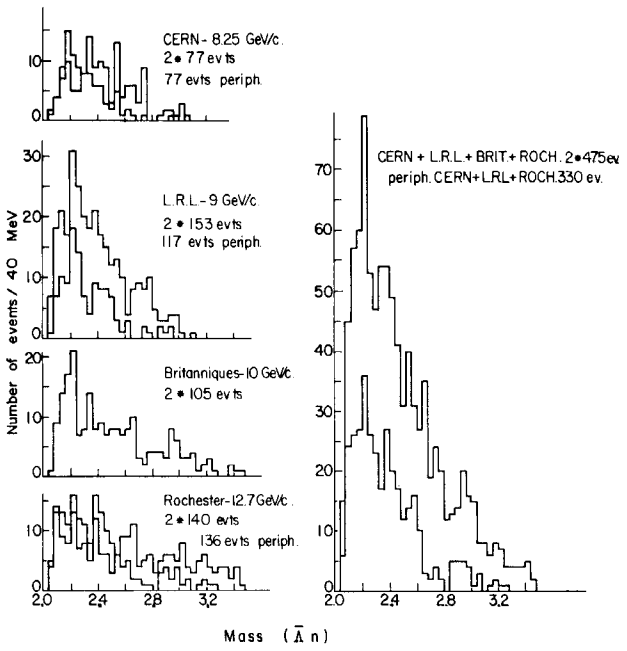

Fig. 72 Compilation of $\bar{\Lambda}N$ effective mass spectra.

4.2 |S| = 1 bosons

During the year we have had evidence presented for a possible $\bar{\Lambda}p$ state at a mass of 2.24 GeV [90]. Of the three contributions submitted to the Conference concerning the reactions

$$K^- p \to pp\bar{\Lambda}$$
$$\bar{p}p\bar{\Lambda}\pi^0$$
$$pn\bar{\Lambda}\pi^*$$

at 8.25 [91], 10.0 [92], and 12.7 GeV/c [93] one of the groups sees the enhancement. Figure 72 shows the compiled data. The existence of this state is still an open question.

5. DISCUSSION

In this last part I would like to discuss some aspects and ideas on meson physics which I find interesting.

5.1 MMS experiment

If we refer back to the meson excited state diagram of Fig. 5 we see that the states which are produced in the MMS experiment, using the Jacobian peak method, are those which lie at the lowest excitation for a given L-value. Except for the δ^-, only states on the ρ trajectory seem to be excited. The B and A_1 are not excited. The dynamics of the MMS experiment might be described by Fig. 73 where the production of a state on the ρ trajectory is formed by the exchange of the next lowest state on the same trajectory together with an angular momentum of $J^P = 2^+$ relative to the incoming π^-. This would then be compatible with the decay channel of the resonant state being identical to the formation channel at the upper pion vertex, viz.

$$\rho^- \to \pi^+\pi^- \text{ with orbital } L^P = 1^-$$
$$A_2^- \to \rho^0\pi^- \qquad = 2^+$$
$$\rho(4\pi)^- \to A_2^0\pi^- \qquad = 2^+$$
$$\text{etc.}$$

It will be interesting to see what states the CERN boson spectrometer produces working at minimum t. Also it would be interesting to see the MMS technique exploring meson production as a function of t. Can there be something special in the production of meson states as a function of t which results in the R, S, T, and U being observed with narrow widths in the special configuration of the MMS? It would also be nice to have a separated beam for counters so that the MMS technique could be used with $K^\pm$ and $\bar{p}$ primaries.

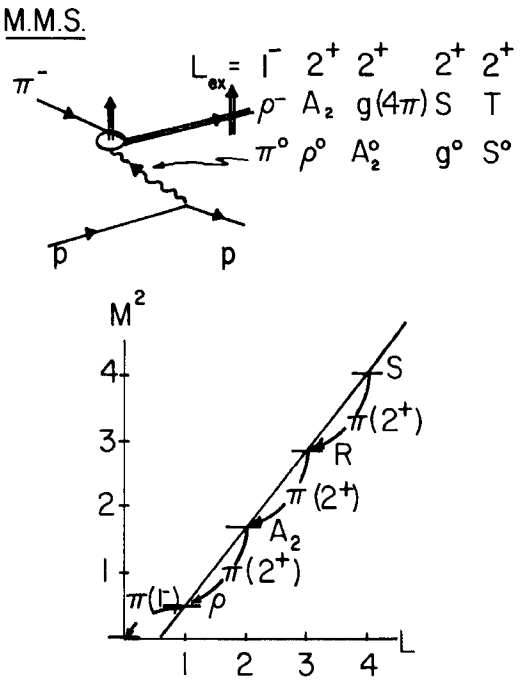

Fig. 73 Diagrams relevant to the MMS experiment showing production and decay mechanisms.

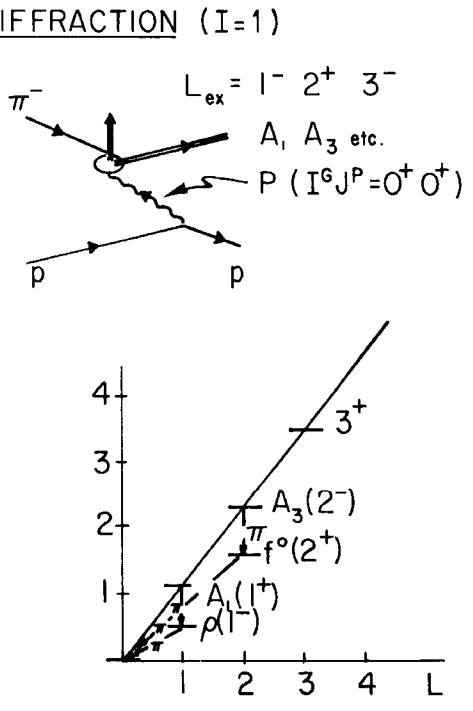

Fig. 74 Diagrams relevant to diffraction mechanism of resonance production and decays of the produced states.

5.2 Diffraction trajectory

Another trajectory upon which it seems possible to excite states by choosing a special dynamical configuration is the "diffraction" trajectory. Figure 74 shows how one might visualize the production of the A_1^- and A_3^- by Pomeron exchange $[I^G J^P(\text{Pom}) = 0^+0^+]$. In this case it is known experimentally that such states are excited at small momentum transfers. These states seem to decay down to lower states via emission of a pion quantum in a state of relative orbital angular momentum 0^+ -- for example, $A_1^- \to \rho^0\pi^-$, $A_3^- \to f^0\pi^-$. It is a pity that counter experiments on deuterium, of the type undertaken by the Johns Hopkins group in their K^-d experiment, viz. $K^-d \to Q^-d$ or $K^-d \to L^-d$ (see Fig. 75), do not yet seem technically feasible due to the low energy of the deuterium recoil. As can be seen in Fig. 75, the Q and L mesons are formed via diffraction production and then decay via other open channels to K*(890) and K*(1400), respectively. The K*(1400) then decays down to either K*(890) or a K via π emission.

5.3 $\bar{p}p$ annihilation

Here my feeling is that we can enter into a boson state at a fixed mass and then cascade down to other bosons lying lower in mass. At this high energy of the boson system we can hope to have a reasonable cross-section for $\bar{p}p \to$ bosons due to the many states available in the higher mass region since, with $M^2 \propto L$ on any given trajectory, the states crowd together at high masses. Furthermore, since the decay width Γ for two-particle decay is given by $\Gamma_\ell \propto [(kR)^\ell/(\ell!!)]^2$ for $kR \ll 1$ (where k is the c.m.s. particle momentum, R the effective radius of interaction, and ℓ the relative orbital momentum), and

$$\sigma(\bar{p}p \to B_\ell^0) = \sigma_\ell \Gamma_\ell(\bar{p}p \to B^0)/\Gamma_\ell \ ,$$

where $\sigma_\ell = \pi\lambda^2(2\ell + 1)$, we see that with decreasing ℓ, Γ_ℓ can become larger and σ_ℓ becomes smaller*). We could then have, for example, the situation shown in Fig. 76 where an antiproton of 740 MeV/c finds many channels available for the formation of boson states. (The higher mass states on Fig. 76 can either be looked upon as radially excited states or daughter trajectories.) Thus once the $\bar{p}p$ has entered into a boson state with a broad width, a K or π can be emitted al-

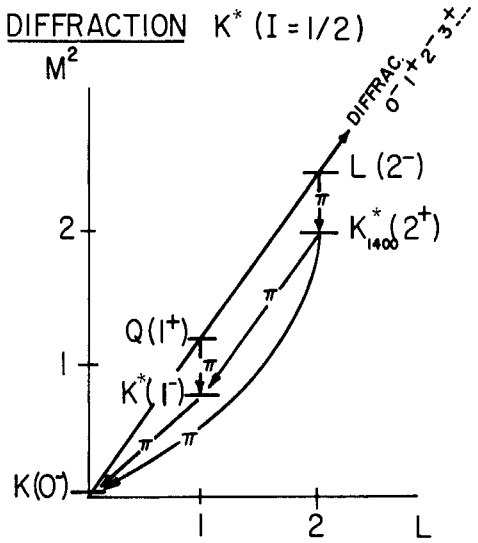

Fig. 75 The K*'s lying on the K* diffraction trajectory and their decay.

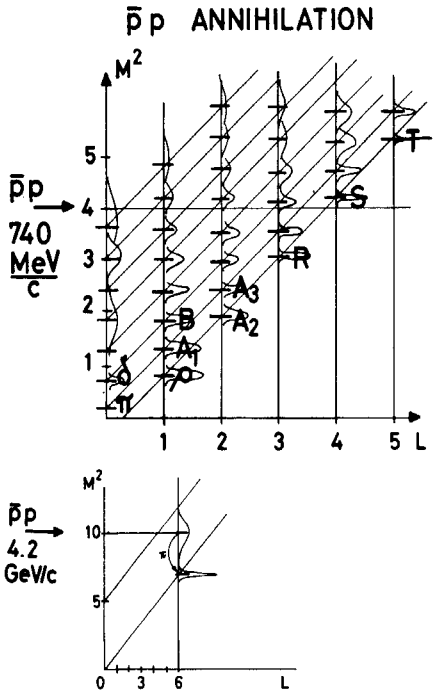

Fig. 76 Excitation diagram showing boson states, which may be available as entrance channels for $\bar{p}p$ annihilation, and an example of the subsequent decay.

*) It is possible that the broad bumps in the total cross-sections seen by Cool et al.[94] result from the compromise of requiring a large $\Gamma(\bar{p}p \to B^0)$ and not too small σ_ℓ; the rapid decrease in Γ_ℓ outweighing the slow increase in σ_ℓ precludes the observation of narrow states with reasonable cross-sections.

lowing the system to drop to a narrower state which may be detected via effective mass plots. Indeed one could go even further and say that if low L, high mass bosons exist, $\bar{p}p$ is a place to look for them. Possible examples of boson formation by antiprotons on protons and their subsequent cascade decay are shown in Fig. 77. Clearly if such a model of annihilation is true we should not be surprised to find rapid changes in the properties of $\bar{p}p$ systems as we change the incident energy. As another example, Fig. 78 shows what happens when we look at what is left in the reactions

$$\bar{p}p \to 2\pi^+ 2\pi^- (\pi^0)$$
$$2\pi^+ 2\pi^- (X^0) \quad M(X^0) < 2M_N$$
$$2\pi^+ 2\pi^- (X^0) \quad M(X^0) > 2M_N$$
$$\bar{p}p\, \pi^+\pi^- (\pi^0)$$

after one π has been emitted -- essentially the missing mass opposite one pion[95]. Evidence for three high mass boson states is seen at masses of 2.82, 3.08, and 3.24 GeV.

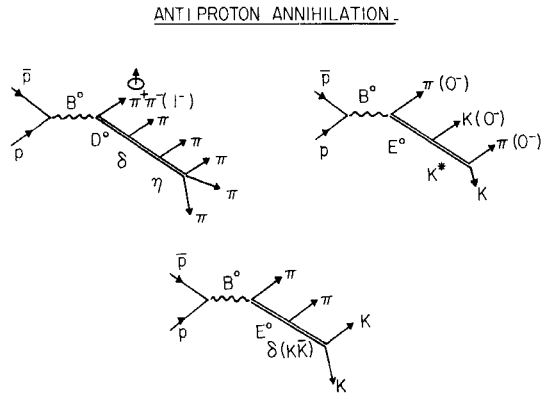

Fig. 77 Examples of the cascade decay of the initial $\bar{p}p$ state via emission of π or K quanta.

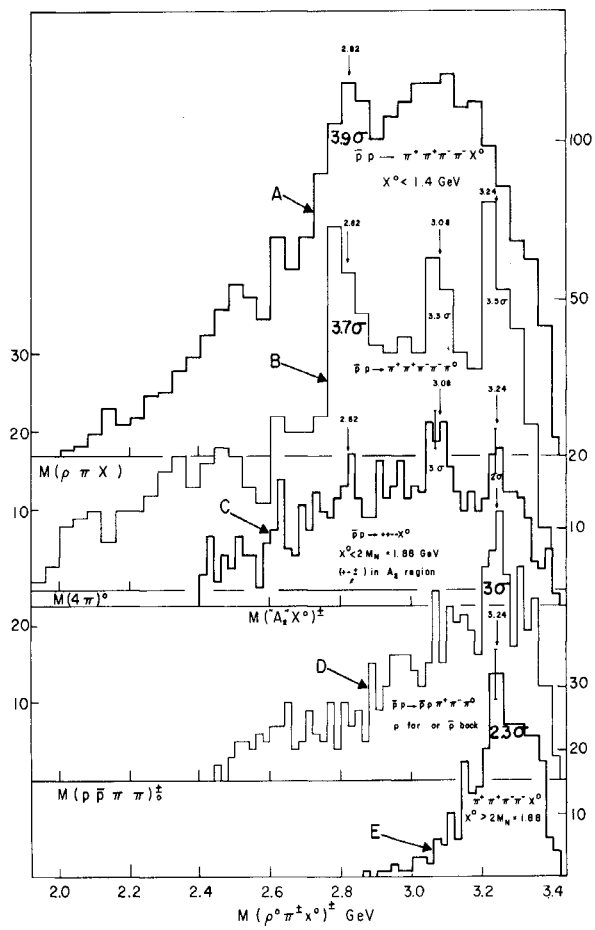

Fig. 78 M mass spectra from the reaction $\bar{p}p \to \pi M$ at 5.7 GeV/c where M $\to (\bar{p}p\pi\pi)$, $\rho^0\pi^\pm X^0$, $A_2^\pm X^0$ [95].

5.4 $\pi p \to p(m\pi)$

We can also look at what one might hope to see in $\pi p \to p(m\pi)$ if this "statistical hadron model" for the decay of highly excited N*'s is valid. In this case either a pion or a proton can be emitted leaving the remaining state to drop down into a lower N* or boson, respectively, as shown in Fig. 79. Figure 80 shows the $\rho^-\pi^+\pi^-$ mass spectrum opposite the proton from the reaction $\pi^- p \to p\pi^+\pi^-\pi^-\pi^0$ at 11 GeV/c [81].

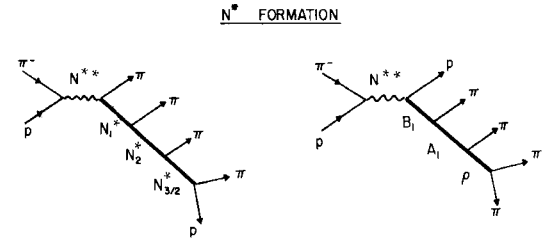

Fig. 79 Diagrams relevant to N* formation by $\pi^- p$ and its subsequent cascade decay.

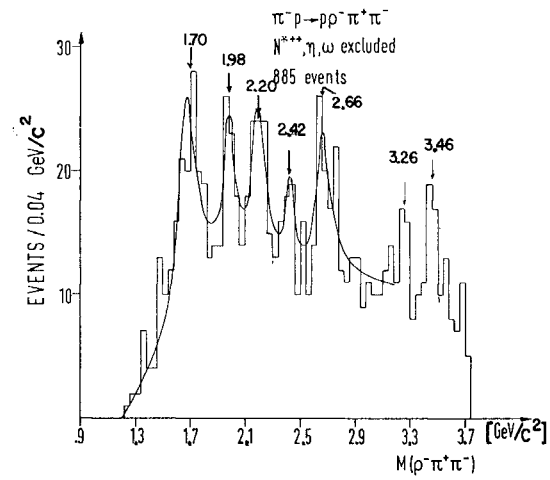

Fig. 80 $\rho^-\pi^+\pi^-$ mass spectrum from the reaction $\pi^- p \to p(\rho^-\pi^+\pi^-)$ and 11 GeV/c [81].

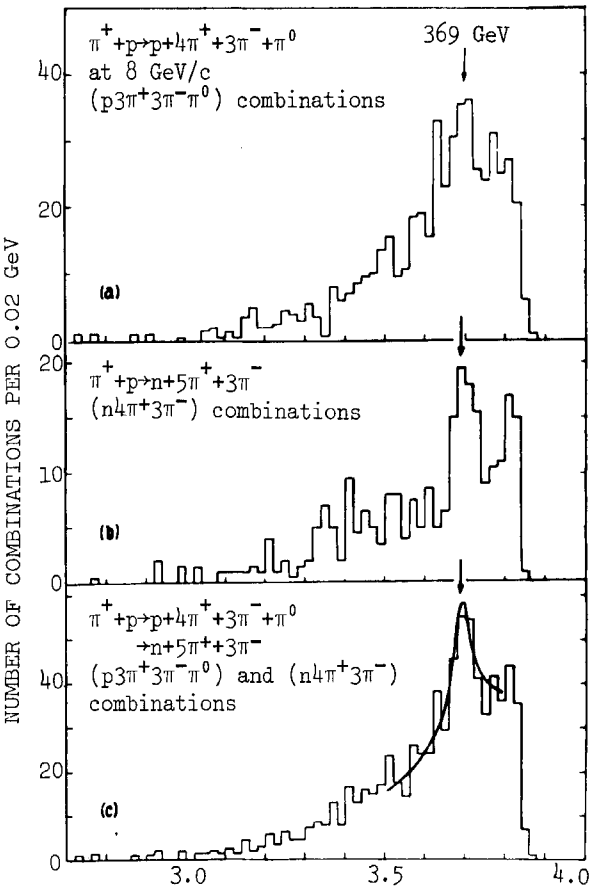

Fig. 81 (Nucleon + 8π) mass spectra from the reaction $\pi^+p \to p4\pi^+3\pi^-\pi^0$ and $n5\pi^+3\pi^-$ at 8 GeV/c [96].

In addition to peaks at 1.70, 1.98, 2.20, 2.42 and 2.66 GeV two other peaks at 3.26 and 3.46 GeV are present, the lower of which corresponds in mass to the peak at 3.24 GeV seen in Fig. 77. As a possible example of a high mass N* we might take that of the ~~Warsaw~~ CRACOW group who, studying the reaction $\pi^+p \to p(8\pi)$ or $n(8\pi)$, obtained evidence for a high mass $N^{*0} \to p(7\pi)$ or $n(7\pi)$ at 3.69 GeV [96], as shown in Fig. 81.

5.5 The ρ trajectory

Another interesting feature of the ρ trajectory, as indicated from the MMS experiment and shown on Fig.3, is that if the trajectory continues in a linear fashion ($M^2 \propto L$) up to high L values, then at L = 14, which corresponds to a boson mass of ∿ 4 GeV, one finds the mass difference between adjacent states on the ρ trajectory is equal to a pion mass. Therefore, the decay $B(J^P = 14^+) \to B(J^P = 13^-)$ via 2^+ pion emission will be prohibited. The next most likely decay is

$$B(J^P = 14^+) \to B(J^P = 12^+) \text{ via } 3^- \text{ pion emission.}$$

Since the decay has a low Q-value the angular momentum barrier will be high and we can expect such states to become very narrow [97]. The problem will be to produce these states with observable cross-sections. The MMS technique involving small momentum transfer to the proton, and hence favouring peripheral collisions, may not favour their production. If, however, we search for these states as the decay products of high mass isobars (in which case the MMS technique must be made sensitive to the detection of evaporation protons in the c.m.s. of the N*), then maybe we will have some success.

One last remark is relevant to Fig. 3. Is it a coincidence that the lowest-lying N*'s, when plotted in terms of their orbital angular momentum, lie on a trajectory almost parallel to the lowest-lying boson trajectory (the ρ trajectory) and separated from it by about the nucleon mass squared?

Acknowledgements

I would like to express my thanks to Drs. I. Butterworth and L. Montanet for discussions and comments on the notes relevant to the talk in Vienna and to Dr. R. Armenteros for kindly reading and commenting on this manuscript. However, responsibility for any blunder is mine. Last, but by no means least, I thank my wife for her understanding.

REFERENCES AND FOOTNOTES

1. A.H. Rosenfeld, N. Barash-Schmidt, A. Barbaro-Galtieri, L.R. Price, P. Söding, C.G. Wohl, M. Roos and W.J. Willis, Rev. Mod. Phys. 40, 77 (1968).

2. A.H. Rosenfeld, Proc. Philadelphia Conference on Meson Spectroscopy, Philadelphia, 1968 (to be published by Benjamin, N.Y., 1968), p. 443.

3. C. Baltay, H.H. Kung, N. Yeh, T. Ferbel, P.F. Slattery, M. Rabin and H.L. Kraybill, paper 18 and Phys. Rev. Letters 20, 887 (1968).

4. M. Gell-Mann, Phys. Letters 8, 214 (1964).

5. G. Zweig, CERN preprint 8182/TH 401 (1964), 8419/TH 412 (1964), and Symmetries in Elementary Particle Physics, Proc. 1964 Int. School of Physics Ettore Majorana,Erice, Italy (Academic Press, N.Y., 1965), p. 192.

6. R.H. Dalitz, Proc. Thirteenth Int. Conf. on High-Energy Physics, Berkeley, California, 1966 (Univ. of Calif. Press, Berkeley, 1967), p. 215.

7. G. Goldhaber, Proc. 1967 CERN School of Physics, CERN 67-24 (1967), Vol. III, p. 4-1.

8. R.H. Dalitz, in Proc. Philadelphia Conference on Meson Spectroscopy, Philadelphia (to be published by Benjamin, N.Y., 1968).

9. M. Goldberg, Symposium on the present status of SU(3) for particle couplings and reactions, ANL, 1967, preprint, p. 17.

10. R.C. Arnold, Phys. Rev. Letters 14, 657 (1965).

11. G. Zweig, in Proc. Philadelphia Conference on Meson Spectroscopy, Philadelphia, 1968 (to be published by Benjamin, N.Y., 1968).

12. D.R.O. Morrison, in Proc. Conference on High-Energy Two-Body Reactions, Stony Brook, April 1966.

13. C. Baltay, Proc. Philadelphia Conference on Meson Spectroscopy, Philadelphia, 1968 (to be published by Benjamin, N.Y., 1968), p. 91.

14. C. Baglin et al., paper 505.

15. J. Kim, C. Baltay, P. Franzini, L. Kirsch, R. Newman, N. Yeh, J.A. Cole, J. Lee-Franzini and H. Yarger, Bull. Amer. Phys. Soc. 13, 16 (1968).

16. A.M. Cnops, G. Finocchiaro, P. Mittner, J.P. Dufey, B. Gobbi, M.A. Pouchon and A. Muller, Phys. Letters, 27 B, 113 (1968).

17. K.C. Wali, Phys. Rev. Letters 9, 120 (1962).

18. A. Barbaro-Galtieri, M. Matison, A. Rittenberg and T.F. Shively, Phys. Rev. Letters 20, 349 (1968).

19. R. Barloutaud, Duong Nhu Hoa, D. Merrill, J.C. Scheur, A. Verglas, W. Hoogland, J.C. Kluyver, A.G. Tenner, S.A. DeWit, S. Focardi, A. Minguzzi-Ranzi, L. Monari, A.M. Rossi, G. Alexander, Y. Eisenberg, G. Lamidey and A. Rouge, Phys. Letters 26 B, 674 (1968).

20. D. Bollini et al., paper 196.

21. A. Barbaro-Galtieri and P. Soding, paper 826 and UCRL 18271.

22. S.Y. Fung, H. Jackson, R.T. Pu, D. Brown and G. Gidal, Phys. Rev. Letters 21, 47 (1968).

23. L.J. Gutay, D.O. Carmony, P.L. Csonka, F.J. Loeffler and F.T. Meiere, paper 789 and Purdue report COO-1428-65.

24. K.J. Braun et al., paper 288.

25. G.A. Smith and R.J. Manning, UCRL-17917.

26. S. Buniatov and D. Schmitt, paper 714.

27. E. Malamud and P.E. Schlein, Phys. Rev. Letters 19, 1056 (1967).

28. I.F. Corbett, C.J.S. Damerill, N. Middlemas, D. Newton, A.B. Clegg, W.S.C. Williams and A.S. Carroll, Phys. Rev. 156, 1451 (1967).

29. T.F. Hoang et al., paper 19.

30. Ch d'Andlau et al., paper 626.

31. I. Butterworth, Proc. Heidelberg Int. Conf. on Elementary Particles. 1967 (North Holland, Amsterdam, 1968), p. 66.

32. K.W. Lai, paper 800.

33. D.H. Miller et al., paper 804.

34. C. Whitehead, J.G. McEwen, R.J. Ott, D.K. Aitken, G. Bennett and R.E. Jennings, Nuovo Cimento 53, 817 (1968).

35. P.B. Johnson et al., paper 23.

36. G. Ascoli, H.B. Crawley, D.W. Mortara and A. Shapira, paper 510 and Phys. Rev. Letters 20, 1411 (1968).

37. V. Barnes et al., paper 259.

38. R. Ammar et al., paper 939.

39. C. Defoix et al., paper 653.

40. Ch. d'Andlau, A. Astier, L. Dobrzynski, J. Siaud, J. Barlow, L. Montanet, L. Tallone-Lombardi, A.M. Adamson, J. Duboc, M. Goldberg, R.A. Donald, D.N. Edwards and J.E. Lys, Nuclear Phys. B5, 693 (1968).

41. M. Deutschmann et al., paper 466.

42. G.F. Chew and A. Pignotti, Phys. Rev. Letters 20, 1078 (1968).

43. B. Junkermann et al., paper 467.

44. G. Ascoli, H.B. Crawley, U. Kruse, D.W. Mortara, E. Schafer, A. Shapiro and B. Terrault, paper 508 and Phys. Rev. Letters 21, 113 (1968).

45. H. Benz et al., paper 240.

46. D.J. Crennell, U. Karshon, K.W. Lai, J.M. Scarr and I.O. Skillicorn, paper 153 and Phys. Rev. Letters 20, 1318 (1968).

47. H. Blumenfeld et al., paper 272.

48. M. Aguilar-Benitez et al., paper 955.

49. M. Aguilar-Benitez et al., paper 760.

50. T.G. Trippe et al., paper 542 and UCLA-1024.

51. G. Bassompierre, Y. Goldschmidt-Clermont, A. Grant, V.P. Henri, I. Hughes, B. Jongejans, R.L. Lander, D. Linglin, F. Muller, J.M. Perreau, I. Saitov, R.L. Sekulin, G. Wolf, W. de Baere, J. Debaisieux, P. Dufour, F. Grard, J. Heughebaert, L. Pape, P. Peeters, F. Verbeure and R. Windmolders, Phys. Rev. Letters 26 B, 30 (1967).

52. P. Antich et al., paper 497.

53. G. Goldhaber, private communication.

54. Birmingham-Glasgow-Oxford Collaboration, paper 217.

55. A. Astier et al., paper 501.

56. R. Palmer, private communication.

57. L. Dubal, M.N. Focacci, W. Kienzle, C. Lechanoine, B. Levrat, B.C. Maglic, M. Martin, P. Schübelin, G. Chikovani, M. Fisher, P. Grieder, H.A. Neal and C. Nef, Nuclear Phys. B3, 435 (1967).

58. A. Forino, R. Gessaroli, L. Lendinara, G. Quareni, A. Quareni-Vignudelli, A. Romano, J. Laberrigue-Frolow, J. Guinquard, M. Sené, W. Fickinger, O. Goussu and A. Rogozinski, Phys. Letters 19, 65 (1965).

59. N. Armenise, B. Gludini, V. Picciarelli, A. Romano, A. Silrestri, A. Forino, R. Gessaroli, L. Lendinara, G. Quarini, A. Quarini-Vignudelli, A.M. Cartacci, M.G. Dagliana, G. di Capariacco, M. Barrier, J. Laberrigue-Frolow, J. Guinquard, M. Sené and J. Loskiewicz, Nuovo Cimento 54 B, 999 (1968).

60. M. Goldberg, F. Judd, G. Vegni, H. Winzeler, P. Fleury, J. Huc, R. Lestienne, G. de Rosny, R. Vanderhaghen, J.F. Allard, D. Drijard, J. Henessy, R. Huson, J. Six, J. Veillet, A. Lloret, P. Musset, G. Bellini, M. di Corato, E. Fiorini, P. Negri, M. Rollier, J. Crussard, J. Ginestet and A.H. Tran, Phys. Letters 18, 354 (1965).

61. D.J. Crennell, P.V.C. Hough, G.A. Kalbfleisch, K.W. Lai, J.M. Scarr, T.G. Schumann, I.O. Skillicorn, R.C. Strand, M.S. Webster, P. Baumel, A.H. Bachman and R.M. Lea, paper 148 and Phys. Rev. Letters 18, 323 (1967).

62. T.F. Johnston, J.D. Prentice, N.L. Steinberg, T.S. Yoon, A.F. Garfinkel, R. Morse, B.Y. Oh and W.D. Walker, Phys. Rev. Letters 20, 1414 (1968).

63. A. Cnops et al., paper 210.

64. J.A. Poirier, N.N. Biswas, N.M. Cason, I. Derado, V.P. Kenney, W.D. Shephard, E.H. Synn, H. Yuta, W. Selove, R. Ehrlich and A.L. Baker, Phys. Rev. 163, 1462 (1967).

65. N. Armenise et al., paper 412.

66. K. Boesebeck, M. Deutschmann, G. Kraus, R. Schulte, H. Weber, C. Grote, K. Lanius, S. Novak, E. Ryseck, M. Bardadin-Otwinowska, H. Böttcher, T. Byer, V.T. Cocconi, E. Flaminio, J.D. Hansen, G. Kellner, U. Kruse, M. Markytan, D.R.O. Morrison and H. Töfte, Nuclear Phys. B4, 501 (1968).

67. T. Ferbel, Proc. Philadelphia Conference on Meson Spectroscopy, Philadelphia (to be published by Benjamin, N.Y., 1968), p. 349.

68. N.N. Biswas, N.M. Cason, A.R. Dzierba, T.H. Groves, V.P. Kenney, J.A. Poirier and W.D. Shephard, Phys. Rev. Letters 21, 50 (1968).

69. C. Caso, F. Conte, G. Tomasini, D. Corels, J. Diaz, P. van Handel, L. Mandelli, S. Ratti, G. Vegni, P. Daronian, A. Daudin, B. Gaudois, C. Kochowski and L. Mosca, Nuovo Cimento 54, 983 (1968).

70. J. Ballam et al., Proc. Heidelberg Inter. Conf. on Elementary Particles, 1967 (North Holland, Amsterdam, 1968), p. 50.

71. I.A. Vetlitsky, V.M. Guszavin, G.K. Kliger, V.Z. Kolganov, A.V. Lebedev, G.S. Lomkazi, V.T. Smoljankin, A.P. Sokolov and E.A. Sisoev, Phys. Letters 21, 579 (1966).

72. J.W. Lamsa, N.M. Cason, N.N. Biswas, I. Derado, T.H. Groves, V.P. Kenney, J.A. Poirier and W.D. Shephard, Phys. Rev. 166, 1995 (1968).

73. M. Ioffredo et al., paper 37.

74. J. Bartsch et al., paper 458.

75. N. Armenise, R. Gessaroli, L. Lendinara, G. Quareni, A. Quareni-Vignudelli, A. Cartacci, M.G. Dagliana, G. Di Caporiacco, G. Porrini, M. Barrier, J. Laberrigue-Frolow and J. Guinquard, Phys. Letters 26 B, 336 (1968).

76. P. Mason et al., paper 645.

77. G.P. Yost et al., paper 65.

78. J.A. Danysz, B.R. French, V. Simak, Nuovo Cimento 51, 801 (1967).

79. R. Donald et al., paper 323.

80. J.A. Danysz, B.R. French, J.B. Kinson, V. Simak, J. Clayton, P. Mason, H. Muirhead and P. Renton, Phys. Letters 24 B, 309 (1967).

81. C. Caso et al., paper 325.

82. M.N. Focacci, W. Kienzle, B. Levrat, B.C. Maglic and M. Martin, Phys. Rev. Letters 17, 890 (1966).

83. J. Bartsh et al., paper 464.

84. P. Antich et al., paper 493.

85. G. Bassompierre, Y. Goldschmidt-Clermont, A. Grant, V.P. Henri, I. Hughes, B. Jongejans, R.L. Lander, D. Linglin, F. Muller, J.M. Perreau, I. Saitov, R.L. Sekulin, G. Wolf, W. De Baere, J. Debaisieux, P. Dufour, F. Grard, J. Heughebaert, L. Pape, P. Peeters, F. Verbeure and R. Windmolders, Phys. Rev. Letters 26 B, 49 (1967).

86. D. Cline et al., paper 287.

87. D. Caro et al., paper 122.

88. Z. Ma et al., paper 186.

89. W. Beusch et al., paper 520.

90. G. Alexander, A. Firestone, G. Goldhaber and B.C. Shen, Phys. Rev. Letters 20, 755 (1968).

91. G. Bassompierre et al., paper 448.

92. Birmingham-Glasgow-Oxford Collaboration, paper 500.

93. J. Berlinghieri et al., paper 16.

94. R. Cool, G. Giacomelli, T.F. Kycia, B.A. Leontic, K.K. Li, A. Lundby and J. Teiger, Phys. Rev. Letters 17, 102 (1966).

95. K. Myklebost, private communication.

96. J. Bartke, O. Czyzewski, J.A. Danysz, A. Eskreys, J. Loskiewicz, P. Malecki, J. Zaorska, K. Eskreys, K. Juszczak, D. Kisielewska, W. Zielinski, G. Pichon and M. Rumpf, Phys. Letters 24 B, 118 (1967).

97. H. Goldberg, Phys. Rev. Letters 21, 778 (1968).

DISCUSSION

SELOVE: Regarding the $\pi\pi$ system near a mass of 700 MeV there is a later result than the one you reported by Gutay et al. from Purdue. A Chew-Low extrapolation analysis has been made for the first time for the $\pi^-\pi^+$ system, using a large collection of data. The results, which are subscribed to by Gutay and Miller of Purdue, along with authors from other laboratories included in the collaboration, are reported in a late contribution to this meeting. They give rather convincing evidence that the T = 0 S-wave phase shift does in fact rise through 90° near 750 MeV more or less rapidly. The effective width is about 100 MeV, although the behaviour is not symmetrical. An additional aspect of the results is that the ambiguity allowing the possible set III solution you showed is removed, and that solution is excluded.

FRENCH: If the width is 100 MeV it is surprising, that it is not seen in the $\pi^0\pi^0$ mass spectrum. To my mind, that is evidence against it having a narrow width.

WALKER: Concerning the S-wave I = 0 phase shift: if a relatively narrow resonance exists with mass $\sim$ 700-750 MeV, then one expects a shoulder in the $\pi^0\pi^0$ spectrum slightly above 750 MeV. Two experiments have been done at Wisconsin, on the $\pi^0\pi^0$ system. We find no such shoulder. Thus we feel there is evidence against the upper family of phase shifts (up-up family).

ZICHICHI: In connection with the five unambiguously identified $\gamma\gamma$ events in the X^0-mass region, I would like to point out that this result is also relevant in order to discriminate between linear or quadratic mass formulae for mesons.

If we use a current-algebra calculation of Baracca and Bramon, our result implies that the quadratic mass formula is favoured with respect to the linear one by a factor of about fifteen to one.

I thought this point was worth mentioning, as this is the first evidence in favour of the validity of quadratic mass formula for mesons.

RATTI: I have two comments: one on the A_1, the other on the 1.7 GeV region in 4π.

Although I agree that the A_1 has not yet a compelling world-wide evidence at 11 GeV/c, the A_1 has been seen in

$$\pi^- p \rightarrow p\pi^+\pi^-\pi^-$$
$$p\pi^-(MM)^0$$
$$n\, 2\pi^+ 2\pi^-$$

at the same position, 1.08 MeV, and with a reasonable width. I would like to stress the danger of compilations. The same washing-out effect could arise in the high-multiplicity events.

The comment on the 4π mass region around 1.7 is the following: from the π data of the Genova-Hamburg-Milano-Saclay Collaboration at 11 GeV/c, it is very unlikely that the $\omega\pi$ and the $\rho\pi\pi$ enhancements are the same. The $\omega\pi$ enhancement is fairly narrow at 1630 MeV with Γ = 60 MeV, while the $\rho\pi\pi$ is broad and centred at 1700 MeV.

CHEW: The concept of "Deck background" should probably not be used in resonance analysis. There exists here exactly the same question of duality that was discussed in the report of Chan. Part of the resonance effect is included in the Deck formula. It would be better for experiments to forget the Deck effect in analysing spectra and to estimate background by old-fashioned methods.

VAN DER VELDE: I would like to take slight exception to your pronouncement that the H meson is "dead" and file a minority report.

First of all, let me point out that there have been no new experiments to look for the H in the reaction in which we saw it, namely, $\pi^+ d$ at 3.5 GeV/c (Phys. Rev. Letters, June 1966).

Secondly, as regards bumps in spectra produced by ρ cuts, we properly took this effect into account in our paper, and found it was not able to explain the data. In doing this we multiplied the independently-estimated 3π phase space by the Dalitz plot fraction curves. It is incorrect to multiply the DPF curves times the observed 3π spectrum, as the California-Riverside Group has done (Phys. Rev. Letters, June-July 1968), since we can "explain" any resonance this way, provided only that its Dalitz plot is approximately uniform. One could in fact cast serious doubt on the existence of the ω^0 by their method.

Thirdly, it is true that the $X^0 \to \pi^+\pi^-\gamma$ branching fraction has increased somewhat since our data were published, so that the possible confusion in our data with this mode is more serious. This has been pointed out by Barbaro-Galtieri and Söding (Philadelphia Meson Conference, April 1968). However, I would point out that in the $X^0 \to \pi^+\pi^-\gamma$ decay the events tend to be near the top of the Dalitz plot, and there was no evidence for such a concentration in our data.

Fourthly, one still has the problem of the mass shift if one wants to attribute the H effect to the $X^0 \to \pi^+\pi^-\gamma$. The H mass we saw was 1000 MeV, whereas the X^0 is 960. A part of this may be due to the incorrect fitting of a π^0 in place of the γ, as Galtieri and Söding have pointed out. However, the main mass shift in their data came from the fact that they did not measure the spectator for $\sim$ 2/3 of their events, whereas in our data only events with measurable spectators were used.

Thus, I beg your permission for the opinion that the H is not dead, although it is admittedly quite dormant, awaiting, I would hope, further experimental investigation.

FRENCH: I would just like to make one comment. These experiments are chosen because you see an enhancement; this enhances the probability that you could be subject to fluctuations. For example, if you take all the experiments that see a $A_{1.5}$ and add them together, you do in fact have an enhancement. But if you are not biased and take the total data, you get the curves I have shown.

RESONANCES – Experimental 2 $(B = 1, S = 0)$

Chairman	R.L. COOL
Rapporteur	A. DONNACHIE
Discussion Leader	G. VALLADAS
Secretaries	R.G. ROBERTS
	F. WAGNER

NUCLEON RESONANCES

A. Donnachie

University of Glasgow, Glasgow

On the basis of the pion-nucleon phase-shift analyses of groups at Berkeley[1], CERN[2] and Saclay[3], it was possible a year ago to conclude[4,5] that there was evidence for the existence of 19 or possibly 20 resonance states of mass less than 2.2 GeV in the pion-nucleon system. The general procedure used to infer the existence of resonance states is to study the Argand diagram of the function $2qf_\ell$, where f_ℓ is the usual partial wave amplitude

$$f_\ell = \frac{1}{2iq}\left[\eta_\ell\ \ell^{2i\delta_\ell} - 1\right],$$

q being the c.m. momentum. If a resonance exists, then this function will describe a counter-clockwise circle, or an appreciable part thereof, in the Argand diagram. This is easily seen by considering the amplitude to be represented by a Breit-Wigner resonance, or as a Breit-Wigner resonance plus background. Some typical situations are shown in Fig. 1. When there is background present, the resonance circle may be distorted considerably and displaced appreciably from the symmetric position, but the amplitude still retains the general resonance features. The same situation occurs in the case of a partial-wave amplitude in an inelastic process, say, $\pi + N \to K + \Lambda$. If there is a resonance present, then the amplitude will describe an appreciable part of a counter-clockwise circle, more or less distorted according to the background. One difference to be noted in the case of an inelastic amplitude is that the imaginary part of the amplitude is no longer restricted to be positive, as it is in the elastic case, and in general there is an arbitrary phase factor involved.

This general feature of a resonance implying a counter-clockwise circle has led to the inference that a counter-clockwise circle automatically implies a resonance, and this is the criterion which has been used in the phase-shift analyses. It was known, however, that this reversal is not necessarily true; for example it is not difficult to show in multi-channel potential scattering that it is possible to produce

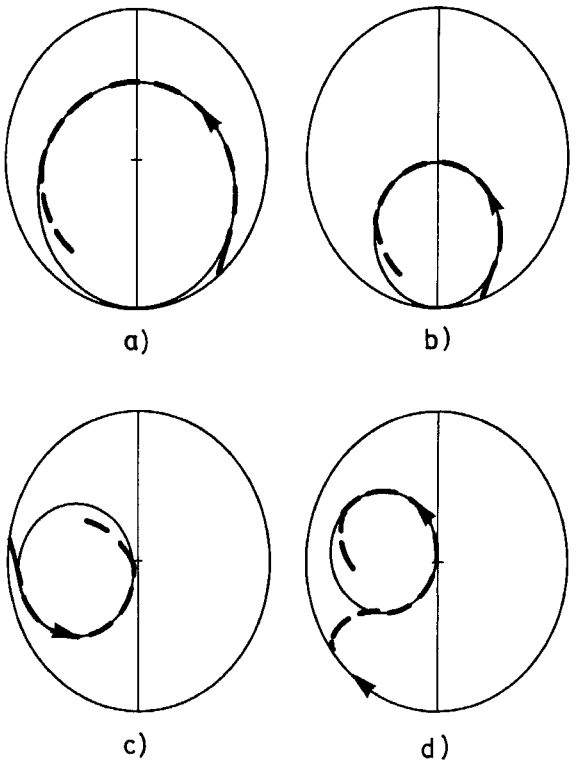

Fig. 1 Typical resonance configurations
a) pure Breit-Wigner, $\Gamma_{el} > 1/2\ \Gamma_{tot}$
b) pure Breit-Wigner, $\Gamma_{el} < 1/2\ \Gamma_{tot}$
c) Breit-Wigner with attractive background
d) Breit-Wigner with repulsive background.

resonance-type circles in any given channel without requiring that there be a resonance. In this context, it is important to recall that "resonance" is synonymous with "a pair of second sheet poles". This point has been given considerable prominence recently, following Schmid's[6] comment that the partial wave projections of Regge-pole amplitudes freely exhibit resonance-type circles, and give at least a qualitative representation of the structure observed in the phase-shift analyses, but explicitly do not have any

second sheet poles. There is now a variety of opinion on this topic[7-9], but its significance, or lack of it, is still unclear. However, one point is ambiguous. The Regge-pole amplitude is a priori a smooth function of energy and cannot give rise to any peaks in total cross-sections, the various partial-wave peaks combining in just such a way as to produce this smooth result. Now both the T = 3/2 and T = 1/2 total cross-sections show considerable structure. In the former, peaks are associated with $P_{33}(1236)$, $F_{37}(1950)$ and the $S_{31}(1640)$, $P_{33}(1690)$, $D_{33}(1690)$ complex which appears as a shoulder on the lower side of the F_{37} peak. In the T = 1/2 case, peaks are associated with $D_{13}(1520)$, $P_{11}(1470)$ which appears as a shoulder on the lower side of the D_{13} peak, the $D_{15}(1680)$, $F_{15}(1690)$ pair and $G_{17}(2190)$. It is very difficult not to associate a resonance with the observed structure in these partial waves. Further, it is my conviction that all the structure observed in pion-nucleon scattering should be associated with resonances, and it is from this viewpoint that this report is written.

1. $\pi + N \to \pi + N$

The results of two new phase-shift analyses, one from Glasgow[10] and one from CERN[11] confirm most of the structure claimed by CERN I*).

Phase-shift analysis is conventionally tackled in one of two ways. Either an energy-dependent analysis is performed parametrizing the partial-wave amplitudes as functions of energy and fitting to all the data simultaneously, or an energy independent analysis is performed, searching extensively at each energy for different solutions and then using continuity between adjacent energies to select among the solutions found. The former approach is a practical one if the number of partial waves is not too great, and if the energy range is sufficiently limited, and it was applied with considerable success in the early days of pion-nucleon phase-shift analysis when these conditions were reasonably well satisfied. In the latter case, imposing continuity is a very serious problem, and sophisticated techniques have been developed to handle it. In the CERN I analysis, a complicated iterative procedure was evolved, making use of partial-wave dispersion relations[12]. In the Berkeley analysis the "shortest-path" technique was developed and used successfully[13]. This is to find the smallest value of the quantity

$$X(k_1, k_2, \ldots) = \left\{ \sum_{i,\ell,j,T} \left(j + \tfrac{1}{2}\right) \left| f_i^{(k_i)}(\ell,j,T) - f_{(i-1)}^{(k_{i-1})}(\ell,j,T) \right|^2 \right\}^{\frac{1}{2}},$$

where $f_i^{k_i}(\ell,j,T)$ is the k^{th} solution at the i^{th} energy for the partial-wave amplitude with orbital angular momentum ℓ, total angular momentum j and isospin T. This technique can be considered as a "resonance eraser", naturally preferring not to go round resonance loops if they can be possibly avoided, i.e. it gives a lower bound on the possible structure.

In the CERN II analysis, this technique has been applied to π^+p scattering, and the results are shown in Fig. 2. The π^+p shortest path is unique up to 1821 MeV (solid line) and qualitatively unique to ∿1950 MeV, the main ambiguity being in the position of the F_{37} resonance. There are still only five branches at 2025 MeV and the dashed continuation shown is the shortest of all. The dotted line in these figures is the dispersion relation fit of CERN I, and is clearly very similar to the shortest path, i.e. the purely experimental lower bound on the amount of structure, as given by the shortest path, is very close to the previous theoretically-favoured dispersion relation fit for π^+p. As in the CERN I analysis, the only structure which appears at all dubious is the D_{35} (∿1950). However, it should be noted that the existence of the $P_{33}(1688)$ structure depends on the experiments at a single energy. It is present if only good solutions are accepted at 1688 MeV (double dot-dashed line), but is absent if the shortest path is allowed to pass through a solution with $P(\chi^2) < 0.001$ (solid line). More π^+p experiments in this region would be valuable. In some solutions there is some evidence for a possible P_{33}(∿2030), but it is not conclusive.

*) To avoid confusion, we shall denote the 1967 CERN analysis[2] by CERN I and the 1968 CERN analysis[11] by CERN II.

The method of search used in the Glasgow analysis was a hybrid one, in which the energy range was broken down into intervals of about 100 MeV and a quadratic energy dependence assumed for the phases and elasticities in each range. The fits were overlapped from range to range, each successive solution, being tied to the last, or the second last point of the previous one. The energy ranges chosen are sufficiently small for the restriction to a quadratic approximation not to be a serious handicap. The amplitudes so obtained, which still contain some awkward corners, were then smoothed further by fitting energy dependent forms to them, the choice being a multichannel Breit-Wigner resonance[14] superimposed on a smooth background. Two results were obtained by this procedure, which are qualitatively very similar not only to each other but also to CERN I. The main differences are that the Glasgow results do not have the $D_{35}(\sim 1950)$, $D_{13}(\sim 1700)$, $D_{13}(\sim 2030)$ and $F_{17}(\sim 1980)$. In fact they change the parity of this last one, and make it $G_{17}(1906)$. CERN I also found some structure in G_{17} at about this mass, but put it down to bad charge-exchange data. This appears to be the most probable explanation and this ambiguous F_{17}/G_{17} structure should not be considered seriously for the present. The evidence of structure obtained in the various phase-shift analyses is summarized in Table 1. From this, it is clear that $D_{35}(1950)$, $D_{13}(1730)$, $F_{17}(1900)$ and $D_{13}(2030)$ are in a precarious state, at least as far as the phase-shift analyses are concerned. Of these four, there is no real evidence elsewhere for $D_{35}(1950)$ and $F_{17}(1980)$, and consequently these two should be rejected, at least for the present. There is some evidence elsewhere for both $D_{13}(1730)$ and $D_{13}(2030)$, particularly the former, so we shall retain both.

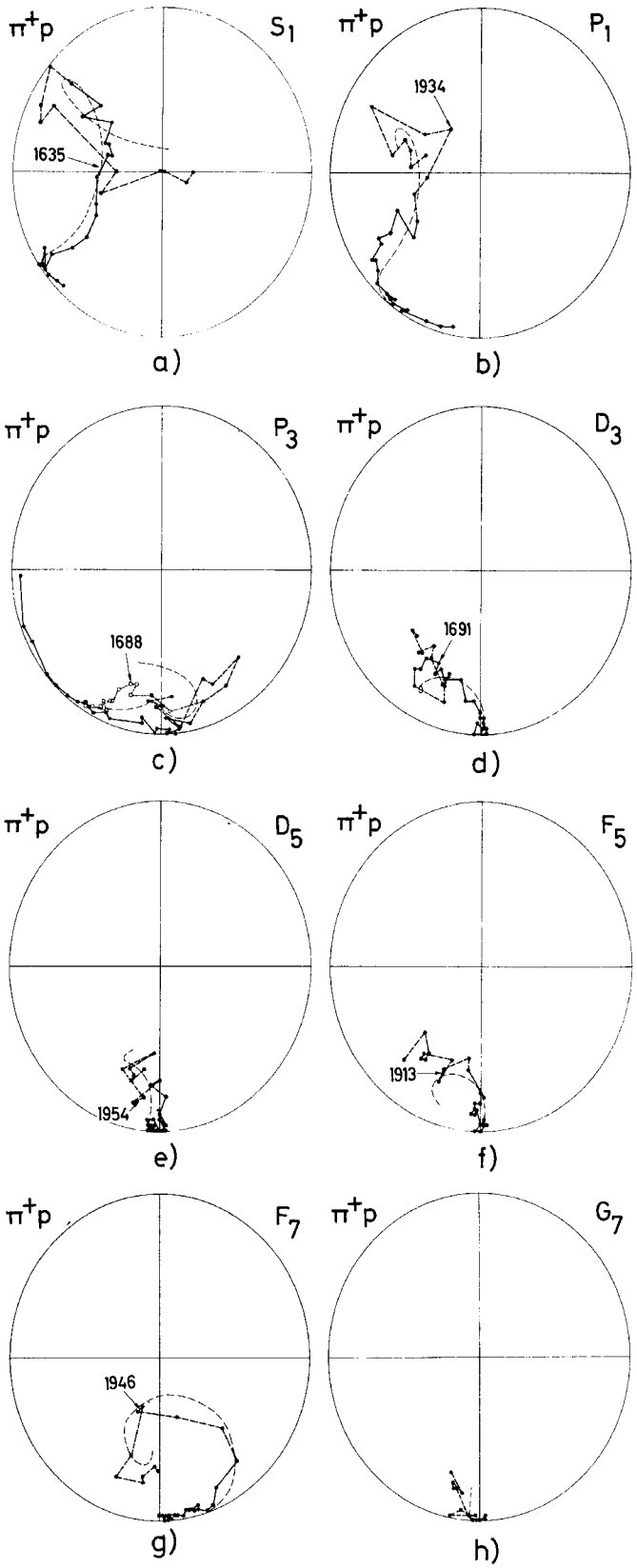

Fig. 2 T = 3/2 pion-nucleon amplitudes. Comparison of CERN I[12] dispersion fit (smooth dot-dash line) with CERN II[11] shortest path.

The proposed structure for this year is shown in Table 2, with the masses, widths and elasticities taken from CERN I and Glasgow (A) and (B) solutions. The variation in the resonance parameters quoted gives some indication of the uncertainties inherent in extracting these parameters from Argand diagrams. This point seems little known, and it is worth stressing. There are three basic causes of these variations. Firstly, different methods of analysis produce somewhat different sets of phase shifts. Secondly, the amplitudes obtained are not smooth with energy, and some smoothing procedure must be applied

before extracting the resonance parameters. There is no "correct" way of doing this, and different choices of smoothing functions will produce somewhat different smoothed results, even starting with the same set of experimental amplitudes. Thirdly, having obtained a smooth plot it is necessary to specify some criterion to separate resonance from background, and different criteria produce, once again, somewhat different results. It is notable that the Argand diagrams of the three solutions quoted differ by much less than would be expected from the differences of their resonance parameters.

All the phase-shift analyses reported above support, to a greater or lesser extent, the structure proposed by CERN I. However, there is the possibility that a qualitatively different solution has been found at Berkeley[15] which contains very little of this structure. This result is still highly provisional and there are some serious objections to it, particularly with respect to the renormalization of some of the experiments (which is allowed in the fit), which in some cases appears to be excessive and with respect to the structure in the solution, which in some amplitudes is extremely rapid, being of the

TABLE 1

Conjectured pion-nucleon resonance assignments below 2.2 GeV mass, with the status of the corresponding structure observed in the five most recent phase-shift analyses.

Possible resonances	Berkeley[1]	CERN I[2]	Saclay[3]	Glasgow[10]	CERN II[11]
$P_{33}(1236)$		We will not argue about this one			
$S_{31}(1640)$	Definite	Definite	Definite	Definite	Definite
$D_{33}(1690)$	Possible	Possible	Ambiguous	Definite	Definite
$P_{33}(1690)$	Probable	Probable	Ambiguous	Possible	Definite
$F_{35}(1910)$	Probable	Probable	Ambiguous	Definite	Definite
$P_{31}(1930)$	Probable	Probable	Ambiguous	Definite	Definite
$F_{37}(1950)$	Definite	Definite	Definite	Definite	Definite
$D_{35}(1950)$	Doubtful	Doubtful	Ambiguous	No	Possible
$P_{11}(1470)$	Definite	Definite	Definite	Definite	-
$D_{13}(1520)$	Definite	Definite	Definite	Definite	-
$S_{11}(1550)$	Definite	Definite	Definite	Definite	-
$D_{15}(1680)$	Definite	Definite	Definite	Definite	-
$F_{15}(1690)$	Definite	Definite	Definite	Definite	-
$S_{11}(1710)$	Definite	Definite	Definite	Definite	-
$D_{13}(\sim1730)$	No	Use imagination	No	No	-
$P_{11}(1750)$	No	Possible	No	Definite	-
$P_{13}(1860)$	No	Possible	No	Definite	-
$F_{17}(1980)$	No	Doubtful	No	Transferred to G_{17}	-
$D_{13}(\sim2030)$	No	Probable	No	No	-
$G_{17}(2190)$	Ambiguous	Definite	-	-	-

"hairpin" variety. It has to be studied in much more detail before it can be entertained as a serious alternative.

Experimentally there has been little to offer in elastic pion-nucleon scattering, the only results presented at the Conference being 12 different $\pi^- p$ cross-sections in the mass range 1500 to 1770 MeV. There are still some serious experimental shortages in the mass range being considered, i.e. below 2.2 GeV. $\pi^+ p$ and $\pi^- p$ differential cross-sections are adequate almost everywhere, except in the 1690 MeV region as noted above, and so is $\pi^- p$ polarization. $\pi^+ p$ polarization data are rather thinly spread and it would be desirable to have more. The information

TABLE 2

Resonances observed in pion-nucleon scattering with a mass of less than 2.2 GeV. The masses, widths and elasticities conjectured in the CERN I[2] analysis and the two results of the Glasgow[10] analysis are shown, together with the "average". In forming this "average", the two Glasgow results were first combined together, and then taken with the CERN I analysis. The differences in the resonance parameters give some guide to the uncertainty in extracting these numbers from Argand diagrams.

Partial wave	CERN I			Glasgow (A)			Glasgow (B)			Composite		
	Mass	Γ_{tot}	Γ_{el}/Γ_{tot}	Mass	Γ_{tot}	Γ_{el}/Γ_{tot}	Mass	Γ_{tot}	Γ_{el}/Γ_{tot}	Mass	Γ_{tot}	Γ_{el}/Γ_{tot}
P_{33}	1236	125	1.00	1238	120	1.00	1238	120	1.00	1237	122.5	1.00
S_{31}	1640	177	0.28	1617	141	0.28	1623	140	0.25	1630	160	0.27
D_{33}	1690	269	0.14	1649	188	0.12	1650	174	0.13	1670	225	0.13
P_{33}	1690	281	0.10	-	-	-	-	-	-	1690	280	0.10
F_{35}	1910	350	0.16	1841	136	0.20	1852	150	0.19	1880	250	0.18
P_{31}	1930	339	0.30	1914	290	0.18	1843	231	0.24	1905	300	0.25
F_{37}	1950	221	0.39	1935	196	0.51	1935	212	0.39	1940	210	0.42
P_{11}	1470	211	0.66	1462	391	0.49	1436	224	0.46	1460	260	0.57
D_{13}	1520	114	0.57	1512	106	0.45	1512	125	0.49	1515	115	0.52
S_{11}	1550	116	0.33	1502	36	0.36	1499	53	0.35	1525	80	0.34
D_{15}	1680	173	0.39	1669	115	0.50	1667	115	0.43	1675	145	0.43
F_{15}	1690	132	0.68	1685	104	0.54	1684	123	0.54	1690	125	0.61
S_{11}	1710	300	0.79	1766	404	0.56	1671	121	0.51	1715	280	0.66
D_{13}	1730?	?	?	-	-	-	-	-	-	1730?	?	?
P_{11}	1750	327	0.32	1770	445	0.43	1867	525	0.30	1785	405	0.34
P_{13}	1860	296	0.21	1844	449	0.40	1854	307	0.26	1855	335	0.27
D_{13}	2030?	290	0.26	-	-	-	-	-	-	2030?	290?	0.26?
G_{17}	2190	300	0.35	-	-	-	-	-	-	2190	300	0.35

available on π^-p charge exchange is poor, and very scarce above 1900 MeV, and the information on π^-p charge-exchange polarization is nil. This latter process will be the most important one in the immediate future, since it is a very sensitive function of the partial-wave amplitudes. The most important test would be provided by the Wolfenstein parameters R and A, which explicitly contain extra information, although presumably this will remain a theoretician's dream for some years to come. Finally, it would be nice to have two measurements of total cross-sections which agree with each other.

2. $\pi + N \to \eta + N$

The important role which inelastic channels can play in helping to elucidate the pion-nucleon resonance structure is clearly evinced by the analyses of the reaction $\pi^- + p \to \eta + n$ which gave the first tangible proof that the structure observed in the S_{11} pion-nucleon amplitude in the vicinity of the η production threshold is indeed due to a resonance, and is not merely a threshold effect. There have been several such analyses, and they are typified by that of Davies and Moorhouse[16], where earlier references may be found. The experimental angular distributions show considerable anisotropy not far above threshold and the nearness of the $D_{13}(1515)$ resonance posed the question of whether the η production proceeds mainly through this resonance, the large S-wave being a scattering length effect only, or whether an S-wave resonance really exists. Davies and Moorhouse, using a rather general multichannel effective range formalism, showed that the latter situation was indeed the case, demonstrating explicitly that their solution has second sheet poles. They also found that the S-wave term is so large that the anisotropy can easily be explained by this interfering with a very small D-wave, the $D_{13}(1515)$ having a partial decay width to ηN of less than 1 MeV.

An interesting energy-dependent analysis of all η-production data below 1900 MeV has been carried out by Deans, Holladay and Rush[17]. They assume the existence of all CERN I T = 1/2 resonances and represent the background by the direct and crossed nucleon pole terms. The resonance and pole couplings are varied to fit the data, but no attempt is made to vary the resonance positions or widths, the level of data not justifying it. Their results are in accord with those of Davies and Moorhouse, with a strong $S_{11}(1525)$ and a small, but non-zero contribution from $D_{13}(1515)$, which cannot seriously be separated from background. They also find non-negligible contributions from $S_{11}(1785)$, which of course, do not contribute close to threshold. All other resonance couplings are consistent with zero.

Some measurements of the reaction $\pi^+ + n \to \eta + p$ are now available[18] near threshold. The variation in cross-section and the production angular distributions are quite in accord with the charge symmetric reaction $\pi^- + p \to \eta + n$.

3. $\pi^- + p \to K^0 + \Lambda^0$

Deans, Holladay and Rush[17] have also analysed this reaction in terms of the CERN I T = 1/2 resonances. In this case the background was represented by the direct channel nucleon pole, the crossed channel Σ pole and a t-channel K^* pole, with vector and tensor coupling. Their analysis takes in all data below 1850 MeV mass, and shows clearly the dominance of the $S_{11}(1710)$ and the D_{11} partial wave, this being shared out between $P_{11}(1460)$ and $P_{11}(1785)$. There are also possible contributions from $P_{13}(1855)$ and the D_{13} partial wave.

Lovelace, Wagner and Iliopoulos[19] have also looked at this process, applying the random search plus shortest path technique to all data below 2025 MeV. Some use was made of the pion-nucleon phase-shift analysis, but only in two respects. Firstly, it was used to determine which partial waves were elastic and could be neglected in this analysis. This turned out to be G_{19} and the H-waves up to 2025 MeV, and F_{17} and G_{17} below 1800 MeV. Because of the waves were retained in the analysis at 1617 MeV, and only S-, P- and D-waves below 1640 MeV. Secondly, the phase-shift analysis was used to find the phase of phase-shift analysis was used to find the phase of those waves containing a Breit-Wigner resonance, i.e. D_{15}, F_{15}. As was mentioned in the Introduction, all partial waves in an inelastic channel can be multiplied by an arbitrary phase factor. However, for a pure Breit-Wigner resonance, the amplitude in any inelastic channel is a real multiple of the ampli-

tude and, since both $D_{15}(1675)$ and $F_{15}(1685)$ have a very regular Breit-Wigner shape in the elastic analysis, it was assumed that the $K\Lambda$ amplitudes for these two waves would be real multiples of the πp up to 1800 MeV. The same assumption was made for G_{17} at higher energies. The real proportionality factors involved were varied in the fit independently at each energy. This is quite different from the analysis of Deans et al.[17], where for each Breit-Wigner the same constant of proportionality was used at all energies. In the case of Lovelace et al.[19], the effect is to reduce the phase ambiguity to a sign ambiguity only. This sign ambiguity was not resolved, and a complete change of sign is possible in one of their solutions. The same is true of the results of Deans et al.[17].

Lovelace et al.[19] find four acceptable solutions, which are shown in Fig. 3. Clearly, the main effect is dominance by S_{11} and P_{11} resonances. There is also some evidence for a smaller resonant contribution from P_{13} or D_{13}, but this is much less clear-cut. In all solutions, the contributions from the D_{15} and F_{15} resonances is very small.

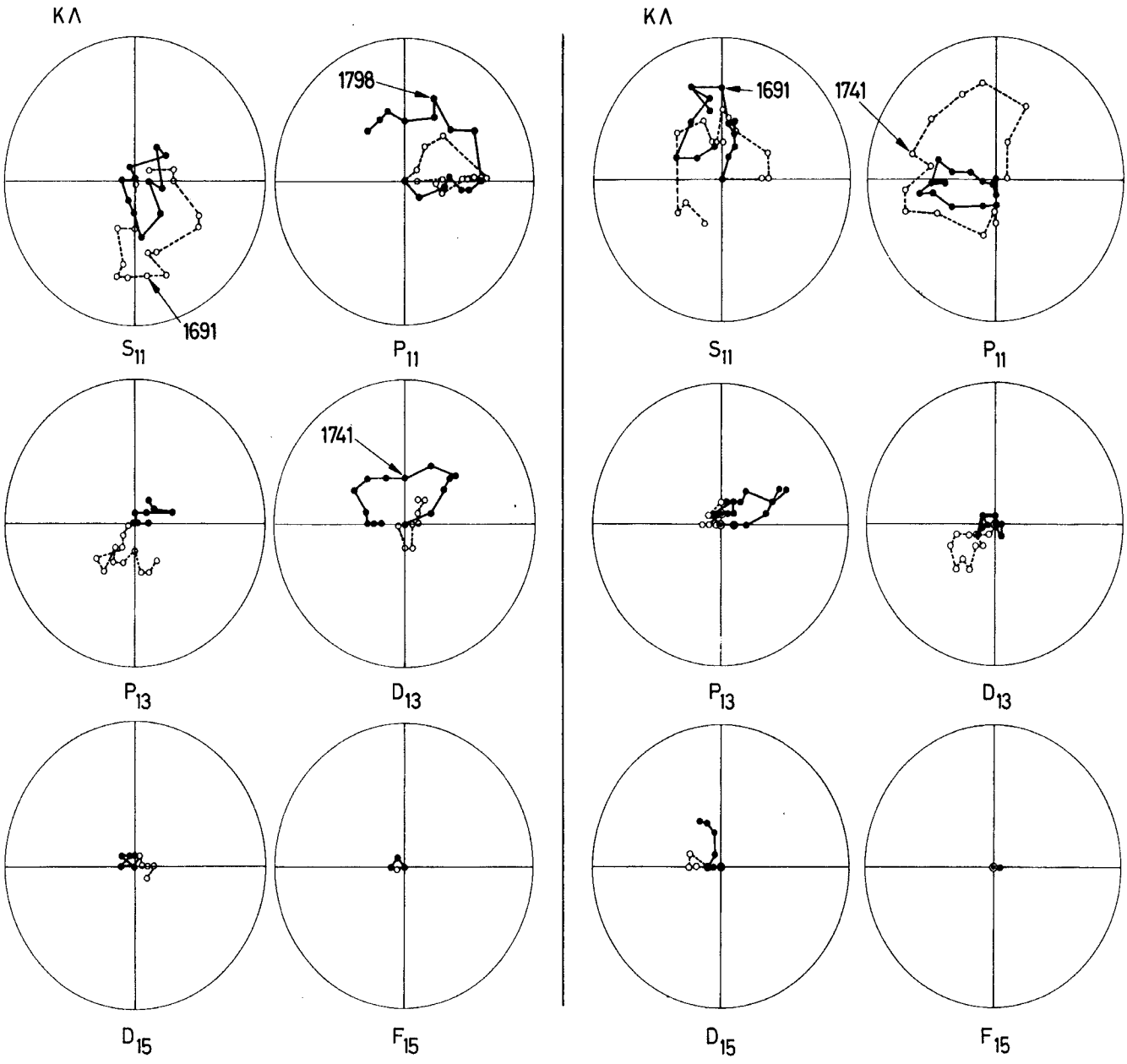

Fig. 3 The four best results of the CERN KΛ analysis. The radius of the circle is half the radius of the unitary circle.

The S_{11} resonance should clearly be identified with the $S_{11}(1715)$, and the P_{11} with the $P_{11}(1785)$. It is also tempting to identify the D_{13}, which appears to have a mass of about 1750 MeV, with the $D_{13}(1730)$, but there is no natural partner for the possible P_{13}, which in $K\Lambda$, if it exists, has a mass of about 1750 MeV, but in πp it has a mass of about 1860 MeV.

The results of Deans et al.[17] and Lovelace et al.[19] are qualitatively very similar, i.e. dominance by the S_{11} and P_{11} partial waves, with some contribution from D_{13}, but there is one apparent difference which should be noted. Deans et al.[17] associate the S_{11} amplitude more with $S_{11}(1525)$ than $S_{11}(1715)$ and the P_{11} amplitude more with $P_{11}(1460)$ than with $P_{11}(1785)$, although both the lower mass resonances are well below the $K\Lambda$ threshold. This can be explained by the fact that, for the resonances, they used a standard Breit-Wigner form, which has a notoriously long tail -- much longer than observed resonances appear to have. The $K\Lambda$ threshold is sufficiently far above the $P_{11}(1460)$ and $S_{11}(1525)$ for this tail to look just like part of the background, which is arbitrary, and to say that they make a large contribution is synonymous with saying that there is a lot of background in $K\Lambda$ in the vicinity of the $S_{11}(1715)$ and $P_{11}(1785)$ resonances. It is obvious by looking at Fig. 3 that there is considerable background. If there were none, the S_{11} and P_{11} resonance circles would be symmetric about the vertical, and they clearly are not. This is yet another example of the resonance/background problem discussed in connection with elastic scattering, and illustrates again the necessity for displaying amplitudes as the result of phase-shift analysis, rather than resonance parameters.

4. $\pi + p \to K + \Sigma$

Lovelace et al.[19] have also studied the preconference data on $\pi^+ + p \to K^+ + \Sigma^+$ up to 1859 MeV, and concluded that the data were not good enough to prove anything.

A measurement of polarization effects in the reaction $\pi^- p \to \Sigma^- K^+$ at 1742 MeV has been made by Edginton et al.[20] who have also attempted an analysis of the three channels $\pi^+ + p \to \Sigma^+ + K^+$, $\pi^- + p \to \Sigma^- + K^+$, $\pi^- + p \to \Sigma^0 + K^0$ up to 1763 MeV. Like Lovelace et al.[19] they found that the data are not good enough to resolve any structure, and the simple parametrization

$$A^{(T)}_{\ell,j} = a^{(T)}_{\ell,j}\, e^{i\psi^{(T)}_{\ell,j}}\, q_\Sigma^{(\ell+\frac{1}{2})}$$

for the partial wave amplitudes is adequate to fit the data.

New data are also available[21] on $\pi^+ + p \to \Sigma^+ + K^+$ at 1856, 1901 and 2016 MeV, and a preliminary analysis has been made at these energies. The angular distributions show no evidence for partial wave higher than F. Since there is a known $\pi^+ p$ resonance, the F_{37}, in this region and the total cross-section (shown in Fig. 4), peaks just in this region, a natural inference is that this will be an important amplitude. With this assumption, a study of the Legendre polynomial coefficients leads Borreani and Kalmus to try the combinations

a) S_{31}, D_{33}, F_{37}

b) S_{31}, P_{31}, D_{35}, F_{37}

c) S_{31}, P_{33}, D_{35}, F_{37}

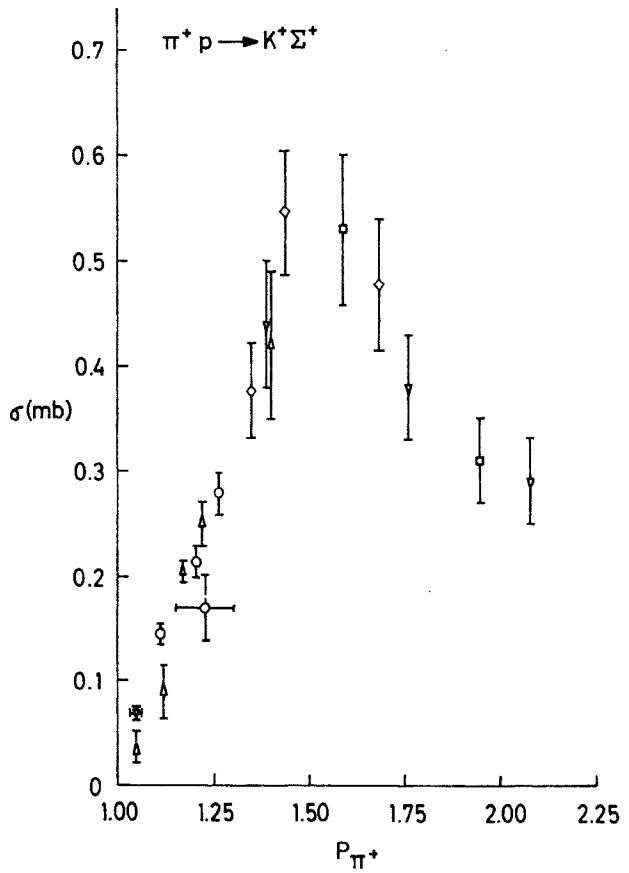

Fig. 4 $\pi^+ p \to K^+\Sigma^+$ total cross-section.

parametrizing background amplitudes by the simple form

$$T = (A + Bk) \exp\{i(c + Dk)\}$$

and using a Breit-Wigner for the resonant amplitudes. The results of the analysis are as yet inconclusive, except to confirm the presence of a strong F_{37}.

5. $\pi + N \to \pi + \pi + N$

Since this is the dominant inelastic channel throughout most of the resonance region, it is clear that a proper understanding of the resonances will not be attained without the inclusion of the three-body channels. This poses a serious problem of analysis. Exactly how should three-body states be treated and how should the results be related to what is known about the elastic amplitudes? The answer has always been to use the isobar model, sometimes blatantly, sometimes discreetly disguised, and until recently inelastic data have not been available in sufficient quantity to warrant anything more sophisticated. This was evident in the analysis of Morgan[22], who applied a generalized version of the isobar model to a study of the T = 1/2 single pion production processes in the range 1450 to 1575 MeV and found that, with the data then available, it was quite unnecessary to go beyond the confines of the isobar model. Morgan's analysis also gave some indication of the value of the information which could be hidden in the three-body data; in particular he suggested that this data required the existence of a second P_{11} resonance, decaying strongly via ρN or $\pi\Delta$ with a mass very roughly between 1500 and 1700 MeV. This suggestion was made simultaneously with, and independently of, the phase-shift analyses of the elastic data finding a second P_{11}, the $P_{11}(1785)$.

New data are now becoming available which will compare favourably in statistical quality with the elastic data, and the time is rapidly approaching when the isobar model will need an appreciable overhaul. In each of the three analyses on which I shall report one of two simplifying assumptions has been made to the isobar model: either that all the three-body events are quasi two-body with negligible background; or there is background but it is incoherent, is given by phase space, and can be removed to leave the "genuine" quasi two-body events. The two assumptions are mutually exclusive and neither is strictly correct. It is unlikely that they will affect the dominant qualitative features obtained in the analyses, since the background is generally estimated to be of the order of 20%-30% at most, but the less dominant features and detailed quantitative features are certainly more in doubt.

A partial wave analysis of the reactions

$$\pi^+ + p \to \pi^+ + p + \pi^0$$
$$\pi^+ + n + \pi^+$$

is being carried out at Saclay, and preliminary results are reported[23] at 1510, 1580, 1640 and 1690 MeV, using the isobar model, with the first of the above two assumptions, in the manner proposed by Deler and Valladas[24] and assuming also that only $\Delta(1236)$ is produced. Only the inelastic angular distributions are used in the fit, and the results are then compared with the three possible invariant mass distributions and with the results of the elastic phase-shift analyses. Agreement is acceptable in the former case, and typical fits are shown in Fig. 5, along with the fitted angular distributions.

The comparison with the elastic data is shown in Fig. 6, where the quantity $\sqrt{1 - \eta^2}$ is plotted. In computing the values from the fitted three-body data, it is necessary to neglect overlap terms, which do not vanish, although generally they appear to be small. The dashed and heavy lines are the values obtained from the CERN I[2] and Saclay[3] analyses. The agreement is acceptable except in the S_{31} amplitude, where it is poor, and it is apparent that the isobar model is breaking down in the simple form in which it has been applied, and that there is background of some kind present. No significant change in the solutions has been found as a result of including production of $P_{11}(1460)$ or the S_{11} attractive interaction in the analysis, and the effect of ρ production is now being investigated.

The same approach has been applied[23] to the reactions

$$\pi^- + p \to \pi^0 + \pi^- + p$$
$$\pi^+ + \pi^- + n$$

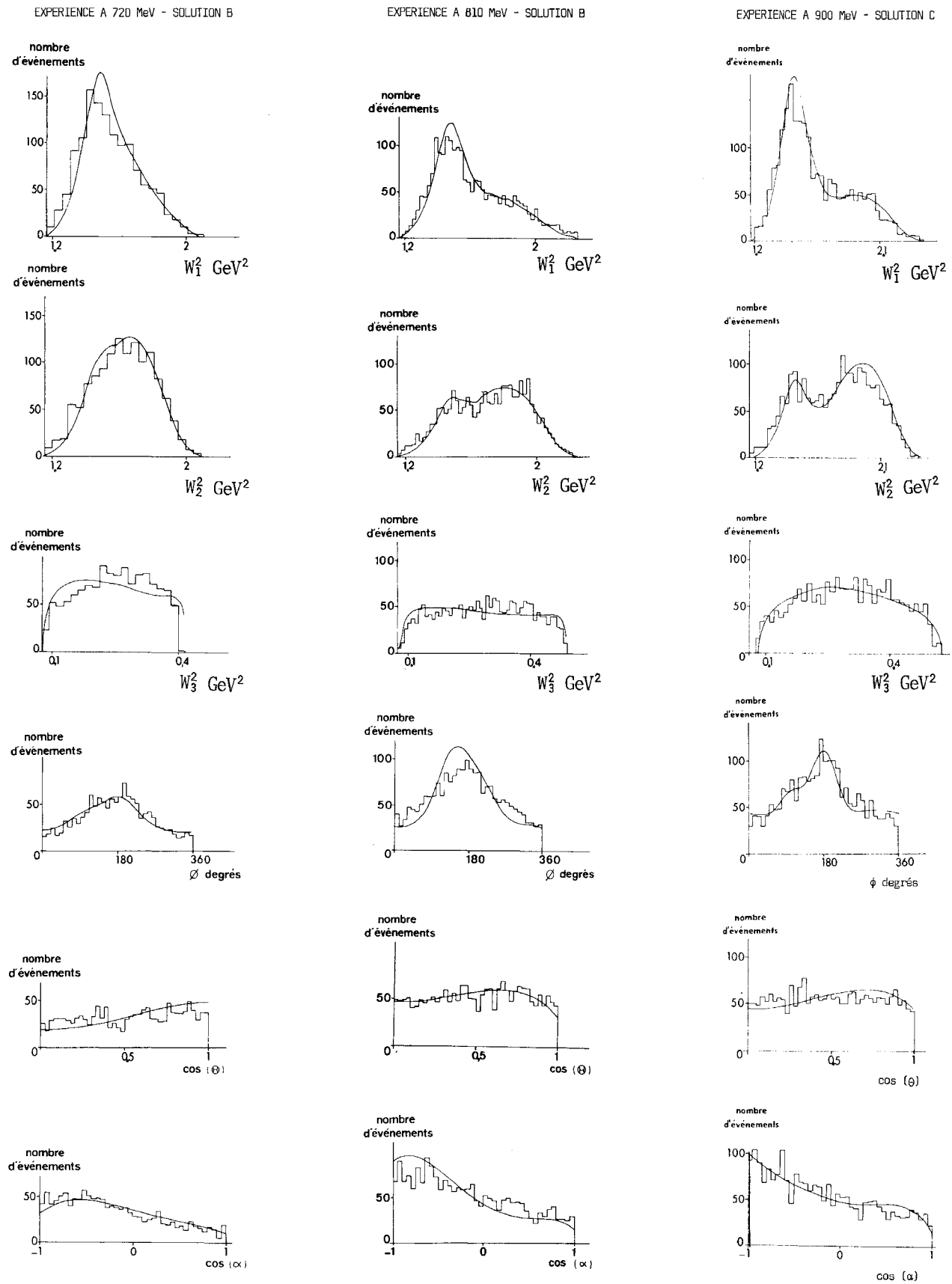

Fig. 5 Comparison of the Saclay[23] fits to $\pi^+ + p \to \pi^+ + \pi^0 + p$ with the experimental histograms at 720 MeV (Brussels), 810 MeV (Saclay) and 900 MeV (Rochester). The variables are as follows:
W_1^2 is the square of the invariant mass of the $(\pi^+ p)$ sub-system,
W_2^2 is the square of the invariant mass of the $(\pi^0 p)$ sub-system,
W_3^2 is the square of the invariant mass of the $(\pi^+\pi^0)$ sub-system,
Θ is the polar angle of the incoming π^+ in the c.m. with respect to the three-body plane,
ϕ is the azimuthal angle of the incoming π^+ in the c.m. system with respect to the three-body plane,
α is the production angle of the nucleon in the c.m. system.

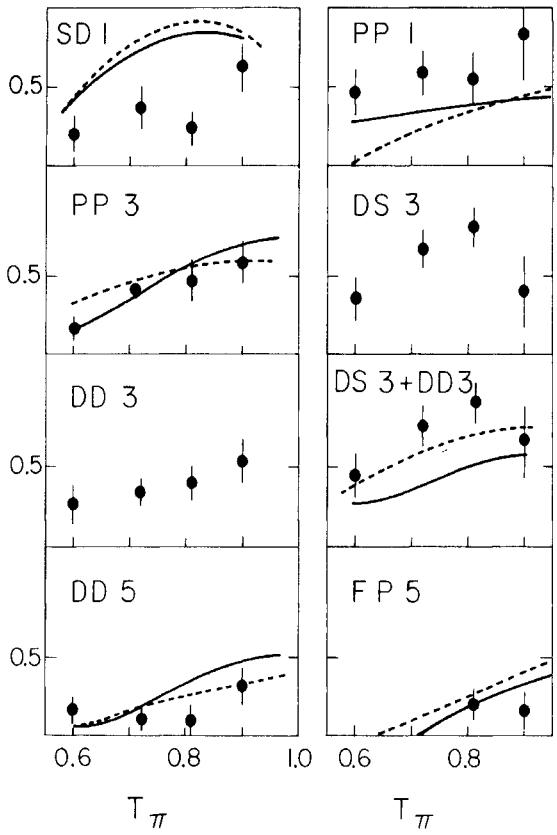

Fig. 6 Comparison of $\sqrt{1-\eta^2}$ from the Saclay[23] fits to inelastic π^+p data and the values obtained from phase-shift analysis. The dotted line is from the CERN I[2] analysis and the solid line from the Saclay analysis[3].

at 1390, 1440, 1485 and 1525 MeV, assuming that the $\pi^0\pi^-p$ final state arises primarily through the {Δ(1236) + π} channel while the $\pi^+\pi^-n$ state involves in addition the {"σ" + n} channel, and the T = 3/2 inelastic channel can be neglected. The results are again in fair agreement with the elastic analyses except for the S_{11} amplitude. The most significant conclusion that they reach is that the partial decay of the $P_{11}(1460)$ into π + Δ(1236) is well established, this resonance decaying in approximately equal parts into πN, σN, πΔ. In common with earlier analyses in this region they find that $D_{13}(1515)$ decays into πΔ with a large branching ratio.

The alternative approach to the isobar model, namely that of making a specific separation of events into quasi two-body and background, has been applied by Brody et al.[25] and Sun Yiu Fung et al.[26].

Brody et al. have studied π^-p interactions at 12 energies between 1500 and 1770 MeV. Their elastic events were used to obtain absolute normalization, normalizing their data with the counter data in the region $-0.8 < \cos\theta < 0.7$, where the elastic cross-sections are rather flat, and checking the result by using the (normalised) forward point. Agreement with the counter data is good. The angular distributions also agree well, and should be a useful piece of extra information for the phase-shift analyses. The reaction $\pi^-p \to \pi^-\pi^+n$ was chosen for detailed analysis since it is dominated by strong $\Delta^-(1236)\pi^+$. This latter channel was separated out explicitly by assuming an incoherent superposition of phase space, together with the channels $\pi^+\Delta^-$, $\pi^-\Delta^+$ and ρ^0n. The best fits to the mass spectra are shown in Fig. 7, which have contributions of 57.6% $\pi^+\Delta^-$, 7.2% $\pi^-\Delta^+$, 0.3% ρ^0n and the rest three-body phase space. The total cross-section for the $\pi^+\Delta^-$ channel is shown in Fig. 8, and it clearly shows an enhancement in the

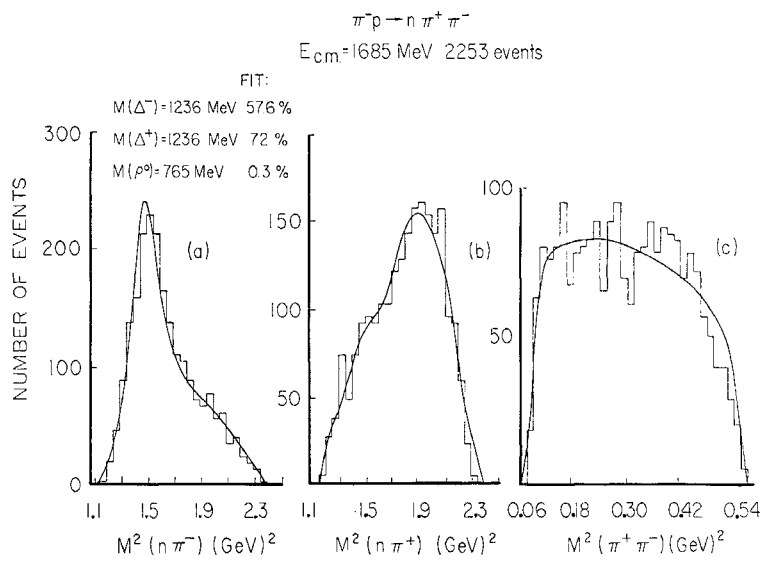

Fig. 7 Maximum likelihood fits to the $\pi^-p \to n\pi^+\pi^-$ data at 1685 MeV.

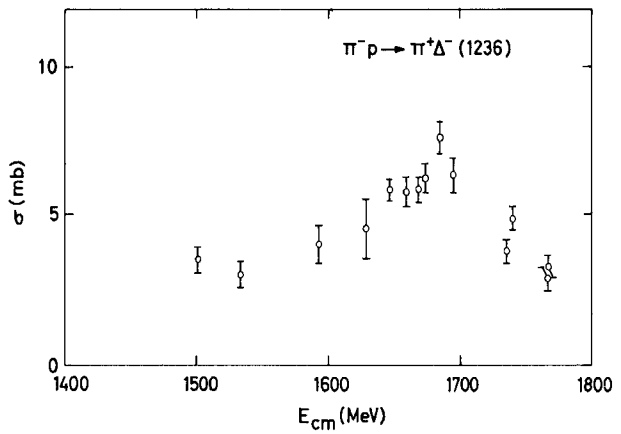

Fig. 8 Total cross-section for $\pi^+ p \rightarrow \pi^+ \Delta^-(1236)$.

region of 1680 MeV, which is presumably associated with $D_{15}(1675)$ and $F_{15}(1690)$. The production angular distributions of the $\pi^+\Delta^-$ channel are shown in Fig. 9 and the corresponding Legendre polynomial expansion coefficients in Fig. 10. The behaviour of the coefficients between 1600 and 1700 is consistent with the presence of the two spin 5/2 resonances, the absense of any dramatic variation of A_1 and A_3 suggesting that the phase difference between these two amplitudes changes very slowly, as is indeed the case in the elastic-scattering data. The behaviour of A_1 and A_2 between 1500 and 1600 MeV, strongly negative but going to zero as the energy increases, implies that the $D_{13}(1515)$ couples in with a negative relative sign to D_{15} and F_{15}. With this as input information, Brody et al. found it possible to obtain a good fit to the data, using the three resonances $D_{13}(1515)$, $D_{15}(1675)$ and $F_{15}(1690)$, parametrized by Breit-Wigner forms, with the addition of a simple

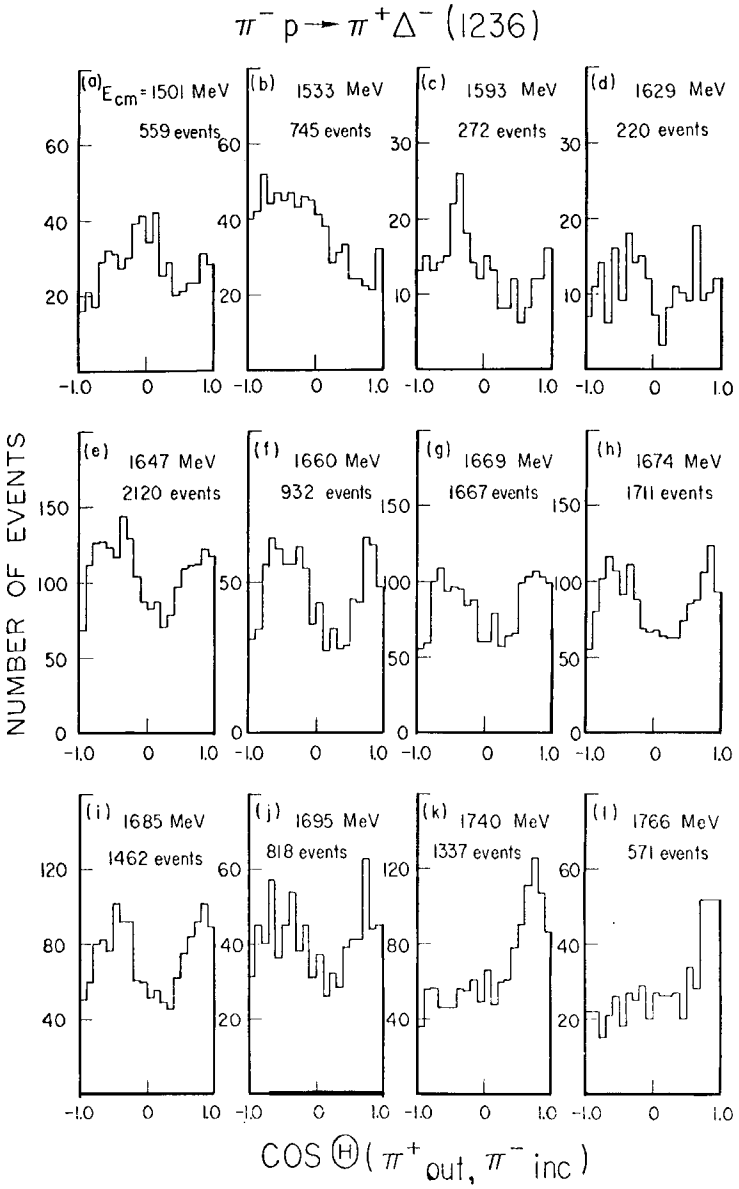

Fig. 9 Centre-of-mass angular distributions for $\pi^- p \rightarrow \pi^+ \Delta^-(1236)$.

$$\pi^- p \longrightarrow \pi^+ \Delta^-$$

$$\frac{d\sigma}{d\Omega} = \Sigma_\ell A_\ell P_\ell \left(\cos \Theta \left[\pi^+_{out}, \pi^-_{inc.}\right]\right)$$

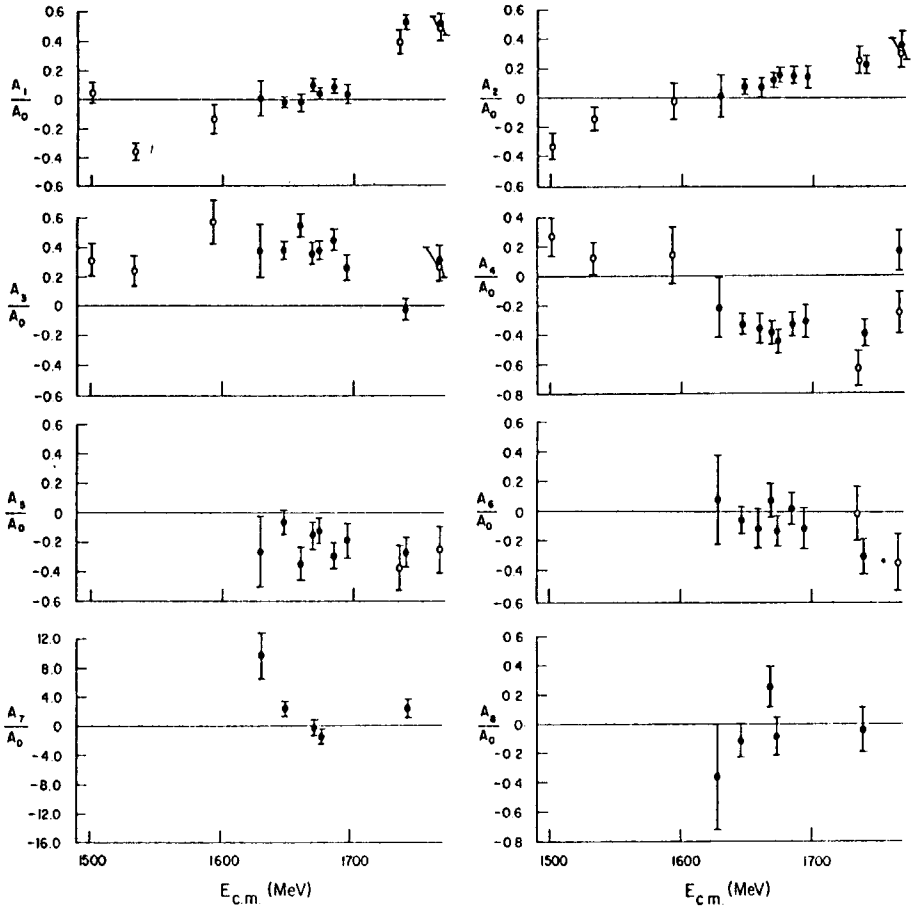

Fig. 10 Coefficients of Legendre polynomial expansion of the c.m. angular distributions of Fig. 9.

linear S-, P-, D- and F-wave background. Using the elasticities of CERN I[2], they obtain the branching fractions

$$\frac{D_{13}(1520) \to \pi\Delta}{\text{All}} \sim 12\%, \qquad \frac{D_{15}(1680) \to \pi\Delta}{\text{All}} \sim 15\%,$$

$$\frac{F_{15}(1680) \to \pi\Delta}{\text{All}} \sim 20\%.$$

Alternative parametrizations are being studied and the fits should not be considered final in any sense. They are, however, a very good guide as to what one may ultimately hope to obtain from these channels.

Sun Yin Fung et al.[26] have adopted a similar approach to the study of the reaction

$$\pi^+ + p \to \pi^+ + p + \pi^0$$

at 1850, 1890, 2010 MeV, and to isolate the channel

$$\pi^+ + p \to \Delta^{++}(1236) + \pi^0$$

using an incoherent superposition of the channel with $\rho^0 + p$, $\Delta^+ + \pi^+$ and three-body phase space. The angular distributions for the $\pi^0\Delta^{++}$ channel are shown in Fig. 11 and the corresponding Legendre polynomial

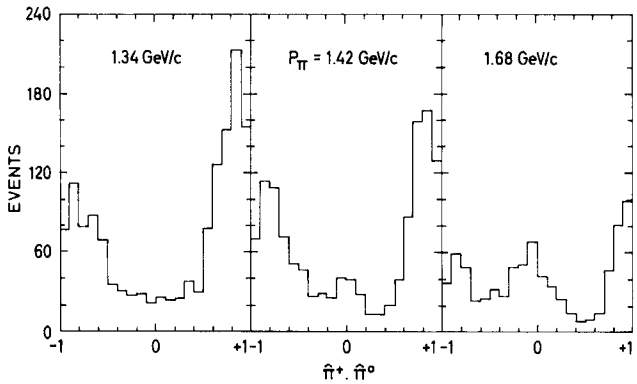

Fig. 11 Centre-of-mass angular distributions for $\pi^+ p \to \pi^0\Delta^{++}(1236)$.

TABLE 3

Coefficients A_n/A_0 obtained by fitting the angular distributions in Fig. 11 with the expansion

$$\frac{d\sigma}{d\Omega} = \lambda^2 \Sigma A_n P_n (\hat{\pi}^+ \cdot \hat{\pi}^0).$$

Momentum (GeV/c)	A_1/A_0	A_2/A_0	A_3/A_0	A_4/A_0	A_5/A_0	A_6/A_0	A_7/A_0
1.34	1.11 ± 0.25	1.35 ± 0.07	0.18 ± 0.10	-0.52 ± 0.09	-0.42 ± 0.13	-0.79 ± 0.11	-0.33 ± 0.13
1.42	1.19 ± 0.26	1.81 ± 0.07	0.40 ± 0.10	-0.65 ± 0.10	-0.43 ± 0.14	-1.74 ± 0.12	-0.27 ± 0.13
1.68	-0.29 ± 0.34	0.57 ± 0.09	0.90 ± 0.14	0.95 ± 0.12	0.22 ± 0.16	-0.86 ± 0.15	0.23 ± 0.17

expansion coefficients are given in Table 3. The large negative A_6 indicates, not surprisingly, that $F_{37}(1940)$ is contributing strongly at all energies. At the present it is difficult to say what other partial waves are contributing appreciably, although D_{35} appears the most likely candidate.

6. $\gamma + N \to \pi + N$

The information on pion-nucleon resonances in photoproduction comes almost entirely from detailed multipole analysis. To date there have been five such analyses, by Schmidt, Schwiderski and Wunder[27], by Chan, Dombey and Moorhouse[28], by Engels, Schmidt and Schwiderski[29], by Walker[30], and by Berends and Donnachie[31]. Analysis of pion-photoproduction is a less objective and a less exact exercise than analysis of elastic scattering, since the data are both less precise and less varied, polarization data in particular being very scarce, and in addition there are many more multipoles than there are partial waves. Consequently, it is not possible to determine weak structural effects, which simply get lost in the background terms, and quantitative precision is lacking. The situation in fact is much the same as in the inelastic channels in πp interactions, and only dominant structure can be seen unambiguously. Resonances in this category are the $P_{33}(1236)$, $S_{11}(1525)$, $D_{13}(1515)$, $F_{15}(1690)$ and $F_{37}(1940)$. The $S_{11}(1525)$ also shows clearly in η-photoproduction[32,33]. The situation with respect to one of the more interesting ones, the $P_{11}(1460)$, is ambiguous. There is some evidence for it, although it is not clear cut and is certainly background-dependent. For example, Berends and Donnachie[31] find two possible solutions, in one of which the transition amplitude to P_{11} is very small and barely distinguishable from zero, and in the other it is quite strong, comparable in magnitude to that of Chan et al.[28], but with the opposite sign. Even at best the production of P_{11} is rather weak, the amplitude, at resonance, for production of P_{11} being not more than one-eighth of the amplitude, at resonance, for production of $P_{33}(1236)$. There is some additional evidence for photoproduction of $P_{11}(1460)$ in a preliminary analysis of $\gamma + p \to p + \pi^+ + \pi^-$ below 1650 MeV by Diambrini Palazzi et al.[34], who conclude that some P_{11} contribution is essential to explain the data.

7. PRODUCTION EXPERIMENTS

Since production experiments are being treated fully in a supplementary report by Rushbrooke[35], only two points which are of special relevance to the N* story will be selected.

The first of these is the continuing accummulation of evidence for the $\pi\Delta$ decay mode of the $P_{11}(1460)$. This is reported in $K^+p \to K^+\pi^+\pi^-p$ at 5.5 GeV/c by Antich et al.[36], in $\pi^+p \to \pi^+p\pi^-\pi^+$ at 16 GeV/c by Ballam et al.[37], in $pp \to pp\pi^+\pi^-$ at 25 GeV/c by Ehrlich et al.[38], in $pp \to pp\pi^+\pi^-$ at 22 GeV/c by Jespersen et al.[39] and in $pp \to pp\pi^+\pi^-$ at 16 GeV/c by Rushbrooke et al.[40]. The second point is further evidence for an enhancement in the vicinity of 1.73 GeV, being seen in the $\pi\Delta$ mode by Rushbrooke et al.[40] and by Ballam et al.[37]. Both of these points are conveniently illustrated in the analysis of Rushbrooke et al.[40], and their $(\pi^-\Delta^{++})$ mass plot is shown in Fig. 12. The cuts in Δ^2 remove Deck background and

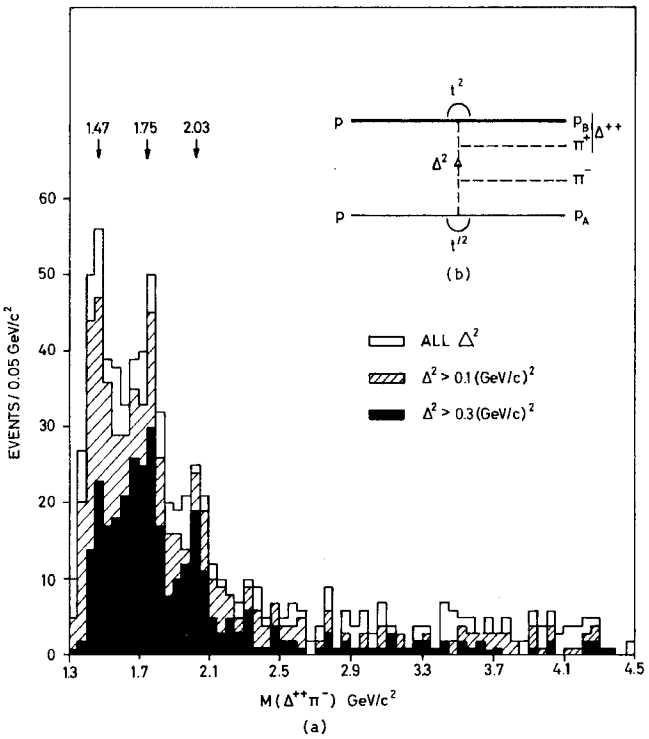

Fig. 12 a) The $m(\Delta^{++}\pi^-)$ spectrum for various Δ^2 cuts in $pp \to pp\pi^+\pi^-$ at 16 GeV/c.
b) Diagram for $pp \to pp\pi^+\pi^-$.

show up the peaks at 1.73 and 2.03 GeV even more clearly. The apparent shoulder on the lower side of the 1.73 enhancement could be associated with the 1.69 D_{15}/F_{15} pair, encouraging the belief that the 1.73 GeV enhancement is indeed something quite different. The peak observed between 1450 and 1500 MeV should be associated with $P_{11}(1460)$, since it is narrower and lower than that indicated by a Deck calculation. The angular distributions in the three peak regions are shown in Fig. 13. That in the $P_{11}(1460)$ region is consistent with isotropy, and the apparent forward peak in the 1.73 GeV enhancement (dotted line) is removed by the cut $\Delta^2 > 0.1$, i.e. by removing the Deck background, leaving a distribution which is symmetrical (and non-isotropic). Thus it is very tempting to associate this peak with $D_{13}(1730)$. A possible candidate for the enhancement at 2.03 GeV is the $D_{13}(2030)$.

The evidence for the pion-nucleon resonances, apart from the phase-shift analyses, is shown in Table 4. None of it by itself is conclusive, but the over-all effect is quite impressive. All the inelastic data are consistent with the resonance assignments of the elastic phase-shift analyses, and in some cases, for example $\pi p \to K\Lambda$, $\gamma p \to \pi p$, many of the resonances are required by the data. The experimental situation is still far from satisfactory, and since it is evident that much information on the pion-nucleon resonances can be gleaned from the inelastic channels, particularly since most of these channels appear to be dominated by small subsets of the isobars, it is to be hoped that the required experimental effort will be forthcoming.

From this, three points stand out. These are the near definite evidence for a strong $\pi\Delta$ decay mode of $P_{11}(1460)$, the accumulating evidence for $P_{11}(1785)$ and, to a somewhat lesser extent, the accumulating evidence for $D_{13}(1730)$.

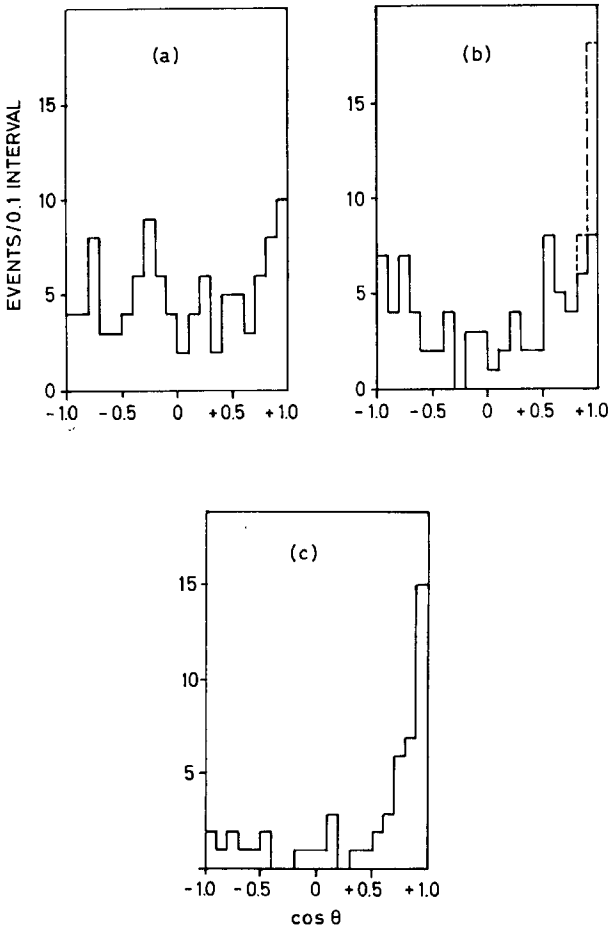

Fig. 13 Angular distributions for the decay of 3-body resonances into a Δ^{++} and π^-.
a) 1.425 GeV/c² < $m(\Delta^{++}\pi^-)$ < 1.525 GeV/c².
b) 1.70 GeV/c² < $m(\Delta^{++}\pi^-)$ < 1.80 GeV/c².
c) 1.80 GeV/c² < $m(\Delta^{++}\pi^-)$ < 1.90 GeV/c².

Finally, it is impossible to resist commenting on the remarkable success attained by the symmetric quark model in classifying the resonances, a point which is discussed in detail by Harari[41]. The situation with respect to the nucleon resonances is shown in Table 5. The only resonance missing in the lowest status is a third P_{33}, and this may well be the possible $P_{35}(2030)$ indicated in the CERN II analysis[11].

TABLE 4

The status of the decay modes of the pion-nucleon resonances observed, other than into pion-nucleon, and the evidence from production experiments. The $P_{11}(1460)$ has a strong σN mode also.

	ηN	$K^0\Lambda^0$	$K^+\Sigma^+$	$\pi\Delta$	ρN	γN	Production
$P_{33}(1237)$						Definite	Definite
$S_{31}(1630)$				Possible			Possible
$D_{33}(1670)$				Possible			
$P_{33}(1690)$				Possible			
$F_{35}(1880)$							
$P_{31}(1905)$							
$F_{37}(1940)$			Probable	Definite	Definite	Definite	
$P_{11}(1460)$				Definite		Probable	Definite
$D_{13}(1515)$				Definite		Definite	
$S_{11}(1525)$	Definite					Definite	Probable
$D_{15}(1675)$				Probable			
$F_{15}(1690)$				Probable		Definite	
$S_{11}(1715)$	Possible	Probable					
$D_{13}(1730)$		Possible					Possible
$P_{11}(1785)$	Possible	Probable		Probable			
$P_{13}(1855)$							
$D_{13}(2030)$							Possible
$G_{17}(2190)$						Possible	

TABLE 5

Classification of pion-nucleon resonances in the ℓ-excitation quark model with parafermi statistics. The empirical rule that only 56, L = $(2n)^+$ and 70, L = $(2n + 1)^-$ supermultiplets are required is obvious. A possible classification of the three resonances in higher levels is:

$$\left.\begin{array}{l} P_{11}(1785) \\ D_{13}(2030) \\ G_{17}(2190) \end{array}\right\} \begin{array}{l} \ell = 4,\ 56,\ L = 0^+ \\ \ell = 3,\ 70,\ L = 3^- \end{array}$$

and the unobserved P_{33} may be filled by the possible $P_{33}(2030)$ reported by the CERN II[11] analysis.

$(1s)^3$	$(1s)^2\ (1p)$	$(1s)^2\ (2s)$, $(1s)^2\ (1d)$, $(1s)\ (1p)^2$		Higher levels
56, L = 0^+	70, L = 1^-	56, L = 0^+	56, L = 2^+	
$8^{1/2}$ $P_{11}(939)$				
$10^{3/2}$ $P_{33}(1237)$				
		$8^{1/2}$ $P_{11}(1460)$		
	$8^{1/2}$ $D_{13}(1516)$			
	$8^{1/2}$ $S_{11}(1525)$			
	$10^{1/2}$ $S_{31}(1630)$			
	$10^{1/2}$ $D_{33}(1670)$			
	$8^{3/2}$ $D_{15}(1674)$			
		$10^{3/2}$ $P_{33}(1690)$		
	$8^{3/2}$ $S_{11}(1714)$			
	$D_{13}(1730?)$			
			$8^{1/2}$ $F_{15}(1687)$	
			$8^{1/2}$ $P_{13}(1855)$	$P_{11}(1785)$
			$10^{3/2}$ $F_{35}(1878)$	
			$10^{3/2}$ $P_{31}(1904)$	
			$10^{3/2}$ P_{33}(unobserved)	
			$10^{3/2}$ $F_{37}(1942)$	
				$D_{13}(2030)$
				$G_{17}(2190)$

REFERENCES AND FOOTNOTES

1. C.H. Johnson, P.D. Grannis, M.J. Hansroul, O. Chamberlain, G. Shapiro and H.M. Steiner, communication to Int. Conf. on Elementary Particles, Heidelberg (1967), by H.M. Steiner.
   C.H. Johnson and H.M. Steiner, UCRL 18001, presented at the Conf. on πN Scattering, University of California, Irvine (1967), by H.M. Steiner.
2. A. Donnachie, R.G. Kirsopp and C. Lovelace, Phys. Letters 26 B, 161 (1968).
3. P. Bareyre, C. Bricman and G. Villet, Phys. Rev. 165, 1730 (1968).
4. C. Lovelace, Proc. Int. Conf. on Elementary Particles, Heidelberg (1967) (North-Holland Publ. Co., Amsterdam, 1968), p. 79.
5. C. Lovelace, CERN preprint TH 839; presented at the Conf. on πN Scattering, University of California, Irvine (1967).
6. C. Schmid, Phys. Rev. Letters 20, 689 (1968).
7. P.D.B. Collins, R.C. Johnson and E.J. Squires, Phys. Letters 27 B, 23 (1968).
8. V.A. Alessandrini, D. Amati and E.J. Squires, Phys. Letters 27 B, 463 (1968).
9. C. Lovelace, paper 258.
10. A.T. Davies and R.G. Moorhouse, paper 925.
11. C. Lovelace and F. Wagner, abstract 254 and paper 255.
12. C. Lovelace, Proc. Roy. Soc. 289 A, 547 (1966).
    A. Donnachie, Particle Interactions at High Energies (Ed. T.W. Priest and L.L.J. Vick) (Oliver and Boyd, Edinburgh, 1967), p. 330.
13. C.H. Johnson, UCRL 17683 (1967).
14. K.T.R. Davies and M. Baranger, Ann. Phys. (NY) 19, 383 (1962).
    C.J. Goebbel and K.W. McVoy, Phys. Rev. 164, 1932 (1967).
15. H.M. Steiner, private communication.
16. A.T. Davies and R.G. Moorhouse, Nuovo Cimento 52 A, 1112 (1967).
17. S.R. Deans et al., paper 479.
18. P.J. Litchfield and J.R. Smith, Rutherford Laboratory preprint.
19. C. Lovelace et al., paper 256.
20. J.A. Edginton et al., paper 207.
21. G. Borreani and G.E. Kalmus, paper 554 and UCRL 18350.
22. D. Morgan, Phys. Rev. 166, 1731 (1968).
23. P. Chavanon et al., paper 947.
24. B. Deler and G. Valladas, Nuovo Cimento 45, 559 (1966).
25. A.D. Brody et al., paper 334.
26. Sun Yin Fung, A. Kernan, G.E. Kalmus and R.W. Birge, paper 555 and UCR-34 P107-72.
27. W. Schmidt, G. Schwiderski and H. Wunder, Proc. Int. Symp. on Electron and Photon Interactions at High Energies, Hamburg (1965) (Ed. G. Höhler et al.) (Deutsche Physikalische Gesellschaft, Hamburg, 1965), Vol. 2, p. 329.
28. Y.C. Chan, N. Dombey and R.G. Moorhouse, Phys. Rev. 163, 1632 (1967).
29. J. Engels, W. Schmidt and G. Schwiderski, Phys. Rev. 166, 1343 (1968).
30. R.L. Walker, CALT 68-158.
31. F.A. Berends and A. Donnachie, paper 556.

32. R.K. Logan and F. Uchiyama-Campbell, Phys. Rev. 153, 1634 (1967).

33. S.R. Deans and W.G. Holladay, Phys. Rev. 161, 1466 (1967).

34. G. Diambrini Palazzi et al., paper 695.

35. J.G. Rushbrooke, Appendix to this report.

36. P. Antich et al., paper 496.

37. J. Ballam et al., paper 335.

38. R. Ehrlich et al., paper 422.

39. R.A. Jespersen et al., paper 948.

40. J.G. Rushbrooke, paper 561.

41. H. Harari, Rapporteur's talk.

DISCUSSION

GREENBERG: I would like to make some remarks about Donnachie's classification of the nucleonic resonances using the parafermi quark model. It is hard to understand why the N(1470), which Donnachie places in a two-quantum excitation, should be lower than the one-quantum excitations. Nelson and I showed that the 3-triplet model can account for all the J^P = = $1/2^+$ and $3/2^+$ states, except for the $P_{33}(1690)$ about which doubt has been raised. Our mass formula gives agreement to within 15 MeV.

SCHLEIN: I would like to comment on a dynamical matter that is of serious concern to those analyses in which one attempts to extract information on the existence of resonances in diffraction dissociation produced systems. In a UCLA-LRL Collaboration result reported to this Conference, we show in a detailed analysis of $pp \to \Delta^{++}p\pi^-$ at 6.6 GeV/c (Colton et al.) that, for low momentum transfers to Δ^{++} and for high $p\pi^-$ mass (that is in the diffraction scattering region), both the shape and absolute magnitude of the $p\pi^-$ spectrum are in quantitative agreement with one-pion-exchange expectations, despite the fact that the $\pi\Delta$ spectrum displays the now well-known features of the $\pi\Delta$ interaction, namely strong N*(1470) production. Our predictions of the $p\pi^-$ mass spectrum are also in agreement with the BNL data on $pp \to p\pi^-\Delta^{++}$ at 28.5 GeV/c. One can thus conclude that it seems incorrect to think in terms of the $\Delta\pi$ spectrum as containing contributions from two separate processes, namely diffraction dissociation production of N*(1470) and a "Deck background". The entire $\Delta\pi$ cross-section is in agreement with OPE (or, if you like, the Deck cross-section), although the shape of the $\Delta\pi$ spectrum reflects the details of the $\Delta\pi$ interaction. The correspondence between the $\Delta\pi$ interaction and the observed $\Delta\pi$ mass spectrum is expected to depend, of course, on the s and $t_{p,\Delta}$ values of the sample considered. These experimental remarks support, therefore, the point of view taken by Chew and Pignotti in their discussion of the Dolen-Horn-Schmidt duality. Corresponding tests of A_1 and Q-bump production in the final states $\rho\pi p$ and $K^*\pi p$ can also be made.

LEFRANÇOIS: You have stated that the P_{11} resonance has now been seen in photoproduction. At one time the story was that it could not be seen in photoproduction on protons but should be seen in photoproduction on neutrons. Could you comment on the present status?

DONNACHIE: The particular statement originally made was based in fact on theoretical calculations which were not entirely certain. In fact, the statement that the P_{11} is seen only very weakly from photoproduction on protons has been confirmed, but the mechanism of the production is quite different from the one assumed in the early calculation. While the statement concerning photoproduction on protons is certainly correct, the statement on neutrons is now open to question. Experimentally it is seen weakly, if at all.

LEITH: You have mentioned the existence of a D_{13} (1730) in $\Delta\pi$. How sure are you of this assignment? In the $\pi^- p \to \Delta^- \pi^+$ formation experiment, we see evidence of $\Delta\pi$ excitation at 1730 MeV in P_{11}. Also in 16 GeV/c $\pi^+ p$ we find a $\Delta\pi$ enhancement at 1730 MeV, which is compatible with P_{11} assignment.

DONNACHIE: The assignment of the quantum numbers to the D_{13} and P_{11} in the πN system are quite definite. The assignments deduced from other channels are doubtful. One cannot make any serious comment about this. It is quite possible to have one or the other, or a mixture of both.

KAMAL: There was a contribution by Tokyo University to this Conference on polarized $\gamma n \to \pi^- p$ around P_{11}. They find no evidence of P_{11} contribution in this channel.

APPENDIX

NUCLEON RESONANCES IN PRODUCTION PROCESSES

J.G. Rushbrooke

Cavendish Laboratory, Cambridge

1. INTRODUCTION

As the subject of nucleon resonances in formation experiments is discussed in Dr. Donnachie's talk[1], I shall be dealing with these resonances in relation to production experiments. The dozen or so papers on the subject, submitted to this Conference, make it clear that it is still too early to pull the results together, and look for patterns and trends in cross-sections and production mechanisms. Rather I shall be reporting on some promising methods of analysis likely to be useful for the high statistics experiments which, need it be said, are required in the future.

The $\Delta(1236)$ is produced very strongly at high energies: for example, 50-70% of events in the reaction $pp \to pp\pi^+\pi^-$ involve Δ^{++} production though the exact fraction is difficult to determine, since the production of low-mass $p\pi^+\pi^-$ resonances would generate kinematically a low-mass peak in the $p\pi^+$ system even if they never decayed into $\Delta^{++}\pi^-$. I shall return to this problem in discussing inelastic decay modes of resonances. I shall be discussing the $\Delta(1236)$ only in this connection. Most papers focus attention on the P_{11} Roper resonance in a context where Deck background is possible, and I shall begin here.

2. KINEMATIC EFFECTS

Previously we had the problem of Deck background; now we have duality to contend with instead. Chew and Pignotti[2] have extended to multiperipheral processes a suggestion made by Dolen, Horn and Schmid[3] that direct channel resonances are already contained, in the sense of a local average, in the cross-channel Regge amplitudes. Thus in a multi-particle production process, say $pp \to p\Delta^{++}\pi^-$, any $\Delta^{++}\pi^-$ enhancement (a Deck peak) predicted by a t-channel model is, therefore, a prediction of resonance(s), and to attempt a

detailed fit to a peaked structure by adding some $\Delta^{++}\pi^-$ resonant amplitude is to risk double counting.

Figure 1 shows an experimental $m(\Delta^{++}\pi^-)$ histogram from $pp \to p\Delta^{++}\pi^-$ at 16 GeV/c [4], compared with theoretical predictions of several t-channel models incorporating one-pion-exchange both Reggeized and un-Reggeized. Though these models give quite good cross-section agreement, discrepancies clearly exist between the histogram and the theoretical curves. At this stage it is not clear whether further refinement of any t-channel model will eliminate this discrepancy completely, or whether $pp \to pN^*$ reactions as well are responsible for the detailed structure. This structure shows more clearly in Fig. 2 [5] after introducing Δ^2 cuts to remove diffractive background, which sharpens the peaks at 1470, 1750, and 2030 MeV (though the 1470 starts to be sheared off for phase-space reasons) and make it fairly certain that resonances in the vicinity of these masses are being observed.

The histogram of Fig. 1 is typical of experiments in the range 5-28.5 GeV/c from which data is now available. Colton et al.[6] have analysed the above reaction $pp \to p\Delta^{++}\pi^-$ in terms of a one-pion-exchange model, using the off-mass-shell modifications proposed by Dürr and Pilkuhn[7]. For events with $m(p\pi^-) > 1.6$ GeV, from which most of the low-mass $\Delta^{++}\pi^-$ peak comes, all the parameters of the model are determined from fitting $d\sigma/dt$ distributions of the quasi-two-body reactions $\pi^+p \to \rho^0\Delta^{++}$, $\bar{p}p \to \bar{\Delta}^{++}\Delta^{++}$, $pp \to \Delta^{++}n$, and $\pi^-p \to \rho^0 n$ over a large range of beam momenta. In Fig. 3 the resulting theoretical cross-section for events with $|t| < 0.3$ (GeV/c)^2, $m(p\pi^-) > 1.6$ GeV and $m(\Delta^{++}\pi^-) < 1.5$ GeV (i.e. the vicinity of the P_{11} resonance) is shown (labelled $\sigma_{\Delta\pi}$) as a function of beam-momentum and the experimental points at 6.6 GeV/c [6], 16 GeV/c [4] and 28.5 GeV/c [8] are in fair

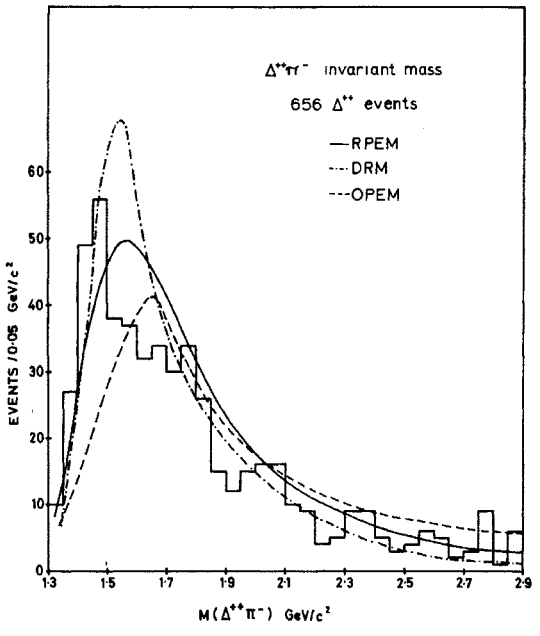

Fig. 1 Experimental low-mass ($\Delta^{++}\pi^-$) spectrum from a Cambridge-Imperial College (London) 16 GeV/c study of $pp \to p\Delta^{++}\pi^-$. The dashed curve is predicted by a single one-pion-exchange model, and the solid and dot-dashed curves by two Reggeized one-pion-exchange models[4]. The selection $\Delta^2 < 1.0$ (GeV/c)^2 has been made for model calculations.

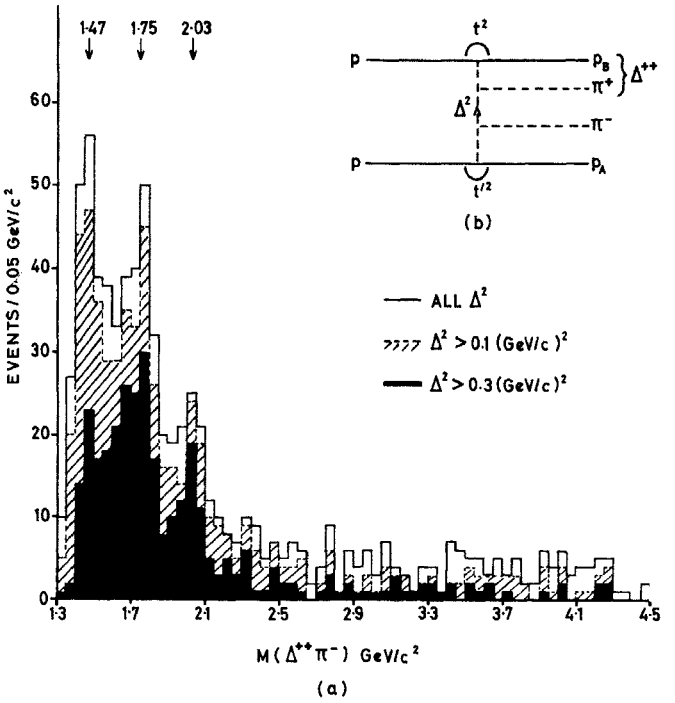

Fig. 2 a) The $m(\Delta^{++}\pi^-)$ spectrum of Fig. 1 with various other Δ^2 cuts. b) Diagram for $pp \to pp\pi^+\pi^-$ with various momentum transfers defined.

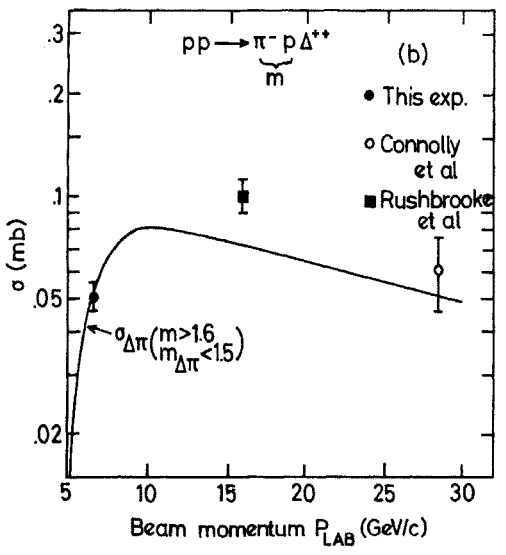

Fig. 3 The curve labelled $\sigma_{\Delta\pi}$ calculated from a one-pion-exchange model[6] compared with data at 6, 16 and 28.5 GeV/c.

agreement with theory. Note that the theory has the appealing feature of predicting a roughly constant cross-section, as expected with diffraction dissociation. The actual $\Delta^{++}\pi^-$ mass-spectrum at 6.6 GeV/c [6] (Fig. 4) is again only approximately described by this t-channel model, though the model itself could be made to reproduce the P_{11} peak by ad hoc adjustment of the off-shell π^-p elastic-scattering distribution in (θ,ϕ). The model is highly constrained and why simple one-pion-exchange works is itself a mystery; presumably with detailed form-factors it makes an effective parametrization.

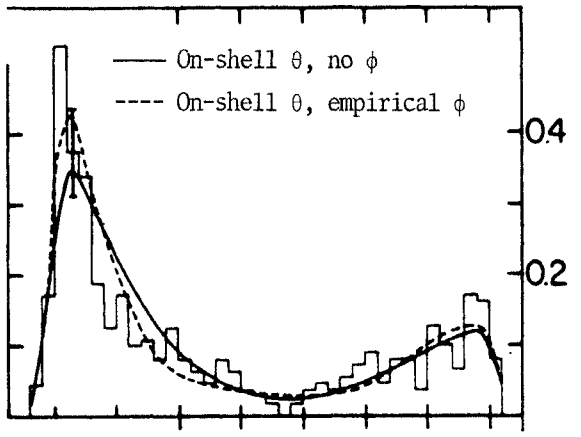

Fig. 4 Experimental $m(\Delta^{++}\pi^-)$ spectrum from $pp \to p\Delta^{++}\pi^-$ at 6 GeV/c with the selection $1.6 < m(p\pi^-) < 2.0$ GeV. Theoretical curves are from the one-pion-exchange model with Dürr-Pilkuhn form-factors[6].

In conclusion, it appears that the procedure of subtracting Deck background is incorrect as one is at the same time removing genuinely resonant events. Therefore in such cases a very good understanding of t-channel dynamics is needed before a quantitative assessment of resonance production can be made. Perhaps double-counting could then be avoided by analysing the t-channel amplitude into partial-waves of the $\Delta^{++}\pi^-$ system (in this example) and subtracting the resonant partial-waves from the full Deck amplitude before adding in resonant amplitudes.

3. Nπ MODES

The P_{11} Roper resonance has been clearly identified in a 7 GeV/c study[9] of the reaction $pd \to p_s pp\pi^-$ by the Weizmann Institute group. The proton spectator behaves in accordance with the Hulthén wave function for the deuteron so that events of the type $pn \to pp\pi^-$ may be studied. In Fig. 5a the momentum

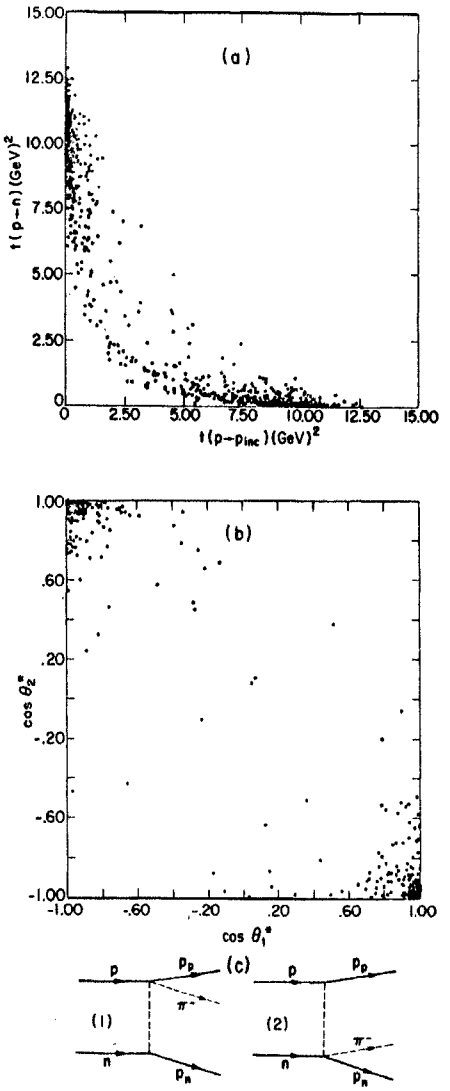

Fig. 5 a) $t(p \to p_{inc})$ versus $t(p \to n)$ from 7.0 GeV/c $pn \to pp\pi^-$ from Weizmann group[9]. b) Plot of c.m.s. angles of outgoing protons. c) Diagrams for $pn \to pp\pi^-$.

transfer $t(p \to p_{inc})$ of each final state proton with respect to the incoming proton is plotted versus $t(p \to n)$ the momentum transfer of the same proton with respect to the neutron target. The events cluster into two groups. In Fig. 5b $\cos\theta_1^*$ is plotted versus $\cos\theta_2^*$, where θ_1^* and θ_2^* are the c.m.s. angles of the first and second final state proton with respect to the incoming nucleon. Figures 5a and b demonstrate the peripheral nature of the reaction and strongly suggest the diagrams of Fig. 5c where each final state proton is labelled according to its association with one of the initial nucleons. Figures 6a and c are sections of the two Chew-Low plots pertaining to Fig. 5c. Figures 6b and d are the corresponding $p\pi^-$ mass projections which display a clear difference in shape. The peak at 1.44 is seen in

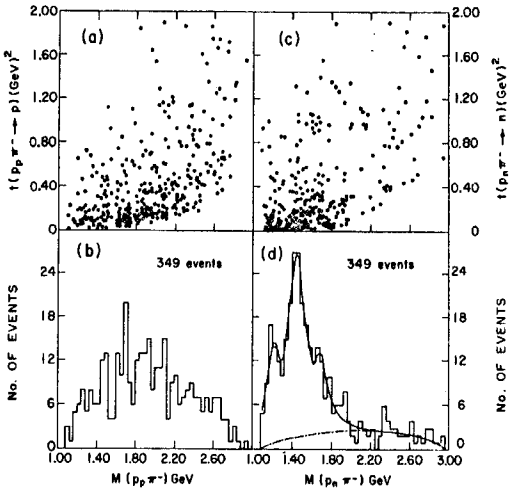

Fig. 6 a), c) Sections of Chew-Low plot for $m(p_p\pi^-)$ versus $t(p_p\pi^- \to p)$ and $m(p_n\pi^-)$ versus $t(p_n\pi^- \to n)$ in $pn \to pp\pi^-$ at 7.0 GeV/c. b), d) Invariant mass distributions for the $p_p\pi^-$ and $p_n\pi^-$ combinations in the same reaction.

the $m(p_n\pi^-)$ distribution, but is absent in the $m(p_p\pi^-)$ distribution, and events in the peak are produced with small momentum transfers. Values of the ratio $R = \sigma(1)/\sigma(2)$ between the cross-sections for diagrams (1) and (2) for various I-spin values of the exchanged particle I(x), and of the $p\pi^-$ system $I(p\pi^-)$, assumed to exist in a pure I-state, are given below.

$I(p\pi^-)$	I(x)	R
1/2	0	0
1/2	1	4
3/2	1	1

The absence of the 1.44 peak in the $m(p_p\pi^-)$ distribution indicates $R \ll 1$ (consistent with $R = 0$); hence the peak corresponds to an I = 1/2 state and the production mechanism of the peak is dominated by I = 0 exchange. Taken with the fact that the N*(1470) acquires the same quantum numbers as the nucleon (see Section 5) this is indicative of Pomeranchuk exchange. By fitting Fig. 6d to Breit-Wigner's for the Δ(1236), N*(1690) and variable N*(1470) plus invariant phase space, they get M = 1446 ± 11 MeV and Γ = 198 ± 40 MeV for mass and width of the P_{11} state, to be compared with 1460 ± 10 and 259 ± 48 MeV when derived from phase-shift analyses[1].

The reaction $pp \to p\pi^+(p\pi^-)$ also permits observation of $p\pi^-$ decay modes (now with I = 0 exchange disallowed) and data[4] from Cambridge - Imperial College at 16 GeV/c illustrates the crucial role played by momentum transfers in selecting resonant events according to production mechanism. In Fig. 7 we show $m(p_A\pi^-)$ when $p_B\pi^+$ forms a Δ^{++}. There is some evidence for double isobar production with final states $\Delta^{++}\Delta^0$, $\Delta^{++}N^*(1470)$ and $\Delta^{++}N^*(1700)$. Examination of the Dalitz plot ($p_A\pi^-$ against $\Delta^{++}\pi^-$) shows these are not reflections of the $\Delta^{++}\pi^-$ resonances already mentioned. We may exclude the possibility of $\Delta^{++}(1236)$ $\Delta^0(1690)$ as no evidence for the charge-symmetric final state $\Delta^0(1236)$ $\Delta^{++}(1690)$ is seen, which would be present in equal strength. The 1700 peak must therefore contain one or more of the I = 1/2 states, as many as five having been reported in this region by phase-shift analysis[1]. For events with no Δ^{++} combination, $p\pi^-$ resonances were detected by choosing the less diffractive proton as being the more

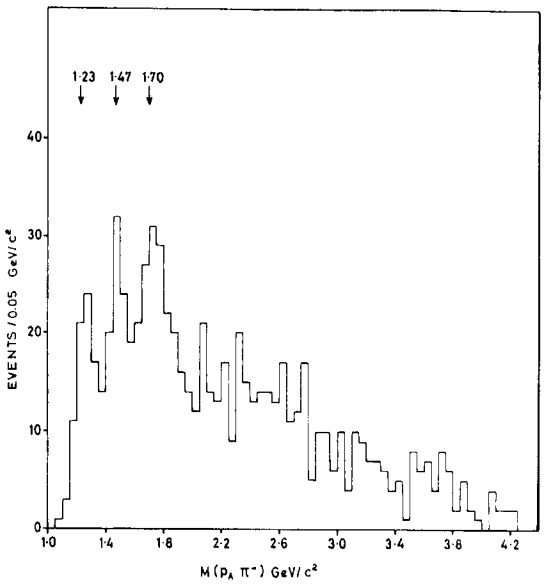

Fig. 7 $p_A\pi^-$ invariant mass distribution for the 752 events forming a Δ^{++} with proton p_B from 16 GeV/c $pp \to pp\pi^+\pi^-$, Cambridge-Imperial College experiment.

likely to form a resonance. If this proton is labelled p_A [i.e. $t^2 < t'^2$ in Fig. 2b], $m(p_A\pi^-)$ is as given in Fig. 8. The Δ^0, N*(1470) and N*(1700) resonances are apparent, and the lack of any such structure in the $m(p_B\pi^-)$ distribution (Fig. 9) lends support to the selection according to t^2/t'^2. Considering $p\pi^-$ resonances irrespective of their mode of production, the data of Fig. 7 and Fig. 8 have been com-

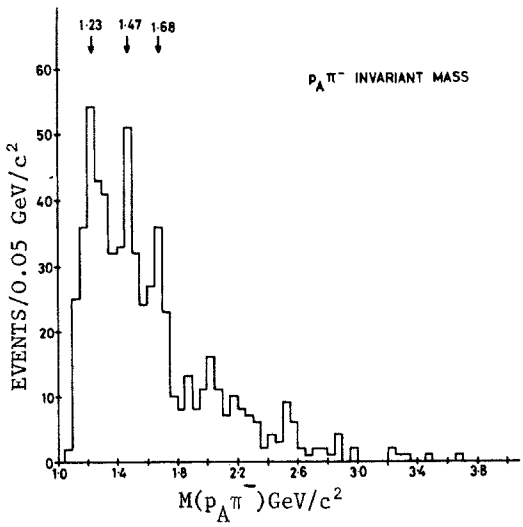

Fig. 8 $p_A\pi^-$ invariant mass distribution for the 618 events containing no Δ^{++}. p_A is chosen such that $t^2 < t'^2$ in Fig. 2b.

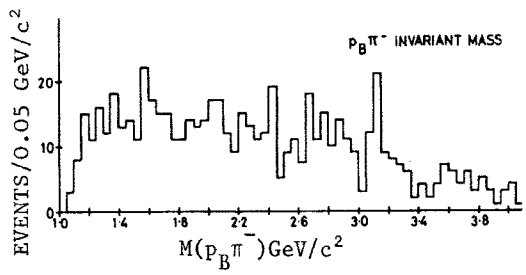

Fig. 9 $p_B\pi^-$ mass distribution when p_A is defined as in Fig. 8 (also 618 events).

bined in Fig. 10 with the additional requirement $t'^2 > 0.5$ (GeV/c)^2. This is intended to limit the effects of background processes diffractive in t'^2, and results in very distinctive resonant structure,

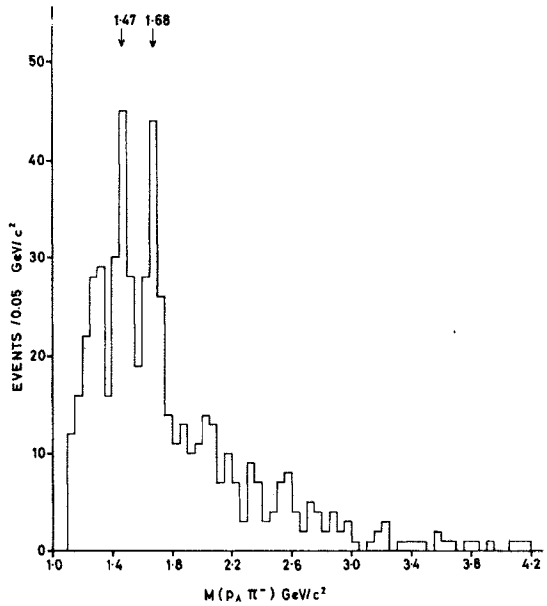

Fig. 10 The sum of the $p_A\pi^-$ invariant mass distributions of Figs. 7 and 8, with the additional requirement that $t'^2(p, p_A) > 0.5$ (GeV/c)^2. The plot contains 541 events. Cambridge-Imperial College (London) Collaboration.

perhaps consistent with 100% resonances (note that some events on the low-mass side of the Δ^0 are removed for reasons of phase space). Note the narrow widths in these production reactions, much less than phase-shift analysis widths.

Similar structure has been seen in $p\pi^-$ distributions at other beam momenta, though the N*(1470) peak often appears centred at a mass near 1.48 - 1.50 GeV, and is probably a composite structure containing N*(1518) as well, particularly at the lowest momenta and except at very low momentum transfers.

The Wisconsin group reported[10] seeing structures at 1480 and 1700 in the final states $\pi^-p \to \pi^-(\pi^+n)$, $\pi^-(\pi^0p)$ and $\pi^-(\pi^+\pi^-p)$ in experiments at 7 and 25 GeV/c, the 1480 resonance having a width of only 40 ± 10 MeV. Figure 11 shows the momentum transfer dependence $\alpha(M^*)$ as a function of M^* for two of these reactions fitted to the form $e^{\alpha t}$. In each case they are looking at the momentum transfer from incident to outgoing (non-resonant) π^-. The 1480 resonance region does show a simple $e^{\alpha t}$ dependence, which is taken as a perfect example of diffraction dissociation, a $1/2^+ \to 1/2^+$ transition.

Various authors have tried to account for the earlier counter measurements of cross-sections for

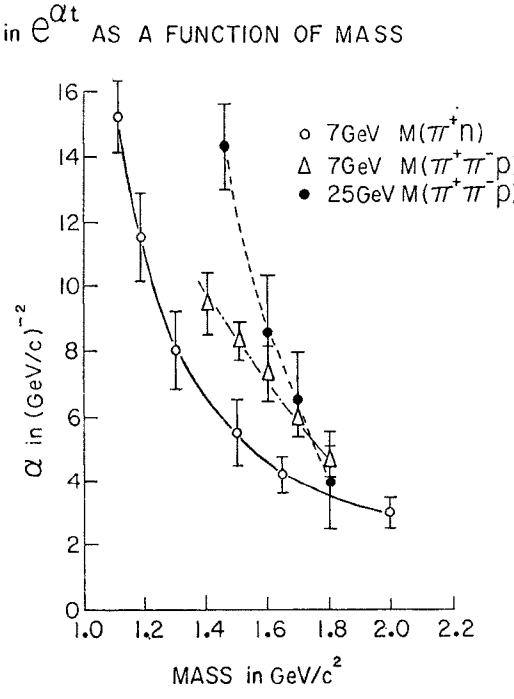

Fig. 11 Four-momentum transfer dependence parametrized as $e^{\alpha(M)t}$ from reactions $\pi^-p \to \pi^-\pi^+n$, $\pi^-p \to \pi^-\pi^+\pi^-p$ at 7 and 25 GeV/c [10].

the production of various resonances including the P_{11} resonance. The Weizmann group estimated[9] a cross-section of 0.5 mb for the reaction pn → $pN^{*0}(1470) \rightarrow p(p\pi^-)$ and therefore 1.5 mb for pn → $pN^{*0}(1470) \rightarrow p(N\pi)$; since they have proved I = 0 exchange this also means 1.5 mb for pp → pN*(1470) → p(Nπ), appreciably higher than the 0.5 ± 0.2 mb found in a missing-mass counter experiment by Blair et al.[11] at adjacent momenta. This would certainly imply that the 1400 enhancement observed in missing-mass experiments is dominantly in the Nπ mode, in conflict with other results (see Section 4). However, both experiments are subject to considerable background uncertainties. Also the Weizmann result is obtained in deuterium; an indication that the spectator proton may be affecting the reaction comes from the value $\alpha = 9.1 \pm 2.1$ $(GeV/c)^{-2}$ found from a maximum likelihood fit of the form $Ae^{\alpha t}$ to N*(1470) events, whereas counter experiments[11] and bubble chamber studies[12] of pp → pN*(1470) obtained $\alpha \sim 20$ $(GeV/c)^{-2}$ at nearby momenta. In fact a large slope parameter α seems to be an agreed hallmark of the Roper resonance.

Comparable data on the reaction channel pp → pN*(1470) → p(Nπ) is available at nearby beam momenta. At 5.5 GeV/c a cross-section of 1.16 mb was obtained, based on the final state $pn\pi^+$ only, falling to only 0.27 mb at 10 GeV/c [12]. This particular channel also gives evidence for the $\Delta^{++}(1920)$ in $p\pi^+$ over this beam momentum range. At higher beam momenta 1C fits become increasingly unreliable, so a recent attempt at Brookhaven to work with missing neutrals at 28.5 GeV/c is of interest.

The Brookhaven group have studied[8] a wide variety of final states including neutrals in pp interactions at a beam momentum of 28.5 GeV/c, using missing-mass techniques. By measuring low-momentum (recoil) protons p_R in two- and four-prong events they isolate

$$p + p \rightarrow p_R + MMX \qquad (1)$$

where elastic events, i.e. MMX incorporates a proton mass, have been eliminated by 4C-fitting. They also isolate

$$p + p \rightarrow p_R + \pi^+ + MMn \qquad (2)$$

where events with MMn within the neutron peak are now selected, most of which also gave reliable 1C-fits to the final state $p\pi^+n$. The authors point out that a loss of events with $|t| \lesssim 0.06$ $(GeV/c)^2$ between target and recoil protons occurs due to a scanning bias against short recoil-proton tracks (there would also appear to be events lost where neither proton is slow enough to be identifiable though these correspond to events having large |t|), but apart from this due to beam-target symmetry, one-half of the events remain, corresponding to production of "forward isobars". The upper histogram of Fig. 12 represents the cross-section for producing MMX in two-prong events of reaction (1), i.e. the particle combinations $n\pi^+$, $p\pi^0$, $n\pi^+\pi^0$ and $p\pi^0\pi^0$. The lower histogram refers to reaction (2), i.e. to the final state $(MMn + \pi^+) = (n\pi^+)$ only. Both plots are restricted to events with $|t| < 0.12$ $(GeV/c)^2$, and a broad enhancement at about 1400 MeV is present in this data which is found to

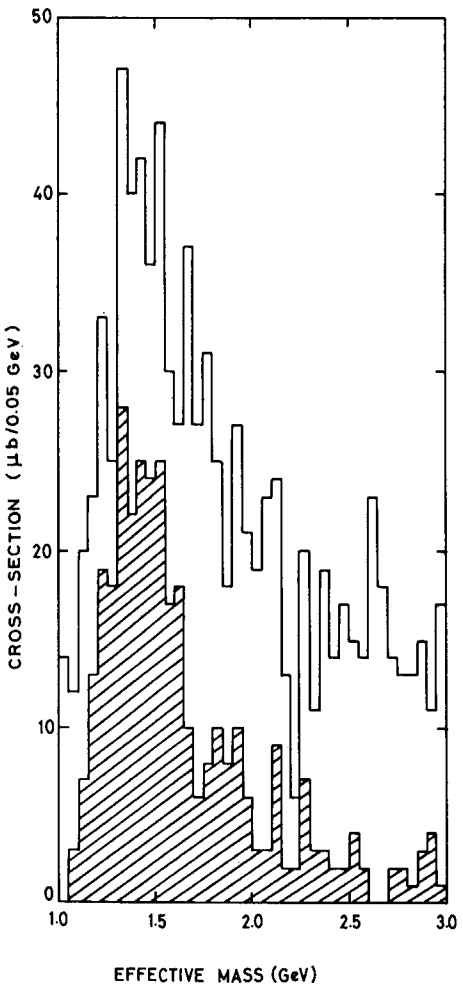

Fig. 12 Distribution of $(MMn + \pi^+) = n\pi^+$ (dashed) and MMX in two-prong events with $|t| < 0.12$ from 28.5 GeV/c pp interactions[8].

disappear when the selection $|t| > 0.12$ $(GeV/c)^2$ is made, indicative of an experimental slope in t roughly equal to twice the elastic slope [i.e. $\alpha \sim 16$-20 $(GeV/c)^{-2}$]. The final state $pp\pi^+\pi^-$ was also studied after making 4C fits to four-prong events and selecting only $p\pi^+\pi^-$ combinations in the backward hemisphere, and the effective mass of $p\pi^+\pi^-$ is shown in

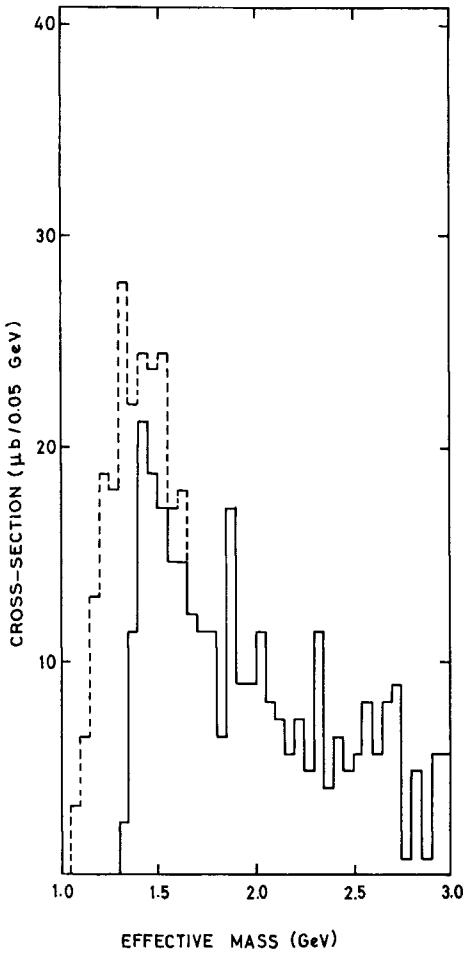

Fig. 13 Distribution of $p\pi^+\pi^-$ effective mass from $pp \to pp\pi^+\pi^-$ (solid line) compared with $n\pi^+$ in $pp \to p\pi^+n$, both for $|t| < 0.12$ from 28.5 GeV/c pp interactions[8].

Fig. 13, again for $|t| < 0.12$ $(GeV/c)^2$, with the $n\pi^+$ mass distribution of Fig. 12 shown again for comparison. Considering events in the interval 1250 to 1550 MeV, there are 235 events in MMX (two-prong) and 142 events in $n\pi^+$. Then assuming the 1400 enhancement is I-spin 1/2, which gives a ratio $(n\pi^+)/(p\pi^0) = 2$, they obtain

$$\frac{n\pi^+\pi^0 + p\pi^0\pi^0}{n\pi^+ + p\pi^0} \approx \frac{22}{213} = 0.1 \ .$$

They are unable to quote a figure for $N\pi\pi/N\pi$ because of the unknown effect of low $|t|$ losses for two-prong events.

In this experiment an enhancement in the 1600-1700 MeV region was also found for $|t| > 0.12$ with a small slope in t ($\sim 1/2$ the elastic slope), consistent with counter data[13].

The authors observe that comparing the $n\pi^+$ and $p\pi^+\pi^-$ spectra in Fig. 13, the $n\pi^+$ spectrum spreads to lower masses and is broader. Their mass resolution is about ±100 MeV. They go on to suggest that the inelastic decay mode $\Delta^{++}\pi^-$ could cause a shift of the position of the $p\pi^+\pi^-$ peak to higher mass, due to the higher threshold for production. However, experiments at lower beam momenta and better mass resolution do not appear to see any significant shift, allowing for the fact that the $\Delta^+(1236)$ is probably contributing to the lower part of the $n\pi^+$ enhancement in this $|t|$ range.

Although there would seem to be formidable event-selection difficulties, and great care is needed to interpret results in the presence of biases, this technique looks promising.

4. $N\pi\pi$ (INCLUDING $\Delta\pi$, $N\sigma$ ...) MODES

The first question here is do $\Delta(1236)\pi$ decay modes of the observed N*'s exist or not? There are two important experimental difficulties in deciding the issue: i) as mentioned above a low-mass $N\pi\pi$ resonance automatically means a large proportion of $N\pi$ combinations within the Δ-mass region for kinematic reasons; ii) a concentration of $p\pi^+$ mass combinations near the Δ^{++} in a sub-Dalitz plot for fixed $p\pi^+\pi^-$ mass does not imply a genuine $\Delta^{++}\pi^-$ decay mode, as there are many background Δ^{++}'s around from competing channels. Several authors[5,12,14] have attempted maximum likelihood analyses to determine the branching ratios of $p\pi^+\pi^-$ enhancements into $\Delta^{++}\pi^-$, $\Delta^0\pi^+$ and non-resonant $p\pi^+\pi^-$ in the final state $pp\pi^+\pi^-$. Figure 14 shows the fraction of events in which a Δ^{++} is produced (the Δ^0 contribution may be neglected on I-spin grounds) as a function of $p\pi^+\pi^-$ mass in an analysis[14] at 24.8 GeV/c. The most significant feature is a dip near the mass of the 1700 MeV enhancement, indicating a substantial decay into non-$\Delta^{++}p\pi^+\pi^-$. They therefore estimate that the branching ratio

$$\frac{N^*(1700) \to \Delta^{++}\pi^-}{N^*(1700) \to p\pi^+\pi^-} < 0.17 \ .$$

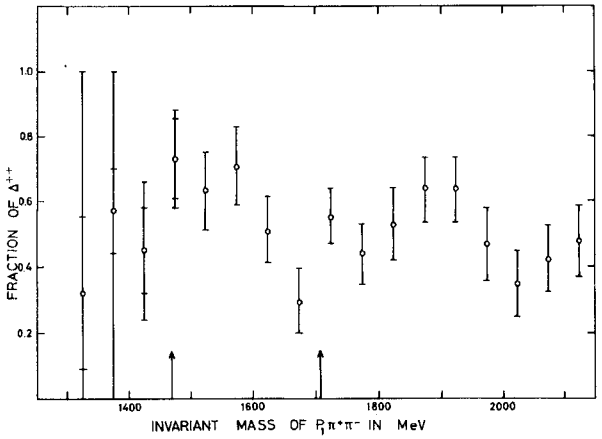

Fig. 14 The fraction of Δ^{++} in each $p_1\pi^+\pi^-$ mass interval as determined from a maximum likelihood fit at 24.8 GeV/c[14]. p_1 is the proton in the $p_1p_2\pi^+\pi^-$ final state which combined with the π^+ gives an effective mass closer to the Δ^{++} than the other proton p_2.

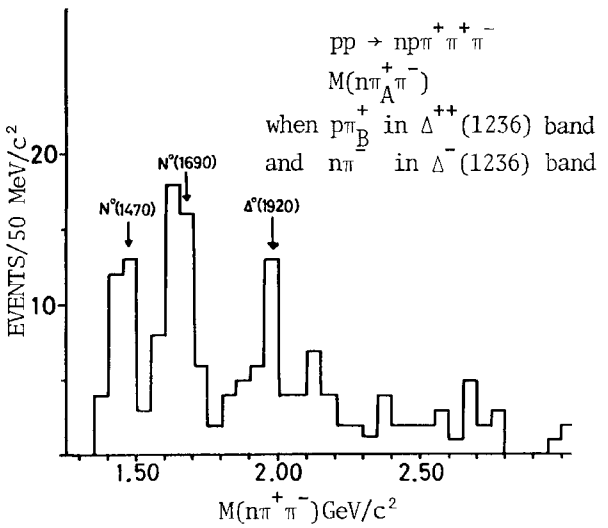

Fig. 15 $m(\Delta^-\pi^+)$ distribution from reaction $pp \to \Delta^{++}\Delta^-\pi^+$ at 19 GeV/c studied by the Scandinavian Collaboration[15].

An earlier analysis at 10 GeV/c [12] obtained the value 0.31 ± 0.17, and higher values have been obtained. A fit such as that of Fig. 14 can probably give a positive indication that the $\Delta\pi$ decay mode exists only in the form of a sharp discontinuity, peak or dip, since background events would be a priori less likely to produce such an effect. Taking all the evidence together some $\Delta\pi$ decay of the N*(1450) probably exists, but one cannot yet give quantitative estimates of the branching ratio from production experiments.

The Wisconsin π^-p data[10] mentioned above is important because of the relative absence of $\Delta^{++}(p\pi^+)$ background combinations. They conclude that the dominant decay of their 1480 MeV $p\pi^+\pi^-$ state is into $p(\pi\pi)^0$ on the basis of $p\pi^+$, $p\pi^-$ and $\pi^+\pi^-$ mass distributions (all phase-space-like) and decay angular distributions. The 1700 enhancement indicates only a small amount of $\Delta^{++}\pi^-$ decay.

A Scandinavian group observe[15] the reaction $pp \to \Delta^{++}\Delta^-\pi^+$ in the final state $(p\pi^+)(n\pi^-\pi^+)$ at 19 GeV/c. This reaction is interesting because placing the pion other than in the diagram

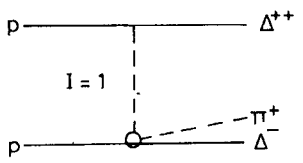

would involve double charge exchange. The mass distribution of $\Delta^-\pi^+$ is shown in Fig. 15 and is characterized by peaks which they associate with $N^0(1470)$, $N^0(1690)$ and $\Delta^0(1920)$. Note once again that the histogram is perhaps consistent with 100% resonances. Note also that I = 1 exchange is required and that the position of the middle resonance is below 1700 MeV, as was the case with the $p\pi^-$ enhancement shown in Figs. 7, 8 and 9 where I = 1 exchange is also demanded. On the other hand where I = 0 exchange is allowed this peak appears to move to higher mass, e.g. in the $\Delta^{++}\pi^-$ spectrum (Fig. 2), from 16 GeV/c pp interactions, it occurs at 1750 MeV. A SLAC 16 GeV/c π^+p experiment[16] sees a clear signal for $\pi^+p \to \pi^+N^*(1720) \to \pi^+(p\pi^+\pi^-)$ also allowed by I = 0 exchange. In view of the many resonances in this region it is interesting to observe that the proposed[1] $P_{11}(1750)$ is a likely candidate for production by diffraction dissociation at high energy.

The Scandinavian group also observe the $N^0(1470)$ and $N^0(1690)$ in the $(p\pi^+)(n\pi^-\pi^+)$ final state when $n\pi^-\pi^+$ systems are chosen having low $|t|$, as shown in Fig. 16. However they see little or no sign of the $N^*(1470)$ and $N^0(1690)$ in the final state $(p\pi^+)(p\pi^-\pi^0)$, which suggests that there is non-negligible $N\sigma$ decay mode present (where σ means an I = 0, J = 0 $\pi\pi$ system) since $N\sigma \not\to p\pi^-\pi^0$ but $N\sigma \to n\pi^-\pi^+$; alternatively, a $\Delta\pi$ decay mode gives $(n\pi^-\pi^+)/(p\pi^-\pi^0) = 5/2$ in qualitative agreement with the observed behaviour of both resonances.

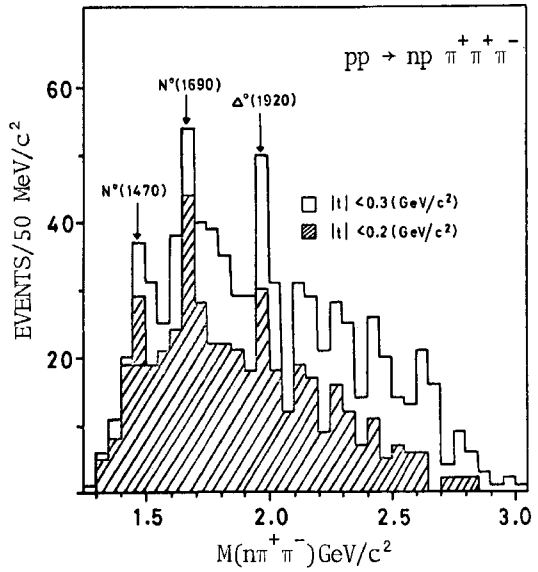

Fig. 16 $m(n\pi^+\pi^-)$ in $pp \to np\pi^+\pi^+\pi^-$ when $|t| < 0.3$ $(GeV/c)^2$ and when $|t| < 0.2$ $(GeV/c)^2$ (cross-hatched histogram) at 19 GeV/c [15].

As the final state $(p\pi^+)(n\pi^-\pi^+)$ is free from Deck effect complications, it is interesting to make a rough comparison of two- and three-body decay modes of the N*(1470). In the same Scandinavian 19 GeV/c experiment they find a cross-section of 0.14 ± 0.03 mb for the reaction $pp \to (p\pi^+)N^{*0}(1470) \to (p\pi^+)(p\pi^-)$, which gives 3/2 (0.14) = 0.21 mb for $pp \to (p\pi^+)N^{*0}(1470) \to (p\pi^+)(N\pi)$ allowing for the unseen decay mode $n\pi^0$. The cross-section for $pp \to (p\pi^+)\, N^{*0}(1470) \to (p\pi^+)(n\pi^+\pi^-)$ was about 0.06 ±0.02 mb; allowing for unseen decay modes means multiplying by a factor 9/5 assuming Δπ decay, or 3/2 if Nσ decay, so in either case $pp \to (p\pi^+)N^{*0}(1470) \to (p\pi^+)(N\pi\pi)$ has a cross-section of about 0.10 mb. Hence

$$\frac{N^*(1470) \to N\pi\pi}{N^*(1470) \to N\pi} \approx 0.50 \pm 0.25 \ .$$

This is consistent with the phase-shift result[1] of about 0.75.

In the case of the 1700 MeV resonance, 10 GeV/c data[12] is available for the same final states. This can only give the result

$$\frac{N^*(1700) \to n\pi^+\pi^-}{N^*(1700) \to N\pi} \approx \frac{0.16}{0.24} = \frac{2}{3} \ ,$$

since the assumption of dominant Δπ decay is almost certainly unjustified for N*'s in this region[1].

This may be compared with the result from an earlier 5.7 GeV/c $\bar{p}p$ experiment[17] that the $N\pi\pi/N\pi$ ratio has a value $\gtrsim 0.8$. This same experiment also concluded there was no evidence for a Δπ decay mode.

5. J^P ASSIGNMENTS

The distributions of polar and azimuthal angles, defining the π^- in the $p_n\pi^-$ system for events with $1.36 < m(p_n\pi^-) < 1.52$ GeV from the Weizmann pd experiment[9], are shown in Figs. 17a and b. The cos θ* distribution is consistent with isotropy and hence with J = 1/2 for the N*(1470).

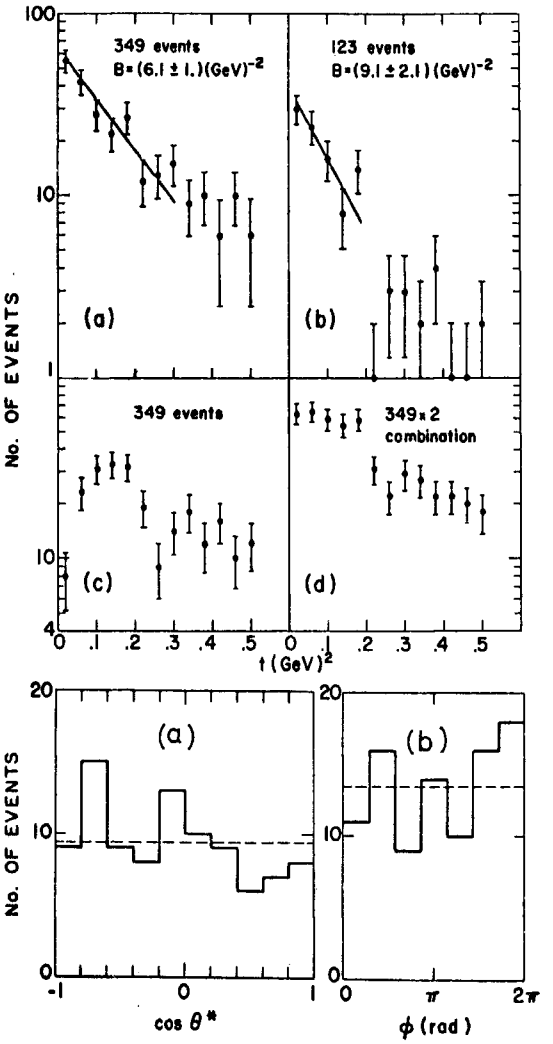

Fig. 17 Distributions in cos θ* and φ describing the π^- direction in the $p_n\pi^-$ system for events $pn \to pp_n\pi^-$ when $1.36 < m(p_n\pi^-) < 1.52$ GeV.

The 7 and 25 GeV/c π^-p data of the Wisconsin group[10] have been used to examine the angular distribution between target and the normal to the decay plane [see definitions of Figs. 18a and b] and are

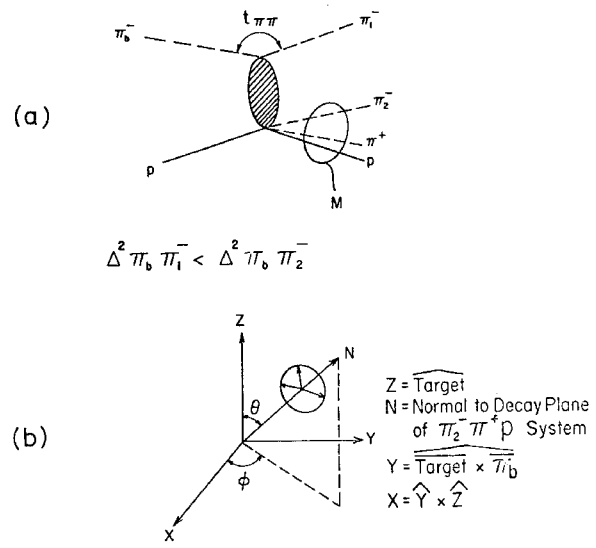

Fig. 18 a) Feynman diagram of the diffraction dissociation process for $\pi^- p \to \pi^- \pi^+ \pi^- p$. b) Coordinate system used to define angles.

shown in Fig. 19 for the 1470 and 1700 MeV regions of $m(\pi^-\pi^+ p)$. At both energies the results for the 1470 are consistent with isotropy and hence $1/2^+$ for J^P. They also claim that the results for the 1700 MeV state are consistent with J = 5/2. If J = 1/2 and the decay were $N^* \to \Delta\pi$, then the Δ would have to be produced in helicity states $\lambda = \pm 1/2$. This would result in a $(1 + 3\cos^2\theta)$ decay angular distribution (in the Δ rest frame) with respect to its direction of flight in the N* rest frame. For the 1470 the observed distribution is isotropic, consistent with little Δπ decay.

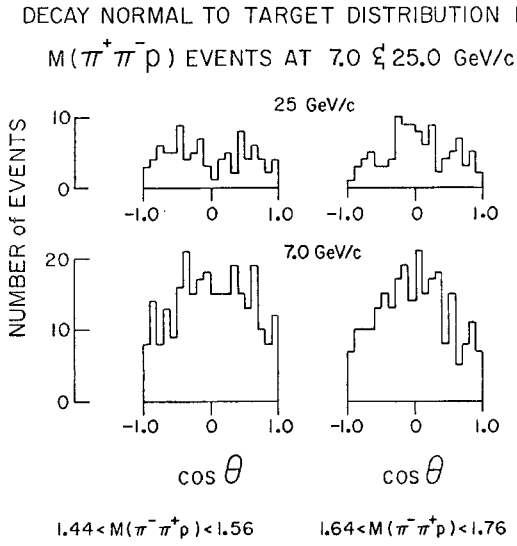

Fig. 19 Distribution of cosine of normal to the decay plane dotted into the target in the $p\pi^+\pi^-$ rest frame for $\pi^- p \to \pi^-(\pi^+\pi^- p)$ at 7 and 25 GeV/c [10].

On the other hand a Maryland group[18] observe the reaction $K^+ p \to K^+ N^*(1450) \to K^+(p\pi^+\pi^-)$ at 5.5 GeV/c. They considered the distribution in the cosine of the angle between the π^+ and the target proton in the $p\pi^+$ rest frame and find that $(1 + 3\cos^2\theta)$ fits very well, as shown in Fig. 20. This is characteristic of m = ±1/2 alignment with respect to the target proton direction, but this may be just an indication of pion-exchange (θ is here the Jackson angle)

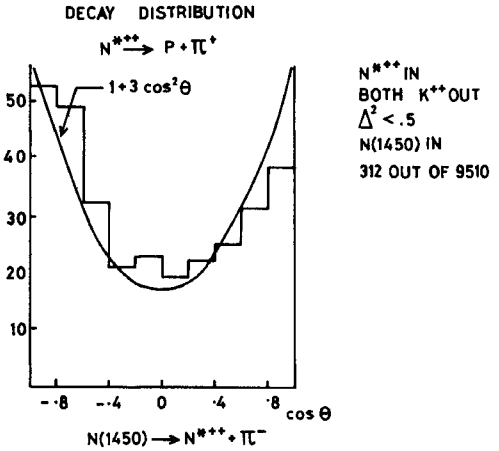

Fig. 20 Cosine distribution of the angle between π^+ and target proton in the $p\pi^+$ c.m.s. for events $K^+ p \to K^+ p\pi^+\pi^-$ at 5.5 GeV/c when $p\pi^+\pi^-$ lies in the mass interval 1350 to 1550 MeV [18]. The curve shown is $1 + 3\cos^2\theta$.

rather than of a Δπ decay mode. They also find striking differences in the angular distributions of π^+ and π^- with respect to target proton direction as viewed in the N*(1450) rest frame, which argues against any dominant pσ decay mode. This result is significant in the absence of background Δ^{++} events, although they find that the 1450 enhancement is correlated with low $K^+\pi^-$ masses and is not purely a resonant effect.

Finally, we note a Legendre polynomial analysis of the distribution in cos θ, defined as the angle between an incident proton and the outgoing Δ^{++} in the $p\pi^+\pi^-$ rest system in the reaction $pp \to pp\pi^+\pi^-$ at 24.8 GeV/c [14]. The Legendre coefficient a_8 is plotted in Fig. 21 as a function of $p\pi^+\pi^-$ mass. For $m(p\pi^+\pi^-) > 1900$ MeV they claim that all coefficients differ significantly from zero, owing to a sharply forward peaked cos θ distribution. In the lower mass region a_8 exhibits a fluctuation from a smooth variation at 1650-1750 MeV. The authors claim that the presence of a component of $\cos^8\theta$ implies that the

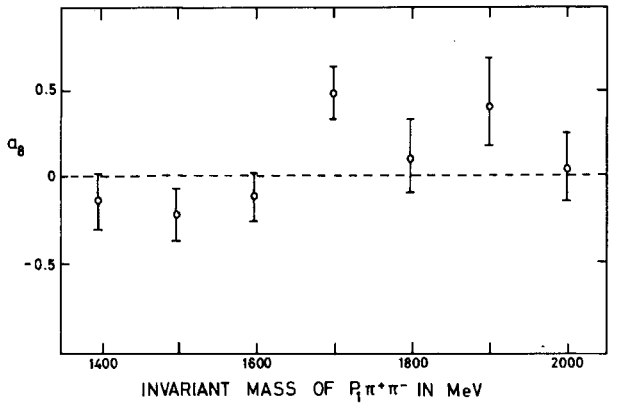

Fig. 21 The Legendre polynomial coefficient a_8 for an expansion to the cos θ distribution for each $p\pi^+\pi^-$ interval in $pp \to pp\pi^+\pi^-$ at 24.8 GeV/c [14]. Cos θ is the angle between an incoming proton and the outgoing $p\pi^+$ system in the $p\pi^+\pi^-$ rest system.

orbital angular momentum in the decay $N^*(1700) \to \Delta^{++}\pi^-$ is at least 4 [though in the same experiment the authors say they see little Δπ decay of the N*(1700) -- see Section 4 above], which implies $J \geq 5/2$. If J = 5/2, then $J^P = 5/2^-$, and this enhancement may be at least partly attributed to the D_{15} N*(1680).

6. SUMMARY

We conclude by attempting in Table 1 to identify -- highly tentatively -- with phase-shift analysis resonances some of the enhancements with their widths and decay modes as seen in production experiments. The additional references given in the table refer only to recent work not mentioned in the text above. The values quoted for widths are highly dependent on assumptions made about background, resonance position, presence of other resonances, etc.

TABLE 1

Phase-shift resonances[1]	Observed positions of produced resonances (MeV)	Approximate widths (MeV)	Decay modes
$P_{11}(1470)$	1450 - 1490	40 - 200	Nπ, Nππ/Δπ/Nσ
$D_{13}(1520)$	1520[a]	35[e] - 100	Nπ, Nππ/Δπ
$D_{15}(1680)$, $F_{15}(1690)$, $[S_{11}(1710)]$	1660 - 1720[e,f]	70 - 120	Nπ, Nππ/Δπ, ΛK
$D_{13}(1730)$, $P_{11}(1750)$	1730 - 1750[b]	∿ 50	Nππ/Δπ
$D_{13}(2030)$	2030 - 2080	40 - 100	Nπ, Nππ/Δπ, Δρ[d]
$G_{17}(2190)$	2175 - 2190	40	Nπ[e], Δππ/Δρ[d]
$P_{33}(1237)$			
$S_{31}(1630)$, $D_{33}(1670)$, $P_{33}(1690)$	1680[f]	55	Nππ
$F_{37}(1950)$	1900 - 2020	∿ 200	Nπ[c], Nππ[f], ΣK

a) Often unresolved from P_{11} resonance.
b) Not always distinguishable from the 1700 enhancement.
c) The exotic decay modes Δρ, Δππ and $Y_1^*(1385)K$ have all been observed[19] in 6 GeV/c pp interactions.
d) See Ref. 20.
e) See Ref. 21.
f) See Ref. 22.

REFERENCES AND FOOTNOTES

1. A. Donnachie, Rapporteur's talk.
2. G.F. Chew and A. Pignotti, Phys. Rev. Letters 20, 1078 (1968).
3. R. Dolen, D. Horn and C. Schmid, Phys. Rev. 166, 1768 (1968).
4. J.G. Rushbrooke et al., paper 560.
5. J.G. Rushbrooke et al., paper 561.
6. E. Colton et al., paper 541.
7. H.P. Dürr and H. Pilkuhn, Nuovo Cimento 40, 899 (1965).
8. W.E. Ellis et al., paper 816.
9. A. Shapira et al., paper 117.
10. A.F. Garfinkel et al., paper 936.
11. I.M. Blair, A.E. Taylor, W.S. Chapman, P.I.P. Kalmus, J. Litt, M.C. Miller, D.B. Scott, H.J. Sherman, A. Astbury and T.G. Walker, Phys. Rev. Letters 17, 789 (1966).
12. S.P. Almeida, J.G. Rushbrooke, J.H. Scharenguivel, M. Behrens, V. Blobel, I. Borecka, H.C. Dehne, J. Diaz, G. Knies, A. Schmitt, K. Strömer and W.P. Swanson, Phys. Rev. (to be published). This contains a full list of references to earlier work on pp interactions.
    S.P. Almeida, J.G. Rushbrooke, J.H. Scharenguivel, M. Behrens, V. Blobel, H.C. Dehne, J. Diaz, R. Schäfer, W.P. Swanson, I. Borecka and G. Knies, Nuovo Cimento 50, 1000 (1967).
13. E.W. Anderson, E.J. Blesser, G.B. Collins, T. Fujii, J. Menes, F. Turkot, R.A. Carrigan, Jr., R.M. Edelstein, N.C. Hien, T.J. McMahon and I. Nadelhaft, Phys. Rev. Letters 19, 198 (1967).
14. E. Ehrlich et al., paper 422.
15. H. Bøggild et al., paper 779.
16. J. Ballam et al., paper 335.
17. V. Alles-Borelli, B. French, A. Frisk and L. Michejda, Nuovo Cimento 47, 232 (1967).
18. P. Antich et al., paper 496.
19. W. Chinowsky, P. Condon, R.R. Kinsey, S. Klein, M. Mandelkern, P. Schmidt, J. Schultz, F. Martin, M.L. Perl and T.H. Tan, Phys. Rev. 171, 1421 (1968).
20. T.S. Yoon, P. Berenyi, A.W. Key, J.D. Prentice, N.R. Steenberg and W.D. Walker, Phys. Letters 24 B, 307 (1967). See however S.U. Chung, O.I. Dahl, J. Kirz and D.H. Miller, Phys. Rev. 165, 1491 (1968).
21. P. Fleury, R. Vanderhaghen, M. Goldberg, B. Makowski, B. Ghidini, A. Romano and A. Quareni-Vignudelli, Phys. Letters 26 B, 682 (1968).
22. P. Fleury, J. Huc, R. Vanderhaghen, J. Duboc, R. George, M. Goldberg, V. Picciarelli, A. Romano and A. Quareni-Vignudelli, Phys. Letters 26 B, 686 (1968).

RESONANCES — Experimental 3 $(B = 1, S \neq 0)$

Chairman	R.L. COOL
Rapporteur	R.D. TRIPP
Discussion Leader	N.P. SAMIOS
Secretaries	C. DAUM
	H.W.K. HOPKINS

STRANGE BARYON RESONANCES

R.D. Tripp

Lawrence Radiation Laboratory, Berkeley, Calif.

1. INTRODUCTION

During the past few years there has been a considerable increase in our knowledge of Y* resonances, and a number of papers have been submitted to the Conference concerning the detailed examination of Y*'s of intermediate mass. Some much-welcomed news has come in concerning Ξ*'s which adds to our fragmentary knowledge of S = -2 baryon states, whilst the interesting problem of the existence of Z*'s (S = +1) has changed little during the past year. Finally, several papers have been presented concerning resonances in the Λp dibaryon system. In this review I shall discuss the above topics in the reverse order from that mentioned above, and shall finish by summarizing the most substantial information on baryonic resonances within the framework of SU(3).

2. STRANGE DIBARYON STATES

Several experiments have been reported which suggest resonances in the Λp system. From Wisconsin[1] comes a report of a resonance at a mass of 2126 MeV and a width of less than 10 MeV. This mass lies just below the ΣN threshold at 2130 MeV. The evidence is extracted from a low-energy K^-d bubble chamber experiment where the presumed reaction sequence is $K^-p \to \Sigma^+\pi^-$, followed inside the same nucleus by $\Sigma^+n \to \Lambda p$. By making a selection on π^- going forward, one has events in which the Σ^+ is produced backwards in the centre of mass, and thus is nearly at rest with respect to the spectator neutron. Since the second reaction is quite exothermic, one would naturally expect a strong $\Sigma^+n \to \Lambda p$ conversion, as has been previously observed for K^-d at rest[2]. Figure 1 shows the statistically significant enhancement in the Λp mass spectrum which seems to peak slightly below the ΣN threshold and is interpreted by the authors as a resonance. The question naturally arises as to how much of this peaking can be explained away as due to a large absorptive ΣN scattering length coupled with a calculation of the apparent ΣN flux within the dibaryon system after the initial K^- interaction.

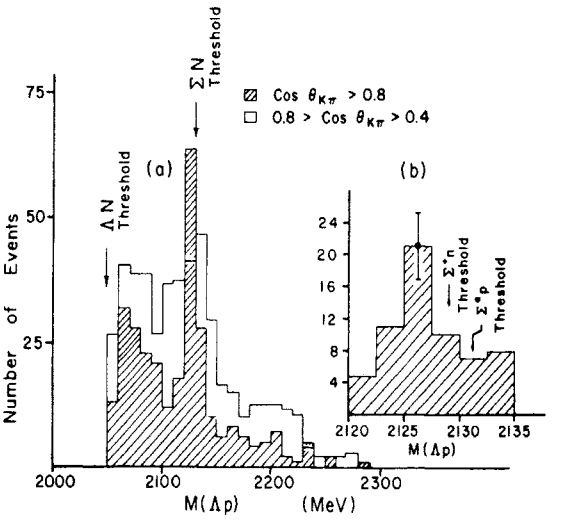

Fig. 1 a) Λp invariant mass spectrum from the Wisconsin experiment[1] for two cos $\theta_{K\pi}$ cuts, where $\theta_{K\pi}$ is the angle between the incident K and the outgoing π in the K^-d centre of mass. b) The mass region of 2120-2135 MeV is shown with 2.5 MeV bins.

These effects are difficult to evaluate, and have not been considered by the authors who present further arguments suggesting that the presumed resonance is in the $^3S_1$-state.

A much cleaner, but experimentally more difficult approach, is to study Λp scattering directly in a hydrogen bubble chamber. This has been pursued over the years with the painstaking accumulation of several hundred scatterings. [For a review, see Alexander and Karshon[3].] Figure 2 shows what is known up to 1 GeV/c, which covers the Λp threshold region in question. The solid curve is an effective range fit to the low-energy region where most of the data lie[4], whilst the dashed curve shows the expected Breit-Wigner resonance cross-section with the above parameters[1], reaching a maximum of $3\pi\lambda^2$. On the basis

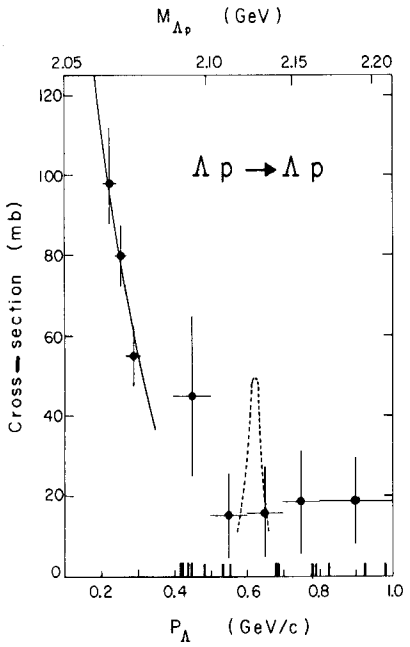

Fig. 2 The Λp elastic scattering cross-section versus Λ lab momentum[4]. The solid line is an effective range fit to the low momentum data, whilst the dashed line shows the expected cross-section for a $^3S_1$ resonance at 2126 MeV with a width of 10 MeV. Lines on the p_Λ axis indicate events.

of very poor statistics, there is no indication of a resonant behaviour. However, the experiment in this momentum region is seven years old[5]. By now there should be enough lambda path-length in bubble chambers to give a definitive judgement on this suggestion of a Λp resonance.

Two papers from Dubna[6] have also been presented on Λp enhancements found in a propane bubble chamber exposed to a 7-8 GeV/c neutron beam. One of the enhancements is near the Λp threshold, and presumably explainable as arising simply from the Λp scattering length, whereas the others at masses of 2200 and 2573 MeV are hardly significant, being based on extremely limited statistics.

3. BARYON RESONANCES WITH S = +1

At the time of the Heidelberg Conference in 1967, there were several interesting anomalies in the KN system, both in I = 0 and I = 1 [7]. These can be accommodated in SU(3) only in at least $\{\overline{10}\}$ and {27} representations, respectively, which in the quark model cannot be constructed from a simple three-quark system. These representations, in turn, imply the existence of Ξ*'s with I = 3/2 and Y*'s with I = 2, neither of which has been observed. One therefore approaches such indications with considerable a priori scepticism. One of the anomalies, involving the K^- spectrum in the reaction $\pi^- p \to K^- (MM)^+$, now appears to be spurious since, when the incident π^- energy was varied, the peak at a mass of about 1600 MeV corresponding to a presumed Z* moved around[8].

The other anomalies were discovered in precise total cross-section measurements at Brookhaven[9] on K^+p and K^+d. Subsequently, these structures were confirmed at Nimrod[10], and a Berkeley bubble chamber experiment in this energy region has been reported[11] for the pure I = 1 K^+p state. Figure 3 reminds you of the data as they existed for the 1966 International Conference, and little on this figure has changed since then. There appears to be no anomalous structure either in the K^+p elastic, single-pion, or double-pion production cross-sections at the mass corresponding to the bump in the total cross-section. This bump appears to be generated in the following manner[11]: the rise in the total cross-section is associated with the rapid increase of $\sigma_{KN\pi}$ above the N* threshold, the flattening and fall-off with the saturation of $\sigma_{KN\pi}$, and the monotonic fall of σ_{KN}; finally

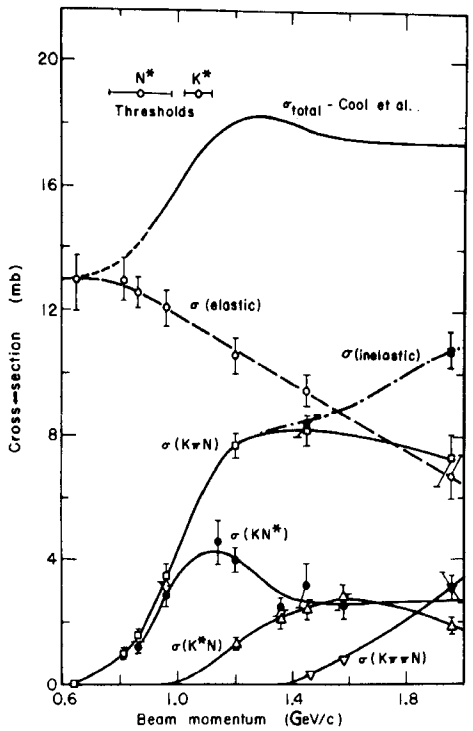

Fig. 3 Total and partial K^+p cross-sections. The partial cross-section curves are intended only to guide the eye.

the drop is arrested with the onset of $\sigma_{KN\pi\pi}$. According to this superficial analysis there is no need to invoke a resonance.

For this Conference, the same Berkeley group[12] has also made a partial wave analysis of the K^+p elastic scattering angular distribution below 1 GeV/c which is well below the bump in I = 1 at 1.25 GeV/c. Since inelastic channels are clearly important, and since polarization data are unavailable, the problem is underdetermined. Nevertheless, from information derived from the inelastic processes it can be inferred that the dominant absorption occurs in the $P_{1/2}$- and $P_{3/2}$-states. Thus the $S_{1/2}$-, $D_{3/2}$-, and $D_{5/2}$-states are assumed to be purely elastic. To restrict the problem further, a certain continuity was assumed between the solutions at the three fitted momenta. Figure 4 shows the Argand plot for the elastic amplitudes. They find two solutions related through a

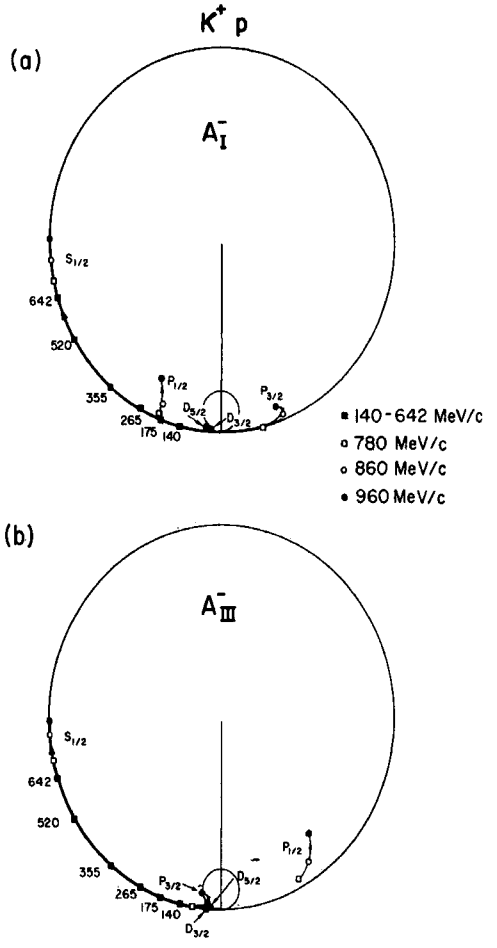

Fig. 4 The Argand diagrams for the K^+p elastic amplitudes for two solutions, as found in the Berkeley analysis[12]. From the size of the total cross-section bump one can conclude that if, for example, the resonance were in J = 3/2, the diameter of the resonant circle would be only 10% as large as the unitarity circle, as indicated by the small circle.

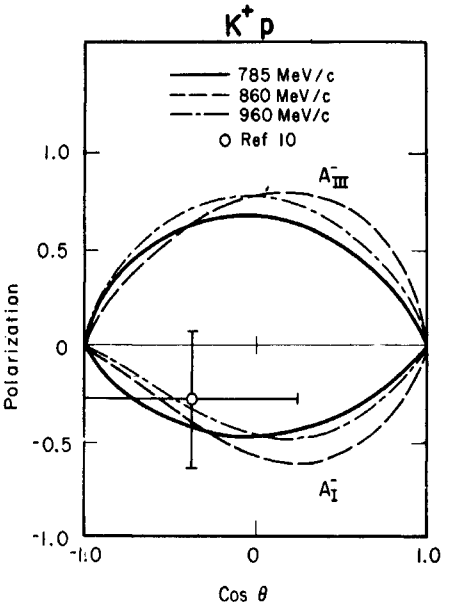

Fig. 5 Predicted polarizations for the two solutions of Fig. 4 and the measured polarization[13] at 780 MeV/c.

Fermi-Yang transformation. K^+p polarization data at 780 MeV/c [13] give a 2.5 standard deviation preference for solution A_I^- as seen in Fig. 5. The three fitted momenta are shown on Fig. 4 as well as some lower energy data. There is no evidence of a resonant structure in any partial wave for solution A_I^-, but it must be emphasized that the highest momentum point is more than a half-width below the conjectured resonance, so that little structure would be apparent up to this energy anyway. Also, from the size of the total cross-section bump one can conclude that if, for example, the resonance were in J = 3/2, the diameter of the resonant circle would be only 10% as large as the unitarity circle and therefore quite difficult to establish conclusively without precise experiments.

In contrast to this analysis, a recent AGS experiment[14] on backward K^+p scattering (Fig. 6) has been phase-shift analysed in an energy-dependent parametrization. The analysis seems not to have included the 780 MeV/c polarization point, since the Argand diagram shown in Fig. 7 resembles solution A_{III}^- extended to higher energy. I do not know whether an A_I^- type solution would also fit the new data as well as satisfy the polarization point. A resonant-like behaviour is seen in Fig. 7 at 1.45 GeV/c (2 GeV mass) which is well above the total cross-section bump at 1.25 GeV/c.

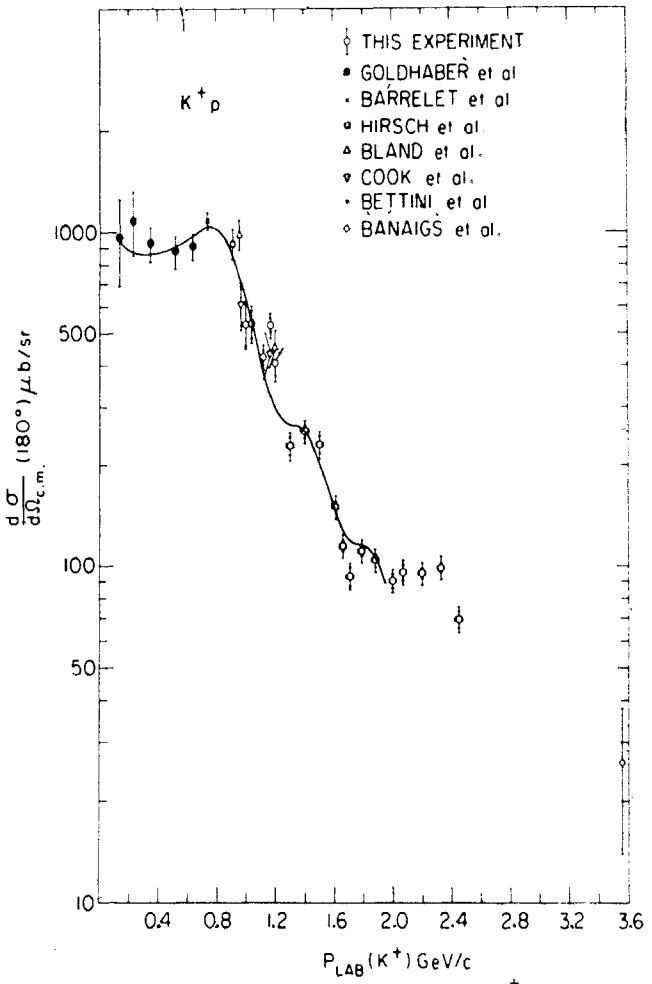

Fig. 6 The 180° differential cross-section for K^+p elastic scattering as a function of incident K^+ momentum. The solid line is the cross-section as obtained from a phase-shift analysis of all K^+p data up to 2.0 GeV/c[14].

The I = 0 bump in the KN system occurs 100 MeV/c below the I = 1 bump, and is nearly twice as large and perhaps slightly narrower. One is thus even more tempted to associate this structure with a resonance. However, since this cross-section must be extracted from the K^+d cross-section after subtraction of an appropriate amount of K^+p cross-section, the question becomes more delicate. First there is the eclipsing effect, namely the Glauber-Wilkins correction. Then there is the effect of the deuteron internal momentum which results in a cross-section averaged over a considerable energy region. That the latter, in particular, has not been given sufficient attention in the region of rapidly varying cross-sections has been shown recently by a group working at Nimrod[15] who have studied these effects in the overdetermined $\pi^\pm p$ and $\pi^\pm d$ systems. In addition to small ($\sim$ 1%) unexplained charge-dependent effects, they observe anomalous fluctuations in the resonance region. When

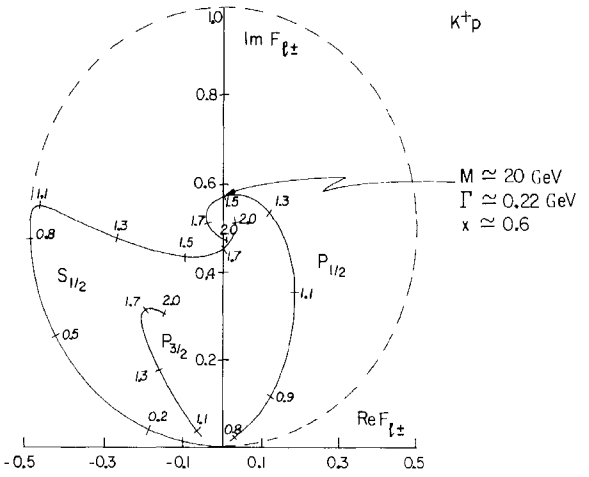

Fig. 7 Argand diagram for K^+p elastic scattering, as presented by Carroll et al.[14].

this anomaly is expressed in terms of the effective inverse mean squared radius of the deuteron required to calculate the difference ["σ(π^+p)" + "σ(π^-p)"] − σ(πd) (where quotation marks refer to the folded cross-section), one finds large excursions (Fig. 8) which coincide with the variations in the cross-sections associated with the πN resonances. In particular, $\langle r^{-2} \rangle$ appears to go negative at about 800 MeV/c. Since the variations coincide with those of the πN cross-section, it is suggestive that some additional effects have not been properly accounted for in the folding procedure.

Some alternative suggestions to account for the negative excursion in Fig. 7 have been put forward at this Conference[16]. One suggestion is that it could be due to the production of an "excited deu-

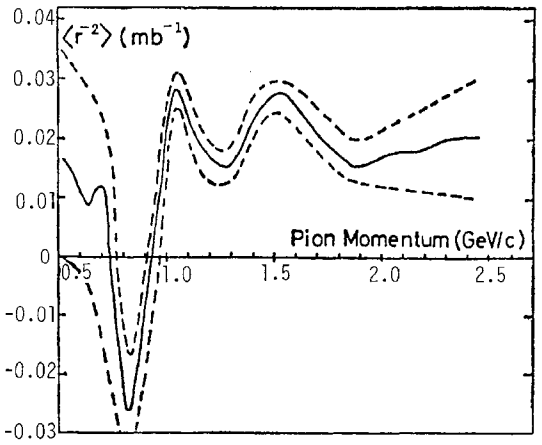

Fig. 8 The deuteron parameter $\langle r^{-2} \rangle$ as a function of momentum as measured at Nimrod[15] with $\pi^\pm p$ and $\pi^\pm d$. The dashed lines indicate estimated limits of experimental error.

teron" (d*) with I = 0 or 1, thereby making the πd cross-section appear larger than the sum of the neutron and proton cross-sections. For the anomaly to occur just above the d* production threshold would require that $M_{d*} = M_d + \sim 500$ MeV. Now if the same effect occurred in the K^+d system, its threshold would occur, interestingly enough, quite near the I = 0 bump found in the KN total cross-section. A rough estimate shows that the bump could be removed by this mechanism, as shown in Fig. 9. (Note also on this figure that the two experimental determinations of the I = 0 cross-sections do not within themselves agree very well.) There seems to be little concrete evidence from other reactions either in support of or in contradiction to this proposal.

The Berkeley K^+ group[17] has also reported an investigation of various reaction channels in a K^+d bubble chamber exposure in the region of the I = 0 bump. Despite the fact that not all charge states are identifiable, with some ingenuity they have separated out the I = 0 elastic and single-pion cross-

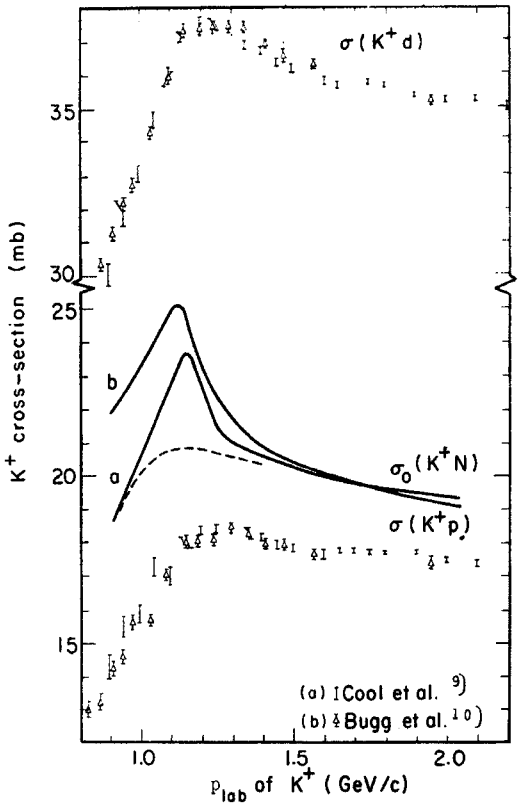

Fig. 9 The K^+d and K^+p total cross-sections. The solid curves are the I = 0 part of the KN cross-section as measured by Cool et al. and Bugg et al., whilst the dashed curve shows the possible effect on the I = 0 bump due to an excited deuteron suggested by Alexander et al.[16].

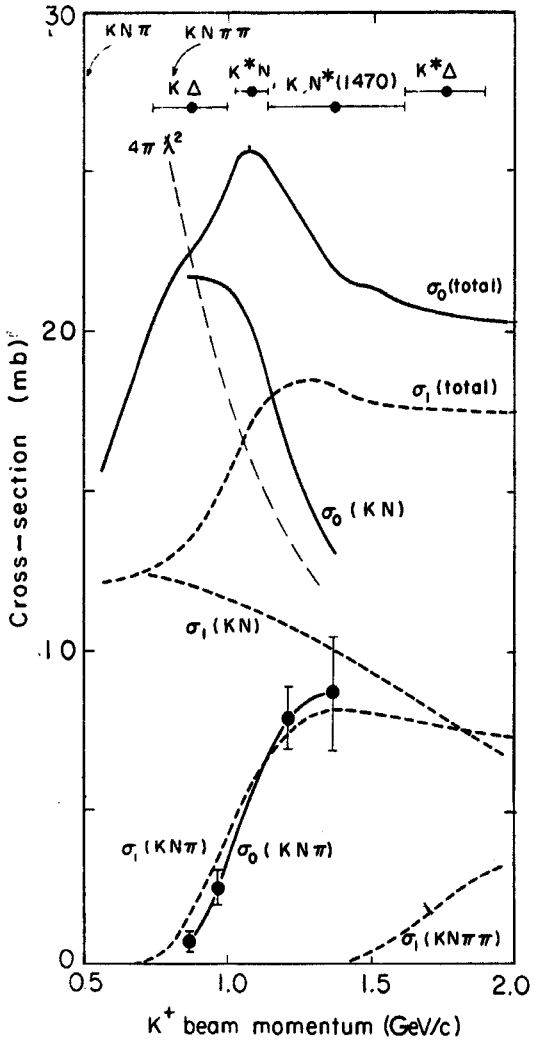

Fig. 10 Isospin 0 and 1 cross-sections from the paper of Hirata et al.[17].

sections using charge independence. Figure 10 shows the cross-sections. There appears to be no structure, but again no detailed partial wave analysis has yet been attempted.

In conclusion, apart from the original evidence for Z* which came from the KN total cross-section bumps, none of the subsequent work has required or even suggested resonance interpretations. However, a definitive statement will have to await a partial wave analysis, which in turn will require detailed polarization measurements. These will be done in the near future at Argonne and at Brookhaven.

4. BARYON STATES WITH S = -2

Because it is impossible to do formation experiments for S = -2 baryons, they have for a long time been the weak point of classification schemes. Frag-

TABLE 1

Ξ branching fractions

Decay mode	Ξ(1830)	Ξ(2030)
$\Lambda\bar{K}$	0.6	0.5
$\Sigma\bar{K}$	0.3	0.5
Ξ(1530)π	0.1	Small*
Ξπ	Small*	Small*

*) No signal detected

mentary data on Ξ*'s have accumulated slowly over the years, but Ξ(1530) is still the only well-understood object. Table 1 shows the Ξ* situation before the Conference. Now a BNL-Syracuse collaboration[18] reports a confirmation of Ξ(1815) and of Ξ(1933). In addition they report the existence of a new resonance Ξ(2030). This work was done in a K^-p bubble chamber experiment at 3.9, 4.6, and 5.0 GeV/c. Figure 11 shows the effective mass distribution for the Ξ(1530)π, $\Sigma^-\bar{K}^0$, Σ^0K^-, and ΛK^- distributions for reactions also containing a K^+. At 1830 MeV all channels have small signals, which together produce a 4 standard deviation enhancement at (1830 ± 10) MeV with a width of (60^{+35}_{-20}) MeV. It should be noted that this experiment yields a prominent $\Sigma\bar{K}$ branching fraction of about 30% in contrast to the complete absence of this mode in the experiment which first found Ξ(1815). Either one of the experiments is wrong (the experiment reported here has not inspected the Σ^+K^- decay mode which provided the strongest evidence against $\Sigma\bar{K}$ in the first experiment) or there are two objects here. The masses are shifted by 15 MeV and the widths are not in good agreement, the latest wallet card giving Γ = (16 ± 8) MeV for Ξ(1815). Since SU(3) calls for a Ξ* for every N* and Δ, such a possibility should not be unwelcome.

Figure 11 also shows a new Ξ(2030), again a 4 standard deviation effect, decaying about equally into $\Lambda\bar{K}$ and $\Sigma\bar{K}$ with no detectable signal in Ξ(1530)π or Ξπ. Its mass and width are quoted as M = (2030 ± 10) MeV and Γ = (50^{+25}_{-20}) MeV. Table 1 lists the branching fractions for Ξ(1830) and Ξ(2030) as given by the above experiment.

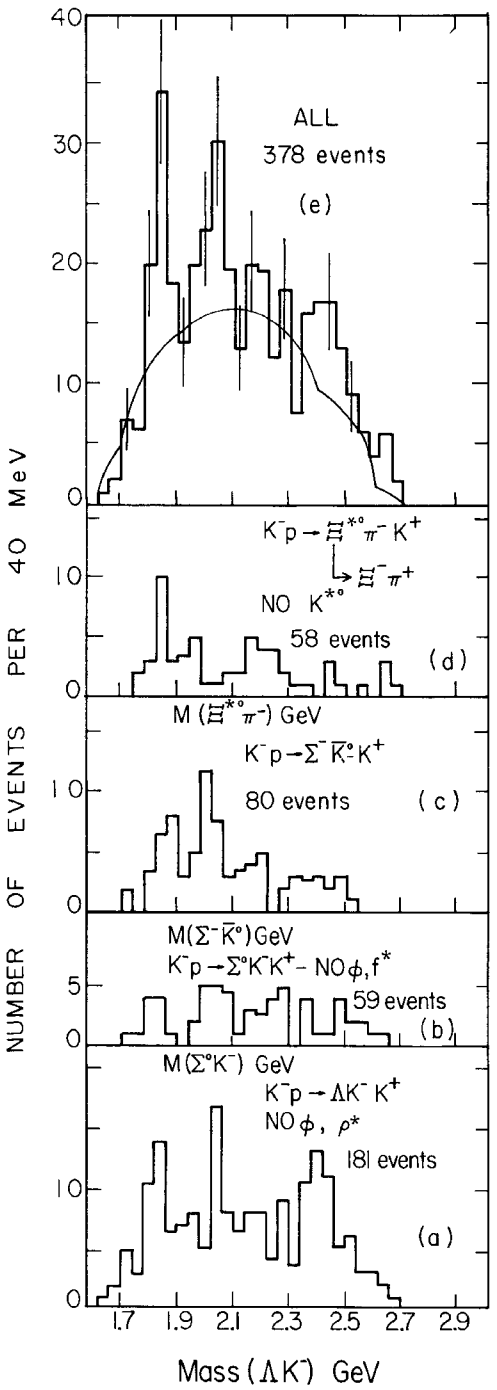

Fig. 11 The mass distributions measured by the Brookhaven-Syracuse group[18] for: a) ΛK^-; b) Σ^0K^-; c) $\Sigma^-\bar{K}^0$; d) Ξ(1530)π^-; e) sum of all channels for the reactions $K^-p \to$ (above combinations) + K^+.

Figure 12 shows the effective Ξπ mass observed for a number of other topologies done in the same experiment[18] at several different K^- energies. A convincing peak is seen at a mass of (1930 ± 20) MeV with a width of (80 ± 40) MeV. Other decay modes such as $\Lambda\bar{K}$ and $\Sigma\bar{K}$ are not seen, but upper limits can be placed on these decay rates which are consistent with SU(3) if this resonance has $J^P = 5/2^-$ (for which

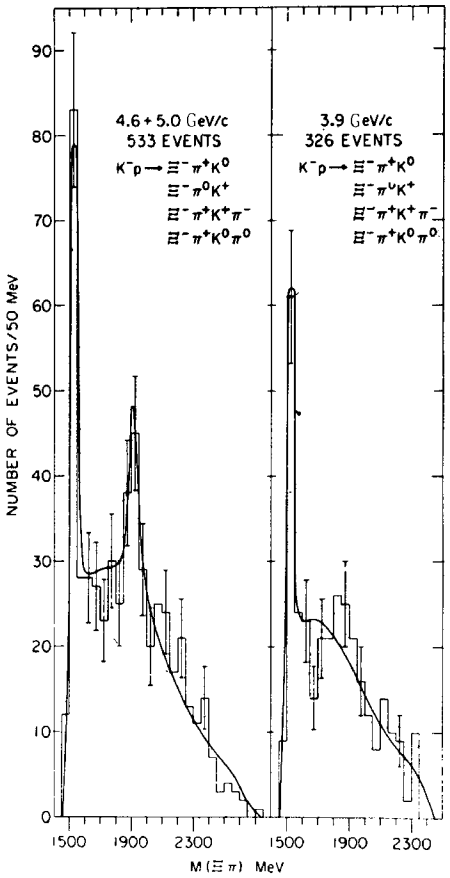

Fig. 12 The $(\Xi^-\pi^+)$ and $(\Xi^-\pi^0)$ mass distributions measured by the Brookhaven-Syracuse group[18] from three- and four-body reactions at incident K^- momenta of a) 4.6 and 5.0 GeV/c, and b) 3.9 GeV/c.

there is no direct evidence). Up to now only the Σ^0K^0 decay mode and not Σ^+K^- has been studied by this group. The latter mode should be nine times more copious when one includes factors of visibility, and could therefore place much more stringent limits on the $\Sigma\bar{K}$ decay rate.

5. BARYON STATES WITH S = -1

The Y*'s are quite well explored, both because of the availability of K^-p formation experiments and because of the variety of easily analysed two-body decay modes.

Somewhat out of the main stream of hyperon research but of considerable intrinsic interest, comes the first good evidence for the radiative decay mode of a known baryon resonance. This has been presented in preliminary form at the Conference by a Berkeley group working with low-energy K^- in a hydrogen bubble chamber[19]. The reaction studied is $K^-p \to \Lambda(1520) \to \Lambda\gamma$, where only the Λ decay is observed in the final state. Figure 13 shows the missing-mass spectrum for

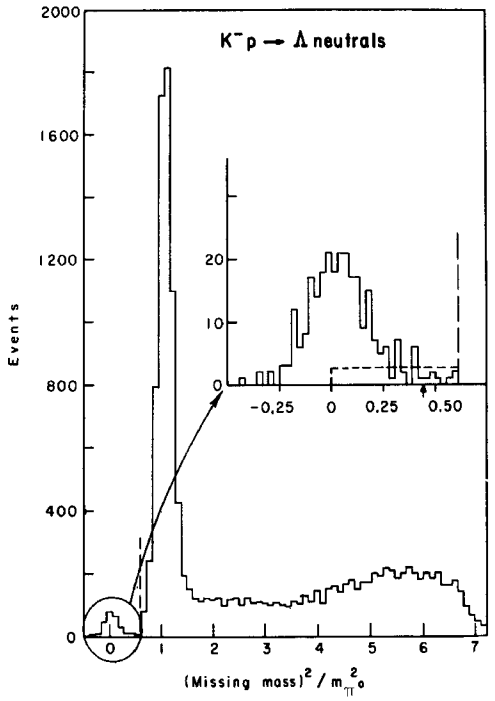

Fig. 13 Events versus (missing mass)^2 as measured by the Berkeley group[19] for the reaction $K^-p \to \Lambda$ + neutrals in which the proton from Λ decay stops in the chamber. The dashed rectangle is the estimated number of $\Sigma^0\gamma$ events.

those Λ events where the decay proton stops in the chamber, so that a precise momentum measurement of the Λ is achieved. In this way a peak at zero missing-mass is clearly separated from the more copious $\Lambda\pi^0$, $\Sigma^0\pi^0$, and $\Lambda\pi^0\pi^0$ reactions. As the K^- beam momentum is varied through the 1520 MeV mass region, an enhancement is observed in the $\Lambda\gamma$ cross-section, as seen in Fig. 14. The fitted curve corresponds to a radiative decay width of (0.15 ± 0.03) MeV, i.e. down by nearly α from the strong decay modes (Γ_t = 16 MeV).

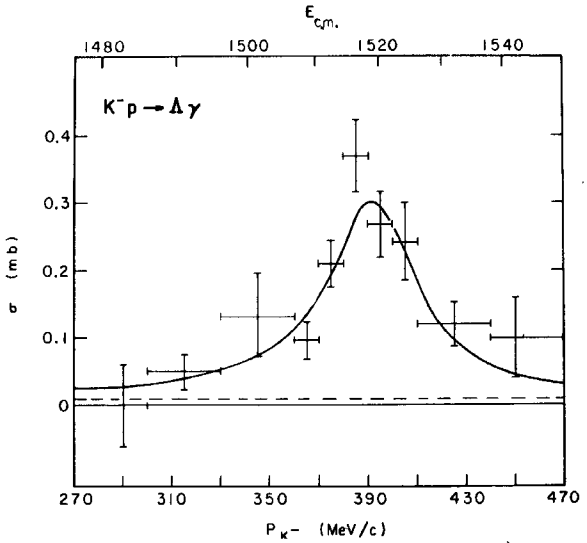

Fig. 14 Cross-section for $K^-p \to \Lambda\gamma$ in millibarns[19]. The upper curve is the fit to a Breit-Wigner + constant background. The dashed curve is the background.

The angular distribution for this mode of Λ(1520) decay, corrected for various experimental cuts, is shown in Fig. 15. It is seen to be consistent with electric dipole and inconsistent with magnetic quadrupole decay. The observed radiative width is comparable to the partial widths of photoproduced N*'s, but since Λ(1520) is a unitary singlet, no currently meaningful comparisons can be made.

Another study of a radiative hyperon decay has been reported at this Conference[20]. This experiment, done at Dubna with a 5.1 GeV/c π^- beam incident on a 1 metre propane bubble chamber, suggests the possibility of a new Y* at a mass of 1327 MeV. Both the Λ and γ were detected and an effort was made to separate the production on protons from the production on carbon. Figure 16 shows the proton events versus the (Λγ) mass. In addition to the Σ^0 peak, there appears to be a peaking at 1327 MeV with a statistical significance of about 3.5 standard deviations. The experimental width of the enhancement is comparable to that of the Σ^0, so presumably it arises mainly from the experimental resolution. Surprisingly enough, in a somewhat larger sample of carbon events, although the Σ^0 peak is clearly present, there is little if any evidence for an enhancement at

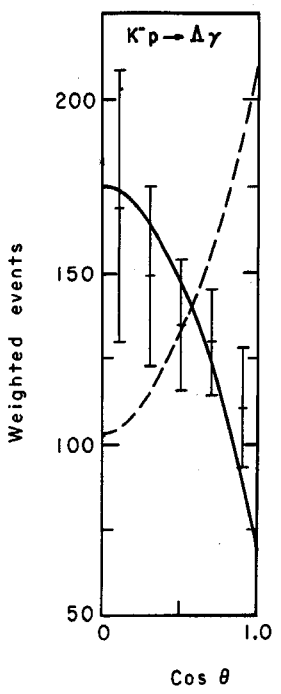

Fig. 15 Weighted events versus production cosine of the γ [19]. The solid curve, normalized to the total number of events, is 5-3 $\cos^2\theta$, corresponding to electric dipole decay. The dashed curve is 1 + $\cos^2\theta$ expected for magnetic quadrupole decay.

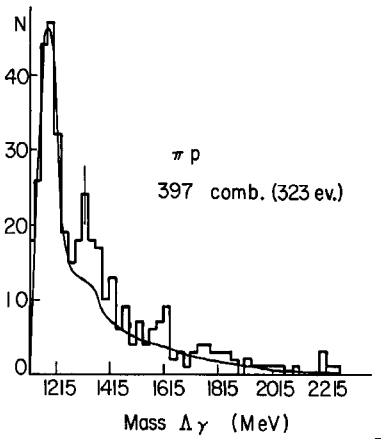

Fig. 16 Events versus (Λγ) effective mass for π^-p reactions, as measured by the Dubna group[20] for 5.1 GeV/c π^- incident on propane. No Λ or γ detection effeciencies have been introduced. The solid curve is a Monte Carlo calculation which includes known cross-sections for $Y_1^*(1385)$, $Y_0^*(1405)$, and $Y_0^*(1520)$.

1327 MeV. A previous experiment at Dubna[21] using a smaller chamber had seen this effect but had ascribed it to the reaction $Y_0^*(1670) \to \Lambda\eta$, where one γ from the η decay was detected. With a larger chamber they are able to materialize both γ's with sufficient efficiency to explore this alternative. No events were found corresponding to this hypothesis when five would be expected. With this alternative explanation eliminated, they conclude that there is evidence for a new hyperon resonance at 1327 MeV. The width is consistent with a purely electromagnetic decay which suggests that the isospin is zero, thereby suppressing the Λπ decay mode. (The mass coincides with the $\Sigma^0\pi^0$ threshold.) It is difficult to fault the experiment in any specific way. However, it is surprising that such a hyperon, produced in this instance with about 10% of the Σ^0 cross-section, would have gone undetected for so long. As an example of experimental situations which should have revealed such a resonance, one may cite the reaction $\pi^- + p \to K^0(\to \pi^+\pi^-) + + MM$ [22], where Λ, Σ^0, $Y_1^*(1385)$, and $Y_0^*(1520)$ are clearly seen at pion energies somewhat below the Dubna experiment, but there is no evidence for an enhancement at 1327 MeV.

The next two figures (Figs. 17 and 18) give a panoramic view of the Y* resonance region as seen from the K^-p system. The first shows $A_0 = \sigma/4\pi\lambda^2$ for elastic scattering and charge exchange. The points from 450 to 1200 MeV/c are those from the extensive CERN-Heidelberg-Saclay (CHS) Collaboration. The very prominent structure in the 1 GeV/c region for charge

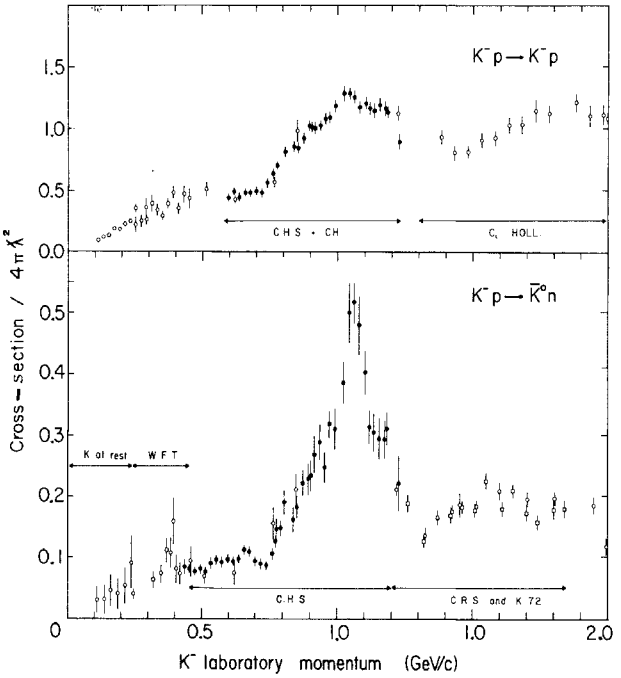

Fig. 17 The A_0 coefficient for K^-p elastic and charge exchange scattering from 0-2 GeV/c.

exchange is due to the highly elastic Σ(1765) and Λ(1815). Near 620 MeV/c, A_0 goes through a minimum. Here is the region of Σ(1660) where confusion continues to reign for lack of sizeable coupling to the K^-p channel. The next figure shows the Σπ and Λπ A_0-coefficients. The latter, in particular, shows the prominent contribution of Σ(1765).

The CHS analysis of differential cross-sections and polarizations (when measurable) in most channels has been completed from 800-1200 MeV/c [23]. Now, the analysis has been extended down to 600 MeV/c [24], and I shall go through the results of their partial wave analysis for the eight low partial waves which are dominant in this region. These are listed in

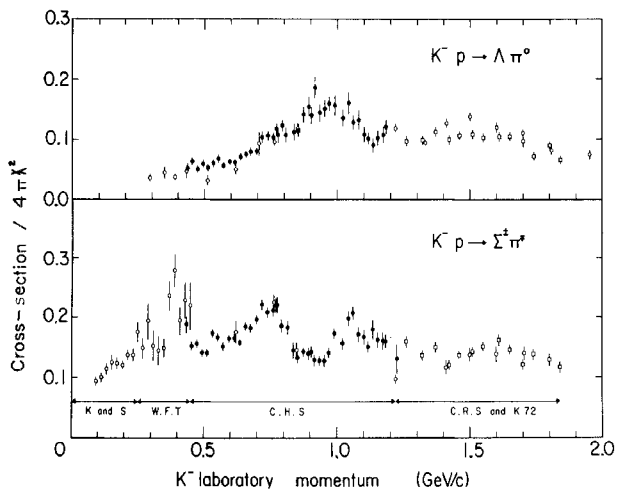

Fig. 18 The A_0 coefficient for Λπ and $(\Sigma^+\pi^- + \Sigma^-\pi^+)$ from 0-2 GeV/c.

TABLE 2

Summary of evidence for Y*'s of J ≤ 3/2 in the 1600-1900 MeV mass region

$L_{I,2J}(J^P)$	Old status	New status					Quality *)
			Mass (MeV)	Width (MeV)	Br. frac. (%)	Laboratory	
$S_{01}(1/2^-)$	Λη resonance at ∿ 1670 MeV	$\bar{K}N$	1663	26	14	CHS	A
		Σπ	1678	26	45		
		Λη	1670	18	28	BNL	
	-	$\bar{K}N$	1750	110	20	Chicago + Heidelberg	C
$S_{11}(1/2^-)$	Λπ enhancement at ∿ 1680 MeV	$\bar{K}N$	-	-	7-10	CHS	B
		Λπ	1650	100	70-93		
		Σπ	-	-	-		
	Ση threshold effect at ∿ 1750 MeV	$\bar{K}N$	1769	123	12	Chicago + Heidelberg	B
$P_{01}(1/2^+)$	-	$\bar{K}N$	1745	147	40	CHS	C
		Σπ	-	-	-		
$P_{11}(1/2^+)$	-	$\bar{K}N$	-	-	2-10	CHS	B
		Λπ	1610	60	20-98		
		Σπ	-	-	-		
		Λπ prod.	1616	60	-	BNL (no J^P det.)	
	-	Λπ	1882	222	-	LRL	C
$P_{03}(3/2^+)$	-	-	-	-	-	-	
$P_{13}(3/2^+)$	-	$\bar{K}N$	-	-	4-10	CHS	C
		Λπ	1660	80	40-96		
		Σπ	-	-	-		
$D_{03}(3/2^-)$	Λ(1690)	$\bar{K}N$	1696	35	18	CHS	A
		Σπ	1681	85	60		
		Σππ	-	-	20		
$D_{13}(3/2^-)$	Σ(1660)	$\bar{K}N$	1668	56	9	CHS	A
		Λπ	1667	50	29		
		Σπ	1661	44	49		
		Λ(1405)π	-	-	≲ 8		
		Λππ	-	-	≲ 10		

*) A stands for "well established"; B for "good evidence but in need of confirmation"; C for "shaky evidence".

Table 2 along with their old and new status as well as evidence coming from other experiments as noted. In the table I classify the resonances A, B, or C according to my judgement of their quality. Category A stands for well-established resonances which any symmetry scheme must accommodate. In this region there are three old ones and no new ones. Category B contains three probable resonances. Category C covers four possible resonances emerging from the data; one may accept or reject these as he chooses. I believe Harari in his Rapporteur's talk has bought them all.

Some of the data and partial wave analyses from which the new conclusions of CHS are derived are shown in Fig. 19 for the $\bar{K}N$ channels, Fig. 20 for the $\Sigma^\pm\pi^\mp$ channels, and Figs. 21 and 22 for the Λπ channel. The Argand diagrams of Fig. 19 show the behaviour of the non-resonant $\bar{K}N$ amplitudes which are parametrized

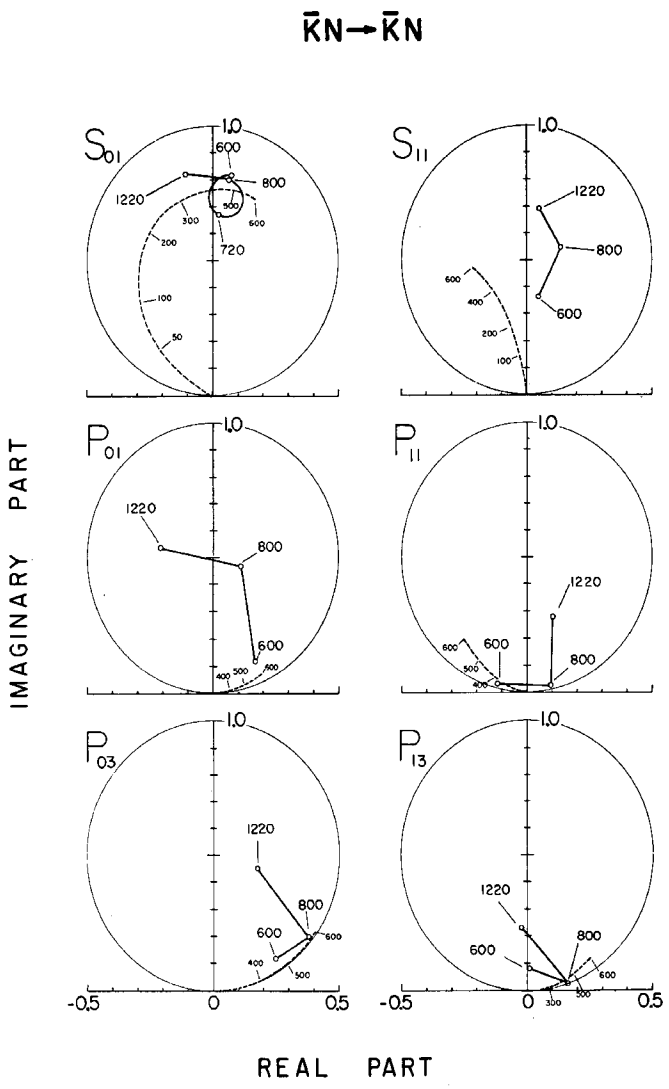

Fig. 19 The Argand diagrams for the S- and P-waves for the reactions $K^-p \to K^-p$ and $K^-p \to \bar{K}^0n$ versus K^- laboratory momentum from the CHS Collaboration experiment.

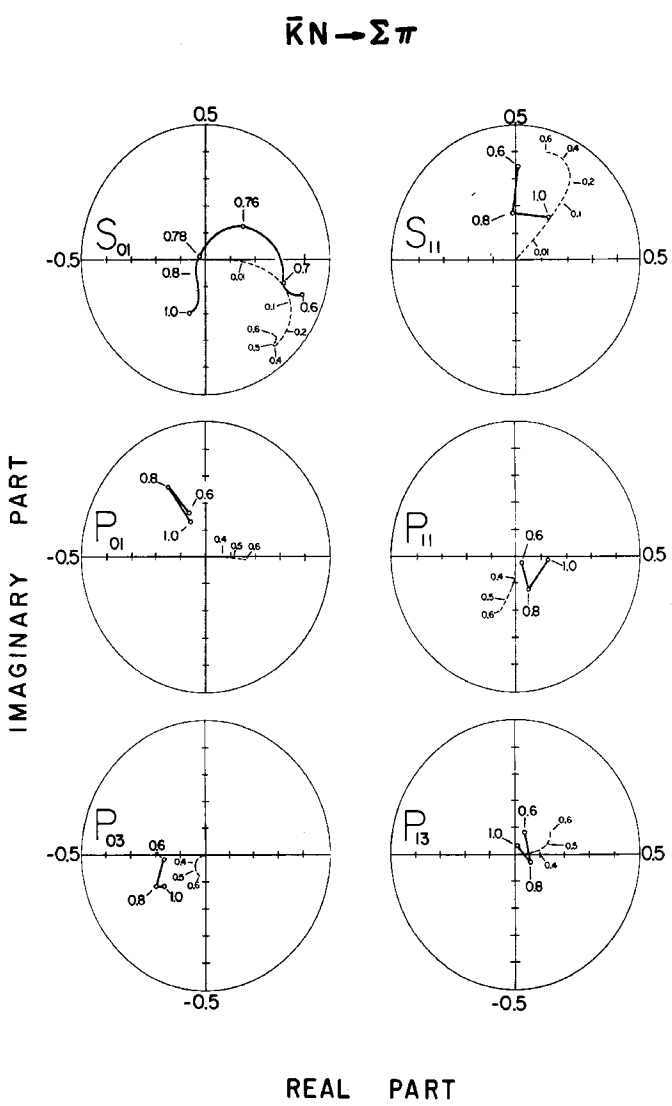

Fig. 20 The Argand diagrams for the S- and P-waves for the reaction $K^-p \to \Sigma^{\pm}\pi^{\mp}$ from the CHS Collaboration experiment.

as linear functions of the laboratory momentum over the range 600-800 MeV/c and over the range 800-1200 MeV/c. For the case of the S_{01} amplitude, a known resonance was also introduced in a way which preserves unitarity by multiplication of non-resonant and resonant S-matrices. The Argand diagrams for the $\Sigma\pi$ channels shown in Fig. 20 were obtained in a similar way, except that here the upper momentum range covered was from 800-1000 MeV/c. The $\Lambda\pi$ channel was, however, treated differently. Since this is a pure I = 1 state and since both angular distributions and polarizations are available, an energy-independent analysis was deemed feasible. In order to circumvent the problem of severe statistical scatter of data points, smoothed (in momentum) curves of the polynomial coefficients were obtained and these were then analysed in terms of amplitudes. Only the energy dependence of the dominant D_{15} amplitude was fixed as a Breit-Wigner resonance with the accepted value for the mass and width of $\Sigma(1765)$. Figure 21 shows the Argand diagrams for the two main distinct solutions found by CHS. With some imagination one can read resonant structures into these amplitudes, and the parameters of the resonances noted in Table 2 are based on the rates of change of the phase angles and the radii of the inferred circles. Figure 22 guides the eye for those who lack imagination. Despite the absence of any large structure [apart from $\Sigma(1765)$] in the $\Lambda\pi$ polynomial coefficients in the 600-800 peak region, there is, according to this analysis, some evidence for several new resonances.

Let us now discuss each particle wave of Table 2 in turn. The S_{01}-state (notation is $L_{I,2J}$) was known from a Brookhaven experiment[25] of several years ago

to have a resonance coupled to Λη near threshold. Now CHS has identified its branching fraction into $\bar{K}N$ and into Σπ, as shown in Table 2. A Chicago-Heidelberg preliminary study[26] of the same 800-1200 MeV/c K^-p, $\bar{K}^0n$ data also suggests a possible resonance at 1750 MeV. The CHS analysis, which uses the Legendre polynomial expansion coefficients rather than fitting the angular distributions directly but is otherwise the same as the Chicago-Heidelberg analysis, neither confirms nor excludes this possibility.

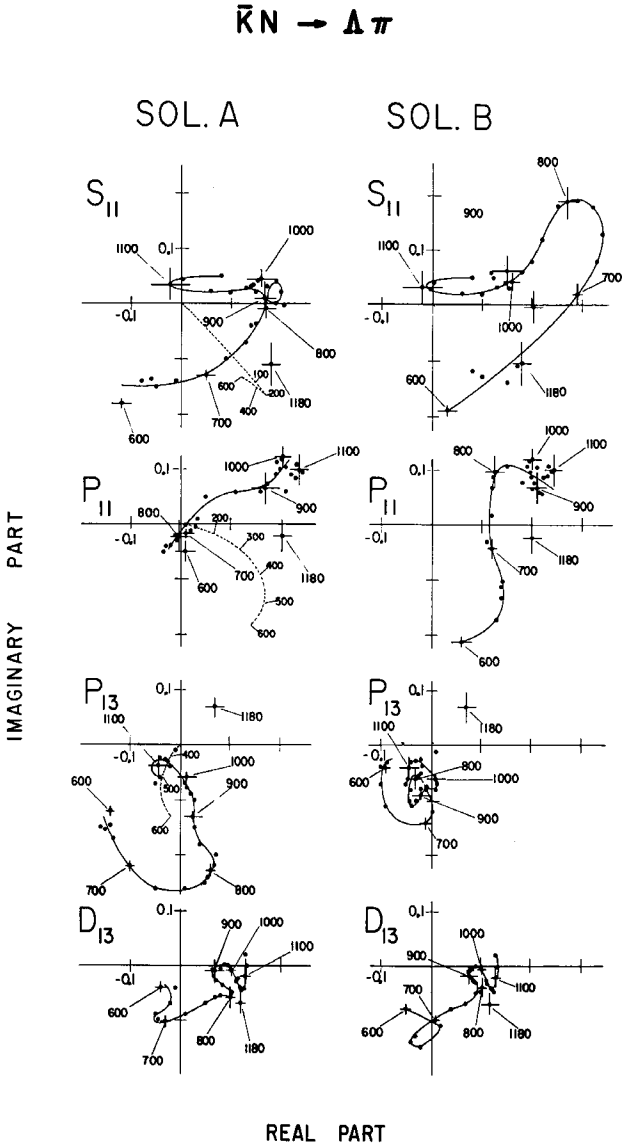

Fig. 21 Amplitudes of the two main solutions of the energy-independent partial wave analysis of $K^-N \rightarrow \Lambda\pi$ by the CHS Collaboration. The points shown every 20 MeV/c describe the momentum dependence of the amplitudes. The continuous line traces the general pattern of this dependence. The errors, shown only every 100 MeV/c, indicate the statistical uncertainty given by the minimizing program. The unitary circles are centred at the origin of each graph and have a radius of 0.5. The D_{15} amplitude, not shown, corresponds to Σ(1765) and is taken at resonance as purely imaginary and positive.

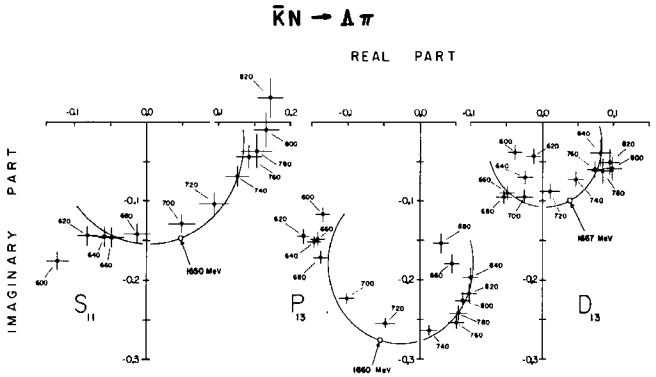

Fig. 22 Amplitudes S_{11}, P_{13}, and D_{13} of solution A in the resonance region. Segments of circles describe possible resonances with arrows indicating the position of the resonant mass.

For the S_{11}-state, a reasonably good circular behaviour has been found on the Argand diagram for Λπ production by CHS. Since it is seen only in the Λπ channel, one is tempted to associate this with the bump found only in Λπ at 1680 MeV by the high-energy production experiment done at Argonne[27] and later confirmed[28]. Also in S_{11} there is a suggestion of a separate Ση resonance near 1750 MeV to partner with Nη and Λη [7]. Now the Chicago-Heidelberg analysis reveals a broad $\bar{K}N$ structure in this region which may be associated with the elastic channel of this resonance.

The P_{01}-state displays a large amplitude in the $\bar{K}N$ channel which, when parametrized as non-resonant, does suggest a resonant behaviour (see Fig. 19). A Breit-Wigner form makes some improvement in the fit, but the evidence is only weak for this resonance.

The P_{11}-state gives some weak indication for resonant structure in Λπ near 1610 MeV but only in solution B of Fig. 21. This could be associated with better evidence for a 1616 MeV bump from a Brookhaven production experiment reported at this meeting[29] which I shall discuss later. A Berkeley formation experiment[30] also sees structure at 1882 MeV, but this is not seen in the CHS formation experiment.

For P_{03} there are no candidates at the present time, while for P_{13} there is a rather large amplitude in Λπ which could be resonant at about 1660 MeV. Note that this is the same state ($J^P = 3/2^+$) and channel which gave the first[31] and much-disputed evidence[32] for the parity of Σ(1660). Thus it may be that both parities of Σ(1660) are correct!

Perhaps the most prominent feature of formation experiments comes from the good evidence for the well-known resonance in D_{03} at 1690 MeV appearing clearly in $\bar{K}N$ and in $\Sigma\pi$ with some evidence for decay into $\Sigma\pi\pi$. The discrepancy between the mass and especially the width of D_{03} as measured in the $\bar{K}N$ and in the $\Sigma\pi$ channels remains unresolved and probably reflects the inadequacy of the parametrization.

Finally we come to the perennial sick man of Y*'s, the $\Sigma(1660)$ of $J^P = 3/2^-$ which may now consist of several resonances. CHS provides new information on the branching fractions in the D_{13}-state as noted in Table 2. Only in the $\Sigma\pi$ channel is the signal really prominent. Much of this comes from spectacular interference effects brought about by the presence of the nearby $\Sigma\pi$ amplitude in the D_{03}-state. These branching fractions are in disagreement with information derived from a Berkeley production experiment presented at the Conference[33]. In this latter experiment done with 2.6 GeV/c K^- on protons, a very peculiar phenomenon is noted: the branching fractions appear to vary markedly with momentum transfer. This is seen in Fig. 23. A strong 1660 signal is seen in the decay channel $\Lambda(1405)\pi$ for small momentum transfer. In fact this is the channel in which the $\Sigma(1660)$ found in production experiments was shown to have $J^P = 3/2^-$ [34]. At larger momentum transfer the $\Sigma\pi$ mode begins to dominate, more in keeping with the CHS branching fractions. The Berkeley authors suggest a possible explanation for this peculiarity: there are two $\Sigma(1660)$ essentially degenerate in mass and width and with the same J^P and I, one made at low momentum transfer (perhaps coupled strongly to the K* exchange diagram) whilst the other is made at large momentum transfer. The formation experiment could be seeing some linear combination of these two states, but predominantly the latter. It is not a pretty picture, but it is perhaps the most economical one which can accommodate the presently observed branching fractions as given by the Berkeley group. This model could possibly do away with the Argonne $\Sigma(1680)$[27], since the most compelling evidence for its difference from $\Sigma(1660)$ comes not from its 20 MeV mass displacement but from its different branching fractions. Of course, since the production mechanism is not understood, an alternative possibility of explaining the

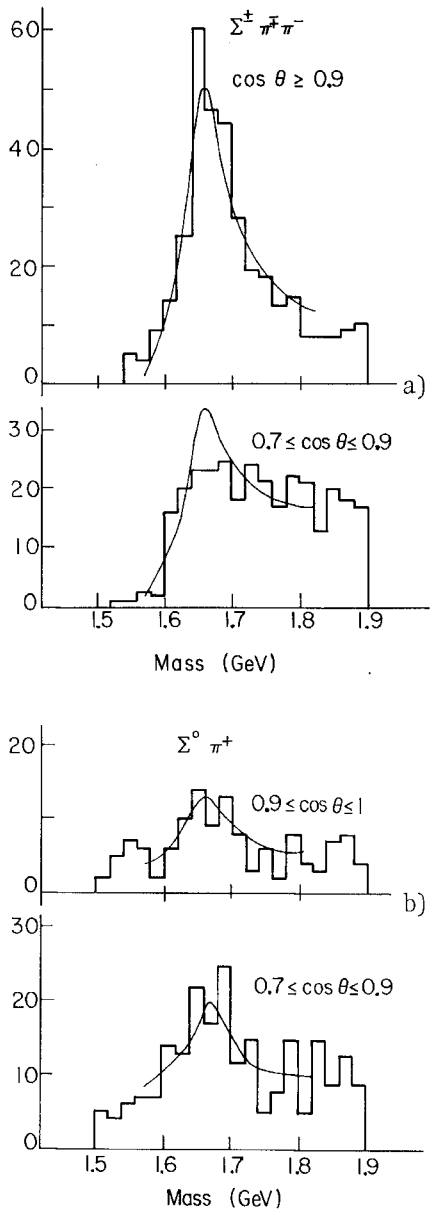

Fig. 23 The effective mass distributions, as measured at Berkeley by Eberhard et al.[33] for a) $(\Sigma^{\pm}\pi^{\mp}\pi^+)$ and b) $(\Sigma^0\pi^+)$ for two different cos θ intervals, where θ is the angle between the incident K^- and the outgoing π^- in the reaction $K^-p \to (\Sigma\pi\pi)^+\pi^-$ and $(\Sigma\pi)^+\pi^-$. The curves represent the best fits to the data assuming a simple exponential dependence of $\Sigma(1660)$ production on momentum transfer: e^{-8t} for $\Sigma\pi\pi$ and e^{-2t} for $\Sigma\pi$.

Berkeley branching fractions of $\Sigma(1660)$ is that through some complicated production mechanism the branching fractions could be distorted by the presence of the other pion or by interference with non-resonant background.

Another piece of evidence for a new Y* resonance in this mass region comes from a BNL-CCNY experiment[29], as mentioned previously. Using K^- of 3.9 GeV/c incident on deuterium, they have studied the reaction $K^-n \to \Lambda\pi^-\pi^-\pi^+$ and observe a significant en-

hancement in the $\Lambda\pi^{\pm}$ mass at (1616 ± 8) MeV with a width of (66 ± 16) MeV, shown in Fig. 24. A corresponding enhancement is not observed in the three-body reaction $K^-n \to \Lambda\pi^-\pi^0$ in which ρ^- appears to be the dominant structure. Particular care was taken to avoid contamination from misidentified Σ^0 events. They report the following ratios of decay rates for this I = 1 state:

$$\Lambda\pi^{\pm} : [\Sigma(1385)\pi]^{\pm} : \bar{K}^0 p =$$
$$= (1.0 \pm 0.16) : (0.2 \pm 0.1) : (0.0 \pm 0.1).$$

The $\Lambda\pi$:$\bar{K}n$ branching fraction is inconsistent with an assignment of this object to a decuplet. Placed in an octet, the above branching fraction would require a $\Sigma\pi$ decay mode comparable in strength to $\Lambda\pi$. This decay mode, however, was not reported to have been studied.

A K^-p polarization experiment done at CERN and reported last year at Heidelberg[7,35] has confirmed the quantum number assignments of $\Sigma(2030)$ and $\Lambda(2100)$ to be $7/2^+$ and $7/2^-$ [36]. Their experiment also extends upwards into the region of $\Sigma(2250)$ and $\Lambda(2350)$. Having lower elasticities, these resonances do not yield their spin parities as conclusively. They have fitted K^-p elastic differential cross-sections and polarizations and total cross-sections using Breit-Wigner resonances in various spin-parity states and background amplitudes parametrized in three different ways. They conclude that $J^P = 9/2^+$ is the preferred assignment for $\Lambda(2350)$; this would fit well as the second Regge recurrence of Λ. Their fits show no clear J^P preference for $\Lambda(2250)$.

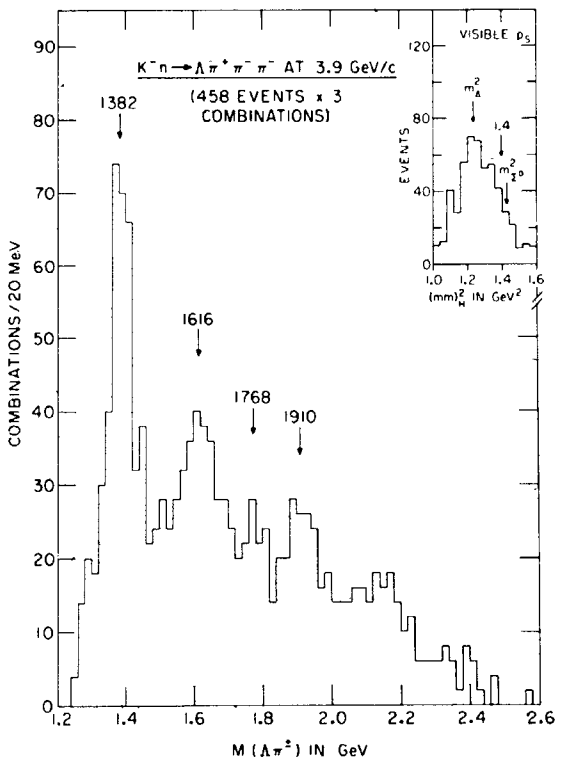

Fig. 24 The $\Lambda\pi^{\pm}$ effective mass in the reaction $K^-n \to \Lambda\pi^+\pi^-\pi^-$ at an incident K^- momentum of 3.9 GeV/c, as measured by Crennell et al.[29]

6. BARYON RESONANCES IN SU(3)

Most of the well-established baryon resonances can be accommodated with considerable success within the framework of SU(3). Not only can the resonances be arranged into singlets, octets, and decuplets in reasonable agreement with mass formulae, but also the partial decay rates are generally in good agreement with currently accepted multiplet assignments. In addition, a particularly striking success of SU(3) is the complete agreement between the observed and predicted relative signs of Y* resonant amplitudes, as measured through interference between different Y* resonances made in formation experiments. There are now at least a dozen measured signs which are found to be in good agreement. The situation was reviewed last year[37], and I shall close by presenting an updated version of the status of decay rates and relative phases of baryon resonance decays into stable baryons and mesons.

Two formulae are needed. For singlets and decuplets one can write the partial width as:

$$\Gamma = c^2 g^2 B_\ell(p) \left(\frac{M_N}{M_R}\right) p ,$$

where c = the SU(3) Clebsch-Gordan coefficient for each decay mode, g = effective coupling constant, $B_\ell(p)$ = centrifugal barrier factor for an angular momentum ℓ, p = c.m.s. decay momentum, M_R = resonant mass, and M_N = nucleon mass (introduced to make g dimensionless). For each decay mode one can then solve for g^2, and each member of the decuplet should yield the same value. Table 3 lists the partial widths employed for this and subsequent SU(3) comparisons. Masses, widths, and branching fractions come generally from UCRL 8030 (August 1968).

TABLE 3

Branching fractions and partial widths

J^P	Mass	Width	Mode	Branching fraction	Partial width	$B_\ell(p)p\ M_N/M_R$	C^2	g^2
Singlets								
$1/2^-$	Λ(1405)	40	Σπ	1.0	40	93.5	3/8	1.14
$3/2^-$	Λ(1520)	16	$N\bar{K}$	0.45	7.2	19.5	1/4	1.48
			Σπ	0.45	7.2	28.0	3/8	0.69
$7/2^-$	Λ(2100)	140	$N\bar{K}$	0.30	42	109	1/4	1.54
			Σπ	0.05	7	82.7	3/8	0.22
			Λη	<0.03	<4.2	44.1	1/8	<0.76
			ΞK	0.02 [a]	2.8	9.70	1/4	1.15
Decuplets								
$3/2^+$	Δ(1236)	120	Nπ	1.0	120	101	1/2	2.38
$3/2^+$	Σ(1385)	35	Λπ	0.86	30	74.2	1/4	1.62
			Σπ	0.14	4.9	21.4	1/6	1.37
$3/2^+$	Ξ(1530)	7.3	Ξπ	1.0	7.3	31.1	1/4	0.94
$7/2^+$	Δ(1950)	220	Nπ	0.40	88	248	1/2	0.71
$7/2^+$	Σ(2030)	120	$N\bar{K}$	0.10	12	173	1/6	0.42
			Λπ	0.35	42	173	1/4	0.97
			Σπ	0.10	12	144	1/6	0.50
			ΞK	<0.025	<3	26.0	1/6	<0.69
Octets								$\sqrt{\Gamma / B_\ell(p)p\ M_N/M_R}$
$1/2^-$	N(1550)	130	Nπ	0.30	39	289		0.367
			Nη	0.70	91	127		0.846
$1/2^-$	Λ(1670)	20	$N\bar{K}$	0.14 [b]	2.8	230		0.110
			Σπ	0.45 [b]	9	230		0.198
			Λη	0.28	5.6	37.1		0.388
$3/2^-$	N(1525)	115	Nπ	0.55	63	154		0.640
			Nη		0.4	3.88		0.321
$3/2^-$	Λ(1690)	40	$N\bar{K}$	0.18 [b]	7.2	117		0.248
			Σπ	0.60 [b]	24	101		0.487
			Λη	<0.005 [b]	<0.2	1.81		0.332
$3/2^-$	Σ(1660)	50	$N\bar{K}$	0.09 [b]	4.5	100		0.212
			Λπ	0.29 [b]	14.5	127		0.338
			Σπ	0.49 [b]	24.5	87.0		0.531
$3/2^-$	Ξ(1815)	16	Ξπ	0.10	1.6	97.4		0.128
			$\Lambda\bar{K}$	0.65	10.4	86.7		0.346
			$\Sigma\bar{K}$	<0.02	<0.32	39.3		0.090
$5/2^-$	N(1680)	170	Nπ	0.40	68	212		0.566
			Nη	<0.025	<4.25	85.9		0.222
			ΛK	<0.016	<2.7	13.2		0.452
$5/2^-$	Λ(1830)	75	$N\bar{K}$	0.08	6	182		0.181
			Σπ	0.42	31.5	159		0.445
			Λη	<0.10	<7.5	65.4		0.339
$5/2^-$	Σ(1765)	100	$N\bar{K}$	0.45	45	156		0.537
			Λπ	0.15	15	171		0.296
			Σπ	0.01	1	135		0.086
			Ση	<0.005	<0.5	1.82		0.524
$5/2^-$	Ξ(1930)	80	Ξπ	<1.0 [c]	<80	146		0.740
			$\Lambda\bar{K}$	<0.5 [c]	<40	148		0.520
			$\Sigma\bar{K}$	<0.75 [c]	<60	106		0.752
			Ξη	?		14.4		
$5/2^+$	N(1690)	130	Nπ	0.65	84.5	117		0.850
			Nη	<0.015	<1.95	23.5		0.288
			ΛK	<0.0013	<0.17	1.43		0.345
$5/2^+$	Λ(1815)	75	$N\bar{K}$	0.70	53.5	88.3		0.778
			Σπ	0.10	7.5	67.3		0.334
			Λη	<0.012	<0.9	12.3		0.270
$5/2^+$	Σ(1910)	60	$N\bar{K}$	0.08	4.8	128		0.194
			Λπ	0.10	6	132		0.213
			Σπ	<0.01	<0.6	100		0.077

References can be found in Ref. 37 except as noted:
a) Ref. 38; b) Ref. 24; c) Ref. 18.

Figure 25 is colour-coded according to the strangeness of the resonance, and shows g^2 evaluated from the decay rates for the famous $3/2^+$ decuplet. Contrary to statements frequently found in the literature, the agreement is not perfect; the Δ(1236) and Ξ(1530) rates differ by about a factor of two from that expected. Since the decuplet is considered to be the best established multiplet among the resonances, this disparity can be considered as setting the scale for expected disagreements with SU(3) among decay rates of less well-established multiplets. Also shown in Fig. 25 is a plot of g^2 for a possible $7/2^+$ decuplet, the presumed recurrence of the $3/2^+$ decuplet. Here again agreement is good to a factor of 2. For unitary singlets there are three good candidates: Λ(1405) of $1/2^-$; the $3/2^-$ Λ(1520); and its presumed recurrence Λ(2100) of $J^P = 7/2^-$. For these resonances, g^2 evaluated for various decay modes are also shown on the figure. At this point it is interesting to note that the sign of the interference between Σ(2030) and Λ(2100) in the $\Xi\bar{K}$ decay mode has recently been observed[38] to be in agreement with their assignments in a decuplet and a singlet. It is also worth while to point out that in spite of the fact that SU(3) makes no connection between the coupling constants of different SU(3) multiplets, the values found are all about the same. In fact, they agree as well between multiplets as they do between different decay modes within a multiplet, despite very different J^P and centrifugal barriers.

The decay rates of members of octets are complicated by the presence of two coupling constants: the symmetrical g_d and antisymmetrical g_f couplings. One therefore writes

$$\Gamma = (c_d g_d + c_f g_f)^2 B_\ell(p) \left(\frac{M_N}{M_R}\right) p$$

which can be solved for each measured partial decay rate

$$c_d g_d + c_f g_f = \pm \sqrt{\Gamma / B_\ell(p) \left(\frac{M_N}{M_R}\right) p}\ ,$$

yielding a linear relation between g_d and g_f. Thus each decay amplitude appears as a straight line plotted on a g_d-g_f plane with the distance from the origin proportional to the square root of the partial

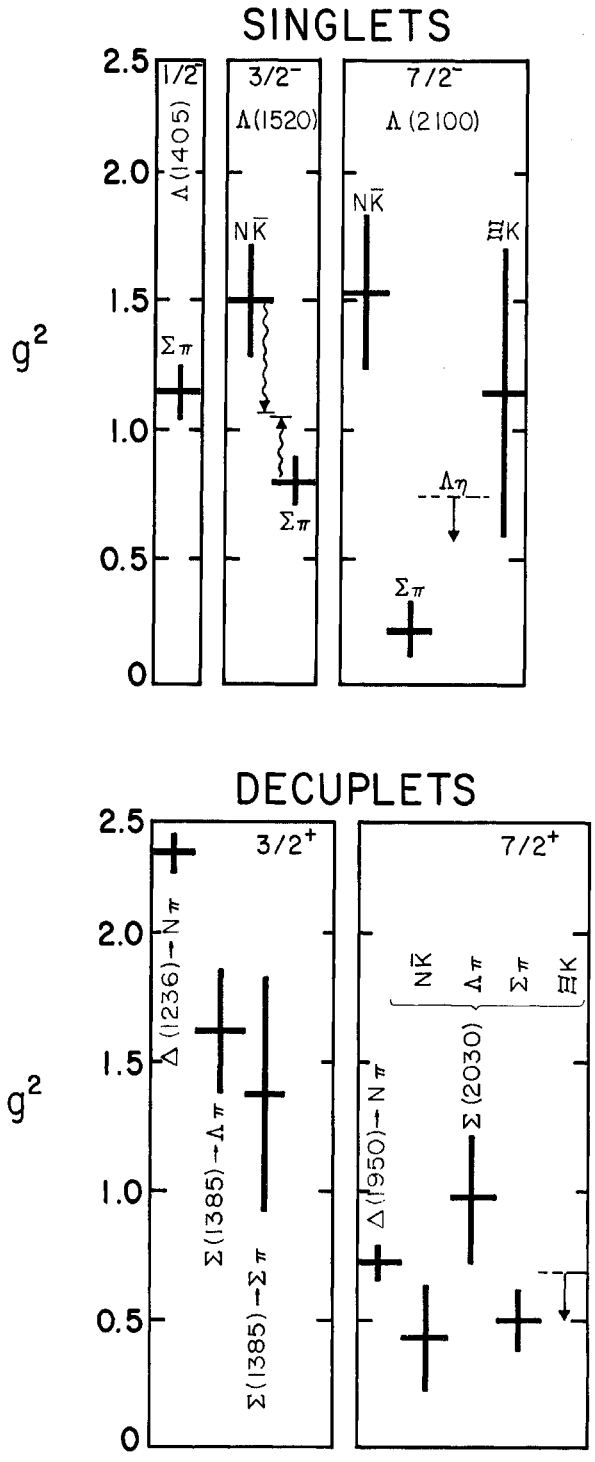

Fig. 25 Display of the relative coupling constants for various decay modes of the $3/2^+$ decuplet and its presumed $7/2^+$ recurrence, and the $1/2^-$, $3/2^-$, and $7/2^-$ states presumed to be unitary singlets. The SU(3) coefficients and corrections for mass differences have been introduced so that within each multiplet all decay modes should have the same value of g^2.

decay rate. The choice of sign is determined by the measured interference between the various Y* resonances. Exact SU(3) would require that all lines intersect at a common point. Plotted in this way, one obtains a global picture showing the consistency of all decay rates and phases; a considerable improvement over methods usually employed in which certain decay rates are arbitrarily fixed in order to predict all the others. At present there are four possible octets for which there is a sufficient number of members to make a meaningful comparison of decay rates.

Figure 26 shows the g_d-g_f plot for the $J^P = 1/2^-$ S-wave baryon-η octet currently containing just two good members: N(1570) and Λ(1670). The partial widths for the somewhat shaky Σ(1750) [7] are too questionable to display. On these plots the thickness of the line is intended to convey the approximate precision of the experimental partial width: the thicker the line, the better the rate is fixed. Thick lines are known to better than 25%, whilst thin lines can be off by a factor of 2 or more. Dashed lines represent upper limits. The new rate shown on this plot is for $\Lambda(1670) \to \Sigma\pi$, presented at this Conference[24]. It disagrees with the other known rates by a factor of 20. It has been suggested[39] that SU(3) impurity should occur most conspicuously in the S-state. Perhaps this is a manifestation.

For the $3/2^-$ octet there is a complete set of candidates, and there is generally good agreement among the decay rates as seen in Fig. 27. Mixing is introduced between Λ(1690) and the singlet Λ(1520), altering the decay rates as shown by the wavy lines and thereby improving the agreement. A good intersection of lines occurs for $g_d = 0.34$ and $g_f = 0.54$ yielding α, the ratio of D to D + F coupling, of $\alpha = 1/(1 + \sqrt{5}\, g_d/3g_f) = 0.46$. Black lines labelled (CHS) and (K&S)[40] indicate the acceptable regions of the plane imposed by the measured relative signs of coupling as determined by two groups of experiments. The plot has been updated by contributions of the CHS Collaboration[24] to this Conference, but they have produced no major change. The outstanding discrepancy associated with the absence of a $\Xi(1815) \to \Sigma\bar{K}$ decay mode can be resolved by using the new decay rates for Ξ(1830) presented at this Conference.

Figure 28 shows the $5/2^-$ octet. The only change here is the confirmation of Ξ(1933) with better-established upper limits on the rates. This octet has no major discrepancy at the present time. The best value of α is 1.16.

Finally, Fig. 29 shows the $5/2^+$ octet. Apart from the complete absence of $\Sigma(1910) \to \Sigma\pi$, good agreement is found with $\alpha = 0.46$. (This is not far from $\alpha = 2/3$ for the $1/2^+$ baryon octet, of which it is the presumed recurrence.) The spin-parity assignment of Σ(1910) remains unconfirmed, so that the disagreement here should not, for the moment, be taken seriously. The newly discovered Ξ(2030), whose J^P is unknown, could complete this octet. Its observed decay rates are in reasonable agreement with the above value of α.

Apart from the $J^P = 1/2^+$ πN resonance (the Roper resonance), this SU(3) summary of decay rates and phases contains all the major baryon resonances and a number of the minor ones as well. We have not attempted similar SU(3) exercises for the multitude of squirms and wiggles recently found on Argand plots for N* [41-43] and for Y* [24]. Neither have we considered the mounting information on decay modes of baryon resonances into baryons and vector mesons, or into baryon resonances and pseudoscalar mesons. Such exercises will probably be done and will deserve scrutiny at future meetings.

Figs. 26-29 Plots of g_d versus g_f for the known decay rates of the presumed octets of $J^P = 1/2^-$, $3/2^-$, $5/2^-$, and $5/2^+$. Colour coding according to strangeness and isospin of the resonant state is as shown on the right. Decay rates indicated by heavy lines are known to about 25%, medium lines are somewhat less well-known, whilst light lines may be uncertain to a factor of 2 or more. Error bars on the heavy and medium lines correspond to 25% and 50% uncertainty in the decay rates, respectively. Dashed lines denote upper limits. The black dashed lines indicate the regions of the figures allowed by the measurements of the relative signs of reaction amplitudes by Kernan and Smart and by the CHS Collaboration. The circle in each figure indicates the approximate values of g_d and g_f that seem to agree best with experiment. The wavy lines in Fig. 27 (and in Fig. 25) exhibit the displacement from the pure octet (and pure singlet) decay rates into $\Sigma\pi$ and NK due to a mixing angle of $-16°$, which is the magnitude suggested by the mass formula.

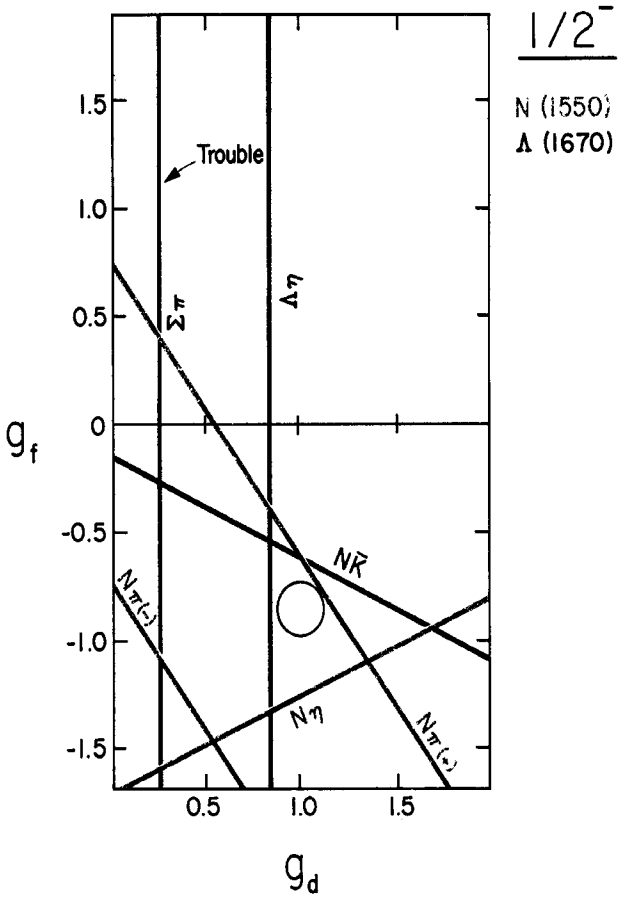

Fig. 26

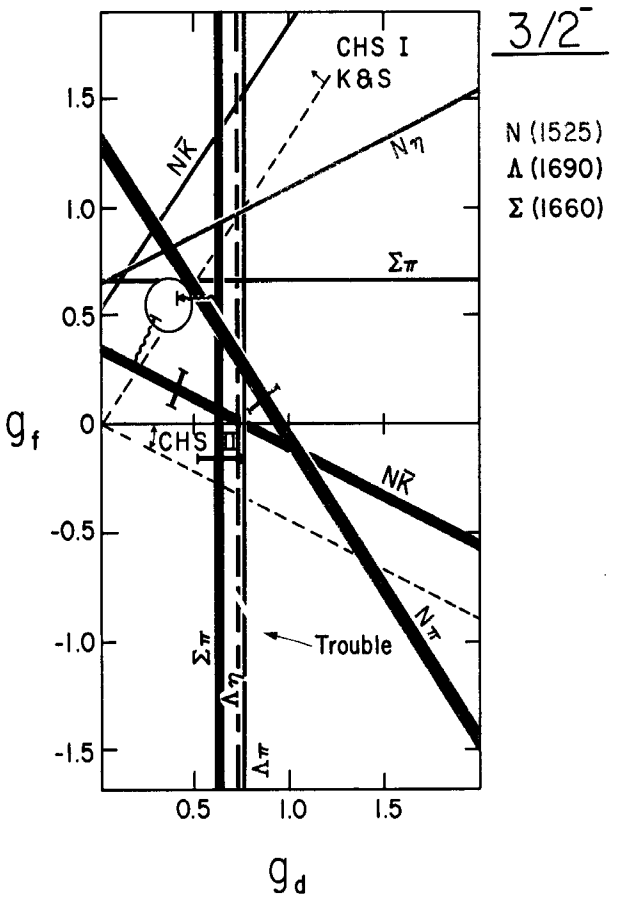

Fig. 27

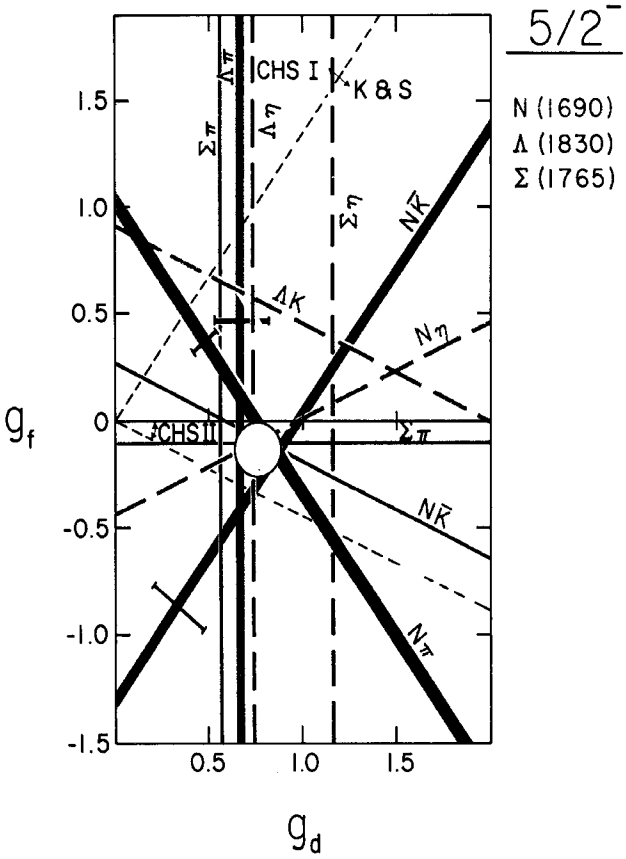

Fig. 28

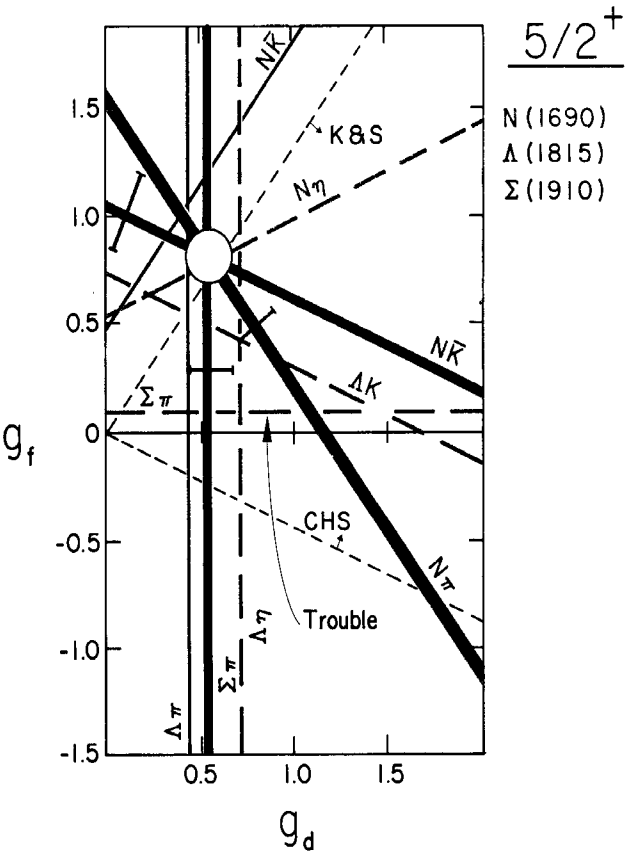

Fig. 29

REFERENCES AND FOOTNOTES

1. D. Cline, R. Laumann and J. Mapp, paper 285; and Phys. Rev. Letters 20, 1452 (1968).

2. O.I. Dahl, N. Horwitz, D.H. Miller, J.J. Murray and P.G. White, Phys. Rev. Letters 6, 142 (1961).

3. G. Alexander and U. Karshon, High-Energy Physics and Nuclear Structure (North-Holland Publ. Co., Amsterdam, 1967), p.36.

4. G. Alexander, O. Benary, U. Karshon, A. Shapira, G. Yekutieli, R. Engelmann, H. Filthuth, A. Fridman and B. Schiby, Phys. Letters 19, 715 (1966).

5. G. Alexander, J.A. Anderson, F.S. Crawford, W. Laskar and L.J. Lloyd, Phys. Rev. Letters 7, 348 (1961).

6. B.A. Shabazian and V.I. Moroz, papers 72 and 73.

7. J. Meyer, Rapporteur's talk at the Int. Conf. on Elementary Particles, Heidelberg (1967), p. 117.

8. R.M. Edelstein, oral communication to this Conference.

9. R.L. Cool, G. Giacomelli, T.F. Kycia, B.A. Leontic, K.K. Li, A. Lundby and J. Teiger, Phys. Rev. Letters 17, 102 (1966).

10. D.V. Bugg, R.S. Gilmore, K.M. Knight, D.C. Salter, G.H. Stafford, E.J.N. Wilson, J.D. Davies, J.D. Dowell, P.M. Hattersbey, R.J. Homer, A.W. O'Dell, A.A. Carter, R.J. Tapper and K.F. Riley, Phys. Rev. 168, 1466 (1968).

11. R.W. Bland, M.G. Bowler, J.L. Brown, G. Goldhaber, S. Goldhaber, V.H. Seeger and G.H. Trilling, Phys. Rev. Letters 18, 1077 (1967).

12. R.W. Bland et al., paper 657.

13. S. Femino, S. Jannelli, F. Mezzanares, L. Monari and P. Serra, Nuovo Cimento 50 A, 371 (1967).

14. A.S. Carroll et al., paper 14.

15. A.A. Carter, K.F. Riley, R.J. Tapper, D.V. Bugg, R.S. Gilmore, K.M. Knight, D.C. Salter, G.H. Stafford, E.J.N. Wilson, J.D. Davies, J.D. Dowell, P.M. Hattersbey, R.J. Homer and A.W. O'Dell, Phys. Rev. 168, 1457 (1968).

16. G. Alexander et al., paper 819.

17. A. Hirata et al., paper 658.

18. J. Alitti et al., paper 379.

19. A. Barbaro-Galtieri, T.S. Mast, F.T. Solmitz and R.D. Tripp, paper 669; UCRL report 18328.

20. N.P. Bogachev et al., paper 87.

21. Van Yun-Chan, Kim Khi In, E.N. Kladnitskaya, G.I. Kopylov, A.A. Kuznetsov, N.N. Mel'nikova, Nguen Din Ty and E.S. Sokolova, Proc. XIIth Int. Conf. on High-Energy Physics, Dubna (1964), Vol. I, p. 615.

22. O.I. Dahl, L.M. Hardy, R.I. Hess, J. Kirz and D.H. Miller, Phys. Rev. 163, 1377 (1967). I thank H.J. Lubatti for bringing this reference to my attention.

23. R. Armenteros, M. Ferro-Luzzi, D.W.G. Leith, R. Levi-Setti, A. Minten, R.D. Tripp, H. Filthuth, V. Hepp, E. Kluge, H. Schneider, R. Barloutaud, P. Granet, J. Meyer and J.P. Porte, $\Sigma(1765) \to \Lambda(1520)\pi$ in Phys. Letters 19, 338 (1965).
R. Armenteros, M. Ferro-Luzzi, D.W.G. Leith, R. Levi-Setti, A. Minten, R.D. Tripp, H. Filthuth, V. Hepp, E. Kluge, H. Schneider, R. Barloutaud, P. Granet, J. Meyer and J.P. Porte, $K^- p \to \Sigma\pi$ in Phys. Letters 24 B, 198 (1967); $K^- p \to \bar{K}N$ in Nucl. Phys. B3, 592 (1967); $\Sigma(1385)\pi$ in Z. Phys. 202, 486 (1967).

24. R. Armenteros et al., papers 524, 627, and 629.

25. D. Berley, P.L. Conolly, E.L. Hart, D.C. Rahm, D.L. Stonehill, B. Thevenet, W.J. Willis and S.S. Yamamoto, Phys. Rev. Letters 15, 641 (1965).

26. R. Levi-Setti, oral communication of Chicago-Heidelberg group to this Confereree.

27. M. Derrick, T. Fields, J. Loken, R. Ammar, R.E.P. Davis, W. Kropac, J. Mott and F. Schweingruber, Phys. Rev. Letters 18, 266 (1967).

28. M. Primer, M. Goldberg, K. Jaeger, V. Barnes, P. Dornan and I. Skillicorn, Phys. Rev. Letters 20, 610 (1968).

29. D.J. Crennell et al., paper 149.

30. W.M. Smart, Phys. Rev. 169, 1330 (1968).

31. M. Taher-Zadeh, D.J. Prowse, P.E. Schlein, W.E. Slater, D.H. Stork and H.K. Ticho, Phys. Rev. Letters 11, 470 (1963).

32. M. Ferro-Luzzi, Rapporteur's talk at the XIIIth Int. Conf. on High-Energy Physics, Berkeley (1967), p. 183.

33. P. Eberhard et al., paper 223.

34. P. Eberhard, M. Pripstein, F.T. Shively, U.E. Kruse and W.P. Swanson, Phys. Rev. 163, 1446 (1967).

35. C. Daum, F.C. Erné, J.P. Lagnaux, J.C. Sens, M. Steuer and F. Udo, Nucl. Phys. B6, 273 (1968).

36. C. Daum, F.C. Erné, J.P. Lagnaux, J.C. Sens, M. Steuer and F. Udo, paper 761; and Nucl. Phys., B7, 19 (1968).

37. R.D. Tripp, D.W.G. Leith, A. Minten, R. Armenteros, M. Ferro-Luzzi, R. Levi-Setti, H. Filthuth, V. Hepp, E. Kluge, H. Schneider, R. Barloutaud, P. Granet, J. Meyer and J.P. Porte, Nucl. Phys. B3, 10 (1967).

38. P. Dauber et al. (to be published in Phys. Rev.).

39. R. Dalitz, Proc. II Hawaii Topical Conference on Particle Physics (1967) (University of Hawaii Press, 1968), p. 325.

40. W.M. Smart, A. Kernan, G.E. Kalmus and R.P. Ely, Phys. Rev. Letters 17, 556 (1966).

41. P. Bareyre, C. Bricman and G. Villet, Phys. Rev. 165, 1730 (1968).

42. A. Donnachie, R.G. Kirsopp and C. Lovelace, Phys. Letters 26 B, 161 (1968).

43. C. Johnson, UCRL-17683 (Thesis).

DISCUSSION

TUAN: You mentioned about the difficulty of obtaining satisfactory agreement (up to a factor of two to four) between SU(3) predictions and decays of $1/2^-$ baryon states, suggesting impurity of SU(3) assignments for S-wave baryon states. There is a recent preprint of Dobson (University of Hawaii) which uses a specific form of SU(3) breaking consistent with the Gell-Mann-Okubo type of symmetry breaking; the sum rules obtained are consistent with presently known decays of $1/2^-$ baryon states. Hence this work suggests that even the $1/2^-$ baryon states can be essentially SU(3) pure (with no strong mixing needed), but with a judicious choice of SU(3) symmetry breaking such as is known to be needed to get the Gell-Mann-Okubo mass formula for the mass spectrum.

SNOW: i) Can you comment on the uniqueness of the phase-shift analyses that went into the determination of the branching ratios that you have been discussing? ii) Can you tell whether any comparison of the fits with dispersion relation have been made?

TRIPP: In the phase-shift analysis many different spin-parity assignments for resonances with differing backgrounds have been tried. The results represent the best fits they obtained and are usually significantly better than the nearest alternatives. I believe that the CHS Collaboration feels that when the waves are dominant, such as some of the rates of resonances in category A, there is very little likelihood of finding alternative possibilities. For the weaker amplitudes where χ^2 differencies are not large, they make no claims of uniqueness. As far as I know, no comparison with dispersion relations have been made for the 600-800 MeV/c data.

BARUT: How sensitive are your results to the choice of the barrier penetration factor $B_\ell(p)$, and what form of this factor have you used?

TRIPP: The barrier penetration factor adopted is the one found in Blatt and Weisskopf with a radius of interaction of one fermi. Other expressions used in the literature differ from this one for $\ell \geq 2$, but

lead to essentially the same result. The choice of radius of interaction is important only when the c.m. momentum in various decay modes is very different. For example in the $3/2^+$ decuplet it will hardly alter the discrepancy between $\Delta(1236) \to N\pi$ and $\Xi(1530) \to \Xi\pi$. However, it will affect the low Q-decay $\Sigma(1385) \to \Sigma\pi$.

LEVI-SETTI: To answer the question by Snow concerning a comparison of the $\bar{K}N$ energy-dependent partial wave analysis of the CHS and Chicago-Heidelberg work with dispersion relation calculations, I wish to show a figure taken from a late contribution by Chicago-Heidelberg to this Conference[1]. This shows

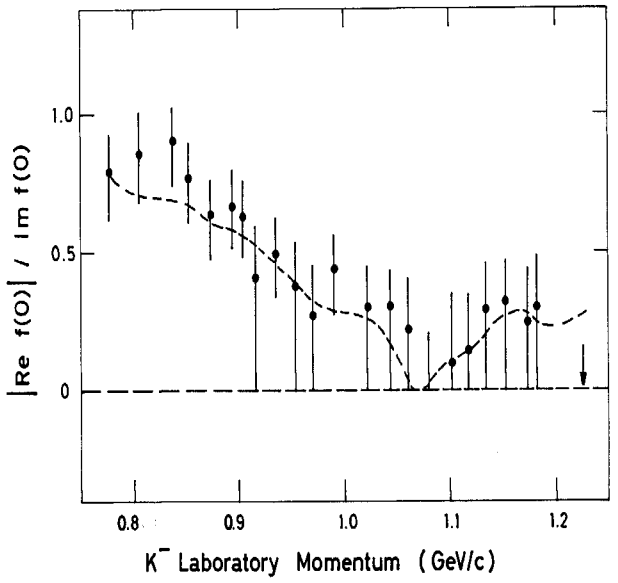

the ratio $|\text{Re } f(0)|/\text{Im } f(0)$ as a function of incident K^- momentum, as obtained a) from a comparison of $d\sigma/d\Omega|_{0^\circ}$ for $K^-p \to K^-p$ with the optical points from $\sigma_{tot}(K^-p)$ (experimental points), and b) from a typical fit of all $K^-p \to K^-p$, $\bar{K}^0n$, and $\sigma_{tot}(K^-p)$ data (dashed curve). The zero observed at ~ 1.08 GeV/c corresponds to Re f(0) becoming negative beyond this momentum. This feature and the over-all behaviour of the curve agree qualitatively with the predictions of Lusignoli et al.[2] based on dispersion relation calculations. In the latter, however, $|\text{Re } f(0)|/\text{Im } f(0)$ is smaller than observed in the region ~ 0.8 GeV/c by almost a factor of two. In contrast, in a similar calculation by Zovko[3], Re f(0) never becomes negative although between 0.8 and 1.2 GeV/c the shape of the predicted curve is still in rough agreement with our fit. A possible cause of discrepancy in these predictions may have been the use of different $\bar{K}NY$ coupling constants. It would be desirable that a comparison be made of our partial wave analysis with dispersion relation calculations based on the most recent determinations of $\sigma_{tot}(K^-p)$ and $\bar{K}NY$ coupling constants.

References

1. B. Conforto, D.M. Harmsen, T. Lasinski, R. Levi-Setti M. Raymund, E. Burkhardt, H. Filthuth, E. Kluge, H. Oberlack and P.R. Ross, EFI Report 68-62 (1968) and late contribution to this Conference.

2. M. Lustignoli, M. Restignoli, G. Violini and G.A. Snow, Nuovo Cimento 45, 792 (1966).

3. N. Zovko, Z. Phys. 196, 16 (1966).